PhD degree in Systems Medicine

(curriculum in Molecular Oncology)

European School of Molecular Medicine (SEMM),

University of Milan and University of Naples “Federico II”

Settore disciplinare: med/04

Polycomb group proteins Ring1A/Ring1B control peripheral B cell homeostasis and terminal differentiation

Federica La Mastra

IFOM, Milan

Matricola n. R11120

Supervisor: Dr. Stefano Casola, Ph.D., M.D.

IFOM, Milan

Academic year 2017-2018

Table of contents

List of Abbreviations

AID	Activation Induced Deaminase
AP-1	Activator Protein- 1
APRIL	Apoptosis-Inducing Ligand
ATAC	Assay for Transposase-Accessible Chromatin
ATF6	Activating Transcription Factor 6
BAFF	B-cell Activating Factor
BAFF-R	BAFF Receptor
Bax	Bcl2-associated X
Bcl-2	B Cell CLL/Lymphoma 2
Bcl-6	B Cell CLL/Lymphoma 6
Bcl-$_{XL}$	B Cell CLL/Lymphoma-extra large
BCMA	B-Cell Maturation Antigen
Bcor	Bcl6 corepressor
BCR	B Cell Receptor
BER	Base Excision Repair
Bim	Bcl2-like protein 11 (Bcl2l11)
BM	Bone Marrow
Bmi-1	Bmi-1 Polycomb ring finger oncogene
bp	base pair
BrdU	BromodeoxyUridine
BSAP	B-cell specific activator proteins
C-term	Carboxy terminus
Casp-glow	FITC-conjugated VAD-FMK, a general caspase inhibitor
Cbx	Chromobox homolog
CD	Cluster of Differentiation
CKI	Cyclin-dependent Kinase Inhibitor
CDK	Cyclin-Dependent Kinase
CDKNA	Cyclin Dependent Kinase inhibitor A
CDKNB	Cyclin Dependent Kinase inhibitor B
cDNA	complementary DNA
CFSE	CarboxylFluorescein Succinimidyl Energy
ChIP	Chromatin Immunoprecipitation
CLP	Common Lymphoid Progenitor
cPRC1	canonical PRC1
CSR	Class Switch Recombination

CXCL13	Chemokine (C-X-C motif) ligand 13
CXCR5	C-X-C chemokine receptor type 5
DAP	Differentially Accessible Promoter
DAPI	4’,6-diamidino-2-phenylindole
DDR	DNA Damage Response
DE	Deletion Efficiency
DEG	Differentially Expressed Gene
DG	DiacylGlycerol
Dll-1	Delta-like 1
DMEM	Dulbecco's Modified Eagle Medium
DNA	Deoxyribonucleic Acid
dNTP	deoxynucleoside triphosphate
DSB	Double-Strand Break
E2a	E2a immunoglobulin enhancer binding factors E12/E47
E2F6	E2F transcription factor 6
Ebf1	Early B-cell factor 1
Eed	Embryonic ectoderm development
EIF4E	Eukaryotic Initiation Factor 4E
ER	Endoplasmic Reticulum
ESC	Embryonic Stem Cell
Ezh2	Enhancer of zeste homolog 2 (Drosophila)
DAPI	4',6-diamidino-2-phenylindole
FACS	Fluorescence Activated Cell Sorting
Kdm2b	lysine (K)-specific demethylase 2B
FDC	Follicular Dendritic Cell
FDR	False Discovery Rate
Flt3	Fms-related tyrosine kinase 3
FO	Follicular
Fw	Forward
g	relative centrifugal force expressed in units of gravity
GC	Germinal Center
GSK3β	Glycogen Synthase Kinase 3
GRK2	G-protein coupled Receptor Kinase-2
Gy	Gray
γH2A.X	phosphorylated Histone H2A.X at Serine-139
H	Histone
Hi	High
H2AK119ub1	mono-ubiquitylated Histone H2A at Lysine 119
H3K27me3	tri-methylated Histone H3 at Lysine 27

H3K36me3	tri-methylated Histone H3 at Lysine 36
H3K4me3	tri-methylated Histone H3 at Lysine 4
H3K79me3	tri-methylated Histone H3 at Lysine 79
H3K9me3	tri-methylated Histone H3 at Lysine 9
Hox	Homeotic
HPH	polyhomeotic Homolog Protein
HSC	Hematopoietic Stem Cell
Ig	Immunoglobulin
IgH	Immunoglobulin Heavy chain
IgL	Immunoglobulin Light chain
IL	Interleukin
IL-7R	IL-7 Receptor
Irf4	Interferon regulatory factor 4
ITAM	Immunoreceptor Tyrosine-based Activation Motifs
ITIM	Immunoreceptor Tyrosine-based Inhibition Motifs
Jag	Jagged
kb	kilobase
kDa	kiloDalton
LN	Lymph Node
lncRNA	Long non-coding RNA
Lo	Low
loxP	locus of X-over of P1
LPS	LipoPolySaccharide
mAb	monoclonal Antibody
MACS	Magnetic-Activated Cell Sorting
MAX	MYC-Associated factor X
Mcl-1	Myeloid cell leukemia sequence 1 (BCL2-related)
MGA	MAX Gene-Associated protein
MHC	Major Histocompatibility Complex
min	minute
MINT	Msx2-Interacting Nuclear Target
miRNA	micro RNA
MLN	Mesenteric Lymph Nodes
MMR	Mismatch Repair
MPP	Multipotent Progenitor
mRNA	messenger RNA
MTA-3	Metastasis-Associated 1 family member 3
mTORC1	mammalian Target Of Rapamycin Complex 1
MZ	Marginal Zone

N-term	Amino terminus
NCOR	Nuclear receptor co-repressor
NCOR2/SMRT	Nuclear receptor co-repressor 2
ncPRC1	non-canonical PRC1
ncRNA	non-coding RNA
NER	Nucleotide Excision Repair
NFAT	Nuclear Factor of Activated T-cells
NHEJ	Non-Homologous End-Joining
O/N	over night
Pax5	Paired box 5
PBS	Phosphate Buffered Saline
PB	Plasma blast
PC	Plasma Cell
PCa	Peritoneal Cavity
PcG	Polycomb Group
PCGF	Polycomb Group ring Finger
PCR	Polymerase Chain Reaction
PDK2	Phosphoinositide-Dependent protein Kinase-2
Pho	Pleiohomeotic
PI3K	PhosphoInositide 3-Kinase
PIP_2	PhosphatidylInositol-4,5-bisphospate
PLCγ2	PhosphoLipase γ-2
Pmaip1	Phorbol-12-myristate-13-acetate-induced protein (Noxa)
pol	polymerase
PP	Peyer's Patches
PRC	Polycomb Repressive Complex
Prdm1	Positive regulatory domain containing 1, with ZNF domain (Blimp-1)
PTK	Protein Tyrosine Kinases
PTP	Protein Tyrosine Phosphatase
PTM	Post-Translational Modification
Ptprc	Protein Tyrosine Phosphatase, Receptor type C
RAG	Recombination Activation Genes
RB1	Retinoblastoma tumor suppressor protein 1
RBC	Red Blood Cell
Ring1	Ring finger protein 1, Ring1A, R1A
RISC	RNA-Induced Silencing Complex
RNA	Ribonucleic Acid
Rnf2	Ring finger protein 2, Ring1B, R1B
rpm	Rotations per minute (centrifugal force)

RSS	Recombination Signal Sequence
RT	room temperature
RT-PCR	Reverse Transcriptase PCR
RT-qPCR	Real-time quantitative PCR
Rv	Reverse
RYBP	Ring1 and Yy1 binding protein
Runx1	Runt related transcription factor 1
S	Serine
S1P	Shingosine-1-Phosphate
S1PR1	Shingosine-1-Phosphate Receptor-1
S1PR3	Shingosine-1-Phosphate Receptor-3
S6K1	S6 kinase 1
Sca1	Stem cell antigen-1; Ly-6A/E
SD	Standard Deviation
Seq	Sequencing
SH	Src homology
SHM	Somatic Hypermutation
SHP-1	Src homology domain-containing phosphatase 1
SLO	Secondary Lymphoid Organ
SPL	Spleen
SSB	Single-Strand Break
Suz12	Suppressor of zeste 12 homolog (*Drosophila melanogaster*)
SWI/SNF	SWItch/Sucrose NonFermentable
TACI	Transmembrane Activator and CAML Interactor
TF	Transcription Factor
T_{FH}	T Follicular Helper cell
TLR	Toll-Like Receptor
TSS	Transcriptional Start Sites
TrxG	Tritorax Group
UPR	Unfolded Protein Response
Wnt	Wingless-related MMTV integration site 1
Xbp1	X-box binding protein 1
Y	tyrosine

Index of figures

Index of tables

1. Abstract

Polycomb group proteins (PcG) are epigenetic modifiers that modulate chromatin accessibility through covalent histone modifications. PcGs are assembled in two main macromolecular complexes, Polycomb Repressive Complex 1 and 2 (PRC1 and PRC2, respectively). Several studies have highlighted the importance of PRC1 and PRC2 in B-cell lymphopoiesis. To study the contribution of PRC1 to peripheral B cell maturation, B cell homeostasis and terminal B cell differentiation, I analyzed mutant mice allowing conditional Cre-dependent inactivation of PRC1 catalytic function starting from late transitional B cells, through combined extinction of the RING1A and RING1B proteins.

In response to induced PRC1 inactivation, peripheral B cells displayed profound alterations in the surface phenotype and a major disturbance of their transcriptional profile. In secondary lymphoid organs (SLOs), numbers of B cells were reduced in PRC1 mutant mice. In particular, we observed a significant impairment in the absolute numbers of PRC1 defective B cells expressing normal levels of marginal zone (MZ) B cell surface markers. PRC1 mutant peripheral B cells expressed lower levels of the Sphingosine-1-phosphate receptor-1 (S1pr1), which is crucial for the migration of B cells to the MZ, and displayed defective *in vitro* migration towards the S1pr1 ligand. Downregulation of S1pr1 in PRC1 mutant B cells could depend on the increased expression of the Polycomb target microRNA mir-125b.

PRC1 mutant B cells showed a reduced response to the B cell survival factor BAFF, reduced fitness when placed in competition with PRC1 proficient B cells in mixed bone marrow reconstitution experiments and heightened sensitivity to pro-apoptotic signals, consequent of the higher levels in these cells of the BIM protein and of the sub-optimal activation of the AKT kinase in response to either BAFF-R or BCR engagement. Upon *in vitro* stimulation with lipopolysaccharide, PRC1 mutant B cells showed premature cell-cycle arrest and onset of the terminal differentiation program to plasma cells. This phenotype was associated, in vivo, with the observed de-repression of Prdm1 gene in a large fraction of follicular B cells. Moreover, we identified a defect of PRC1 mutant B cells in the correct splicing of the *Ptprc* gene encoding for the CD45R phosphatase. The expression of shorter isoforms of the CD45R at the expense of the full-length one correlated in these cells with

an impaired activation of the CD45R substrate, LYN kinase, a positive regulator of BCR signalling.

Transcriptomic analyses revealed that the majority of genes upregulated in PRC1 mutant B cells overlapped with those targeted by PRC2 in resting B cells, pointing to a strict interdependence between PRC1 and PRC2 for correct silencing of shared targets in mature B cells. Our studies also unveiled a subset of PRC1-controlled genes that lacked H3K27me3 deposition at the promoter region. PRC1 inactivation caused the down-regulation of a distinct subset of genes controlling DNA replication and cell cycle, possibly as a result of the interference with cell-cycle regulated E2F and FOXM1 transcription factors. Instead, our study failed to reveal major changes in chromatin accessibility at promoter-distal regulatory regions following PRC1 inactivation.

In summary, this work provides evidence for a crucial role played by PRC1 in peripheral B cell subset differentiation, B cell homeostasis and timing of terminal B cell differentiation.

2. Introduction

2.1 Chromatin and epigenetics

2.1.1 The chromatin architecture

In eukaryotic cells, the DNA is organized in a complex structure with proteins and RNAs called chromatin. The primary function of chromatin is to condense the genetic material in the nucleus; however, it is actively involved also in DNA replication, cell division and transcriptional regulation. The primary structure of chromatin, the nucleosome, is constituted by 147 bp of DNA wrapped around a histone octamer, consisting of two copies of H2A, H2B, H3 and H4 proteins. Also through the linker histone H1, nucleosomes are further condensed into higher-order structures, which are only partially understood. Condensed chromatin is highly organized in the nucleus into discrete domains, usually characterized by similar transcriptional features. Chromatin condensation is a dynamic event, which is tightly regulated by a multitude of factors, including epigenetic modifications (Fyodorov et al. 2018; Kouzarides 2007).

2.1.2 Epigenetics and chromatin

The term ‘epigenetic’ indicates all the processes which influence gene expression, not involving changes in the DNA sequence. Epigenetic processes are categorized in events that alter the chromatin conformation, hence influencing the gene transcription, and in mechanisms which act at the post-transcriptional level, ultimately favouring or inhibiting mRNA translation. The former category includes histone post-translational modification, substitution of classical histones with histone variants, nucleosome remodelling and DNA methylation; the latter is mainly represented by post-transcriptional regulation by non-coding RNAs, among which microRNAs (miRNAs) are the most investigated.

2.1.2.1 The histone code

Histones are globular proteins with a N-terminal tail that protrudes from the nucleosome, which can be subjected to substantial post-transcriptional modifications (PTMs), such as acetylation, phosphorylation, methylation and ubiquitination, and others less investigated.

Histone PTMs influence the transcriptional activity by two mechanisms: on the one hand, the introduction of charged groups favour/inhibit the interaction between histone tail and histone core, thus influencing the status of nucleosome compaction (this mechanism is mainly known for acetylation); on the other hand, histone PTMs are specifically recognized and bound by transcriptional activators or repressors that are indeed targeted to specific loci to regulate gene expression. PTMs are added to histones by a class of enzymatic proteins called “writers” and, vice versa, removed by “erasers” (Biswas and Rao 2018). The reversibility of histone PTMs constitutes a potent and plastic mechanism to control gene expression in response to environmental changes (e.g. induction of differentiation). Importantly, a single histone modification per se in not able to induce any biological change, whereas is the general chromatin environment, given by the combination of different histone PTMs, the so called “histone code”, which impacts on transcriptional regulation. There are two main chromatin environments in the genome, namely active euchromatin and repressed heterochromatin. Euchromatin is characterized by an accessible conformation and is generally marked by high levels of histone acetylation and specific histone PTMs, as tri-methylation of lysine-4 of histone H3 (H3K4me3) at gene promoters and tri-methylation of lysine-36 and di/tri methylation of lysin-79 of histone H3 in gene bodies (H3K36me3 and H3K79me2/3, respectively). On the contrary, heterochromatin is in a condensed status, less accessible to transcription factors (TFs), and marked by di/tri-methylation of lysine-9 and -27 of histone H3 (H3K9me2/3 and H3K27me2/3, respectively). An exception of this dualistic classification is represented by the bivalent domains, which retain both activating and repressive PTMs (usually H3K4me3 and H3K27me3 at gene promoters) and are characterized by a ‘poised’, low-level of transcription. Bivalent domains are particularly present in stem cells or cells undergoing developmental processes, within which they lose either H3K27me3 or H3K4me3, reaching a stable status of transcriptional activation or repression, respectively (Kouzarides 2007).

2.1.2.2 Other chromatin-associated epigenetic marks

Besides being modified by PTMs, canonical histones could be substituted by histone variants, which confer structural and functional features to the chromatin environment. Moreover, the position of nucleosomes along the DNA could be changed by complexes which move, remove and/or reshape their distribution. All these processes, named nucleosome remodelling, directly influence gene expression. Lastly, DNA methylation consists in the addition of a methyl-group to the nucleotides of DNA. In mammals, the main target of this epigenetic process is cytosine that is transformed into 5-methyl-cytosine. At promoters, especially in CpG repeats called CpG island, DNA methylation is associated with transcriptional repression and gene silencing. Chromatin epigenetic modifications influence each other, by the recruitment of different factors. For instance, it is largely known that the deposition of histone PTMs associated to heterochromatin favours the recruitment of DNA-methylases that further silence gene expression.

All these processes contribute, together with histone PTMs, to create a chromatin landscape which in turn influences a large number of nuclear processes, including gene transcription, DNA-replication and repair, chromosome compaction and localization (Kim, Samaranayake, and Pradhan 2009).

2.1.2.3 Micro-RNAs

miRNAs are short non-coding RNAs of about 22 nucleotides that have emerged as important post-transcriptional regulators. miRNAs are usually transcribed in clusters by RNA polymerase (pol) III and then processed by Drosha and Dicer, in the nucleus and cytoplasm respectively, to obtain double-strand oligonucleotides. Next, a miRNA duplex is loaded onto an AGO protein to form an effector complex, named RNA-induced silencing complex (RISC). Within RISC, miRNA duplex is unwound, the passenger strand is removed (usually the 5' strand), whereas the mature or guide miRNA is retained (usually the 3' end). According to the canonical model of action of miRNAs, RISC complex is targeted to the 3' UTR of one or more transcripts by the partial pairing of guide miRNA and transcript sequence. Upon complex binding, target transcript is either cut and degraded or its

translation is inhibited. Both mechanisms prevent protein synthesis, resulting in the down-regulation of the miRNA target gene (Figure 1).

Given their plasticity, miRNAs are involved basically in all biological processes, including cell differentiation and development (Ketting 2010; Lodish et al. 2008).

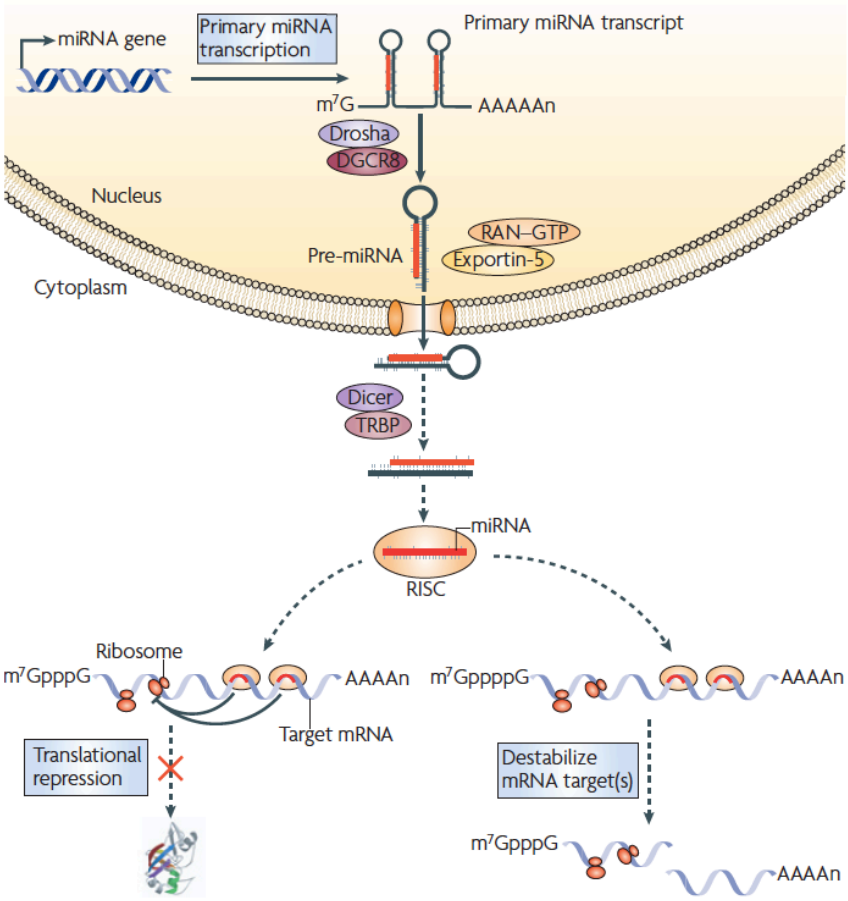

Figure 1. MicroRNA biogenesis and function.

miRNA genes encode long primary mRNA transcripts that in turn produce mature miRNAs through a series of maturation steps: 1) Primary miRNA transcripts are processed into precursor miRNA (pre-miRNA) by Drosha; 2) The pre-miRNA is then actively transported to the cytoplasm by Exportin-5; 3) pre-miRNA is processed into a ~21-nucleotide duplex. 4) The final step of miRNA maturation is the selective loading of the functional strand of the small RNA duplex onto the RISC complex. Mature miRNAs then guide the RNA-induced silencing complex to cognate target genes and repress target gene expression by either destabilizing target mRNAs or repressing their translation. Polycomb group proteins. Adapted from Lodish et al. 2008.

2.2 Polycomb Repressive Complexes

Polycomb group (PcG) proteins were initially identified in *Drosophila melanogaster* where, together with proteins of the Tritorax group (TrxG), they sustained proper development of embryos. In particular, PcG and TrxG proteins were respectively repressors and activators of the Homeotic genes (Hox), which dictate proper body segmentation (Lewis 1978; Di Croce and Helin 2013). Later, PcGs were characterized in all vertebrates, with orthologs increasing in number and in sequence divergency in correlation with the evolution of complex traits (Whitcomb et al. 2007).

Different PcG interact and assemble to form macromolecular complexes that belong to two main families: Polycomb Repressive Complexes 1 and 2 (PRC1 and PRC2, respectively). PRC1 and PRC2 are both writers of histone modifications, but they have different catalytic activities: PRC1 carries E3-ligase activity, through which they transfer a ubiquitin group to the main target lysine-119 of histone H2A (H2AK119ub1) whereas PRC2 are methyl-transferases which target lysin-27 of histone H3 (H3K27me2/3). Both epigenetic marks are linked to chromatin compaction and transcriptional repression.

PRC1 and PRC2 complexes are characterized by a core component that remains constant in all the different variants (Figure 2).

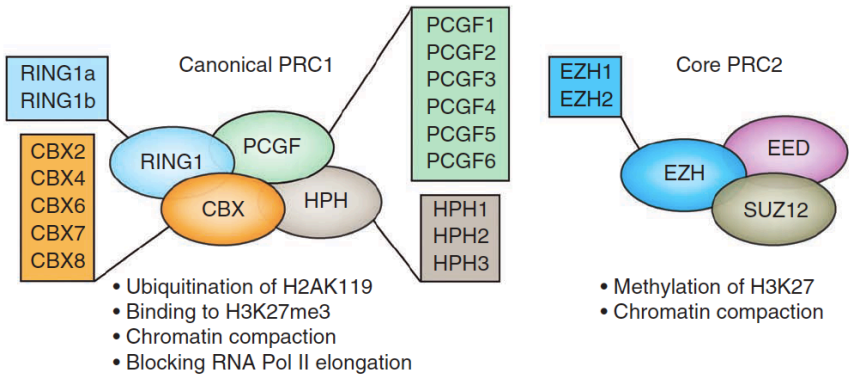

Figure 2. Composition and function of the main Polycomb complexes.

Polycomb group proteins assemble in two main macromolecular complexes in mammal, PRC1 and PRC2. Core components of the two complexes are shown. Variability of the complexes is depicted by the availability of multiple CBX, HPH, PCGF and catalytic subunits. Adapted from Di Croce and Helin 2013.

The core component of PRC1 is constituted by two subunits: the catalytic subunit RING1 (either RING1A or RING1B/RNF2) and a subunit belonging to PCGF family (PCGF1-6), which fosters the catalytic activity. On the contrary, PRC2 core component is formed by the catalytic subunit Enhancer of Zeste Homolog 2 (EZH2) or its homolog EZH1, by the Zinc-finger protein Suppressor Of Zeste 12 Protein Homolog (SUZ12) and by Embryonic Ectoderm Development (EED), which binds to tri-methylated residues by the WD40 repeat domain. The two cores assemble with other proteins of the PcG family that regulate the enzymatic activity or influence the recruitment/localization of the complexes on chromatin. However, while PRC2 variants are few, PRC1 complex has a very diverse composition (Aranda, Mas, and Di Croce 2015).

2.2.1 PRC1 complexity

The core component of PRC1 complex associates with different subunits, whose expression can be cell-context and developmental-stage dependent. PRC1 complexes are usually divided into two subfamilies of canonical and non-canonical PRC1 (cPRC1 and ncPRC1, respectively) (Figure 3).

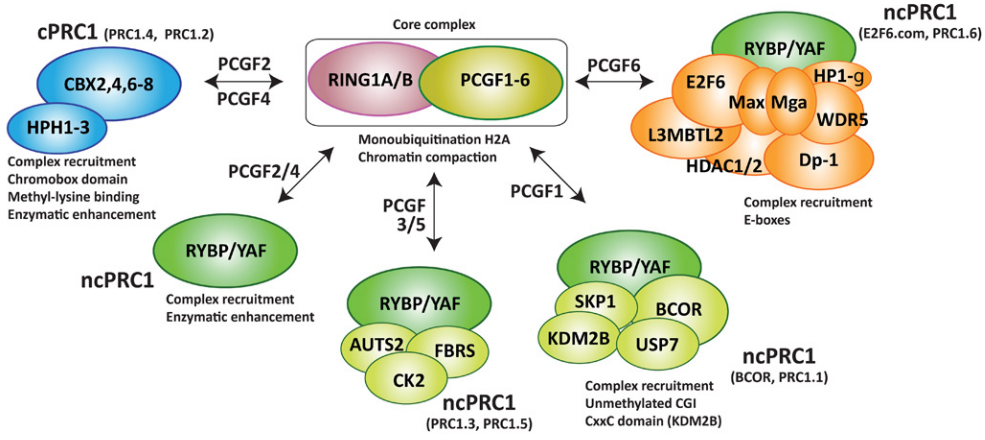

Figure 3. Composition of PRC1 complexes.

The core complex of PRC1 can associate with distinct PCGF proteins, which allows for an alternative nomenclature. Therefore, PCGF2 and PCGF4 are present in the cPRC1 complexes (PRC1.2 and PRC1.4, respectively), PCGF2 and PCGF4 are also associated with ncPRC1-containing RYBP or YAF proteins, PCGF3 and PCGF5 are present in the ncPRC1 complexes (PRC1.3 and PRC1.5), PCGF1 is present in the ncPRC1 complex PRC1.1 (also known as BCOR), and PCGF6 is present in the ncPRC1 complex PRC1.6. Adapted from Mas, Mas, and Croce 2015.

Canonical and non-canonical complexes vary in PCGF subunit composition, with PCGF-4 and -6 belonging to cPRC1 and PCGF-1, -2, -3, and -5 composing ncPRC1 complexes. Usually, PRC1 complexes are classified in six different groups according to the associated PCGF subunit (e.g. PRC1.6 contains PCGF6) (Gao et al. 2012).

In cPRC1, the catalytic core is always associated to a Chromobox (CBX) protein and to a polyhomeotic homolog protein (HPH). The main feature of cPRC1 is that the chromobox domain ensures the recruitment of the complex to H3K27me3-marked chromatin regions, through recognition of the histone mark.

For long time, PRC1 was believed to be recruited to chromatin in a PRC2-dependent manner. However, this model, named hierarchical model, has been challenged by the identification of ncPRC1 complexes, which implies the existence of PRC2-independent chromatin recruitment mechanisms of PRC1. Indeed, ncPRC1 lack a CBX subunit, which is instead replaced by the constant presence of the Ring1B and Yy1-binding protein RYBP, or its homolog YAF2 (Gao et al. 2012). These subunits are particularly able to foster the E3-ligase activity toward H2A and modify histones on chromatin independently on the presence of H3K27me3 (Tavares et al. 2012). The targeting of ncPRC1 to chromatin is still under investigation, but evidences suggest that it is mediated by other PcG proteins. For instance, the histone-demethylase KDM2B included in the ncPRC1 complex PRC1.1, also named BCOR, harbours a DNA-binding domain directing the complex to unmethylated CpG islands (Farcas et al. 2012). Additionally, PRC1.6 includes MAX (MYC-associated factor X) and MGA (MAX gene-associated protein), two DNA-binding proteins that can bind E-box sequences recognized by MYC (Hurlin et al. 1999).

Recently, an extensive biochemical study by Gao et al. unveiled that canonical and non-canonical PRC1 complexes have only a partially-overlapping chromatin localization. In particular, they showed that different PCGF proteins occupy diverse genomic loci, thus controlling subsets of genes associated with specific gene ontologies (Gao et al. 2012). Moreover, in this and other studies, alternative localization was shown for both CBX proteins and RYBP in embryonic stem cells (ESCs). Among CBXs, CBX7 location highly correlates with H3K27me3 co-occupancy and strong silencing of early lineage commitment genes,

whereas CBX2, 4 and 8 inhibit the expression of stem cell self-renewal genes (Morey et al. 2013; Gao et al. 2012). RYBP partially overlaps with CBX7 for repression of developmental genes, whereas in the rest of the genome the two proteins are mutually exclusive. In these regions, RYBP is mainly associated with modest expression of genes involved in the regulation of metabolism and cell-cycle progression (Morey et al. 2013). Together, these observations indicate a complex scenario whereby PRC1 complexes differentially contribute to the transcriptional regulation of different subsets of genes through different molecular mechanisms and interactions.

2.2.2 Targeting Polycomb Complexes to chromatin

Initial studies in *Drosophila* have shown that the recruitment of PcG proteins to chromatin is dictated by the recognition of Polycomb Responsive Elements (PRE), which contain consensus sites for several TFs (Schwartz et al. 2006; Tolhuis et al. 2006; Negre et al. 2006). However, the *Drosphila* TFs involved in this process are not conserved in mammals, except for YY1 and GAF, which, however, do not show major role in PcG protein recruitment in mammals (Mendenhall et al. 2010; Ku et al. 2008; Vella et al. 2012). Moreover, among the several target genes bound by Polycomb complexes, only two functional PREs have been identified in mammals (Sing et al. 2009; Woo et al. 2010). Considering that the genome-wide distribution of PRC1 does not fully correspond to the one of PRC2/H3K27me3 (Gao et al. 2012; Tavares et al. 2012; Morey et al. 2013; O'Loghlen et al. 2012) and that, in some loci, it remains unaffected upon the removal of H3K27me3 (Tavares et al. 2012), it is very likely that multiple molecular mechanisms contribute to PcG targeting to chromatin. Three main molecular mechanisms of Polycomb recruitment have been elucidated so far: 1) interaction with sequence-specific binding factors or DNA sequences; 2) recognition of histone modifications; 3) interaction with long non-coding RNAs (lncRNAs).

The first mechanism of recruitment is supported by the observation that both PRC1 and PRC2 were found to directly interact, in particular circumstances, with DNA-binding factors, such as REST and RUNX1 for PRC1 (Dietrich et al. 2012; Ren and Kerppola 2011; Yu et al. 2012) and SNAIL, REST, PLZF for PRC2 (Herranz et al. 2008; Dietrich et al. 2012;

Arnold et al. 2013). Moreover, the presence of the TFs MAX and MGA in ncPRC1.6 and the moderate enrichment of this complex in E-boxes suggests that the chromatin recruitment of ncPRC1.6 can be mediated by these transcription factors (Qin et al. 2012). Besides this, several evidences have shown that PRC2 is able to bind to CpG islands, especially when they are unmethylated and in an open conformation, inducing gene silencing (Ku et al. 2008; Mendenhall et al. 2010; Riising et al. 2014). Accordingly, EZH2 and SUZ12 displayed high overlapping genome occupancy with Ten-eleven translocation methyl-cytosine deoxygenase-1 (TET1), an enzyme that removes DNA-methylation by converting 5'-methyl-cytosine into hydroxymethyl-cytosine (Wu et al. 2011; Neri et al. 2013). Deletion of TET1 increases DNA-methylation and is corresponded by a reduction in EZH2 binding to the genome (Wu et al. 2011). The link between CpG island and Polycomb recruitment is further substantiated by the observation that the abrogation of DNA-methylation by inactivation of Dnmt1/3 in ESCs is associated with a redistribution of H3K27me3 and H2AK119ub1 histone marks in the genome (Reddington et al. 2013; Cooper et al. 2014). At the molecular level, the recruitment of PRC2 to unmethylated CpG islands could rely on the described ability of some PRC2-subunits to directly bind to unmethylated CpGs (Wu, Coskun, et al. 2010), or on the PRC1-mediated recruitment. Indeed, the ncPRC1 subunit KDM2B recognises unmethylated CpG islands: here, the recruitment of PRC1 and the subsequent deposition of H2AK119ub1 is able to recruit PRC2 complex (Wu, Johansen, and Helin 2013; Farcas et al. 2012; Blackledge et al. 2014).

Several studies highlighted that PcG proteins are recruited to chromatin through the recognition of histone modifications. The main histone modifications that drive PcG recruitment are the Polycomb-dependent ones, namely H3K27me3 and H2AK119ub1. As already mentioned, the CBX subunit of cPRC1 is crucial for its recruitment to PRC2-occupied chromatin regions though the recognition of H3K27me3 (Kaustov et al. 2011). Furthermore, recent evidences have shown that PRC2 is able to recognize and bind to H2AK119ub1, supporting the hypothesis of a PRC1-dependent PRC2 recruitment to some chromatin loci (Kalb et al. 2014; Blackledge et al. 2014; Cooper et al. 2014). Details of the interplay between PRC1 and PRC2 are described in section 2.2.4.

Other, non PcG-dependent histone modifications have been described to influence Polycomb occupancy on the chromatin. Indeed, the H3K9 methyltransferase G9a can directly interact with and recruit an enzymatically active PRC2 to target genes, where they cooperate to establish gene silencing (Margueron et al. 2009; Mozzetta et al. 2014). On the other hand, the presence of acetylation on lysine-27 of histone H3 creates a chromatin environment non-permissive for PRC2 binding, in line with the fact that this modification is mutually exclusive with H3K27me3 (Morey et al. 2008; Reynolds et al. 2012). Incorporation of histone variants in specific regions of the chromatin has also been described to influence PRC1 and PRC2 occupancy (Creyghton et al. 2008; Illingworth et al. 2012; Banaszynski et al. 2013).

PcG proteins, especially of PRC2 complex, have been reported to interact with several coding and non-coding RNAs in different cell types. Recently, Davidovich and co-workers showed that PRC2 interacts with different RNAs, with affinities ranging from mid to low nanomolar *in vitro* (Davidovich et al. 2015). However, the relevance of the uncovered affinities still needs to be established *in vivo*.

In mammals, the first evidence of functional interaction between PRC2 and the lncRNA *Xist* has been described in the context of X-chromosome dosage compensation in females. *Xist* gene is located on the X chromosome; once expressed, *Xist* lncRNA coats the X chromosome and triggers the recruitment of chromatin remodelling machinery, including PRC2, to impose repressive DNA and histone methylation (Plath et al. 2003; Zhao et al. 2008).

Other two lncRNAs, HOTAIR and ANRIL, are crucial for PcG proteins recruitment to specific chromatin loci. HOTAIR is a conserved lncRNA transcribed from the *Hoxc* locus in human and mice and it is crucial for the maintenance of transcriptional silencing throughout the genome, including the *Hox* loci (Gupta et al. 2010; Tsai et al. 2010; Rinn et al. 2007; Chu et al. 2011; Li et al. 2013). This action is mediated by the HOTAIR-dependent recruitment of both PRC2 and the histone demethylase LSD1 to *Hox* and other GA-rich loci, resulting in H3K27me3 deposition and loss of H3K4me3, with subsequent transcriptional repression (Chu et al. 2011; Li et al. 2013).

The antisense lncRNA ANRIL is expressed form the *Ink4* gene and directly interacts with both CBX7 and SUZ12, thus recruiting PRC1 and PRC2, respectively. This leads to the deposition of H2AK119ub1 and H3K27me3 and transcriptional silencing of the *Ink4* locus (Yap et al. 2010; Aguilo, Zhou, and Walsh 2011). Notably, this process is frequently enhanced in tumours because the repression of this locus, encoding for a cell-cycle inhibitor, sustains proliferation and tumor progression.

2.2.3 Transcriptional regulation by Polycomb Repressive Complexes

2.2.3.1 Polycomb-mediated gene silencing

Histone modifications written by Polycomb are thought to inhibit gene transcription mainly by three mechanisms: 1) by holding the poised RNA pol II; 2) by blocking RNA pol II elongation; 3) by favouring chromatin compaction (Di Croce and Helin 2013) (Figure 4).

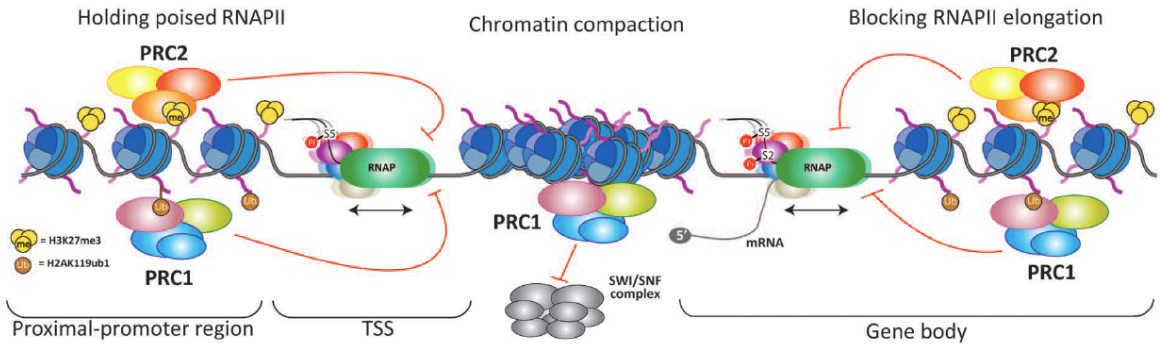

Figure 4. Mechanisms of Polycomb-mediated transcriptional repression.

PcG complexes mediate transcriptional repression by three main mechanisms: 1) by holding the poised RNA pol II at TSS, 2) by blocking the RNA pol II in a poised state, inhibiting the acquisition of a conformation allowing transcriptional elongation and 3) by favouring chromatin compaction. Adapted from Mas, Mas, and Croce 2015.

H3K27me3 is localized in transcriptional start sites (TSS), in gene bodies and distal enhancers. Evidences obtained in *Drosophila* indicate that its presence at proximal promoters inhibits the recruitment of RNA pol II (Chopra et al. 2011), whereas others sustain a preferential function in restraining the poised polymerase to promoters (Chen et al. 2012; Seenundun et al. 2010). Also, H2AK119ub1 is mainly found at TSS where it interferes with transcriptional activation by different mechanisms. In particular, in mouse ESCs Stock et al.

displayed that PRC1-dependent histone mark induces the retention of RNA pol II in a conformation with reduced activity (Zhou et al. 2008); subsequently, H2AK119ub1 was shown to inhibit the recruitment of FACT complex, which initiates transcriptional elongation, to the promoters of chemokines in macrophages (Stock et al. 2007); alternatively, in hepatocytes H2AK119ub1 prevents transcriptional initiation, by impeding di/tri-methylation of H3K4 (Brookes et al. 2012).

Besides RNA pol II regulation, another mechanism of gene repression is the Polycomb-induced chromatin compaction, which is mainly mediated by the presence of PRC1 and independent from its E3-ligase activity. Indeed, *in vitro* assays showed that reconstituted PRC1 complex induces chromatin compaction (Shao et al. 1999; Francis, Kingston, and Woodcock 2004; Grau et al. 2011; Trojer et al. 2011). In line with this finding, chromatin regions occupied by PcG proteins displayed reduced sensitivity to DNA enzymatic digestion compared to non-PcG domains (Bell et al. 2010; Calabrese et al. 2012; Kelly et al. 2012; Beck et al. 2014; Deaton et al. 2016) and decreased transcription factor and polymerase binding (Zink and Paro 1995; McCall and Bender 1996; Fitzgerald and Bender 2001). A recent work pointed out that these features are PRC1- and not PRC2-dependent and that they are specific for promoter regions, while distal elements bound by PcGs show no difference in accessibility (King et al. 2018). Together, these studies propose a model whereby the presence of PcG, and especially of PRC1, at gene promoters favours the compaction of nucleosomes, creating a chromatin environment in a “close” conformation, with poor accessibility for the transcriptional machinery. Interestingly, a recent work in Drosophila highlighted that H2AK119ub1 histone modification is dispensable for the transcriptional repression of PRC1: animals carrying either catalytically inactive Sce (the Ring1B ortholog in fly) or a mutant form of histone H2A lacking the target residue of PRC1 activity were viable and developed without aberration of the anterior-posterior axis segmentation (the typical Polycomb phenotype). However, PRC1 catalytic activity was crucial for viability and required for tri-methylation of H3K27 in the early embryogenesis (Pengelly et al. 2015). The conclusions drawn for Drosophila, yet, apparently are not valid for mammalian organisms, at least in ESC. Indeed, Endoh and colleagues described that

RING1-dependent H2A ubiquitylation is required for efficient repression of PcG-target genes and ESC proliferation (Endoh et al. 2012).

2.2.3.2 Polycomb contribution to active gene transcription

In recent years, emerging evidences proposed a role for PRC1 in favouring transcriptional activation. In mouse ESCs, indeed, the switch in expression from CBX7 to CBX8 ensures the initial activation of developmental genes. This event correlates with the localization of PRC1 also in H3K36me3 active gene bodies, but the molecular mechanisms behind this phenomenon are still under investigation (Creppe et al. 2014). Another study in resting B lymphocytes proposed that PRC1 co-localizes with Aurora B at active promoters: here, Aurora B inhibits the ubiquitylation of histone H2A written by PRC1 and recruits the deubiquitinase USP16. The knock-out of either Aurora B or RING1B causes reduced transcription and diminished binding of RNA pol II to promoters, suggesting that in this scenario PRC1 does not restrain, rather favours the recruitment of the polymerase (Creppe et al. 2014). Another evidence of active promoter occupancy by PRC1 came from the study of Schaaf and co-workers. In Drosophila, the authors demonstrated that PRC1 interacts with cohesins, which are typically located at active promoters to sustain transcriptional activation. Depletion of PRC1 reduced the elongating-associated phosphorylation of RNA pol II with subsequent reduction of transcribed mRNA (Schaaf et al. 2013). Recently, the PRC1-dependent recruitment of the elongation factor Spt5 to active genes was also added to this model (Pherson et al. 2017). Moreover, in the central nervous system, the non-canonical complex PRC1.5 was shown to have a dual activity in sustaining transcriptional activation: on the one hand, the CK2 subunit phosphorylates RING1B at serine-168, inhibiting its catalytic activity; on the other hand, the AUTS2 subunit recruits p300, a histone acetylase which creates an “open” chromatin environment. Additionally, RING1B was revealed to be a co-activator of gene expression by favouring the interaction of enhancer and promoter of the gene *Meis2* (Kondo et al. 2014). Altogether, these evidences highlight important implications of PRC1 not only in transcriptional repression but also in transcriptional activation, although the molecular mechanisms are not fully understood.

2.2.4 The interplay between PRC1 and PRC2 function

For long time, the hierarchical model of PRC2-dependent PRC1 recruitment to chromatin was believed to be the exclusive way to describe the interplay between the two Polycomb complexes. This model emerged from observation of chromatin co-occupancy of PcG at target sites and from the discovery of CBX subunits in PRC1 (Cao et al. 2002; Wang et al. 2004). Although this mechanism is clearly important for PRC1 localization on the chromatin, evidences from the last ten years have challenged this dogma. Indeed, a genome-wide analysis of PcG-histone mark distribution in Drosophila showed that the presence of H3K27me3 is not sufficient to recruit PRC1 (Schwartz et al. 2006); moreover, different observations in mammalian cells highlighted PRC1 recruitment on chromatin and the subsequent ubiquitylation of H2A regardless PRC2 (Schoeftner et al. 2006; Pasini et al. 2007; Tavares et al. 2012). This new model was further substantiated by the discovery of ncPRC1 complexes and their alternative mechanisms to be recruited to chromatin (Tavares et al. 2012; Farcas et al. 2012). Strikingly, *in vitro* assays indicated that H2A-ubiquitilatyon is able to recruit PRC2 and to promote tri-methylation of H3K27 on nucleosomes (Kalb et al. 2014). This evidence fostered different groups to investigate a possible inversion in the hierarchy of Polycomb-recruitment, leading to the discoveries that, in ESC, *de novo* binding of PRC1 and subsequent ubiquitilatyion of H2AK119 recalls PRC2, which contributes to the establishment of new PcG domains (Blackledge et al. 2014), and that the artificial recruitment of PRC1 to pericentromeric regions is followed by PRC2 binding and H3K27me3 deposition (Cooper et al. 2014). To further substantiate this model, the removal of PRC1 subunits was shown to cause H3K27me3 loss, both in Drosophila and mouse ESC (Pengelly et al. 2015; Blackledge et al. 2014). In summary, the mechanism of recruitment between PRC1 and PRC2 is reciprocal: in some regions of the genome PRC2 is the driving force to recall PRC1, whereas in other domains PRC1 is actively and primarly recruited to target sites, then followed by PRC2. Indeed, PRC2 subunits were found to interact with proteins of PRC1 complex (Kalb et al. 2014; Bhatnagar et al. 2014; Cao et al. 2014).

2.2.5 Biological processes controlled by Polycomb group proteins

2.2.5.1 Cell cycle

Cell cycle is the articulated series of events allowing DNA replication and cell division, ultimately producing two daughter cells from one. The cell cycle is divided in four main phases: in G_1 the cell is in resting condition, in S phase the genomic material is duplicated by DNA-polymerases and subsequently equally divided at two poles of the cell during G_2, while in M phase all cellular components (including DNA) are partitioned in two cells by meiosis. The progression through different phases of the cell cycle is ensured by the tightly-controlled expression of Cyclin proteins, which trigger cyclin-dependent kinase (CDKs) that ultimately activate effectors of cell-cycle progression. For instance, the progression from G_1 to S phase is mediated by the Cyclin D/CDK6 complex which, upon mitogenic stimulation, activates through phosphorylation the retinoblastoma tumor suppressor protein 1 (RB1) that subsequently dissociates from the E2F transcription factors, thus promoteing the expression of a substantial number of genes, including several necessary for DNA replication (Nevins 2001). CDKs are restrained by a group of proteins, known as CDK inhibitors (CKIs), which play an important role in cell-cycle checkpoints. Cell-cycle checkpoints consist of strictly controlled mechanisms that temporarily block cell-cycle progression in case of anomalies, such as in case of damaged DNA, to avoid its propagation to daughter cells. The three main checkpoints are the G_1/S checkpoint, the G_2/M checkpoint and the mitotic checkpoint (Elledge 1996).

CKIs are divided in two main families according to their structure: the INK4 family comprises $p15^{INK4b}$, $p16^{INK4a}$, $p18^{INK4c}$ and $p19^{INK4d}$ whereas the Cip/Kip family includes $p21^{Cip}$, $p27^{Kip1}$ and $p57^{Kip2}$. INK4 CKIs bind and inhibit only CDK4 and CDK6, playing a major role in G_1/S checkpoint, while Cip/Kip CKIs are broadly acting inhibitors of multiple CDKs thereby controlling all the three main checkpoints (Sherr and Roberts 1999). Given their role of inhibition of cell-cycle progression, usually CKIs are considered tumor suppressors. Different evidences indicated that PcG control the expression of many CKI genes, belonging to both families (Sauvageau and Sauvageau 2010) (Figure 5).

Subunits of both PRC1 and PRC2 were shown to bind to promoters of $p16^{INK4a}$ and $p19^{INK4d}$ and repress their expression in diverse cell types (Gil and Peters 2006; Maertens et al. 2009). The PRC2 subunit EZH2 represses $p15^{INK4b}$ and $p57^{Kip2}$ transcription (Kheradmand Kia et al. 2009; Yang et al. 2009), while the PRC1 subunit BMI/PCGF4 inhibits the expression of $p21^{Cip}$ in mouse neuronal stem cells and Drosophila (Fasano et al. 2007; Gong et al. 2006). In line with the latter finding, recently Bravo and co-workers showed that depletion of both RING1A and RING1B induces p21-dependent cell-cycle arrest in mouse embryonic fibroblasts (Bravo et al. 2015).

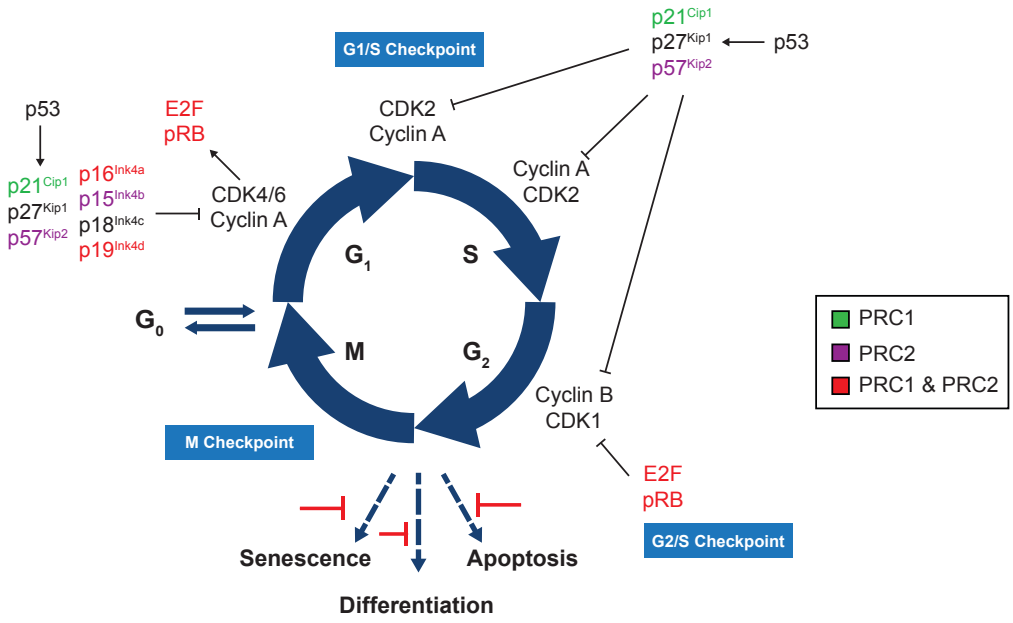

Figure 5. Regulation of cell cycle by PcG proteins.

Cell cycle and cell-cycle regulators. Cyclin-dependent inhibitors and other cell-cycle regulators are indicated in different colors according to the differential PRC1-dependent transcriptional regulation. Re-adapted from Sauvageau and Sauvageau 2010.

Besides a transcriptional control on CKI genes, Polycomb complexes contribute to cell replication also by transcriptional-independent mechanisms. By the E3-ligase activity, PRC1 complex ubiquitinates Geminin, an inhibitor of the DNA-replication factor CDT1; ubiquitination of Geminin targets the protein to proteasomal-degradation, thereby releasing CTD1 for the initiation of S phase (Ohtsubo et al. 2008). Moreover, PRC1 and PRC2 localize at the replicating-fork during S phase, contributing to fork progression (Piunti et al. 2014; Bravo et al. 2015). Although all molecular mechanisms behind this contribution have not

been unveiled yet, recently it was proposed, at least for PRC1, that RING1B is essential to promote pericentromeric chromatin replication, both dependently and independently from the H2AK119ub1 histone mark (Bravo et al. 2015).

Considering all the contributions of PRC1 and PRC2 to cell cycle and DNA-replication, the majority of PcG genes prevent the onset of senescence (Gil and Peters 2006; Jacobs et al. 1999; Kamminga et al. 2006).

2.2.5.2 Survival and apoptosis

Apoptosis is a process of programmed cell death typical of multicellular organisms, that results in the removal of damaged or stressed cells. The B-cell lymphoma-2 (Bcl-2) family of genes encodes for pivotal regulators of this cellular process. Members of the Bcl-2 family are divided in three main categories according to their structure and function in the apoptotic pathway: the anti-apoptotic "guardian" proteins (BCL-2, BCL-$_{XL}$, BCL-W, MCL-1, A1 and BCL-B), the pro-apoptotic "sensors" (BIM, BAD, PUMA, BID, NOXA, BMF) and the pro-apoptotic "effectors" (BAX and BAK) (Figure 6).

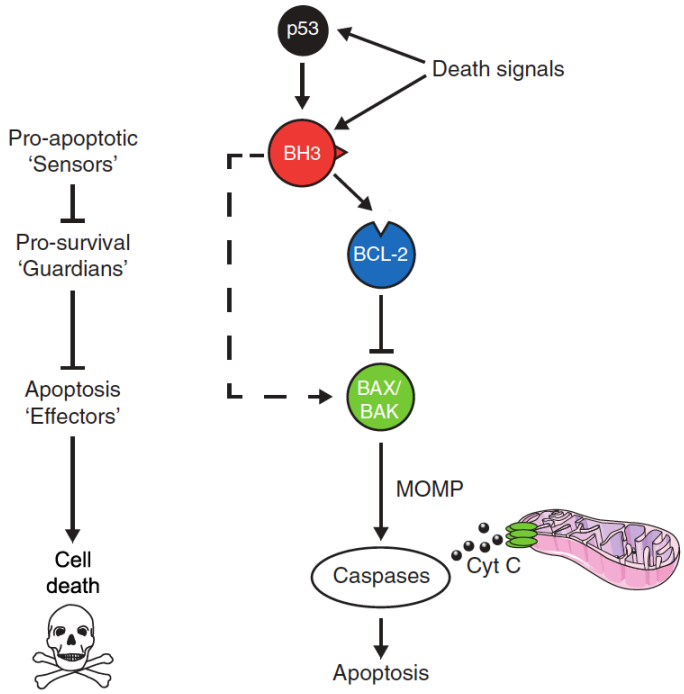

Figure 6. Bcl-2 family of apoptotic factors.

The anti-apoptotic factors can bind to pro-apoptotic sensors as well as to pro-apoptotic effectors, preventing their activation. The pro-apoptotic sensors are activated by different stress-activated pathways, including p53. Once activated, they favour the

activation of effectors both by directly interacting with them and by titrating away the anti-apoptotic factors. Pro-apoptotic effectors oligomerize, forming pores in the mitochondria, resulting in caspase activation and cell death. Adapted from Merino et al. 2016.

In normal conditions, pro-apoptotic sensors and effectors are inhibited by the direct interaction with anti-apoptotic factors; however, an excess of sensors, which is induced by stress stimuli through p53, fosters the activation of the apoptotic pathway by activating the apoptotic effectors This event is mediated both by the direct interaction of sensors and effectors and by the fact that sensors titrate out the inhibitors, leaving the effectors free to oligomerize and activate the programmed cell death (Merino et al. 2016).

The role of PcG proteins in apoptosis in not fully understood, but emerging evidences support a role for Polycomb complexes also in this biological process. The gene encoding for the mitochondrial apoptotic factor *Noxa* is a direct target of the PRC1 subunit BMI1 (Yamashita et al. 2008), while *Bim* is targeted by PRC2 complex (Wu, Zheng, et al. 2010). Interestingly, *Bim* was found up-regulated upon deletion of *Ring1B* in T lymphocytes, where it was responsible for their apoptosis-susceptible phenotype; the authors suggest a direct regulation of the gene by PRC1 since they found low but significant binding of Ring1B at its promoter by chromatin immunoprecipitation analysis (Suzuki et al. 2010). The anti-apoptotic function of PcG proteins is also mediated by the expression of miRNA, as shown in a recent work by Zhang and colleagues. Specifically, EZH2 suppresses the expression of miR-31 which, in turn, negatively regulates the stability of E2F transcription factor 6 (E2F6) transcript: as a result, the expression on the anti-apoptotic protein E2F6 is increased, hence conferring apoptosis resistance to cancer cells (Zhang et al. 2014).

Besides regulation of pro- and anti-apoptotic gene expression, both PRC1 and PRC2 repress the locus encoding for $p19^{INK4d}$ tumor suppressor, which induces p53-dependent apoptosis (Pomerantz et al. 1998; Zhang, Xiong, and Yarbrough 1998; Kamijo et al. 1998). Coherently with this observation, the inactivation of Bmi1 in ESCs is sufficient to block cell proliferation and to induce p53-dependent cell death (Park et al. 2003). Moreover, RING1A and RING1B were independently shown to interact directly with MDM2 and p53, favouring the MDM2-dependent and the RING-dependent ubiquitylation of p53, followed by its

degradation. Conversely, loss of either Ring1 proteins resulted in p53 stabilization and induction of apoptosis (Su et al. 2013; Wen et al. 2014; Shen et al. 2018).

Lastly, PRC1 represses the expression of *p21,* which is a master regulator of apoptosis. The main function of p21 is anti-apoptotic through transcriptional inhibition of E2F and Cyclin-D and -E genes, by encoding for factors that promote cell-cycle progression and apoptotic cell-death, or through direct inhibition of c-JUN that induces c-Myc expression (Soria and Gottifredi 2010; Wu, Zheng, and Yu 2009; Jung, Qian, and Chen 2010). However, it has also been shown that the interaction between p21 and NF-κB and STAT restricts some anti-apoptotic proteins, such as BCL-2 and BCL-X_L, thus favouring the apoptotic process.

2.2.5.3 DNA damage response

The DNA damage response (DDR) is a complex response triggered by cells upon sensing DNA damage, accounting for cell-cycle arrest and check-point activation, transduction of the damage signal and eventually assembly of the repair machinery. Resolution of the damage allows cell-cycle resumption, whereas failure to repair DNA damage leads to senescence or apoptosis. Upon single- or double-strand breaks (SSB and DSB, respectively), the site of damage is marked by different post-translational modifications, among which the first and most important one is the phosphorylation of serine-139 of histone H2A.X (γH2A.X) (Ciccia and Elledge 2010). Growing evidences implicates a role for PcG proteins as regulators of the DDR. The ubiquitylation of H2A was found to accumulate at sites of damage, together with RING1B, BMI1 and other subunits of the PRC1 complex that contributed also to the ubiquitylation of histone H2A.X (Chou et al. 2010; Gieni et al. 2011; Ginjala et al. 2011; Pan et al. 2011). It is still controversial whether the presence of PRC1-dependent histone mark is able to coordinate the DDR, for instance by fostering the recruitment of 53BP1. However, cells devoid of Bmi-1 displayed increased sensitivity to ionizing radiation, emphasizing the pivotal role of this PRC1 subunit in the DDR (Facchino et al. 2010; Ismail et al. 2010). Moreover, evidences sustain the involvement of RING1B/H2AK119ub1 in some DNA repair pathways, such as in nucleotide excision repair

(NER) and non-homologous end-joining (NHEJ) (Chitale and Richly 2017; Bartocci et al. 2014). The first observation about PRC2 involvement in DDR was reported by Zeidler and co-workers, who highlighted a decreased expression of the homologous-recombination protein RAD51 upon EZH2 over-expression with a subsequent increase of aneuploidy and cell death (Zeidler et al. 2005). Moreover, recruitment of PRC2 subunits was reported at DSBs, where they possibly participate in the NHEJ repair pathway (Hong et al. 2008; Rouleau et al. 2007). In addition, PRC2 and EZH2 colocalize with PCNA at the replication fork, and the PRC2-mediated H3K27me3 modification positively correlates with late replication of large DNA segments (Hansen et al. 2008; Sauvageau and Sauvageau 2010). Indeed, the removal of PRC2 subunits increases cell sensitivity to ionizing radiations (Caganova et al. 2013; Campbell et al. 2013).

2.2.6 Polycomb in stem cell self-renewal and cell fate determination

ESCs are endowed of two important features: on the one hand, they have the ability to self-renew, thereby guaranteeing the maintenance of an undifferentiated state, and, on the other hand, they undergo multilineage differentiation upon proper stimulation. Hence, ESC genome should be plastic, ensuring the expression of pluripotency-specific genes and, at the same time, able to quickly rewire the expression pattern in response to differentiation stimuli. This plasticity is largely achieved by epigenetic modulation, including the one ruled by PcG proteins. In ESCs, Polycomb complexes repress genes driving differentiation processes, like the Hox cluster gene and *Dlx*, *Fox*, *Pax*, *Sox* and *Wnt* genes; these loci are usually marked both by H3K27me3 and H2AK119ub1 at the pluripotent/multipotent stage, while the marks are progressively lost during ESC differentiation (Boyer et al. 2006; Lee et al. 2006; Ku et al. 2008). Recent observations, however, indicated that ESCs are able to maintain the pluripotency also in the absence of PcG proteins, while they fail to maintain the proper expression of lineage-specific genes in the absence of PRC1 or PRC2 (Boyer et al. 2006; Pasini et al. 2007; Chamberlain, Yee, and Magnuson 2008; Leeb et al. 2010; Leeb and Wutz 2007; Shen et al. 2008; van der Stoop et al. 2008). These notions conveyed the idea that PcG protein have a seminal role in the dynamics of gene expression regulation

during cell fate determination. Indeed, H3K27me3 and H2AK119ub1 were frequently found to co-localize with H3K4me3 modification in active chromatin domains, usually silent or minimally transcribed in pluripotent stem cells and expressed during differentiation. These bivalent genes, where the presence of PcG at promoters ensures the poised RNA pol II configuration, undergo epigenetic changes during cell-fate specification either by losing H3K27me3 and acquiring an active transcriptional status, or, vice versa, by losing H3K4me3 which leads to stable silencing (Mikkelsen et al. 2007; Pan et al. 2007). Deletion of PcG proteins in ESCs induces the aberrant activation of lineage commitment genes, which contribute to abnormal differentiation and, in some instances, to impaired proliferation (Bernstein et al. 2006; Roman-Trufero et al. 2009).

2.2.7 Polycomb control of early hematopoiesis

Hematopoietic stem cells (HSCs) are multipotent cells endowed with the ability to self-renew and differentiate into all blood cell types. Similar to ESCs, also HSCs carry bivalent domains at promoters of lineage-specific TFs, which are differentially modulated by epigenetic modifications during cell specification. The essential role of the Polycomb axis in hematopoiesis id underlined by several studies reporting hematologic dysfunctions in mouse PcG mutants (Cales et al. 2008; Su et al. 2003; van der Lugt et al. 1994). The first PcG protein showed to be important for HSCs was BMI1, a PCGF subunit of PRC1 complex, whose expression is elevated in stemness states, whereas decreased with cell differentiation. Indeed, depletion of Bmi1 causes severe post-natal anemia due to progressive HSCs exhaustion, despite unaltered fetal hematopoiesis (van der Lugt et al. 1994). Upon bone marrow transplant, Bmi1-deficient HSCs were not able to self-renew and to sustain long-term hematopoiesis. Consistent with this phenotype, $p16^{INK4a}$ and $p19^{INK4d}$ were consistently up-regulated, with a consequential cell-cycle arrest and p53-dependent apoptosis; genes associated with stemness, cell survival and encoding for TFs were also altered (Park et al. 2003). Moreover, cells derived from Bmi1-deficient animals showed impaired mitochondrial function, with subsequent increase of reactive oxygen species levels and sustained activation of the DDR pathway, suggesting a protective role for Bmi1 against

oxidative stress (Liu et al. 2009). In addition to loss of self-renewal ability, Bmi1$^{-/-}$ HSCs prematurely expressed genes of B-cell progenitors, such as *Ebf1* and *Pax5*, and displayed an accelerated lymphoid lineage specification (Oguro et al. 2010). Overall, BMI1 activity is crucial to sustain HSCs, by supporting their proliferation and protection from genotoxic damage, and by limiting lineage differentiation.

A role in HSCs maintenance was identified also for other PCGF subunits. Removal of Pcgf1 determines a mild expansion of progenitors *ex vivo* (van den Boom et al. 2013). Analogously to *Bmi1*, *Mel18* knock-out mice displayed severe immunodeficiency caused by impaired proliferation of lymphoid precursors upon Il-7 stimulation (Akasaka et al. 1997). Interestingly, subsequent studies reported increased proliferation of HSCs in Mel18-defiecent mice (Kajiume et al. 2004) or reduced proliferation of B cells in Mel18-overexpressing mice (Tetsu et al. 1998). Collectively, these discrepancies may underline different functions of *Mel18* depending on the stage of differentiation.

CBX subunits show distinct patterns of expression dependent on the specific stage of HSC differentiation. Indeed, the removal of the different subunits in HSCs is associated with diverse phenotypes. Over-expression of *Cbx7*, which is highly expressed in HSCs, enhances self-renewal ability and favours leukemia; conversely, the over-expression of *Cbx2*, *Cbx4* and *Cbx8* promotes the differentiation and the exhaustion of HSCs (Klauke et al. 2013).

The ncPRC1 subunit KDM2B is required for HSCs maintenance: the knock-out of this subunit in adults induces the reduction of both pools of HSCs and CLPs, in parallel with an accelerated differentiation towards myeloid lineage; vice versa, its over-expression promotes the expansion of progenitors (Andricovich et al. 2016; He, Nguyen, and Zhang 2011).

Selective inactivation of Ring1b in HSCs resulted in overall BM hypoplasia, with a concomitant enlargement of the fraction of immature linage-negative (Lin$^-$) cells, probably caused by the induction of cyclin D2. The hypoplastic phenotype is induced by the selective up-regulation of p16^{INK4a} with consequent cell-cycle arrest. Indeed, it is rescued by the concurrent inactivation of *Cdkn2a* locus (Cales et al. 2008). Recently, HSCs exhaustion

was reported upon ablation of *Mysm1*, a de-ubiquitylase of PRC1-dependent histone modification. The phenotype depends on the ability of MYSM1 to activate the commitment regulator *Ebf1* and the cell-cycle regulator *Gfi1* genes (Wang et al. 2013; Jiang et al. 2011). Comparing to PRC1, the role of PRC2 in hematopoiesis is mainly dependent on EZH protein family. EZH2 is present in all HSCs, whereas EZH1 starts to be expressed only in adults HSCs. Ezh2 loss-of-function studies revealed no alterations in HSCs homeostasis nor enhanced myeloid development. Instead, these studies highlighted that the loss of Ezh2 resulted primarily in impaired B- and T-cell development, as a result of inefficient VDJ recombination (Su et al. 2003). On the other hand, the enforced expression of EZH2 prevents HSCs exhaustion during serial transplantation. In contrast with this, loss of Eed or Suz12 PRC2 subunits enhances the proliferative capacity of HSCs (Majewski et al. 2008; Neff et al. 2012; Tanaka et al. 2012).

Overall, these observations show that removal of PcG activity affects HSCs homeostasis, with different, and sometimes opposing, outcomes depending on the stage of differentiation where PcG function is lost and the specific PcG component that is inactivated.

2.3 B cell development

B cell development is a step-wise tightly modulated process through which cells progressively differentiate from HSCs and acquire immunological competence. Research carried out over the past decades has dissected the main molecular events underlying B lineage specification, allowing now the accurate investigation of processes instructing each development step.

In the description of the numerous molecular events that drive B-cell development, I will give particular emphasis to the part that are related to my study.

2.3.1 Early B cell development

In human and mouse, early B cell development occurs in the bone marrow (BM) where HSCs reside. HSCs are multipotent cells that originate all the blood cell types by

progressively restricting their developmental potential upon stimulation with diverse differentiating factors (Figure 7).

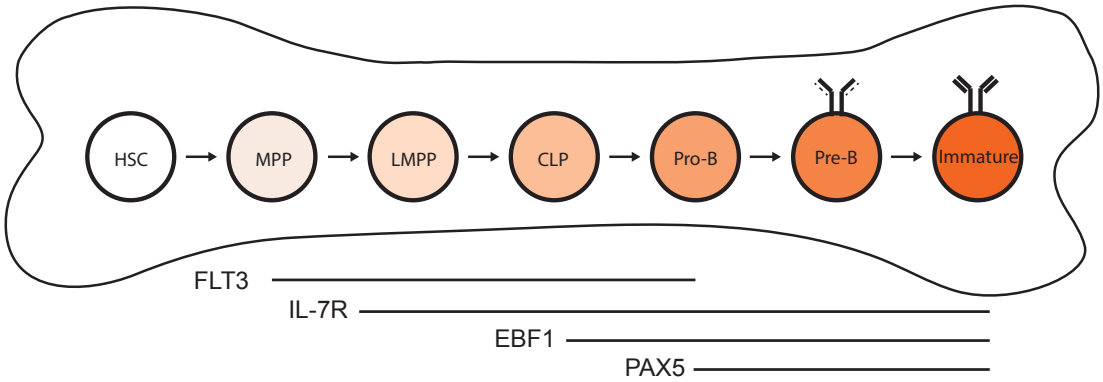

Figure 7. Early B-cell development in the bone marrow.

Schematic representation of early B-cell developmental steps, from HSC to immature B cells. Bars shown below the scheme represent the expression of the main TFs driving B-cell differentiation. HSC = hematopoietic stem cell; MPP = multipotent progenitor; LMPP = lymphoid multipotent progenitor; CLP = common lymphoid progenitor.

The first step toward differentiation is the transition from HSCs to multipotent progenitors (MMP), that lose the self-renewal potential. MMPs can be of two types: lymphoid-lineage MMPs or erythroid-cell MMPs (Kondo, Weissman, and Akashi 1997; Akashi et al. 2000). A specific feature of lymphoid MMPs is the expression of FMS-related tyrosine kinase 3 (FLT3), driven by Ikaros and PU.1 TFs (Adolfsson et al. 2001; Adolfsson et al. 2005; Yoshida et al. 2006). In response to Flt-3 ligand and IL-7 stimulation, MMPs start expressing early B cell factor 1 (EBF1) and the TF E2A, which definitely mark the entry into the common lymphoid progenitor (CLP) pool (Medina et al. 2004; Nutt and Kee 2007). Upon further stimulation of IL-7 receptor (IL-7R), CLPs up-regulate Paired box protein 5 (Pax5) also known as B-cell specific activator proteins (BSAP), a master regulator of B-cell development that drives the differentiation towards the B-cell lineage (Hagman and Lukin 2006; Cobaleda et al. 2007; Medvedovic et al. 2011). The expression of Pax5 fosters the differentiation to early B cell progenitors, mainly by repressing genes associated to multipotency as *Flt3* (Holmes et al. 2006). The progression through further stages of development, like pro-B cells and pre-B cells, is accompanied by the rearrangement of the immunoglobulin (Ig)

locus. Indeed, the ability of lymphocytes to exert their function relies on the recognition of pathogens, mediated by the mature immunoglobulin receptor on the surface of B and T lymphocytes, called B-cell and T-cell receptor (BCR and TCR, respectively). The BCR consists of two identical Ig heavy (H) and light (L) chains, assembled together by disulfide-bonds. Each receptor is composed by a variable region, responsible for the recognition of pathogenic antigens, and by a constant region which mediates the effector functions of the receptor. The constant region can exist in two different conformations. In early stages of development, Ig H retains a transmembrane and a cytoplasmic domain, which anchors the receptor to the membrane and triggers a signalling cascade downstream the receptor. In this case the Ig molecule is also called BCR. Otherwise, upon activation of B cells, alternative transcriptional events exclude the trans-membrane domains from the Ig H transcript, thus favouring the secretion of the entire molecule, usually named secreted immunoglobulin or antibody.

The variable region of Ig is assembled during the early stages of B cell development through a gene rearrangement process called V(D)J recombination, whereby starting from an array of different variable (V), diversity (D) and joining (J) gene segments, single V, D and J are joint together in the Ig H locus. This process takes place also in the IgL locus but involves only V and J gene segments (Tonegawa 1983). VDJ recombination process is initiated by the Recombination Activating Genes 1 and 2 (RAG1 and RAG2), which bind to and cleave DNA at specific recombination sequences (Recombination Sequence Signals – RSSs) flanking V, D and J gene segments (Eastman, Leu, and Schatz 1996; McBlane et al. 1995; Melek, Gellert, and van Gent 1998; van Gent et al. 1995). Upon RAG-dependent cleavage, DNA ends are brought in close proximity and are ultimately joined by the components of classical NHEJ repair pathway (Difilippantonio et al. 2000; Li et al. 1995). IgH chain is rearranged in the transition from pro-B cells to pre-B cells. Successful rearrangements lead to the expression on the surface of pre-BCR, whereby the heavy chain is combined with a surrogate IgL chain. This receptor is functional and the signalling, among other functions, inhibits further rearrangement of the IgH chain, process called allelic exclusion (Li et al. 2018). Following clonal expansion, pro-B cells stop dividing and rearrange the IgL chain

genes. Once the L chain has been successfully synthesized, it is paired with IgH to form a functional BCR expressed on the surface of B cells. This molecular change marks the transition from pre-B cells to immature B cells. Immature B cells are highly sensitive to antigen binding to BCR: if they autoreact to antigens present in the BM, they quickly undergo cell death. Hence, only the non-autoreactive immature B cells egress from the BM and migrate to secondary lymphoid organs (SLOs) to complete their maturation (Rajewsky 1996).

2.3.1.1 Immature B cells

Immature, or transitional, B cells that escaped from cell death in the BM migrate to SLOs (Allman, Ferguson, and Cancro 1992; Allman et al. 1993). Here, the vast majority of them die within few days, while a small fraction gives rise to the mature B cells subsets (Allman et al. 1993). Feature of immature B cells is the expression of the early differentiation surface markers CD24/HSA and CD93/AA4.1. However, while the former marker can also be expressed by activated B cells and marginal zone B cells, AA4.1 is specific for the immature population. Moreover, transitional B cells are divided in two subpopulations according to the expression of additional surface markers. T1 B cells are defined as $CD23^{-}$ $CD21/35^{lo}$ IgM^{+} IgD^{-} while T2 B cells, the precursors of the long-lived mature B cell pool, acquire the expression of CD23, CD21/35 and IgD (Loder et al. 1999; Allman et al. 2001). An additional subset named T3 B cells, differing from the T2 population only for the expression of IgM, has been identified but its function in B cell development is still unclear (Allman et al. 2001). Besides surface marker expression, T1 and T2 immature B cells show diverse localizations and BCR reactivity. Indeed, within the spleen, T1 localize outside of the follicle, in the outer area of the periarteriolar lymphoid sheath, whereas T2 are embedded in the follicles with mature B cells (Loder et al. 1999; Liu 1997). Additionally, T1 cells retain the sensitivity to negative selection upon BCR activation, like immature B cells in BM; on the contrary, upon BCR engagement T2 cells are able to proliferate and to up-regulate pro-survival molecules like cyclin D2, $Bcl\text{-}_{XL}$ and A1 which favour their survival (Su and Rawlings 2002; Petro et al. 2002). The difference between the two cell subsets probably relies on the acquired

sensitivity of T2 to T-helper stimulation (Chung, Silverman, and Monroe 2003). The antigen-driven activation of BCR together with T-helper derived-signals seem to be the driving force for differentiation of T2 cells into mature B cells. However, it was also highlighted that the signalling from the B-cell activating factor (BAFF) receptor is crucial for T1 to T2 and T2 to mature B cell progression. *In vivo* studies with Bromodeoxyuridine (BrdU) labeling by Allman and colleagues showed a rapid turnover of transitional B cells, including T2 cells, in contrast to the one of the mature B cell compartments. These observations reflect the shorter lifespan of transitional B cells (1-4 days) compared to the one of long-lived mature B cells (80-120 days) (Allman et al. 1993).

2.3.2 Peripheral B cell development

In the mouse, mature B cells are divided in three main subsets, which are phenotypically and functionally different: Follicular B cells (FO), Marginal Zone B cells (MZ) and B-1 B cells (Figure 8).

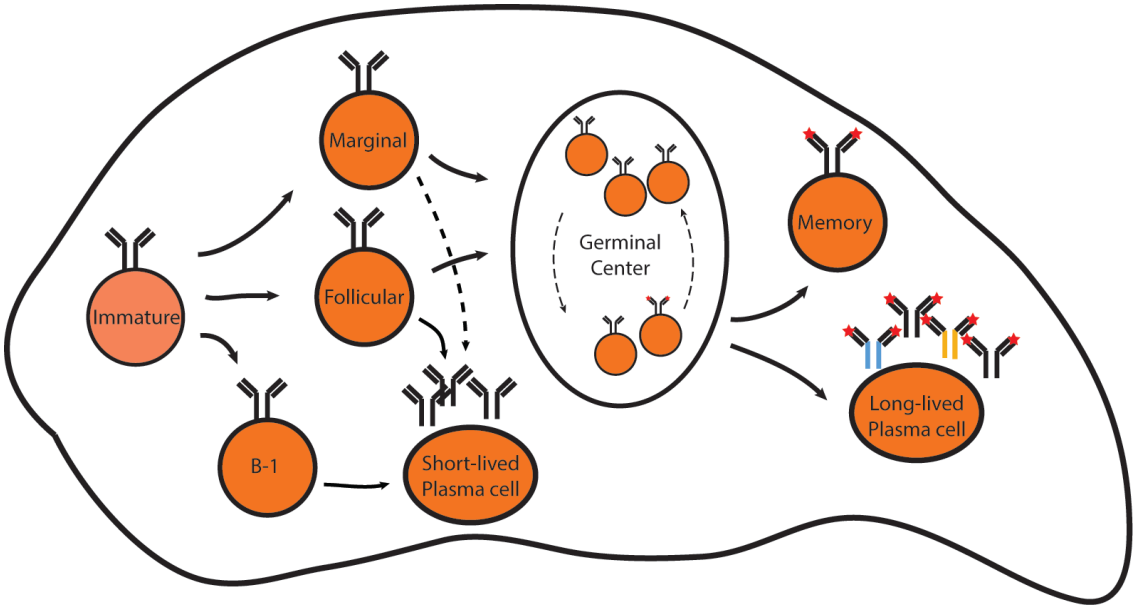

Figure 8. Peripheral B-cell development in the spleen.

Schematic representation of peripheral B-cell developmental steps, from immature to the three main mature B cell subpopulations, namely B-2 Follicular, Marginal zone and B-1 B cells. Upon antigen encountering, mature B cells are recruited in the germinal center reaction, which ultimately leads to the production of memory B cells and high-affinity antibody secreting plasma cells. Mature B cells can also differentiate directly into short-lived plasma cells without undergoing the germinal center reaction.

2.3.2.1 Follicular B cells

Follicular B cells, also called B-2 B cells, are the most abundant subset of mature B cells in SLOs. Phenotypically, they are identified as $CD23^{+}$ $CD21^{lo}$ IgM^{+} IgD^{+}. FO B cells derive directly from T2 transitional cells: once they maturate in SLOs, they localize in the follicles of spleen, Peyer's patches and lymph nodes where they may present antigens to activated T cells; otherwise, relying on their recirculating capacity, FO B cells also home to the BM, where they preferentially localize around vascular sinusoids (Cariappa et al. 2007). FO B cells are the main mediators of the T cell-dependent immune responses to protein antigens, although they can also participate to T cell-independent responses (Allman and Pillai 2008; Casola 2007).

2.3.2.2 Marginal zone B cells

MZ B cells are identified as $CD23^{lo}$ $CD21^{hi}$ IgM^{+} IgD^{-} and they are also positive for the markers CD38 and CD1d. Loder and collaborators proposed that MZ B cells derive from a MZ precursor ($CD23^{+}$ $CD21^{hi}$ $CD1d^{hi}$ IgM^{+} IgD^{+}), which in turn is derived from T2 transitional cells (Loder et al. 1999; Pillai and Cariappa 2009). Investigations in conditional Rag-2 knock-out mice at specific times after birth suggested that MZ B cells persist longer than FO B cells in the spleen of mice with a block in BM influx (Hao and Rajewsky 2001). However, later observations clarified that MZ cells are more sensitive to radiation and to cyclophosphamide, indicating that their homeostasis is founded on either self-renewal or on the presence of proliferating precursors (Kumararatne, Gagnon, and Smart 1980).

In the mouse, MZ B cells are sessile, residing in the marginal sinus of the spleen, where they are retained by the activity of two sphingosine-1-phosphate receptors, S1PR1 and S1PR3 (Cinamon et al. 2004; Vora et al. 2005; Cinamon et al. 2008). MZ B cells are mainly involved in T-cell independent immune responses and represent the first line defense against blood-borne pathogens: upon sensing foreign antigens through the BCR, they migrate out of the MZ in the red pulp where they rapidly proliferate and differentiate into short-lived plasma cells (Martin and Kearney 2002). Evidences argue that MZ cells can also mediate the transport of antigens in the form of immune complexes to FO B cells residing

in the nearby follicle, thus contributing also to T-cell dependent responses, as well as in responses to lipid antigens (Allman and Pillai 2008; Attanavanich and Kearney 2004; Song and Cerny 2003).

2.3.2.2.1 Mechanisms sustaining the B cells cellular entry and retention in the marginal zone

Homing of transitional cells to the spleen is mainly guided by selectin and integrin molecules which mediate the interaction between lymphocytes and endothelial cells. Once bound to the endothelial cells, the specific interaction between the lymphocytic integrins LFA-1 and $\alpha 4\beta 1$ and their ligands ICAM-1 and VCAM-1 expressed by stromal cells in the spleen allows the entry of lymphocytes into the white pulp (Lo, Lu, and Cyster 2003). Here, cells are exposed to two opposite chemokine gradients which drive the migration of B cells to either the follicular or to the marginal zone. Chemokine (C-X-C motif) ligand 13 (CXCL13), released by follicular dendritic cells (FDCs), is sensed by B cells through the C-X-C chemokine receptor type 5 (CXCR5), thus mediating the proper formation of B cell follicles (Forster et al. 1996; Reif et al. 2002). Conversely, S1P, a sphingolipid highly concentrated in the blood, attracts cells outside the follicle towards the marginal sinus. This signalling lipid is sensed through S1PR1 and S1PR3, which are expressed at higher levels by MZ B cells than by FO B cells. Indeed, knock-out of S1PR1 or S1P in mice, as well as their treatment with inhibitor of the receptor (FTY720), induced mislocalization of MZ B cells into follicles. Notably, this phenotype is rescued by the concurrent inactivation of CXCR13 (Cinamon et al. 2004; Cinamon et al. 2008).

S1PR1 is a G-protein coupled receptor molecule which activates a signalling cascade upon interaction with S1P ligand. Among other processes, this cascade includes a feedback regulatory loop mediated by the G-protein coupled receptor kinase-2 (GRK2), which phosphorylates the C-terminal domain of S1PR1 and subsequently induces receptor internalization and proteasomal-mediated degradation (Oo et al. 2007; Watterson et al. 2002; Arnon et al. 2011). In the absence of S1P, the desensitization effect is naturally lost and the receptor re-expressed on the surface. These findings led to the proposal of a model

whereby in the spleen MZ B cells first migrate to the MZ area attracted by S1P molecule; here, the progressive S1P-dependent desensitization of S1PR1 favours the migration towards the follicle driven by the CXCL13-CXCR5 interaction. Low S1P amount in the follicular environment induces resensitization of S1PR1 which, in turn, guides B cells back to the MZ area (Arnon and Cyster 2014). The continual migratory movement of MZ B cells in follicles is named MZ shuttling and it is believed to be at the base of MZ B cell participation to T-cell dependent immune responses (Cinamon et al. 2008).

Despite the antagonistic CXCL13 and S1P gradients, other molecules contribute to B cell retention into the MZ, including integrins. Deletion of signalling molecules involved in the integrin signalling in mice is associated to the lack of MZ (Girkontaite et al. 2001; Guinamard et al. 2000; Fukui et al. 2001; Sanui et al. 2003; Croker et al. 2002). Interestingly, in these cases the MZ subset is completely absent in the spleen of the mouse, and it is not mislocalized as reported for the S1PR1 knock-out mouse, suggesting that integrin signalling sustains the formation of MZ B cells, additionally to their localization.

2.3.2.3 B-1 B cells

In the mouse, B-1 B cells, identified as $CD23^{lo}$ $CD19^{hi}$ $B220^{lo}$ IgM^{+} IgD^{-}, reside in the peritoneal and pleural cavities and at mucosal sites. Moreover, they can home from the peritoneum to mesenteric lymph nodes and to the intestinal lamina propria; although the mechanisms which drive their migration are still under investigation, a role for S1PR1 has been suggested (Kunisawa et al. 2007). As MZ B cells, B-1 B cells are mainly involved in T-cell independent immune responses against antigens that reside in the cavities or mucosal sites. In the peritoneal cavity (PCa), B-1 B respond to bacterial antigens to rapidly differentiating into short-lived IgM-secreting PCs, whereas in the intestinal mucosa they mainly contribute to IgA immune responses (Alugupalli et al. 2004; Fagarasan and Honjo 2003; Hardy 2006). Based on surface marker expression of CD5, B-1 B cells are categorized in B-1a ($CD5^{+}$) and B-1b ($CD5^{-}$) B cell subsets (Stall et al. 1992). B-1a B cells predominantly originate from fetal liver progenitors, while B-1b derive from BM progenitors (Baumgarth 2017). Despite their different origin, B-1a and B-1b reside in the PCa together

with a small fraction of B-2 cells (Hastings et al. 2006; Berberich, Forster, and Pabst 2007). Moreover, while B-1a contribute to innate-like immune responses, B-1b participate to adaptive immunity, possibly representing a special type of IgM memory B cells derived from B-2 B cells in a T-cell independent fashion (Alugupalli et al. 2004; Haas et al. 2005).

2.3.2.4 Molecular determinants controlling peripheral B cell homeostasis

2.3.2.4.1 BAFF

The B-cell activating factor (BAFF) represents one of the most important molecules that sustain peripheral B cell survival. There are two BAFF family ligands, the B-cell activating factor belonging to TNF family (BAFF also called BLyS) and the apoptosis-inducing ligand (APRIL). BAFF ligands are mainly expressed by mononucleated cells of the blood, whereas in the spleen and lymph nodes they are produced by diverse cell types, including FDCs, monocytes and macrophages. BAFF ligands are produced as homotrimeric transmembrane proteins which are proteolytically cleaved to produce trimeric soluble cytokines. BAFF soluble molecules are sensed by three main receptors, namely BAFF receptor (BAFF-R), B-cell maturation antigen (BCMA) and transmembrane activator and CAML interactor (TACI) (Mackay and Ambrose 2003). BAFF receptors are expressed on the surface of B lymphocytes (Bossen and Schneider 2006; Li et al. 2008), activated and regulatory T cells (Mackay and Leung 2006), monocytes and dendritic cells (Chang et al. 2006; Chang, Mihalcik, and Jelinek 2008). In B cells, BAFF-R is dispensable for the maintenance of T1 transitional cells, while it is crucial for the generation of T2 cells and for the maintenance of FO and MZ mature B cell subsets (Schiemann et al. 2001; Schneider et al. 2001; Thompson et al. 2001). Conversely, it is not required for B-1 B cell persistence (Crowley et al. 2008; Scholz et al. 2008).

Stimulation of BAFF-R in B cells potently activates the alternative or non-canonical NF-κB pathway and, to a minor extent, the classical NF-κB pathway, whereas TACI mainly sustains the latter one. Both pathways are crucial for B cell survival but it was showed that B cells can be sustained by the activation of BAFF-R alone (Mackay and Leung 2006). In the alternative NF-κB pathway, engagement of BAFF-R activates the NF-κB-inducing

kinases Nik and Ikk which lead to the phosphorylation-dependent cleavage of p100 and the subsequent release of p52, that dimerizes with RelB and translocates into the nucleus (Siebenlist, Brown, and Claudio 2005). RelB/p52 is a transcription factor targeting genes of the Bcl-2 family (*Bcl-$_{XL}$* and *A1*), and genes encoding for cytokines and other ligands (*Il-8*, *Cd40/Cd154*) (Fu et al. 2009).

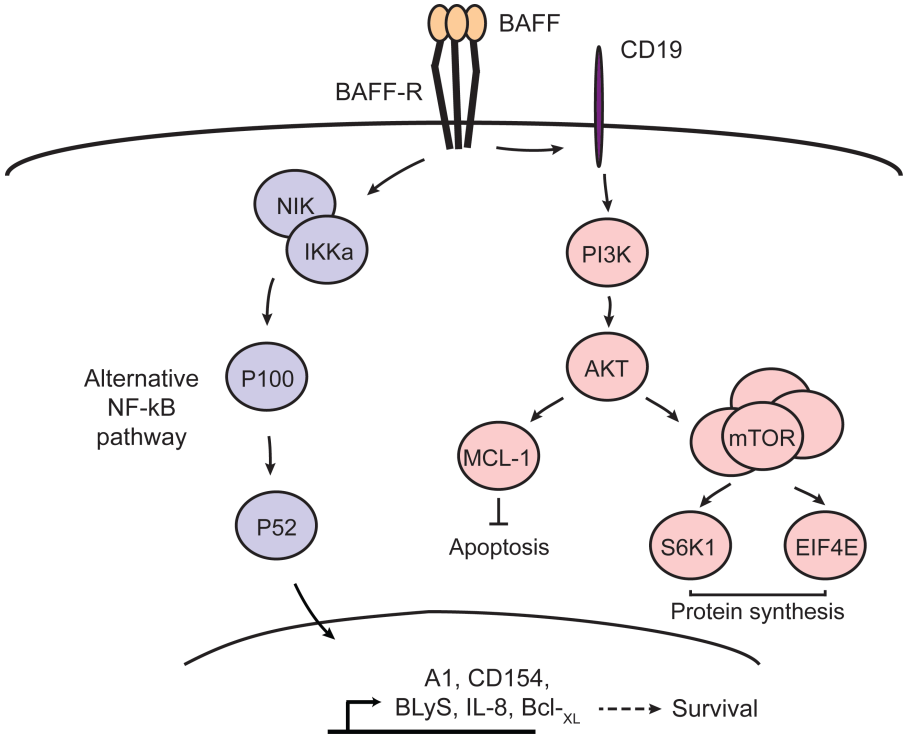

Figure 9. Signalling pathways activated by BAFF receptor.

BAFF receptor activates the alternative NF-κB pathway, which leads to the transcription of pro-survival genes. At the same time, BAFF-R triggers the CD19-PI3K-AKT pathway that promotes cell survival and protein synthesis.

Besides increasing the expression of anti-apoptotic proteins, BAFF-R signalling promotes B cell survival through the activation of the protein kinase mammalian target of rapamycin complex 1 (mTORC1) (Patke et al. 2006; Woodland et al. 2008). The activation of this complex relies on the ability of BAFF-R signalling to cross-talk with BCR signalling, through the activation of CD19 receptor (Jellusova et al. 2013) (see Paragraph 2.3.2.4.2 for BCR signalling). mTORC1 activates S6 kinase 1 (S6K1) and the eukaryotic initiation factor 4E (EIF4E), which promote mRNA translation and protein synthesis (Patke et al. 2006). Furthermore, the activation of BAFF-R through BCR signalling leads to the positive

transcription and protein stabilization of the anti-apoptotic factor MCL-1, which counteracts BIM at the protein level (Wang et al. 1999; Maurer et al. 2006), and prevents the nuclear translocation of the apoptotic inducer protein kinase Cδ (Woodland, Schmidt, and Thompson 2006). In summary, the BAFF-R activation sustains B cell survival by promoting an anti-apoptotic response and, simultaneously, by favouring protein synthesis (Figure 9).

2.3.2.4.2 BCR

Continuous signalling through the BCR is critical for the survival of peripheral B cells. Indeed, acute ablation of BCR signalling components results in the rapid disappearance of the mature B cell subsets (Kraus et al. 2004; Lam, Kuhn, and Rajewsky 1997). Additionally, various evidences indicated that the strength of BCR signalling is important for mature B cell-fate determination (Casola 2007). Cells receiving strong signalling through BCR are thought to differentiate towards the B-1 B cell compartment, modest signalling favours the development of MZ B cells whereas basal signalling allows the differentiation to FO B cells (Casola et al. 2004; Wen et al. 2005).

The BCR expressed on the surface of B lymphocytes is composed by immunoglobulins (IgH and IgL) associated with the Igα (CD79a)/Igβ (CD79b) heterodimer. After BCR stimulation, the ITAM (immunoreceptor tyrosine-based activation motif) domains within the cytoplasmic portion of both Igα and Igβ are phosphorylated by protein tyrosine kinases (PTKs) such as LYN, SYK and BTK, which are recruited at the site of activated BCR. The phosphorylation of ITAMs activates different signalling cascades, including the PI3K (phosphoinositide 3-kinase) and PLCγ2 (phospholipase γ-2) pathways (Figure 10).

PI3K is activated by BCR signalling though CD19 and BCAP (Rickert, Rajewsky, and Roes 1995; Okada et al. 2000). Active PI3K phosphorylates AKT at Threonin-508 (Y508), partially activating the protein, whereas the full activation is assured by phosphorylation at Serine-473 by PDK2 (phosphoinositide-dependent protein kinase-2). AKT is a serine/threonine kinase with multiple targets. For instance, by phosphorylation, AKT activates mTORC1 (Patke et al. 2006; Woodland et al. 2008) and inhibits p27 (Shin et al. 2002), GSK3β (Cross

et al. 1995) and the TF FOXO1, by sequestering the protein to the cytoplasm (Matsuzaki et al. 2003).

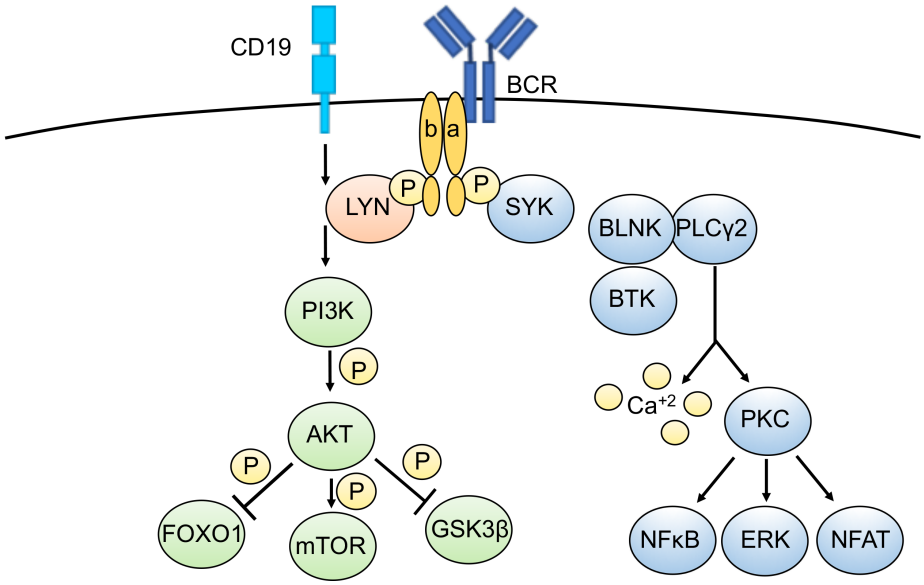

Figure 10. Signalling pathways activated by BCR.

BCR mainly activates two different signalling pathways: 1) the PI3K-AKT pathway and 2) the PLCγ2 pathway which leads to the release of intracellular Ca^{++} and the activation of the Ca^{++}-dependent enzyme PKC.

PLCγ2 is activated by the SYK-dependent phosphorylation of BLNK, a modification that allows BLNK to interact with PLCγ2, SYK and BTK. Once brought in close proximity, SYK and BTK phosphorylate PLCγ2, which starts to produce diacylglycerol (DG) and phosphatidylinositol-4,5-bisphospate (PIP_2). The latter are small soluble molecules that function as second messengers in the cell (Kurosaki 2011). Specifically, they induce the release of Ca^{++} stored in the endoplasmic reticulum, event that can differentially impact on diverse pathways in B cells, like the NFAT (Nuclear factor of activated T cells) and the NF-κB pathways (Dolmetsch et al. 1997; Healy et al. 1997).

2.3.2.4.2.1 CD45 receptor: structure, alternative splicing and regulation of BCR signalling

CD45R, encoded by *Ptprc* gene encompassing 33 exons, is one of the most abundant cell surface protein in all nucleated hematopoietic cells, with increasing levels with cellular maturation (Thomas and Lefrancois 1988; Hermiston, Xu, and Weiss 2003). CD45R is a glycoprotein containing a large extracellular domain, a single transmembrane domain and

an intracellular part containing protein tyrosine phosphatase (PTP) domains. The extracellular domain can exist as multiple isoforms depending on the alternative splicing of three exons (exon 4, 5 and 6, usually named as A, B and C, respectively). Despite poor homology of the sequence (~ 35%), the ABC splicing system is conserved through multiple species, suggesting functional importance *in vivo* (Thomas 1989; Hermiston, Xu, and Weiss 2003). Interestingly, the pattern of CD45R isoform expression on different hematopoietic cells is highly conserved, pointing to a physiological relevancy of the different isoforms (Hermiston, Xu, and Weiss 2003; Thomas and Lefrancois 1988). ABC exons contains multiple sites for O-liked glycosylation, whereas the remaining portion of the extracellular domain is endowed with sites for N-linked glycosylation; both modifications can dramatically influence size and charge of the surface protein. In T cells, diverse evidences support the hypothesis that differential extracellular glycosylation may influence the interaction of CD45R with lectins and their subsequent organization in microdomains, possibly altering their function as PTP or their interaction with substrates (Earl and Baum 2008; Hernandez et al. 2007; van Vliet et al. 2006; Chen, Chen, and Demetriou 2007). Alternative splicing of exons A, B and C potentially originates 8 different protein isoforms, named according to the retained exons. Myeloid cells usually express the shortest R-O isoform (lacking all exons 4, 5 and 6) until, upon activation, they switch to R-A; naïve T cells primarily express the isoforms containing exon B, and they switch to the R-O upon activation. Resting B cells are characterized by the expression of the longest CD45-ABC isoform, also named B220, the pan-B cell marker, because of its molecular weight of 220 kDa (Figure 11A). Similarly to T cells, upon activation, they switch the expression to R-O.

The mechanisms behind the isoform expression regulation are only partially understood. In 2008, two research groups discovered that the heterogenous ribonucleoprotein hnRNPLL is a key regulator of the alternative splicing of *Ptprc* transcript: the over-expression of this protein facilitates the switching from the CD45R-ABC to shorter isoforms, whereas its inhibition prevents normal expression of CD45R-O in activated T cells (Oberdoerffer et al. 2008; Topp et al. 2008). Later, this notion was further confirmed in T and in B cells by other groups (Yabas et al. 2011; Cho et al. 2014; Chang, Li, and Rao 2015). In particular,

hnRNPLL was identified as a master regulator of splicing in plasma cells, critical for tuning the transcriptome of terminally differentiated B cells (Chang, Li, and Rao 2015). By RNA immunoprecipitation assays, hnRNPLL was shown to bind to CA repeats at the beginning of exon 4 and 6 of *Ptprc* transcript, fostering their exclusion in the splicing process (Preussner et al. 2012). In contrast, the exclusion of exon 5 is less dependent on hnRNPLL, but it is regulated by the mutually exclusive DNA-methylation and CTCF binding to this exon. In particular, binding of CTCF to DNA slows down the processivity of RNA pol II and splicing machinery, which favour the inclusion of the exon in the transcript. Conversely, the presence of DNA methylation in the exon sequence prevents the binding of CTCF, thus allowing exon exclusion (Shukla et al. 2011) (Figure 11B).

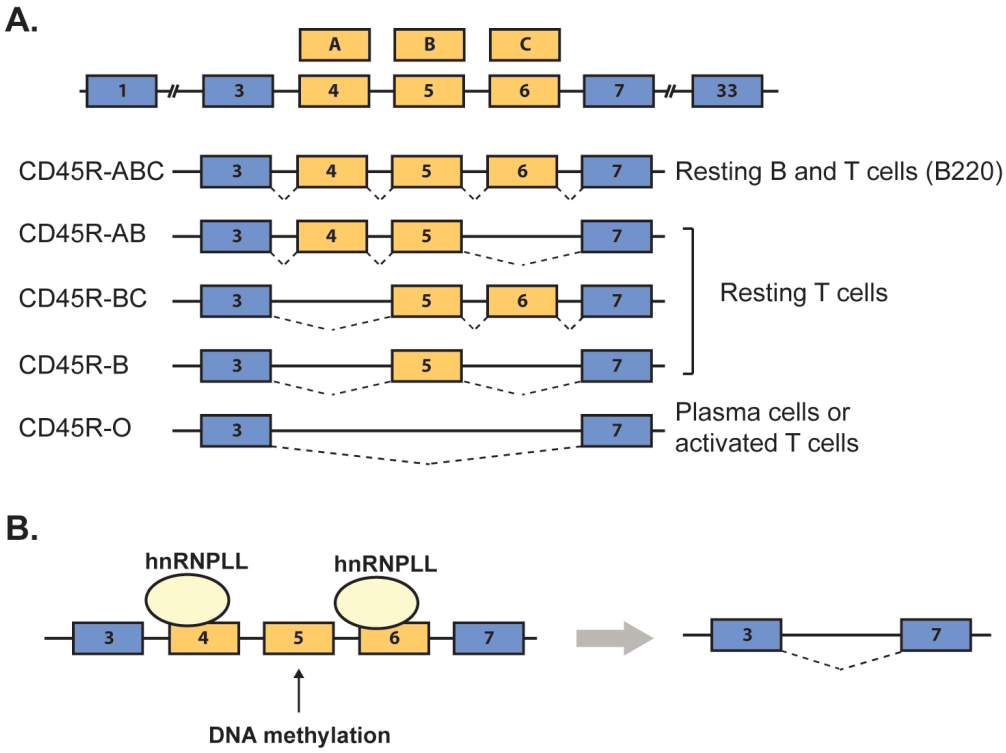

Figure 11. CD45R structure, expression and alternative splicing regulation.

A. CD45R exon composition and isoform expression among B and T cells. **B.** Regulation of Ptprc/CD45R alternative splicing by hnRNPLL and DNA methylation. Re-adapted from Chang et al. 2015.

CD45R intracellular domain is highly conserved in mammals and composed by two phosphatase domains, D1 and D2. Both domains are required for optimal phosphatase function *in vivo*, although only D1 owns the catalytic activity. Crystal structure analyses indicated that the dimerization of the cytoplasmic portion of CD45R could inhibit the

phosphatase activity, providing a further level of regulation (Bilwes et al. 1996; Majeti et al. 1998).

CD45R is one of the most critical phosphatases of PTKs belonging to the Src family (Src family kinases – SFKs) in hematopoietic cells. SFKs are localized nearby the cytoplasmic membrane, where they directly influence the activation of different receptor signalling, such as Fc receptors, growth factor receptors, immunoglobulin receptors, integrin and cytokine receptors (Lowell 2004). SFKs exist in an “open” and “closed” conformations, based on the phosphorylation of a highly conserved tyrosine residue situated in the C-terminal tail (Lowell 2004; Palacios and Weiss 2004). The presence of the phospho-group on this residue favours the interaction between the C-term domain with the SH2 domain of the protein, leading to the “closed” conformation whereby the access to the substrate-binding site is blocked. Conversely, the absence of the phospho-group guarantees the “open”, yet not “active”, conformation whit an accessible catalytic site. The “active” conformation, with full kinase activity, is achieved by SFK-dependent transphosphorylation of another tyrosine residue located in the activation loop of the catalytic domain (Hermiston, Zikherman, and Zhu 2009). Hence, the activation of SFKs relies on a fine equilibrium between phosphorylation and dephosphorylation of their regulatory residues. In B cells, CD45R together with CD148, mainly dephosphorylates the C-terminal inhibitory tyrosine of SFKs, thus favouring the “open” conformation (Shrivastava et al. 2004; Katagiri et al. 1999).

In B cells, the main SFKs are LYN, FYN and BLK. Of these, LYN has the unique role as positive and negative regulator of BCR signalling. The positive effect is mediated by the phosphorylation of the ITAM motifs of the Igα /Igβ heterodimer, which result in the recruitment of SYK and the subsequent signalling cascade. Conversely, the negative effect relies on the phosphorylation of the ITIMs domains (immunoreceptor tyrosine-based inhibition motifs) of BCR. This modification recruits inhibitory molecules such as the phosphatases Src homology 2 (SH2) domain-containing phosphatase 1 (SHP-1) and SH2 containing 5’-inositol phosphatase 1 (SHIP-1), that down-regulate the BCR response. While the positive effect on BCR is redundant with FYN and BLK activities, activation of inhibitory feedback loop upon BCR stimulation effect is unique of LYN. Probably due to its dual

function on BCR signalling, loss or constitutive activation of LYN in mice results in autoimmunity (Chan, Lowell, and DeFranco 1998; Hibbs et al. 1995; Hibbs et al. 2002).

2.3.2.5 Transcriptional control of B cell identity and peripheral B cell subset differentiation

2.3.2.5.1 PAX5

PAX5 is a transcription factor crucial for B cell development and B-cell identity maintenance. Pax5 belongs to the Pax family of TFs, accounting for nine members, but is the only one expressed in hematopoietic cells. PAX5 can act both as transcriptional activator and transcriptional repressor, depending on the interacting partners and/or recruitment of epigenetic modifiers, including chromatin-remodelling and histone-modifying complexes (McManus et al. 2011). PAX5 expression begins at the pro-B stage of development where, together with E2A and EBF1, guarantees the activation of transcriptional programs which sustain the B-cell lineage commitment (Medvedovic et al. 2011). Indeed, the deletion of any of these TFs causes the block of B cell development at early stages (Busslinger 2004). Despite restricting the developmental options of lymphoid progenitors, PAX5 maintains B cell identity by activating B cell specific genes and by repressing lineage-inappropriate genes (Cobaleda et al. 2007). PAX5 sustains the expression of many genes contributing to the BCR and co-stimulatory receptors, like *Cd79a*, *Cd19*, *Cd72* and *Cd21*, or involved in BCR signalling cascade, such as *Blnk* (Nutt et al. 1998; Kozmik et al. 1992; Horcher, Souabni, and Busslinger 2001; Ying et al. 1998; Schebesta, Pfeffer, and Busslinger 2002). Moreover, PAX5 induces the expression of TFs that sustain B cell identity, namely *Irf4*, *Irf8*, *Bach2*, *Aiolos* and *Spib* (Pridans et al. 2008; Schebesta et al. 2007). PAX5 is also crucial for Ig V-DJ rearrangement, by mediating a contraction of the Ig locus and subsequent looping (Fuxa et al. 2004; Sayegh et al. 2005), probably though the recruitment of PRC2 (Su et al. 2003). Among PAX5-repressed genes, different studies identified myeloid and T cell lineage-specification genes (e.g. Csf1r and Notch1), surface receptors and signalling molecules of progenitors and other lineages (Flt3, Sca1, Ramp1, Lilrb4) and adhesion molecules involved in migration (Ccl3, Ccl5, Itgal, Cd47) (Cobaleda et al. 2007).

Furthermore, Pax5 prevents the expression of genes involved in the plasma cell differentiation program, indeed it is repressed during terminal plasma cell differentiation (Adams et al. 1992).

2.3.2.5.2 NOTCH2

Whereas Notch1 is crucial for driving T-cell commitment at the expenses of B cells, Notch2 pathway plays an important role in the development of the MZ mature B cell subset in the spleen (Saito et al. 2003; Pillai and Cariappa 2009). Among the four Notch receptor molecules, Notch2 is expressed on mature B cells. Notch ligands are integral membrane proteins expressed by a variety of cells; they are divided in two families according to their structure, the Delta-like (DLL) family including DLL-1, -3 and -4 and the Jagged (JAG) family including JAG-1 and -2 (Radtke et al. 2004). In the spleen, DLL-1 and JAG-1 are the main Notch ligands, produced by FDCs (Yoon et al. 2009). Upon interaction with a ligand, the intracellular domain of Notch is released by proteolytic cut and translocated into the nucleus where it forms a ternary complex with RBP-J and Mastermind. The trimer constitutes an active transcription factor, targeting Notch genes (e.g. *Deltex1*, *Hes1*) for expression (Saito et al. 2003; Shimizu et al. 2000; Tan-Pertel et al. 2000). Besides the positive effect on transcription, recent work from Strobl's group pointed to a repressive transcriptional activity of Notch pathway towards some genes (e.g. *Klf2*, *Itgb7*) in resting B cells (Strobl et al., personal communication).

The first evidence of the involvement of Notch pathway in MZ B cell development came from the observation that the conditional deletion of RBP-J in B cells totally impairs the formation of MZ B cells, favouring instead the FO B cell compartment (Tanigaki et al. 2002). Successively, Notch2 knock-out studies on B-cell specific conditional mice showed that MZ B cells lack completely upon biallelic ablation of the receptor (Saito et al. 2003), while they are reduced when only one allele is inactivated (Witt et al. 2003). Knock-out mice for DLL-1 phenocopies the full Notch2 knock-out for MZ formation (Hozumi et al. 2004). Conversely, the inactivation of Notch inhibitor MINT (Msx2-interacting nuclear target) correlates with increased number of MZ B cells to the detriment of FO B cells (Kuroda et al. 2003).

Altogether, these evidences indicate the involvement of Notch2 signalling pathway in MZ development.

2.3.2.5.3 IRF4

Interferon regulatory factor 4 (IRF4) is a transcription factor endowed with a DNA-binding domain, an interferon-associated domain (IAD) which supports its homo- and hetero-dimerization with other TFs of the IRF family or other families, and a nuclear-localisation signal (Brass, Zhu, and Singh 1999). IRF4 is induced in response to stimuli activating the NF-κB pathway, such as lipopolysaccharide (LPS), interleukin-4 (IL-4) and CD40 (Gupta et al. 1999; Honma et al. 2005; El Chartouni, Schwarzfischer, and Rehli 2010). Besides being essential for early B-cell development for Ig receptor editing and central tolerance (Pathak et al. 2008; Cadera et al. 2009; Bevington and Boyes 2013), IRF4 is important for cell fate decision in mature B cells. Indeed, a recent study by Simonetti and co-workers displayed that IRF4 restricts the MZ B cell pool in a cell intrinsic manner. Genetic inactivation of *Irf4* in mature B cells is associated with their increased retention into the MZ area. This defect is mainly contributed by the induction, in the lack of Irf4, of the transmembrane receptor and transcriptional regulator NOTCH2, which normally favours the differentiation of B cells into the MZ subset and their retention into the MZ area. The aberrant activation of NOTCH2 in Irf4-deficient FO B cells is sufficient to cause their aberrant retention into the MZ area during their entry or egress from the spleen, through the induction of integrins and chemokine receptors, including S1PR3, known to mediate the migration and retention into this anatomical site. Notably, the administration of a NOTCH2-inhibitory antibody is sufficient to revert the $Irf4^{-/-}$-induced phenotype (Simonetti et al. 2013).

2.3.2.5.4 KLF2

Krüppel-like Factor 2 (KLF2) is a zinc-finger transcription factor belonging to the Krüppel-like Factor family. KLF2 is expressed in the B-cell lineage starting from the pre-B cell stage. Importantly, in the three mature peripheral B cell subsets, the expression of this TF is diverse: its expression is the highest in B-1 B cells, it is reduced in FO B cells and it is

minimal in MZ B cells (Hart et al. 2011). A recent study showed that the limited expression of Klf2 in the MZ B cell subset is ensured by ZFP36L1, which inhibits the translation of *Klf2* transcripts at the post-transcriptional level (Newman et al. 2017). In line with the expression profile, genetic ablation of *Klf2* in committed B cells caused a drastic reduction in B-1 B cells and a considerable increase in MZ and transitional B cell numbers (Hart et al. 2011). Notably, Hart and co-workers showed that the reduced B-1 B cell number scored in Klf2-mutant mice is not due to impaired differentiation or short-term cell survival, rather to an impairment of the long-term maintenance of this subset (Hart et al. 2012). Moreover, Klf2 was shown to be important for the maintenance of FO B cell identity, since the lack of this TF is associated with the acquisition by the latter population of MZ B cell characteristics, such as the expression of several signalling molecules. Besides sustaining B-1 B cell maintenance and FO B cell identity, Klf2 was shown to be crucial for B cell activation. Indeed, upon BCR cross-linking or LPS-stimulation, Klf2-deficient B cells displayed increased apoptosis and impaired cell proliferation (Hart et al. 2011; Winkelmann et al. 2014).

2.3.2.5.5 FOXO1

FOXO proteins are members of a large group of TFs, characterized by the presence of a forkhead DNA binding domain. Forkhead proteins are subdivided in different families, alphabetically named from FOXA to FOXR. FOXO family comprises four proteins: FOXO1, FOXO3A, FOXO4 and FOXO6 (Calnan and Brunet 2008). Among the FOXOs, FOXO1 is the most abundantly expressed in B cells, where it plays a crucial role in their survival, differentiation as well as in the germinal center reaction (Yusuf et al. 2004). In B cells, FOXO1 activity is repressed by the AKT-depend phosphorylation on serine-256, which sequesters the protein into the cytoplasm, thus preventing it to act as TF. Besides BCR signalling, other cytokine receptors contribute to FOXO1 regulation. When activated, FOXO1 translocates into the nucleus where triggers a transcriptional program that sustains cell survival and proliferation (Ushmorov and Wirth 2018). In early stages of B cell development, FOXO1 is necessary for the induction of *Il7r* and *Rag* genes and for the

survival of both pre- and pro-B cells. Indeed, the knock-out of this gene in early B cell progenitors blocked the progression of B cell differentiation beyond the pro-B cell stage (Amin and Schlissel 2008; Lin et al. 2010; Ochiai et al. 2012), whereas its inactivation in committed B cells caused a developmental arrest at the pre-B cell stage (Dengler et al. 2008). Subsequently, Chen and co-workers further investigated the latter mouse model, revealing that the ablation of Foxo1 is associated with a reduction of FO B cells, mirrored by an increase in the number of the MZ B cell subset (Chen et al. 2010). The ability of Foxo1 to favour MZ B cell development was further substantiated by the observation that the lack of the MZ B cell subset suffered from CD19-deficient animals is reversed by the concomitant deletion of Foxo1 (Chen et al. 2010).

Recently, FOXO1 has been characterized as a crucial TF for the germinal center reaction, and in particular for the formation of the dark zone of the GC, where it is mainly expressed. Opposed to PI3K signalling, which inhibits FOXO1 and that is mainly active in B cells of the light zone (Sander et al. 2015), FOXO1 instruct a transcriptional program that is essential to sustain the formation of the dark zone part of the germinal center. Indeed, its genetic ablation in mice abrogates the formation of the dark zone and affects both affinity maturation and class switch recombination (Dominguez-Sola et al. 2015).

2.3.2.5.6 NF-κB

The Nuclear Factor kappa-light-chain-enhancer of activated B cells (NF-κB) is a family of transcription factors, including RELA (p65), NF-κB1 (p50/p105), NF-κB2 (p52/p100), c-REL and RELB (Verma et al. 1995; Ghosh, May, and Kopp 1998). All these proteins contain a dimerization, a nuclear-localisation and a DNA-binding domain. c-REL, RELB and RELA proteins also harbour a trans-activation domain, which strongly activates transcription of target genes. Instead, the other REL proteins, lacking the trans-activation domain, substantially act as transcriptional repressors (May and Ghosh 1997). NF-κB proteins are usually retained in the cytoplasm in an inactive form, as a result of their association with the IκB proteins (IκBα, IκBβ and IκBε). In response to different signalling pathways, IκB proteins, and especially IκBα, are phosphorylated by the kinases of the IKK family and

degraded, allowing NF-κB protein translocation into the nucleus, where they regulate the transcription of their targets (Verma et al. 1995). NF-κB proteins are divided in canonical and non-canonical signalling pathways, activated by different stimuli. The canonical pathway is triggered by proinflammatory cytokines such as TNFα and IL-1, leading to the activation of RELA- or c-REL-containing complexes (Karin and Ben-Neriah 2000). The alternative pathway is activated for instance by CD40L, BAFF and the receptor activator NF-κB ligand (Senftleben et al. 2001; Bonizzi et al. 2004; Novack et al. 2003), resulting in the activation of RELB/p52 complexes (Bonizzi and Karin 2004).

In peripheral B cell development, NF-κB canonical and alternative pathways are absolutely essential. Indeed, compound deficient mice of NF-κB1/NF-κB2 and c-Rel/RelA displayed profound arrest in the transition from T1 to T2 transitional B cells and almost complete absence of FO and MZ mature B cells (Franzoso et al. 1997; Grossmann et al. 2000; Claudio et al. 2002; Gerondakis et al. 2006). Similar phenotypes were scored upon genetic ablation of p100/ NF-κB2 (Tucker et al. 2007) and of NEMO, the activator of the canonical NF-κB pathway (Pasparakis, Schmidt-Supprian, and Rajewsky 2002). A milder reduction in FO B cells resulted from the sole inactivation of NF-κB1/c-Rel (Gerondakis et al. 2006; Pohl et al. 2002).

Among the three mature B cell subsets, the generation of the MZ subset is particularly sensitive to perturbations in the NF-κB activity. Single deficiency of NF-κB1, NF-κB2 or RelB and, to a lesser extent, RelA or c-Rel in mature B cells caused the reduction of MZ B cell number (Caamano et al. 1998; Franzoso et al. 1997; Cariappa et al. 2000; Weih, Yilmaz, and Weih 2001; Guo et al. 2007; De Silva et al. 2016). Furthermore, De Silva and colleagues showed that the combined inactivation of both RelB and NF-κB2 leads to a dramatic reduction in peripheral B cells and especially in the ones belonging to the MZ B cell compartment; the defects induced by the simultaneous ablation of the genes are B-cell intrinsic, indeed they cannot be rescued by the activation of the canonical NF-κB pathway under physiological conditions (De Silva et al. 2016). Similar conclusions were drawn for the canonical NF-κB pathway, upon the combined deletion of RelA and c-Rel. Indeed, also in this case, the simultaneous deletion of both genes caused a severe block in B cell

development in the T1 to T2 transition, and consequent reduction of mature B cells, fewer and smaller B-cell follicles and counterselection of the MZ B cell compartment (Milanovic et al. 2017). These findings, combined together, suggest that both the canonical and non-canonical NF-κB pathways are critical to support the physiological generation and maintenance of mature B cells. Notably, also the inactivation of IKK2, a NF-κB activator kinase, abrogates MZ B cell formation (Pasparakis, Schmidt-Supprian, and Rajewsky 2002).

B1-B mature B cell development is also impaired when factors belonging to the NF-κB pathway are perturbed. Concomitant deletion of NF-κB1 and NF-κB2 (Claudio et al. 2002) as well as deficiency of the sole NF-κB1 reduced B-1B cell numbers, whereas the combined inactivation of NF-κB1 and c-Rel completely abrogated their formation (Gerondakis et al. 2006; Pohl et al. 2002). Coherently, also IKK2 genetic inactivation was combined with absence of B-1 B cells (Pasparakis, Schmidt-Supprian, and Rajewsky 2002).

2.3.2.5.7 NFATc1

Nuclear factor of activated T cells (NFAT) are calcium-inducible TFs that, in B cells, are activated upon calcium release induced by BCR cross-linking or CD40 signalling (Ho et al. 1995; Timmerman et al. 1997; Venkataraman et al. 1994; Verweij, Guidos, and Crabtree 1990). The family is composed of four TFs, of whom NFATc1, c2 and c3 are expressed in B cells. Lack of NFATc1, but not NFATc2, in B cells leads to selective loss of the B-1a B cell compartment through a cell intrinsic mechanism. Notably, the role of NFATc1 in sustaining B-1a B cell development could not be compensated by NFATc2, as well expressed in this B cell subset (Berland and Wortis 2003).

2.3.3 B cell immune responses

B cells are equipped to recognize foreign antigens of different nature through the binding to different set of membrane-bound receptors. Whereas the BCR confers high specificity in the recognition of foreign antigens, innate immune receptors such as Toll-like receptors

(TLR) ensure all B cells to recognize conserved pathogen-associated molecular patterns. These include different types of microbial products including lipopolysaccharide (LPS) and CpG DNA, binding respectively to TLR4 and TLR9.

The engagement of the BCR alone or in conjunction with triggering of one or more TLRs represent a critical step in the activation of B cells and in their subsequent recruitment into an immune response. There are two main types of B cell immune response, differing in the extent to which T cells are recruited.

T-cell-dependent (TD) B cell immune responses are triggered in response to antigen (mostly in the form of protein)-driven engagement of the BCR. Antigens stimulating TD B cell immunity include polypeptides in the form of soluble immune-complexes or haptens conjugated to carrier proteins. After the binding to the antigen, BCR/antigen complexes get internalized and proteolytic cleaved. 11-to-30 amino acid-long peptides, resulting from antigenic processing, are ultimately loaded onto Major Histocompatibility Complex Class-II (MHC-II) molecules to be presented to CD4-positive follicular T-helper cells (T_{FH}) (Rammensee, Friede, and Stevanoviic 1995). Initial T-B cell interactions are crucial for the subsequent recruitment of antigen-specific B cells into the GC reaction. GCs are structurally divided in two microenvironments, named dark zone and light zone according to their histological appearance (Victora et al. 2012; Victora and Nussenzweig 2012). The dark zone is densely packed by high-rate proliferating B cells, known as centroblasts, whereas the light zone is composed by resting B cells, known as centrocytes, T_{FH}, macrophages and FDCs. Within the dark zone, centroblasts undergo clonal expansion and diversify the Ig variable region locus though a molecular process called somatic hypermutation (SHM). SHM is the result of point mutations within the portion of the V gene coding for the hypervariable regions (also called complementarity determining regions or CDRs), which creates the idiotype for antigen binding. Point mutations are introduced at the Ig locus by the Activation-induced cytidine deaminase (AID), whose expression is induced in GC B cells (Muramatsu et al. 2000), and fixed by low-fidelity DNA repair systems. Indeed, B cells with mutated BCR then migrate to the light zone, where they turn into resting centrocytes and they are selected on the basis of improved antigen binding via their BCR (Rajewsky 1996).

Only cells expressing high-affinity antigen receptors, that therefore can capture the antigen presented by FDCs and T_{FH} and receive co-stimulatory signals, are positively selected (Vinuesa et al. 2005). T_{FH} cells also provide signals that promote Ig class-switch recombination (CSR), a process whereby B cells exchange their constant region (from IgM/IgD to other isotypes) through a recombination mechanism initiated by AID, to improve the effector function of their BCR (Kawabe et al. 1994; Vinuesa et al. 2005). The end result of T-cell dependent immune response is the generation of high-affinity long lived antigen-specific memory B cells and antibody-secreting plasma cells (Klein and Dalla-Favera 2008; Basso and Dalla-Favera 2015).

T cell independent (TI) type-2 immune responses are triggered by proteins featuring repetitive structural motifs recognized by the BCR in the absence of T-cell help. BCR crosslinking leads to potent B cell activation followed by intense proliferation outside the GC and final differentiation into short-lived plasma cells. B cells can also recognize T-cell independent type-1 antigens that are composed of microbial products such as LPS. In this case the relevant inducers of B cell activation, proliferation and terminal differentiation are commonly TLR ligands. Antibodies produced in response to TI immune responses are on average of low affinity for the antigen, given the failure of the responding B cells to undergo extensive Ig somatic hypermutation and selection within the GC reaction. TI immune responses driven by bacterial products still require the integrity of BCR tonic signalling. Indeed, as elegantly shown by Otipoby and colleagues, conditional BCR ablation in mouse B cell *in vitro* prevents these cells to proliferate in response to LPS or CpG stimulation.

2.3.3.1 T-cell independent B cell responses: innate immunity receptors

T-cell independent immune responses are initiated by the activation of BCR or TLRs. TLRs are a family of non-catalytic surface receptors, which recognise structurally conserved molecules derived from microbes, such as LPS, lipoproteins or non-methylated CpG DNA. After ligand binding, TLRs dimerize and undergo a conformational change that allows the recruitment of the downstream signalling molecules, including the adaptor molecule myeloid differentiation primary-response protein 88 (MyD88), IL-1R-associated kinases (IRAKs),

transforming growth factor-β (TGF-β)-activated kinase (TAK1), TAK1-binding protein 1 (TAB1), TAB2 and tumor-necrosis factor (TNF)-receptor associated factor 6 (TRAF6). All TLRs signalling, except for the one of TLR3, is MyD88-dependent. Indeed, MyD88 is crucial for the recruitment of IRAK proteins. This event triggers a signalling cascade which ultimately leads to the activation of the canonical NF-κB pathway and MAP kinases, activating cell proliferation and migration, and the expression of cytokines, chemokines and type I interferons (INFs), that protect the host from microbial infection (Akira and Takeda 2004). Among the genes induced by the activation of canonical NF-κB there is also AID, which is critical for class-switch recombination. Alternatively, TLRs can activate also the MyD88-independent TRIF-dependent pathway which activates the IRF3 transcription factor, which triggers the expression of type I INFs.

Despite TLR engagement is sufficient to trigger the innate immune response, recent evidences have shown that it synergises with BCR to induce CSR in T-cell dependent and T-cell independent antibody responses to microbial pathogens. Indeed, BCR triggering, together with simultaneous TLR engagement, leads to enhanced B cell differentiation and antibody responses (Pone et al. 2010; Pone et al. 2012). Furthermore, as previously mentioned, the presence of the BCR is critical to sustain B cell proliferation in response to TLR triggering (Otipoby et al. 2015).

2.3.4 Plasma cell differentiation

Plasma cells are classified in short-lived and long-lived PCs. Short-lived PCs derive from both MZ, FO and B-1 B cells that have been activated after antigen encounter. They resides in SLOs where they undergo apoptosis after few days of intense switched low-affinity antibody secretion (Smith et al. 1996). Conversely, long-lived PCs derive from the germinal center reaction, hence they secrete switched high-affinity antibodies. Long-lived PCs reside in bone marrow niches as well as in the spleen, where they can survive for more than three months (Manz, Thiel, and Radbruch 1997).

Differentiation into functional antibody-secreting PCs is a step-wise process that requires the combined expression of different TFs, among which the most important are IRF4 and

BLIMP-1 (Tellier and Nutt 2018). IRF4 is important to sustain the initial steps of PC differentiation, whereas the activation of BLIMP-1 is critical for the later stages, also by repressing the transcriptional programs of mature B cells. PCs, being the result of a lineage switch, are phenotypically different from mature B cells. Indeed, they lose B-cell specific markers including CD19, CD23, Ig and B220. The latter is substituted by the shorter version of the receptor, CD45R-O, and *Ptprc* transcript is down-regulated. Moreover, PCs acquire new surface markers such as CD138/Syndecan1 (Tellier and Nutt 2017).

2.3.4.1 IRF4

IRF4 is a TF essential for PC development (Klein et al. 2006; Sciammas et al. 2006). Its expression is not restricted to PC, as *Irf4* is required also for early developmental stages (Mittrucker et al. 1997; Lu et al. 2003) and for B cell activation, sustaining CSR and GC B cell formation (De Silva et al. 2012). Indeed, *Irf4* levels are low in centroblasts but rise in centrocytes as a result of CD40 signalling (Sciammas et al. 2006). IRF4 binds to DNA weakly on its own, whereas the binding is strengthened by interaction with binding partners, such as NFAT and AP-1 (activator protein-1) (Glasmacher et al. 2012; Rengarajan et al. 2002). In B cell development, *Irf4* functions as a rheostat depending on its expression levels. Indeed, resting B cells express Irf4 at low level; in the GC reaction intermediate amounts of Irf4 triggers GC formation and CSR by inducing the expression of some crucial genes, including *Aicda* (encoding for AID) (Klein et al. 2006) and *Bcl6* (Sciammas et al. 2006; Ochiai et al. 2013); at high levels, instead, Irf4 favours the activation of PC differentiation path, by activating *Prdm1* and *Xbp-1*, and by repressing *Bcl6* (Klein et al. 2006; Sciammas et al. 2006). Coherently with this crucial role in the activation of the PC differentiation program, Irf4 genetic inactivation in mice is associated to the lack of plasma cells (Klein et al. 2006; Sciammas et al. 2006; Ochiai et al. 2013).

2.3.4.2 BLIMP-1

BLIMP-1 is a TF encoded by the gene *Prdm1* (positive regulatory domain containing 1). Within B cell development, BLIMP-1 is expressed exclusively in developing PCs and tightly

repressed in all the other stages, since its ectopic expression is able to induce plasmacytic differentiation (Turner, Mack, and Davis 1994). BLIMP-1 is required for the development of both short-lived and long-lived PC (Angelin-Duclos et al. 2000; Kallies et al. 2004; Shapiro-Shelef et al. 2003), but not for the initiation of plasmablast formation. Indeed, depletion of BLIMP-1 in B cells arrests the PC differentiation to the pre-plasmablast stage (Kallies et al. 2007). In GC B cells, *Prdm1* is repressed by the concerted actions of BCL6 and MTA3 (metastasis-associated 1 family member 3) (Fujita et al. 2004; Tunyaplin et al. 2004), while in late GC B cells the induction of the gene depends on the combined action of STAT3 and IRF4. Specifically, STAT3 is activated by the stimulation of IL-21 receptor, whereas *Irf4* is transcriptionally up-regulated by CD40-induced activation of NF-κB. Together, STAT3 and IRF4 bind to an IL-21 responsive element upstream the *Prdm1* gene and mediate its full expression (Kwon et al. 2009). Notably, recent evidence from our group demonstrates that EZH2-dependent H3K27me3 limits the induction of *Prdm1* in response to IL-21 stimulation, thereby contributing to the persistence of B cells within the GC (Caganova et al. 2013).

BLIMP-1 acts both as transcriptional activator and repressor. A recent evidence showed that BLIMP-1 induces the expression of almost hundred genes important for PC differentiation, including *Irf4*, *Xbp-1*, and *Ell2* and *Eaf2*, the latter being two important factors acting at Ig mRNA level and promoting antibody secretion. On the other hand, BLIMP-1 is crucial for the repression of B-cell stage genes, such as *Pax5*, *Myc* (Lin et al. 2002), *Ciita* (encoding MHC-II), *SpiB* and *Id3* (Shaffer et al. 2002), and for the maintenance of PC identity (Tellier et al. 2016). Importantly, Minnich and co-workers showed that repression of these genes is mediated by the BLIMP-1-dependent recruitment on the chromatin of PRC2, chromatin remodelling complexes like BAF and NuRD, as well as histone-deacetylates such as NCor and SIN3 co-repressor complexes (Minnich et al. 2016). Additionally, BLIMP-1 has been demonstrated to interact with histone-modifiers associated to transcriptional repression in non-B lymphoid cell types (Gyory et al. 2004; Su et al. 2009; Yu et al. 2000). Altogether, these findings indicate that BLIMP-1 represses its target genes by recruiting of chromatin-remodelling and histone-modifying complexes to its binding sites.

2.4 Linking Polycomb group proteins to B cell development

Accumulating evidence implicates several members of the Polycomb family in the regulation of lymphocyte development. Indeed, as previously mentioned, conditional ablation of Ezh2 results in impaired rearrangement of immunoglobulin (Ig) genes, resulting in B cell lymphopenia and severe immunodeficiency (Su et al. 2003). Members of PRC1 have also been implicated in B cell development, with *Mel18* dictating mitotic response to IL-7 stimulation in HSCs (Akasaka et al. 1997), and restraining proliferation of mature B cells following BCR stimulation (Tetsu et al. 1998).

The expression of PcG proteins in mature B cells, in particular upon recruitment into an immune response, is known since long time (Raaphorst, van Kemenade, Fieret, et al. 2000). Moreover, subunits of either PRC1 and PRC2 are frequently deregulated or mutated in B cell Hodgkin and non-Hodgkin lymphomas derived from mature B cells (Raaphorst, van Kemenade, Blokzijl, et al. 2000; van Kemenade et al. 2001; Bea et al. 2001; Morin et al. 2010).

Apart from *Mel18*, other two subunits of PRC1 have been shown to be involved in early B cell development. *Phc1*, also named *Rae28*, encodes for a subunit of cPRC1 complex. BM transplantation experiments of Phc1-deficient HSCs revealed a severe B-cell maturation arrest, with a block between the pro-B and pre-B stages in development, despite no alterations in the T-cell developmental path (Tokimasa et al. 2001). On the other hand, conditional inactivation of *Rybp* in the early hematopoietic compartment results in an unbalance between B-1 and B-2 progenitors. Specifically, B-1 progenitors increased in numbers at the expenses of B-2 progenitors (pro-B and pre-B), with a subsequent skewing towards B-1 B cell differentiation (Cales et al. 2015). This evidence, together with the aforementioned observation that depletion of Bmi1 and Kdm2b associated with accelerated B lymphopoiesis or favoured myelopoiesis, suggests that PRC1 is critical for the choice of cell fate and lineage commitment. A clear example of PRC1-dependent maintenance of cell fate is the conversion of T-cell progenitors to B cells after the ablation of both *Ring1* genes in T cell precursors. Specifically, upon selective ablation of *Ring1* genes in T-cell progenitors, Ikawa and co-workers observed severe block in T-cell development at the

immature stage. Strikingly, after BM reconstitution of immunodeficient mice, PRC1-deficient progenitors generated $CD19^+$ IgM^+ functional B cells. The authors suggest that this phenotype is caused by the de-repression of a B-cell transcriptional program commanded by *Pax5*, although the up-regulation of this gene, by itself, is not able to reprogram T cells to B cells (Ikawa et al. 2016).

In agreement with studies that reported relevant frequencies of Ezh2 gain-of-function mutations in human and large B cell lymphoma that originate from GC B cells (Morin et al. 2010) and a therapeutic efficacy of molecules targeting Ezh2 in non-Hodgkin lymphomas (McCabe et al. 2012), recently our group has shown that Ezh2 function is crucial to prevent premature B cell terminal differentiation. This regulation is mainly exerted through the direct repression of the PC determinants *Prdm1* and *Irf4* (Caganova et al. 2013). Besides EZH2, a role for ncPRC1 complexes in the formation and maintenance of GC reaction has been recently established. Indeed, canonical components of PRC1 are repressed within early GC B cells and, in parallel, non-canonical components such as *Bcor*, *Kdm2b* or *Pcgf1* are induced. This allows the formation of a PRC1-BCOR complex containing CBX8, which is recruited to target loci for repression in a PRC2- and BCL6-dependent manner. Notably, *Cbx8* loss-of-function mirrors the effects of *Ezh2* ablation in normal and malignant GC B cells, indicating a crucial role for this factor at this stage of B-cell development (Beguelin et al. 2016).

In line with the close relationship between PRC1 and PRC2 complexes, as already mentioned, several evidences indicate that also PRC2 is relevant for early (Su et al. 2003) and peripheral B cell development and activation (Caganova et al. 2013; Beguelin et al. 2013).

3. Aim

Polycomb proteins are largely implicated in developmental processes, including B cell development. In particular, several evidences support a role for PRC1 in early B-cell development and in the GC reaction. However, to our knowledge the understanding of PRC1 functions in the differentiation process between immature and mature B cells and in the maintenance of mature B cell subsets is still missing. Considering the variety of PRC1 complexes and the functional redundancy of RING1 proteins, we have challenged this question though the characterization of compound mutants of *Ring1A* and *Ring1B* to disrupt any PRC1 activity.

The initial characterization of these mice, in which the germline *Ring1A* knock-out is combined with a conditional *Ring1B* knock-out allele inactivated selectively in transitional B cells using the Cd23-cre transgene, was performed by Dr. Federica Alberghini and reported in her PhD thesis. PRC1-deficient resting B cells showed an aberrant transcriptional program with expression of several lineage determinants, besides the retention of immature B cell markers such as CD93/AA4.1 and CD24/HSA. Moreover, mature B cell numbers were marginally affected, with a detectable decrease only in FO B cells. The most relevant and investigated phenotype of PRC1-deficient mice was the substantial impairment of germinal center (GC) responses. Specifically, the GC formation was impaired *in vivo* upon T-cell dependent antigen stimulation, with subsequent severe reduction in high-affinity antibody responses and decreased number in long-lived plasma cells and memory B cells. *In vitro* experiments with LPS stimulation showed increased apoptosis and accelerated plasmablast differentiation; however, the apoptotic phenotype was not detectable in stimulation settings not associated with the induction of AID, suggesting AID-driven cell-death in PRC1-deficient B cells.

This work led some open questions, such as: 1) how does the absence of PRC1 specifically impact on the development of the three mature B cell subsets? 2) is the fitness of mature B cells affected upon PRC1 inactivation? 3) how does PRC1 influence B cell activation and terminal differentiation? 4) are the defects displayed by PRC1-deficient mice B-cell autonomous?

Therefore, the aim of the present study is to elucidate the role of PRC1 in resting B cell maturation and to unveil the mechanisms which explain the defects of B cell activation and terminal differentiation.

4. Materials and methods

4.1 Mice

BL6C57/J and Ly5.1 (B6.SJL-*Ptprc*^{a}*Pepc*^{b}/BoyCrl) mice were purchased from Charles River. Ring1a$^{-/-}$Ring1b$^{fl/fl}$CD23-cre mice were generated by crossing Ring1a$^{-/-}$Ring1b$^{fl/fl}$ mice (L. D'Artista, S. Casola, personal communication) with CD23-cre mice (Kwon et al. 2008). JHT mice were used as recipients for bone marrow transplantation assay. Mice were housed and bred in animal facility at the IFOM-IEO Campus Institute, Milan, Italy. Experimentations were performed under the protocol numbers 80/2016 and 880/2017 approved by the Italian Ministry of Health and the IFOM OPBA Committee.

4.1.1 Mutants (genetic background)

Ring1a$^{-/-}$ (del Mar Lorente et al. 2000)

Ring1b$^{fl/fl}$ (Cales et al. 2008)

4.1.2 Cre line (genetic background)

Cd23-cre (Kwon et al. 2008)

4.2 Genomic DNA extraction for tail biopsy

1 cm of a tail biopsy was incubated in 400 µl of Tail lysis buffer with Proteinase K (100 µg/ml) at 56 ˚C, shaking at 850 rpm, O/N in Thermomixer Compact (Eppendorf®). The lysate was spun at 13000 rpm for 1 min, then transferred into a new tube. 1 ml of isopropanol was added, tube was mixed by inverting and centrifuged at 13000 rpm for 1 min. DNA pellet was dissolved into 300 µl of TE 1X buffer by incubation at 60 ˚C for 20 min.

Tail lysis buffer: 100 mM tris-HCl pH 8.5, 5 mM EDTA, 200 mM NaCl, 0.2 % SDS, in ddH_20.

TE buffer: 10 mM Tris-HCl pH 8.1, 5 mM EDTA pH 8, in ddH_20.

4.3 Genotyping strategy

The genotypes of all mice were analyzed by polymerase chain reaction (PCR) amplification performed on genomic DNA extracted from tails. Primers and annealing temperature (T_A) used are listed in Table 1, while PCR reagents in Table 2. PCR conditions are summarized in Table 3. PCRs were run in automatic thermocycler GeneAmp PCR System9700 (Applied Biosystems).

Table 1. Primers used for genotyping and annealing temperatures.

PCR product	Primer ID	Sequence	T_A
Ring1B WT vs fl	Ring1b Del Fw	TAATTCCATGAAAGCATCAAAGT	58 ˚C
	Ring1b Fl Rv	GTTCCATTTGTCTGCACAGCCTGAG	
	Ring1b Del Rv	AGCACTGTGCTCCTTTTTGAT	
Ring1A WT vs KO	Ring1a WT Fw	CTTCCGCAGACCTCTCTCAG	60 ˚C
	Ring1a WT Rv	TTGCGCTCATCTTAGGCTTT	
	Ring1a KO Fw	TGCTCGAGATGTCATGAAGG	
Cd23-cre	Cd23-cre Fw	GATGTGAGGGACTACCTCCTGTACC	60 ˚C
	Cd23-cre Rv	CCAGCATCCACATTCTCCTT	

Table 2. PCR reagents.

Component	Final volume (µl)
5X Flexi buffer	5
MgCl2 solution, 25 mM	2
PCR Nucleotide Mix, 2.5 mM each	2
Forward primer, 50 µM	0.2
Reverse primer, 50 µM	0.2
GoTaq® DNA Polymerase (5u/µl)	0.2
Template DNA	1
Nuclease-Free Water	14.4
Total	25

Table 3. Genotyping PCR conditions.

Temperature (˚C)	Time (min:sec)
94	2:30

94	0:30	x 33 cycles
T_A	0:30	
72	0:30	
72	5:00	
4	hold	

4.4 Bone marrow chimeras

JHT mice, used in bone marrow chimera experiments, are Ly5.2$^+$ (CD45.2 allotype) C57BL/6 congenic mice. CD23-cre or Ring1a$^{-/-}$Ring1b$^{fl/fl}$CD23-cre mice Ly5.2$^+$ (CD45.2 allotype) were used as donor mice, as test cells, in combination with C57BL/6 Ly5.1$^+$ (CD45.1 allotype), as competitor cells. JHT recipient mice were sub-lethally irradiated (5 Gy) and reconstituted with a total of 5×10^6 total donor bone marrow cells (test + competitors) + 2x10^6 total splenic cells (from C57BL/6 Ly5.1$^+$) by intravenous injection. Reconstituted mice were administered with antibiotics (2.5 mg/ml ampicillin, 4 mg/ml kanamycin 1.6 mg/ml metronidazole) in their drinking water for four weeks post-reconstitution. Transplantation efficiency was checked after 4 weeks by immunostaining for Ly5.1 and Ly5.2 surface markers on blood obtained by recipient tail bleeding. Mice were analysed 14-16 weeks post-transplantation.

4.5 *In vivo* turnover assay

BrdU (Sigma Aldrich) was administered in drinking water (0.8 mg/ml) for one week. Splenocytes and bone marrow cells were retrieved as indicated in 4.6.1 and stained with anti-BrdU antibody.

4.6 Cell culture techniques

4.6.1 Preparation of cell suspension from lymphoid organs

For B cell analysis, mice of 4-8 months of age were used. Spleens, lymph nodes, peritoneal cavity wash, tibias and Peyer's patches were collected from mice. For cell suspension, spleen, lymph nodes and Peyer's patches samples were smashed between frosted slide glasses and subsequently filtered through 40 µl nylon meshes (Becton Dickinson, USA); tibias were flushed using a syringe containing 1 ml of B cell medium to obtain bone marrow cells. Erythrocytes lysis was performed on spleen and bone marrow preparations by incubating cell suspensions in 1 ml of Red Blood Cells (RBC) lysis buffer for 3 minutes on ice. Reaction was stopped by adding 10 ml of B cell medium; cells were washed (centrifugation at 1200 rpm for 5 minutes at 4 ˚C) and resuspended in B cell medium before counting. Live cells were counted using Erythrosine B dye to distinguish alive and dead cells.

B cell medium: DMEM, 10% heat-inactivated FBS, 0.1 mM NEAA, 1 mM Na Pyruvate, 50 µM β-ME and 2 mM L-glutamine (Invitrogen)

RBC lysis buffer: 1 part solution A + 9 parts solution B

Solution A: 0.17 M Tris-HCl pH 7.65, in ddH_20.

Solution B: 0.15 M NH_4Cl, in ddH_20.

4.6.2 B cell purification

Starting from splenic cell suspension, CD43-expressing B cells (activated B cells, plasma cells and B-1a cells), T cells, NK cells, dendritic cells, macrophages, granulocytes, and erythroid cells were indirectly magnetically labeled by using a cocktail of biotin-conjugated antibodies against CD43, CD11b, CD11c, Ter-119, CD4, CD8, and CD3 and followed by Anti-Biotin MicroBeads (Myltenyi Biotec) incubation (antibodies details are listed in Table 4). B cells were then purified through LS columns (Miltenyi Biotec) following manufacturer's B Cell Isolation Kit depletion protocol (Miltenyi Biotec). For antibody staining and

purification, cells were resuspended in MACS buffer. This procedure allows the isolation of untouched resting B cells from single cell suspensions of lymphoid tissues.

MACS buffer: 1X PBS, 0.5 % BSA, 2 mM EDTA, in ddH_20.

Table 4. Antibodies used for negative B cell purification.

Antibodies	Clone	Company	Dilution
Monoclonal Rat anti-mouse CD43 (biotin)	S7	eBioscience	1/800
Monoclonal Rat anti-mouse CD11b (biotin)	M1/171	eBioscience	1/800
Monoclonal Armenian hamster anti-mouse CD11c (biotin)	N418	eBioscience	1/800
Monoclonal Rat anti-mouse Ter-119 (biotin)	TER-119	eBioscience	1/800
Monoclonal Rat anti mouse CD4 (biotin)	GK1.5	eBioscience	1/400
Monoclonal Rat anti mouse CD8 (biotin)	53-6.7	eBioscience	1/400
Monoclonal Armenian hamster anti mouse CD3 (biotin)	145-2C11	eBioscience	1/200

4.6.3 *In vitro* B cell culture

For survival experiments, purified B cells were cultured in B cell medium and stimulated with different concentration of BAFF (50, 25, 12, 6 or 0 ng/ml) (Peprotech – Recombinant Human BAFF – 310-10). Cells were plated at a density of $5x10^5$ cells/ml at 37 ˚C and 5 % CO_2.

For activation experiments, purified B cells were cultured in B cell medium and stimulated with 20 µg/ml LPS (Lipopolysaccharide, Sigma Aldrich) with or without 1 ng/ml of IL-4 (Recombinant Murine Interleukin 4, 214-14, Peprotech). Alternatively, 1 µg/ml anti-RP105 (Monoclonal rat anti-mouse CD180, functional grade purified RP/14, eBioscience) was added to the medium. Cells were plated at a density of $5x10^5$ cells/ml at 37 ˚C and 5 % CO_2.

For survival and growth curves, viable cell number was determined using Muse™ Cell Count & Viability Assay kit (Millipore) and MUSE Cell analyser instrument, according to the manufacturer's protocol.

MACS buffer: 1X PBS, 0.5 % BSA, 2 mM EDTA, in ddH_20.

4.6.4 *In vitro* cell proliferation assay with CFSE

Purified B cells were resuspended at $1x10^6$ cells/ml final concentration in pre-warmed (37 ˚C) 1X PBS. CFSE was added (ab145291, Abcam) at a 2.5 µM final concentration and cells were incubated at 37 ˚C in the dark for 10 minutes. Labelling was quenched by adding five volumes of B-cell medium and incubating cells for 5 minutes at RT. Then, cells were centrifuged, washed once in medium, and plated at $5x10^6$ cells/well in a six-well dish in the presence of LPS with or without IL-4, as previously described (4.6.3). Variations in the intensity of CFSE labelling were detected with the FACSCalibur™ (BD Bioscience) at 72 hours. Cells were collected and further stained with IgG1 or IgG3 to identify labelled B cells switched to IgG1/IgG3 isotype.

4.6.5 *In vitro* chemotaxis assay

Total splenic cell suspension, after treatment with RBC lysis, was resuspended in resensitization medium at 10^7 cells/ml and incubated at 37 ˚C for 40 min. In the meantime, S1P chemokine was diluted to the concentration of 10 or 100 nM in experimental medium. 580 µl of chemokine-containing medium or chemokine-free medium were aliquoted in wells of a 24-well plate. Wells containing chemokine-free medium were added for inputs and to test the spontaneous migration. Transwells (5 µm pore size) were allocated in each well and then 100 µl of cell suspension was added on the top. For input, 20 µl of cell suspension was plated directly into the medium. Each condition was tested in triplicate. Transwell plate was incubated at 37 ˚C for 3 hours, avoiding vibrations. At the end of the incubation time, transwells were gently removed, cells were resuspended by pipetting 10 times and transferred into a FACS tube for counting. Migrated cells were enumerated by collecting events with the FACSCalibur™ (BD Bioscience) for 60 sec at low speed and analysed with FlowJo software. Then, cells were stained with antibodies anti-CD23, -CD21, -CD19 and -B220 and collected again.

Migration index was calculated as follow:

$$Migration\ index = \frac{(cells\ migrated\ in\ response\ to\ chemochine) - (cells\ migrated\ spontaneously)}{Number\ of\ cells\ in\ input} * 100$$

Resensitization medium: RPMI, 10 mM Hepes, 2 % BSA fatty-acid free.

Experimental medium: RPMI, 10 mM Hepes, 0.5 % BSA fatty-acid free.

4.7 Imaging techniques

4.7.1 Immunostaining for flow cytometry and cell sorting (FACS)

For FACS, $1x10^6$ cells were stained for 20 minutes on ice in 50 µl FACS buffer (PBS 1 %, BSA 0.01 %) containing the appropriate mixture of fluorescently labeled antibodies (listed in Table 5). For FACS-sorting, $1x10^7$/100 µl cells were stained for 15 minutes at 4 ˚C on rotation in FACS buffer. Cells were then washed twice, resuspended in PBS 2% FBS and sorted using FACSAria™ (BD Bioscience). After sorting, cells were collected in PBS 33% FBS, centrifuged at 6000 rpm 4 ˚C for 5 min and immediately resuspended in the appropriate buffers or frozen at -80 ˚C.

FACS buffer: 1X PBS, 0.01 % BSA, in ddH_20.

Table 5. Antibodies used for flow cytometry.

Antibodies and antigens	Company	Dilution
Monoclonal Rat-anti mouse CD19 (Cy7 PE)	eBioscience	1/400
Monoclonal Rat-anti mouse CD21/CD35 (PE)	eBioscience	1/1000
Monoclonal Rat-anti mouse CD23 (FITC)	eBioscience	1/100
Monoclonal Rat-anti mouse CD38 (APC)	eBioscience	1/600
Monoclonal Rat-anti mouse CD1d (biotin)	eBioscience	1/800
Monoclonal mouse-anti mouse CD95/Fas (PE)	eBioscience	1/170
Monoclonal Rat-anti mouse CD93/AA4.1 (APC)	eBioscience	1/600
Monoclonal Rat-anti mouse CD24/HAS (PE)	eBioscience	1/400
Monoclonal Rat-anti mouse/human CD45R (B220) (Cy7PE)	eBioscience	1/400

Monoclonal Rat-anti mouse/human CD45R (B220) (FITC)	eBioscience	1/200
Monoclonal Rat-anti mouse CD268/BAFF-R (APC)	Biolegend	1/400
Monoclonal mouse-anti mouse CD45.2 (Cy7PE)	eBioscience	1/200
Monoclonal mouse-anti mouse CD45.1 (FITC)	eBioscience	1/100
Monoclonal hamster-anti mouse anti-TCRβ (APC)	eBioscience	1/600
Monoclonal mouse-anti mouse MHC-II (PE)	eBioscience	1/200
Monoclonal Rat-anti mouse IRF4 (Alexa 488)	Biolegend	1/800
Monoclonal Rat-anti mouse IgG1 (biotin)	BD Bioscience	1/2000
Monoclonal Rat-anti mouse IgG3 (biotin)	BD Bioscience	1/500
Monoclonal Rat-anti mouse CD138 (PE)	BD Bioscience	1/200
Monoclonal Rat-anti mouse IgM clone R33.24.12 (Alexa 488)	Home-made	1/400
Polyclonal Goat-anti mouse IgM Fab2 (Alexa 647)	Jackson Immunoresearch	1/800
Monoclonal Rat-anti mouse IgD (PE)	eBioscience	1/3000
Monoclonal Rabbit-anti mouse H3K27me3 (Alexa 647)	Cell Signaling	1/1000
Monoclonal Rat-anti mouse CD5 (PE)	eBioscience	1/200
Monoclonal Rat-anti Mouse PAX5 (PE)	Biolegend	1/200
Monoclonal Mouse-anti mouse BLIMP-1 (DyLight 650)	Novus Biologicals	1/100
Streptavidin (PE)	eBioscience	1/600
Streptavidin (APC)	eBioscience	1/800

4.7.2 Intracellular immunostaining for flow cytometry

Cells were stained in 10 µl / $1x10^6$ of FACS buffer containing antibodies of choice (Table 5) for 20 min at 4 ˚C in the dark and subsequently washed twice with 200 µl of FACS buffer as described before in 4.7.1. For intracellular protein stainings True Nuclear™ Transcription Factor kit (Biolegend) was used. Surface stained cells were fixed and permeabilized in Transcription Factor 1X Fix solution buffer for 40 min on ice in U bottom 96 well microplate and washed 3 times by Transcription Factor 1X Perm Buffer and centrifugation. Cell were then stained in 100 µl of Transcription Factor 1X Perm Buffer, in which antibodies listed in Table 5 were diluted, for 1 hour at RT shaking. Cells were washed twice with Transcription Factor 1X Perm Buffer and resuspended in 100 µl 1X PBS. Samples were acquired using

FACSCalibur™ (BD Bioscience) and analysed FlowJo software. All centrifugation steps were performed at 400 g for 3 min at RT.

4.7.3 Immunostaining of splenic sections

Spleens were fixed in liquid nitrogen. Frozen 3 µm sections were thawed, air-dried, fixed in 80 % ethanol for 10 minutes, washed with 1X PBS, blocked with Blocking solution for 1 hour, and stained O/N at 4 ˚C in a humidified chamber with primary antibodies (light protected) diluted in Blocking solution. Sections were washed three times with 1X PBS, stained for 1 hour with secondary antibodies, washed, counter-stained with DAPI for 5 minutes, washed with 1X PBS immediately after. Slides were mounted in Mowiol (Calbiochem) + antifade (DABCO, Sigma Aldrich) and stored at 4 ˚C until acquisition. Images were acquired on a Full Manual BX51 (Olympus) Microscope. Image analysis was performed using ImageJ software (NIH). Antibodies used are listed in Table 6. Quantifications of signal intensity and marginal zone width were performed using ImageJ.

Blocking solution: 1X PBS, 0.02 % FBS, 0.01 % w/v BSA, in ddH_20.

Table 6. Antibodies used for immunofluorescent staining of splenic sections.

Antibodies and antigens	**Type**	**Company**	**Dilution**
Monoclonal mouse-anti mouse CD45.2 (Alexa 647)	Primary	eBioscience	1/10
Monoclonal mouse-anti mouse CD45.1 (biotin)	Primary	eBioscience	1/20
Anti-mouse IgM clone R331.12 (Alexa 488)	Primary	Home-made	1/10
Monoclonal Rat-anti mouse MOMA-1 (biotin)	Primary	eBioscience	1/10
Streptavidin (Alexa 555)	Secondary	Life Technologies	1/200

4.7.4 Immunostaining of *in vitro* activated B cells

Cell suspensions were harvested, seeded on Polysine™ Microscope Adhesion Slides (ThermoFisher Scientific) and air-dried for 30 minutes. Fixation was performed with 100 % ice-cold methanol for 10 min. Slides were washed 3 times with 1X PBS, blocked with Blocking solution for 1 hour, and stained with primary antibodies diluted in Blocking solution (light protected) in a humidified chamber at 4 ˚C O/N. Slides were washed three times with Washing buffer, stained for 1 hour with secondary antibody diluted in Blocking solution, washed, counter-stained with DAPI for 2 minutes, washed with 1X PBS immediately after. Cells were treated with ethanol solutions (70 %, 95 % and 100 %) to dehydrate and remove aspecific signals. Slides were mounted in ProLong Gold Antifade Mountant (ThermoFisher Scientific) and stored at 4 ˚C until acquisition. Antibodies used for stainings are listed in Table 7. Images were acquired on a Full Manual BX51 (Olympus) Microscope. Image analysis was performed using ImageJ software (NIH). Quantification of γH2A.X foci was performed using Cell Profiler software tools.

Blocking solution: 3%BSA, 0.5% Triton-X, 3% donkey serum, in 1X PBS.

Washing buffer: 0.2 % BSA, 0.1 % Triton-X, in ddH_20.

Table 7. Antibodies used for immunofluorescent staining of activated B cells.

Antibodies and antigens	**Type**	**Company**	**Dilution**
Monoclonal Rabbit-anti mouse γH2A.X	Primary	Cell Signaling	1/1000
Monoclonal Donkey-anti rabbit (Alexa 488)	Secondary	Jackson ImmunoResearch	1/400

4.7.5 *In situ* hybridization of splenic sections

For *in situ* single and double-target mRNA hybridization, formalin-fixed and paraffin-embedded (FFPE) 4 µm-thick sections were cut and air-dried O/N. Tissue sections were deparaffinized at 60° C for 1 hour, rehydrated and air-dried before pre-treatments. The

unmasking technique was performed using Target Retrieval maintained at a gentle boiling temperature (98 to 104° C) using a hot plate for 15 min. After protease treatment at 40° C for 15 min in a HybEZ hybridization oven (Advanced Cell Diagnostics), the target probes listed in Table 8 were incubated. Detection of specific probe binding was revealed with RNAScope 2.5 HD Reagent kit – brown (Advanced Cell Diagnostic) and RNAScope 2.5 HD Duplex Assay kit (Advanced Cell Diagnostic).

To quantify the co-localization of *Prdm1* and *Pax5* signal a semiautomatic segmentation was performed. The segmentation should be considered semi-automatic because it required the initial manual sampling of some BLUE and RED spots on a random subset of images (10% of the whole dataset) in order to identify the appropriate threshold values to be used with the multiresolution approach described by Sciortino and co-workers (Sciortino, Tegolo, and Valenti 2017). To consider the different magnifications of the microscope, the fourth and fifth wavelet planes were considered. The overlap areas of BLUE and RED spots were measured in micrometers (µm), as well as the distances between each BLUE spot and all the RED spots in each image. In particular, a histogram representation allows to express quantitatively the number of BLUE spots at a given distance from the RED spots, providing indication on some kind of density. For a quicker comparison of all the results, we computed also the average distance.

Table 8. Probes used for *in situ* hybridization.

Probe	Accession number	Target region	Usage
Mus musculus-*Prdm1*	NM_007548.4	1871-2808	Experimental
Mus musculus-*Pax5*-C2	NM_008782	5-1146	Experimental
Mus musculus-*Ubc*	NM_019639.4	34-860	Positive control

4.7.6 Immunostaining for detection of apoptosis

For detection of apoptotic cells CaspGLOW™ Fluorescein Active Caspase Staining Kit (BioVision) was used with specific modifications in protocol. *Ex vivo* or *in vivo* cultured B cells were incubated in 100 µl of B cell medium containing 1 µl of FITC-VAD-FMK (carbobenzoxy-valyl-alanyl-aspartyl-[O-methyl] fluoromethylketone), a cell-permeant pan-

caspase inhibitor that irreversibly binds to the catalytic site of caspase proteases, at 37° C and 5 % CO_2 for 1 hour. Cells were collected by centrifugation (2000 rpm for 30 seconds) and washed with 200 µl of wash buffer. Subsequently, surface staining was performed as described before in 4.7.1. Cells were acquired by FACSCalibur™ (BD Bioscience) and analysed using FlowJo software.

4.7.7 Cell-cycle analysis

For this procedure, cells were treated with reagents of Fixation/Permeabilization Solution Kit (BD Bioscience). $1x10^6$ of *in vitro* activated B cells were collected by centrifugation at 1500 rpm for 5 min, then they were resuspended in 1 ml of medium supplemented with BrdU (33 µM, Sigma Aldrich) and incubated at 37° C and 5 % CO_2 for 40 min. Cells were washed in 1X PBS, fixed in 100 µl of BD Cytofix/Cytoperm™ (C/C) buffer for 20 min at RT and washed with Perm/Wash™ (P/W) buffer. Cells were resuspended in 70 µl of 10 % DMSO in FBS solution and incubated at RT for 10 minutes. After washing in P/W buffer, cells were re-fixed in 100 µl of C/C buffer at RT for 5 min and washed by P/W buffer again. Cells were resuspended in DNase solution (1X PBS, 300 µg/ml DNase) and incubated at 37° C for 1 hour. After washing with P/W solution, cells were stained in 50 µl of P/W buffer with anti-BrdU (BD Bioscience) at RT for 20 min. After washing with P/W buffer, for DNA staining cells were resuspended in 1 ml of cold propidium iodide (50 µg/ml) + RNase (250 µg/ml) and incubated at 4° C O/N. Samples were collected in doublet discrimination mode by FACSCalibur™ (BD Bioscience) and analysed using FlowJo software.

4.7.8 Neutral comet assay

Neutral comet assay was performed using CometAssay® Reaction Kit (Trevigen), following manufacturer's instructions. Briefly, $1x10^5$ cells were resuspended in 50 µl of 1X PBS and mixed with prewarmed 500 µl of molten LMAgarose at 37 ˚C. 50 µl of the mixture was pipetted onto CometSlide™. Slides were refrigerated at 4 ˚C for 10 min, then transferred in 1X Lysis Solution O/N. Slides were immersed in 50 ml of ice-cold 1X Neutral

Electrophoresis Buffer for 30 min, then electrophoresed in 850 ml of the same buffer with CometAssay® ES unit (Trevigen), at 21 V for 45 min at 4 ˚C. Slides were then immersed in DNA Precipitation Solution for at RT 30 min and successively in 70% ethanol solution at RT for 30 min. Slides were air dried for 30 min and stained with 100 µl of diluted SYBR Gold Staining Solution (ThermoFisher Scientific) at RT for 30 min. Next, slides were air dried at RT O/N. All the passages of the procedure were performed in the dark. Samples were acquired on a Full Manual BX51 (Olympus) Microscope. Image analysis was performed using OpenComet plugin of ImageJ software (NIH).

10X Neutral Electrophoresis Buffer: 1 M Tris Base, 5 M NaAc, in ddH_20.

DNA Precipitation Solution: 7.5 M NH_4Ac, in 95 % ethanol.

SYBR Gold Staining Solution: 1/10000 SYBR Gold in TE buffer, pH 7.5.

TE buffer: 10 mM Tris-HCl pH 8.1, 5 mM EDTA pH 8, in ddH_20.

4.8 Biochemical techniques

4.8.1 Immunoblot analysis

Primary or *in vitro* stimulated B cell extracts were washed once in 1X PBS, then resuspended in RIPA buffer containing Benzonase and incubated on ice for 1 hour. Sonication was performed for 5 cycles (30 sec ON/ 30 sec OFF) using Bioruptor^{TM} Next Gen (Diagenode). Lysates were centrifuged at 15000 rpm for 15 min at 4 ˚C, then transferred to a new tube. 20-30 µl of lysate was mixed with 1X Laemmli loading buffer. Samples and protein marker (NOVEX® Sharp PreStained protein standard – Invitrogen) were electrophoresed by 4-12 % SDS-PAGE (Invitrogen) in an XCell SurelockTM Mini-cell apparatus (Life Technologies) in NuPAGE MOPS or MES SDS running buffers (ThermoFisher Scientific) and transferred to nitrocellulose membranes (iBlot® Transfer Stuck, Invitrogen), by iBlot2® Dry Blotting Device (Invitrogen). After blotting, the membranes were stained with Ponceau S staining solution to verify equal loading and transfer. Membranes were briefly washed in distilled water and blocked in Blocking solution

at RT for 1 hour. After blocking, membranes were incubated with primary antibodies (Table 9) diluted in Blocking solution, at 4 ˚C O/N. After three washes, of 5 min each in TBS-T, membranes were incubated with the horseradish peroxidase conjugated secondary antibody diluted in Blocking solution for 1 hour at RT. Membranes were washed three times in TBS-T for 5 min and the bound secondary antibody was revealed using the ECL Western Blotting Substrate (Pierce) and detected using the Chemidoc^{TM} XRS + imaging System (Biorad). Image analysis was performed using the Image Lab^{TM} 5.2.1 software tool.

RIPA buffer: 50 mM Tris-HCl pH 7.4, 150 mM NaCl, 1 % Triton, 5 mM $MgCl_2$, 1X PMSF, 1X Protease inhibitor cocktail (Roche), 1/1000 Benzonase nuclease (Novagen), in ddH_20.

Laemmli loading buffer: 4X NuPAGE® (Invitrogen), 2 mM DTT, 4X PMSF, 4X Protease inhibitor cocktail (Roche).

Ponceau S staining solution: 0.1 % Ponceau S (w/v) and 5 % acetic Acid (w/v), in ddH_20.

TBS-T: 20 mM Tris HCl pH 7.4, 500 mM NaCl, 0,1 % Tween, in ddH_20.

Blocking solution: 5 % BSA in TBS-T.

Table 9. Antibody used for immunoblot protein detection.

Primary Antibodies	Clone	Company	Dilution
Rabbit anti-mouse RING1A	2820S	Cell Signaling	1/1000
Rabbit anti-mouse RING1B	D22F2	Cell Signaling	1/1000
Rabbit anti-mouse BIM	C34C5	Cell Signaling	1/1000
Rabbit anti-mouse p100/p52	Polyclonal	Cell Signaling	1/1000
Rabbit anti-mouse AKT (total)	C67E7	Cell Signaling	1/1000
Rabbit anti-mouse AKT (phospho-Serine 473)	D9E	Cell Signaling	1/1000
Rabbit anti-mouse FOXO1 (total)	C29H4	Cell Signaling	1/1000
Rabbit anti-mouse FOXO1 (phospho-Serine 256)	Polyclonal	Cell Signaling	1/1000
Rabbit anti-mouse LYN (total)	Polyclonal	Cell Signaling	1/1000
Rabbit anti-mouse LYN (phospho-Tyrosin 508)	Polyclonal	Cell Signaling	1/1000
Rabbit anti-mouse BTK	D9T6H	Cell Signaling	1/1000

Rabbit anti-mouse GSK3β	D85E12	Cell Signaling	1/1000
Rabbit anti-mouse H2A	Polyclonal	Merck Millipore	1/1000
Rabbit anti-mouse H4	Polyclonal	Abcam	1/1000
Rabbit anti-mouse H2AK119ub1	D27C4	Cell Signaling	1/1000
Rabbit anti-mouse H3K27me3	C36B11	Cell Signaling	1/1000
Secondary Antibody	**Clone**	**Company**	**Dilution**
Goat anti-rabbit HRP-linked	Polyclonal	Cell Signaling	1/2000

4.8.2 Chromatin immunoprecipitation (ChIP)

$1x10^6$ cells were FACS-sorted as described previously in 4.7.1 and cross-linked with 1 % formaldehyde in 1X PBS for in rotation at RT 10 min. Cross-linking was quenched with 1 ml of 0.125 M glycine, then cells were washed twice in ice-cold 1X PBS, resuspended in SDS buffer and incubated at -80 ˚C at least for one O/N. Samples were defrosted gradually, centrifuged at 40000 rpm at 16 ˚C for 10 min and resuspended in 130 µl of Sonication buffer. Sonication was performed for 10 cycles (30 sec ON/ 30 sec OFF) using Bioruptor® (Diagenode) followed by sonication with Covaris M220 (peak power 175.0, duty factor 10.0, cycles/burst 100). Chromatin was centrifuged at 1500 rpm at 16 ˚C for 10 min and supernatant transferred in a new tube. 1 ml of IP buffer was added together with 8 µl of Rabbit anti-mouse H3K27me3 (Cell Signaling). 10 µl of chromatin were saved before addition of antibody as Input. Tubes were incubated in rotation at 4 ˚C O/N. 20 µl of protein G dynabeads (Invitrogen) were added to each sample and incubated in rotation at 4 ˚C for 4 hours. Beads were retrieved with a magnet, washed four times with Washing buffer, once with TE buffer, then resuspended in 250 µl of Elution buffer. Samples were boiled at 95 ˚C for 5 min and supernatant transferred in a new tube (two times). 490 µl of Elution buffer were added to the Inputs. 10 µl of Proteinase K (20 mg/ml) were added to all samples. Tubes were incubated in a Thermomixer Compact (Eppendorf®) at 55 ˚C for 4 hours and then at 65 ˚C O/N. DNA was purified by Phenol/Chloroform purification, followed by Na-Acetate and ethanol precipitation. Briefly, 500 µl of Phenol/Chloroform/Isoamylalcohol 25:24:1 (Sigma Aldrich) were added to the de-cross-linked DNA. Tubes were vortexed for 30 sec, then pun at 10000 rpm at RT for 10 min. the upper phase was transferred in a new

tube containing 1 µl of glycogen. 75 µl of 3 M Na-Acetate and 1 ml of 100 % ethanol were added to the tube, that was subsequently vortexed for 30 sec. Tubes were incubated at -80 ˚C for 1 hour, then centrifuged at 13000 rpm at 4 ˚C for 20 min. Supernatant was discarded. 1 ml of 70 % ethanol was added, the tube vortexed briefly and centrifuged at 13000 rpm at 4 ˚C for 10 min. Supernatant was discarded. Tubes were air-dried for 10 min at RT. 30 µl of 1X TE were added on the DNA pellet and DNA dissolved in a Thermomixer Compact (Eppendorf®) at 56 ˚C for 30 min. DNA was stored at -20 ˚C until library preparation.

SDS buffer: 0.5 % SDS, 50 mM Tris-HCl pH 8.1, 100 mM NaCl, 5 mM EDTA pH 8, in ddH_20.

Sonication buffer: 1 % SDS, 50 mM Tris-HCl pH 8.1,10 mM EDTA pH 8, in ddH_20.

IP buffer: 0.5 % Triton X-100, 50 mM Tris-HCl pH 8.1, 150 mM NaCl, 1 mM EDTA pH 8, in ddH_20.

Washing buffer: 0.5 % Triton X-100, 50 mM Tris-HCl pH 8.1, 150 mM NaCl, 5 mM EDTA pH 8, in ddH_20.

TE buffer: 10 mM Tris-HCl pH 8.1, 5 mM EDTA pH 8, in ddH_20.

Elution buffer: 100 mM $NaHCO_3$, 50 mM Tris-HCl pH 8.1, 150 mM NaCl, 1 % SDS, in ddH_20.

4.8.3 Assay for Transposase-Accessible Chromatin (ATAC)

For ATAC-seq sample preparation, I adapted the protocol published by Buenrostro and co-workers to primary B cells (Buenrostro et al. 2015). Specifically, I performed the set-up of the biochemical and library preparation part (described in 4.10.4) to get good quality samples also starting from a non-homogenous and resting cell population such as splenic B cells.

For the characterization of PRC1-proficient and -deficient resting B cells, cells were FACS-sorted as described previously in 4.7.1. $1x10^5$ cells were transferred in a new tube, washed with 500 µl of ice-cold 1X PBS and resuspended in 300 µl of Lysis buffer, incubated at 4 ˚C for 15 min. Tubes were flicked every 5 min. Cells were centrifuged and washed twice with Lysis buffer. The nuclei pellet was then resuspended in 20 µl of Tagmentation mix. Tubes were incubated in a Thermomixer Compact (Eppendorf®) at 37 ˚C, 300 rpm, for 40 min.

DNA was then purified by Qiagen Minelute kit according to the manufacturer's protocol. DNA was eluted in 12 µl and stored at -20 ˚C until library preparation. Each centrifugation was performed at 500 g, 4 ˚C, 10 min.

Lysis buffer: 10 mM Tris-HCl pH 7.4, 10 mM NaCl, 3 mM $MgCl_2$, 0.01 % IGEPAL (CA-630), in ddH_20.

Tagmentation mix (per each sample): 10 µl 2x TD buffer, 2 µl Transposase (Illumina), 8 µl nuclease free H_20.

4.9 Molecular biology techniques

4.9.1 RNA and DNA extraction

For cell pellets or sorted cells, total RNA and DNA was extracted using Qiagen RNeasy AllPrep Micro Kit following the manufacturer's protocol. This kit enables the separate elution of total RNA and genomic DNA from one cell pellet.

For microRNA detection and quantification, total miRNAs were extracted from cell pellets using Qiagen miRNeasy Mini Kit following the manufacturer's protocol.

4.9.2 cDNA synthesis

Complementary DNA (cDNA) was produced using SuperScript™ III Reverse Transcriptase Kit (ThermoFisher Scientific) following the manufacturer's protocol. Specifically, 50-100 µg of RNA were incubated with Mix 1 (Table 10) at 65 ˚C for 5 minutes, then chilled on ice for 1 minute. Mix 2 (Table 10) was added to the reaction mix. Reaction was performed according to the program indicated in Table 11. Eventually, cDNA was used for PCR or RT-qPCR (real-time quantitative PCR).

Table 10. cDNA synthesis reagents.

Mix 1	Final volume (µl)
Random primers	1

10 mM dNTP mix	1
Nuclease-Free Water	to 13
Mix 2	Final volume (µl)
10X RT buffer	2
25 mM $MgCl_2$	4
0.1 M DTT	2
RNase OUT™ (40 U/µl)	1
SuperScript™ III RT (200 U/µl)	1
Total	20

Table 11. cDNA synthesis conditions.

Temperature (˚C)	**Time (min:sec)**
25	5:00
50	60:00
72	15:00
4	hold

4.9.3 PCR

For gene amplification, PCR was performed using GoTaq® DNA Polymerase (Promega) following the manufacturer's protocol. Specifically, 1.5 µl of cDNA were mixed with PCR reagents in Table 12. Primers and annealing temperature (T_A) used are listed in Table 13, while PCR conditions are summarized in Table 14.

Table 12. PCR reagents.

Component	**Final volume (µl)**
5X Green GoTaq® Reaction Buffer	5
PCR Nucleotide Mix, 10 mM each	1
Forward primer, 10 µM	0.25
Reverse primer, 10 µM	0.25
GoTaq® DNA Polymerase (5u/µl)	0.25
Template cDNA	1.5
Nuclease-Free Water	16.75
Total	25

Table 13. Primers used for PCR and annealing temperatures.

PCR product	Primer ID	Sequence	T_A
Ptprc exons 2-7	Ptprc Ex2 Fw	CCTTTGGATTTGCCCTTCTGGACA	58˚ C
	Ptprc Ex7 Rv	TGCTTCGTTGTGGTAGCTATGG	

Table 14. PCR conditions.

Temperature (˚C)	Time (min:sec)	
94	2:00	
94	0:30	x 40 cycles
58	0:30	
72	0:30	
72	5:00	
4	hold	

4.9.4 Real time quantitative PCR (RT-qPCR) reaction and analysis

For gene expression analysis RT-qPCR was performed using 1 µl of cDNA, 500 nM primers mix and 10 µl of LightCycler® 480 SYBR Green I Master containing Hot-start polymerase (Roche) in a final volume of 20 µl per reaction in 96-well format. Reaction conditions are indicated in Table 15. The same conditions were used in qPCR performed on 15 ng of DNA to measure allelic deletions. Accumulation of fluorescent products was monitored using a LightCycler® 96 Real-Time PCR System (Roche). *Rplp0* (cDNA analyses) or *Gapdh* (DNA analyses) were used as control house-keeping genes for normalization. Transcript fold enrichment was calculated by DDct method.

Table 15. RT-qPCR conditions.

Temperature (˚C)	Time (min:sec)	
95	5:00	
95	0:10	x 45 cycles
60	0:10	
72	0:10	
to 95 (melting curves)		

To measure the deletion efficiency (DE) of Ring1B lox-P flanked exon 2, RT-qPCR analysis was performed on genomic DNA. Ring1BΔ primers were used to detect remaining Ring1B exon 2 and primers annealing to *Gapdh* gene used as a loading control. DE was calculated as DE (%) = 100 % - retained exon 2 (%) for Ring1B$^{fl/fl}$. Primers are listed in Table 16.

Table 16. Primers used for RT-qPCR and target molecules.

PCR product	Primer ID	Sequence	Target molecule
Dtx1	Dtx1 Fw	GCCACATGTATCACCTGCTC	cDNA
	Dtx1 Rv	ATGGCTTTGCAGGTTGGA	
Hes1	Hes1 Fw	AGGTGACCCGCTTCCTGT	cDNA
	Hes1 Rv	TCTGGGTCATGCAGTTGG	
Klf2	Klf2 Fw	CGGCACGGATGAGGACCTAAAC	cDNA
	Klf2 Rv	TCGGGAGGATTTTCGGCG	
S1pr1	S1pr1 Fw	GTGTAGACCCAGAGTCCTGCG	cDNA
	S1pr1 Rv	AGCTTTTCCTTGGCTGGAGAG	
Bcl2	Bcl2 Fw	TGAAGCGGTCCGGTGGATAC	cDNA
	Bcl2 Rv	GGCGGCGGCAGATGAATTAC	
Bcl-XL	Bcl-XL Fw	CACTGTGCGTGGAAAGCGTA	cDNA
	Bcl-XL Rv	CTCGGCTGCTGCATTGTTCC	
Mcl-1	Mcl-1 Fw	GGACGACCTATACCGCCAGT	cDNA
	Mcl-1 Rv	CGGAGCATGCCCTGGAAG	
Puma	Puma Fw	ATGCCTGCCTCACCTTCATCT	cDNA
	Puma Rv	AGCACAGGATTCACAGTCTGGA	
Noxa	Noxa Fw	GAGTTGTGACAAGTCAACACAAACC	cDNA
	Noxa Rv	GAAGATAAAGCGTAACAGTTGTAAGATAACC	
Bim	Bim Fw	GAGTTGTGACAAGTCAACACAAACC	cDNA
	Bim Rv	GAAGATAAAGCGTAACAGTTGTAAGATAACC	
Bax	Bax Fw	TGAAGCGGTCCGGTGGATAC	cDNA
	Bax Rv	GGCGGCGGCAGATGAATTAC	
Cd154	Cd154 Fw	AGCAAGCCAAGTGATCCACAGA	cDNA
	Cd154 Rv	ATAGGGAAGACTGCCAGCATCA	
Il8	Il8 Fw	TTCCACCGGCAATGAAGCTTCT	cDNA
	Il8 Rv	GGTCTCCCGAATTGGAAAGGGAAA	
p15	p15 Fw	GCAGGCCTTCCAAAACTTGA	cDNA
	p15 Rv	AGCTGCAGAAAATGCGTAGGA	

p16	p16 Fw	CAATGTCCTGTGACGTTTGG	cDNA
	p16 Rv	GGCTTCAGCAGACCTTCTGCT	
p18	p18 Fw	AAATGGATTTGGGAGAACTGC	cDNA
	p18 Rv	AAATTGGGATTAGCACCTCTGA	
p21	p21 Fw	CCACAGCGATATCCAGACATTC	cDNA
	p21 Rv	CGGAACAGGTCGGACATCA	
p27	p27 Fw	CAGACAATCCGGCTGGGTTA	cDNA
	p27 Rv	GCCCTTTTGTTTTGCGAAGA	
p57	p57 Fw	CGAGGAGCAGGACGAGAATC	cDNA
	p57 Rv	GAAGAAGTCGTTCGCATTGGC	
Prdm1	Prdm1 Fw	GACGGGGGTACTTCTGTTCA	cDNA
	Prdm1 Rv	GGCATTCTTGGGAACTGTGT	
Pax5	Pax5 Fw	ATGGCCACTCACTTCCGGGC	cDNA
	Pax5 Rv	GTCATCCAGGCCTCCAGCCA	
Ptprc ex4	Exon 4 Fw	TTCTGCCTCAAAGTGACCCCTTAC	cDNA
	Exon 4 Rv	TGTGGTCTCTGAAGAGCCATTTCC	
Ptprc ex5	Exon 5 Fw	AGGAGCTGACACTCAGACAT	cDNA
	Exon 5 Rv	GTGAGTGTGGGATTGTCAGCTT	
Ptprc ex6	Exon 6 Fw	ATTCCTGCAGACACAGCCTTTC	cDNA
	Exon 6 Rv	TCTGTGGTGCTGACATTGGA	
Ptprc ex7	Exon 7 Fw	CAGCCTCACAACTCTTACACCATC	cDNA
	Exon 7 Rv	TATGGTTGTGCTTGGAGGGTCAGT	
Rplp0	Rplp0 Fw	TTCATTGTGGGAGCAGAC	cDNA
	Rplp0 Rv	CAGCAGTTTCTCCAGAGC	
Ring1bΔ	R1bΔ Fw	GTTCCATTTGTCTGCACAGCCTGAGA	gDNA
	R1bΔ Rv	AGATGCTGAAGACTGGAGGGGTGT	
Gapdh	Gapdh Fw	AGCGCTGACCTTGAGGTCTCCTTG	gDNA
	Gapdh Rv	GTTGCCTACGCAGGTCTTGCTGAC	

4.9.5 Quantitative RT-qPCR for microRNA

miRNA-125b-5p was quantified using TaqMan® MicroRNA Assay (Applied Biosystems) and the specific probe hsa-miR-125b (A/N MI0000446). Reverse transcription was carried out using the TaqMan® MicroRNA Reverse Transcription Kit (A/N 4366596) according to the manufacturer's instructions. Each reaction contained 15 ng DNase-treated RNA as template. Real-time qPCR was performed using TaqMan Universal PCR Master Mix as

recommend by the manufacturer. Sno135 was used as control house-keeping snRNA for normalization (A/N TM001230). Transcript fold enrichment was calculated by DDct method. Accumulation of fluorescent products was monitored using a 7900 HT Fast Real-Time PCR System (ThermoFisher Scientific).

4.9.6 Gel purification

PCR reactions were loaded on 0.8 % agarose gel added with DNA dye (GelRed® Nucleic Acid Gel Stain, Biotium). Samples and DNA ladder (100 bp DNA ladder, Promega) were electrophoresed at 100 V for 2 hours, then detected using the Chemidoc™ XRS + imaging System (Biorad). Image analysis was performed using the Image Lab™ 5.2.1 software tool. PCR amplicons were excised from agarose gel and purified using Qiagen Gel extraction kit (Qiagen) according to the manufacturer's instructions. DNA was eluted in 20 µl.

4.10 Sequencing techniques

4.10.1 Sanger sequencing

DNA obtained by gel purification was sequenced by Sanger sequencing by using the same primers used for cDNA amplification, listed in Table 13.

4.10.2 RNA-sequencing

Cells were FACS-sorted as described previously in 4.7.1. Total RNA was purified from cells using the All prep DNA/RNA micro kit (Qiagen). RNA was quantified with a microvolume UV spectrophotometer (NanoDrop ND-100). 500 ng/sample of total RNA were used to prepare cDNA libraries for strand-specific RNA sequencing with Ion Total RNA Seq kit v2 (ThermoFisher Scientific). Sequencing reactions was performed with an Ion Proton™ instrument (Ion Torrent, ThermoFisher Scientific).

4.10.3 ChIP-sequencing

Immunoprecipitated DNA was used to prepare libraries for sequencing with Library preparation kit for Ion Torrent (KAPA Biosystem). DNA concentration of ChIP-seq libraries was quantified with Qubit HS ds DNA assay (ThermoFisher Scientific). Bioanalyzer 2100 (Agilent Technologies) run was performed to assess the size distribution of ChIP-seq libraries and possible contaminations by adapter dimers. Sequencing reactions were performed on Ion ProtonTM instrument (Ion Torrent, ThermoFisher Scientific).

4.10.4 ATAC-sequencing

Libraries were created by amplifying DNA first for 9 cycles with NEBNext High Fidelity enzyme (New Englan Biolabs) and Nextera PCR barcoded primers, using reagents and conditions listed in Table 17 and Table 18. Then, PCR products was purified with AMPure XP beads (Agencourt), with 0.65X and 1.8X beads ratio. Briefly, 32.5 µl of AMPure XP beads were added to 50 µl PCR reaction. After mixing carefully, tubes were incubated at RT for 5 min and magnetized for 4 min. The supernatant was transferred to a new tube, containing 57.5 µl of AMPure XP beads. After mixing carefully, tubes were incubated at RT for 4 min and magnetized for 4 min. Supernatant was discarded and beads were washed twice with 80 % ethanol. Tubes were air-dried at RT for 4 min, then beads resuspended in 22 µl of EB buffer. After magnetizing for 4 min, the supernatant containing eluted DNA was transferred into a new tube. The second PCR reaction was performed using 10 µl of eluted DNA and the same conditions described for the previous PCR, with 5 cycles of amplification. Final PCR products were purified with AMPure XP beads (Agencourt), with 2X beads ratio. For this, 70 µl of AMPure XP beads were added to 50 µl PCR reaction. After mixing carefully, tubes were incubated at RT for 5 min and magnetized for 4 min. Supernatant was discarded and beads were washed three times with 80 % ethanol. Tubes were air-dried at RT for 4 min, then beads resuspended in 22 µl of EB buffer. After magnetizing for 4 min, the supernatant containing eluted DNA was transferred into a new tube. DNA concentration of ATAC-seq libraries was quantified with Qubit HS ds DNA assay (ThermoFisher Scientific). 1 µl of each sample was run on Bioanalyzer 2100 (Agilent) using High Sensitive

DNA kit (Agilent) for quality control. Libraries were sequenced with HiSeq 2500, 100 bp PE, with a coverage of 30 million reads per sample.

Table 17. PCR reagents for ATAC-seq library preparation.

Component	Final volume (µl)
2X NEBNext High Fidelity PCR Master Mix	25
Nextera PCR Ad1_no MX primer, 25 mM	2.5
Nextera PCR Ad2.n barcoded primer, 25 mM	2.5
Template DNA	10
Nuclease-Free Water	10
Total	50

Table 18. PCR conditions for ATAC-seq library preparation.

Temperature (˚C)	Time (min:sec)	
72	5:00	
98	0.30	
98	0:10	x 9 or 5 cycles
63	0:30	
72	1:00	

4.11 Bioinformatic analyses

4.11.1 Bioinformatic analyses on RNA-seq data

Reads were aligned to the mouse mm10 transcriptome using TopHat version 2.1.1 (Trapnell, Pachter, and Salzberg 2009). Differentially expressed genes (DEGs) were called with DESeq2 (Love, Huber, and Anders 2014) using the read counts per transcripts calculated by HTSeq (Anders, Pyl, and Huber 2015). Only genes with a False Discovery Rate (FDR) < 0.05 and $\log_2$ fold change > +0.25 or < -0.25 were defined as DEGs. Unsupervised hierarchical clustering and heatmaps were made with the R/Bioconductor package pheatmap (Raivo Kolde (2018). R package version 1.0.1. (https://CRAN.R-project.org/package=pheatmap). For sashimi plots, RNA-seq reads aligned to the mouse

mm10 genome using Bowtie 2 (Langmead and Salzberg 2012) and were analysed using IGV_2.4.8 (Broad Institute).

4.11.2 Bioinformatic analyses on ChIP-seq data

Reads were aligned, -end-to-end, to the mm10 genome using Bowtie 2 version 2.2.9 (Langmead and Salzberg 2012). To identify genomic regions enriched for H3K27me3 (peaks) in immunoprecipitated samples relative to the input samples, we used MACS2 (version 2.1.1) (Zhang et al. 2008) with default parameters, broad option. Target genes were defined according to the presence of a peak in an interval of +/- 1.5 kb around the TSS.

4.11.3 Bioinformatic analyses on ATAC-seq data

Reads of minimum length of 50 bp were aligned to the mouse reference genome mm10 with Bowtie 2 version 2.2.9 (Langmead and Salzberg 2012), with the parameters -end-to-end and -X2000 which allowed to map fragments of length up to 2 kilobases. Reads marked as unmapped, as PCR or optical duplicates, with multiple alignments, with quality score < 30 and mapping to mitochondrial chromosome were removed. Peaks were called with MACS2 (version 2.1.1) (Zhang et al. 2008) setting the parameters –nomodel—shift 37—extsize 73. Peaks mapping to a set of regions known to give false positive were filtered out. Target genes were defined according to the presence of a peak in an interval of +/- 1.5 kb around the TSS.

4.11.4 Enhancer analysis

Genomic regions defined enhancer are endowed with the following requirements: 1) peak of H3K27ac1+, using the broad peaks called in $CD19^+$ resting wild-type B cells extended of 100 bp at each end before their intersection with the intersectBed utility of BEDTools v2.27.1 (Quinlan and Hall 2010); 2) peak of H3K4me1+, using the narrow peaks called in $CD19^+$ resting wild-type B cells extended of 100 bp at each end before their intersection with the

intersectBed utility of BEDTools v2.27.1 (Quinlan and Hall 2010); 3) not mapping in promoters (TSS +/- 5 kb); 4) FANTOM5 mouse enhancers. The mm9 robust phase 1 and 2 CAGE peaks for mouse enhancers were downloaded from FANTOM5 (Lizio et al. 2015) (http://fantom.gsc.riken.jp/5/tet/#!/sources) and subsequently converted to the mouse genome mm10 assembly with the liftOver utility of the UCSC Genome Browser. The target genes of FANTOM5 enhancers mapping within the H3K27ac+/H3K4me1+ regions in both $PRC1^{+/+}$ and $PRC1^{-/-}$ $CD19^{+}$ B cells were defined by identifying the closest TSS with the closest utility of BEDTools v2.27.1 (Quinlan and Hall 2010).

4.11.5 Intersection of RNA-seq, ChIP-seq and ATAC-seq data

Venn diagrams displaying the overlap among different list of genes were produced using the VennDiagram package (Chen and Boutros 2011) (https://CRAN.R-project.org/package=VennDiagram). Enrichment analyses and pathways analyses were performed using the EnrichR tool (Chen et al. 2013; Kuleshov et al. 2016) (http://amp.pharm.mssm.edu/Enrichr/). The Gene lists provided by EnrichR were ranked based on the p-value.

4.12 Statistical analysis

Statistical analysis of normally distributed values (Gaussian) was performed by two-tailed unpaired Student's t-test. Mann-Whitney test was applied in case of non-normal distribution, whereas Welch test was used for unequal variances. Chi-squared test was used to test different distribution of B and T cells in bone marrow chimeras. Differences were considered significant at *p-value* < 0.05.

5. Results

5.1 The PRC1 complex regulates B cell homeostasis and maturation in secondary lymphoid organs

5.1.1 Targeting PRC1 function in mature B cells in the mouse model

To study the role of PRC1 in peripheral B cell maturation, given the diversity of PRC1 complexes, we decided to inactivate them all through the inhibition of the catalytic activity of the complex. To this aim, we considered a series of data available in our laboratory at the time of the start of the project. First, it was shown that the Ring1A catalytic subunit of PRC1 is dispensable for embryogenesis and post-natal life (del Mar Lorente et al. 2000). Moreover, our laboratory had shown that Ring1A mutant mice display normal B cell development and germinal center responses (Dr. Federica Alberghini, PhD thesis work). Second, we observed that conditional inactivation of the other PRC1 catalytic subunit Ring1B, using the Cr2-Cre strain, was dispensable for peripheral B cell maturation. Most importantly, mice mutants in B cells for either of the two E3 ligases contributing to PRC1 function displayed normal levels of Histone H2A lysine-119 mono-ubiquitylation (L. D'Artista master thesis; Dr. F. Alberghini, PhD thesis work). The latter result suggested functional redundancy between Ring1B and Ring1A in B cells, which is in line with previous evidences obtained from the analysis of other cell types (Roman-Trufero et al. 2009; Posfai et al. 2012; de Napoles et al. 2004).

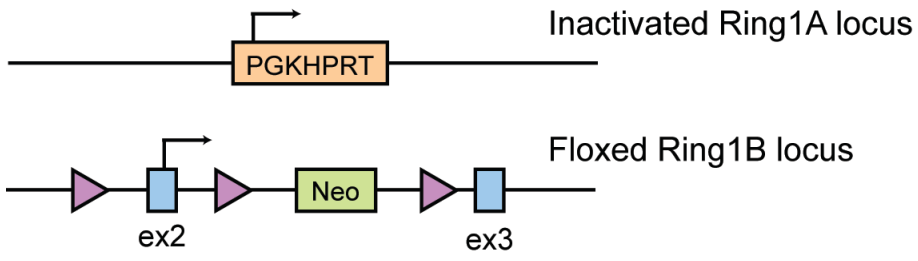

Figure 12. Structure of conditional Ring1A-null and Ring1B alleles in PRC1 mutant mice.

Schematic representation of the inactivated Ring1A allele ($Ring1A^{-}$) and of the floxed Ring1B locus ($Ring1B^{fl}$).

To overcome this, we developed a PRC1 conditional knock-out mouse model in which a germline *Ring1A* mutation (Ring1A^{KO} or Ring1A^{-}) was combined to a conditional *Ring1B/Rnf2* knock-out allele (Ring1B^{fl}) (Figure 12). Inactivation of PRC1 in late transitional B cells was achieved using the *Cd23-Cre* BAC transgene (Kwon et al. 2008). In the latter strain, the Cre transgene is under the control of *Cd23/FcεRII* regulatory regions, leading to recombinase expression starting from late, T2 stage, immature B cells. This approach allowed us to follow immature B cells lacking PRC1 function in their commitment to differentiate into the three major subsets of mature B cells (Figure 13), namely Follicular (FO)/B-2, Marginal Zone (MZ) B and B-1 B cells.

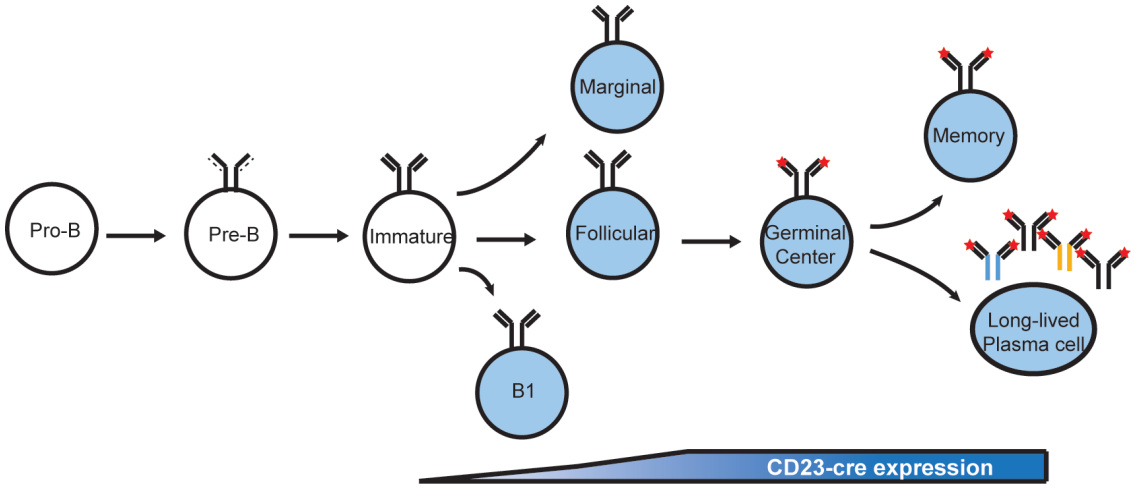

Figure 13. Schematic view of B cell development and timing of CD23-Cre mediated deletion.

In blue are indicated the mature B cell subsets in which the activation of Cre, under the control of *Cd23* gene, induces the recombination of LoxP sites flanking exon 2 of Ring1B alleles. This genetic recombination ultimately inhibits the expression of RING1B protein.

Quantitative PCR performed on genomic DNA retrieved from splenic CD19^{+} B cells of representative *Ring1A*$^{-/-}$; *Ring1B*$^{fl/fl}$; *Cd23-cre*, compound mutant animals displayed close-to-complete Cre-mediated recombination at the *Ring1B*^{fl} locus (Figure 14). In line with these results, immunoblotting analyses revealed over 70% reduction in RING1B protein levels, and around 50% less H2AK119 mono-ubiquitylation when compared to control wild-type and to Ring1A knock-out B cells (Figure 15).

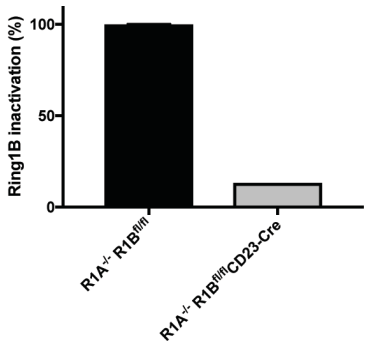

Figure 14. Ring1B allele inactivation in conditional mutant mice.

Genomic qPCR analysis to quantify *Ring1B* gene copy number in CD19^{+} splenic B cells purified from R1A$^{-/-}$R1B$^{fl/fl}$ and R1A$^{-/-}$R1B$^{fl/fl}$CD23-Cre mutant mice (n=3). Data are normalized to *Gapdh* gene and shown as relative to R1A$^{-/-}$R1B$^{fl/fl}$ control sample.

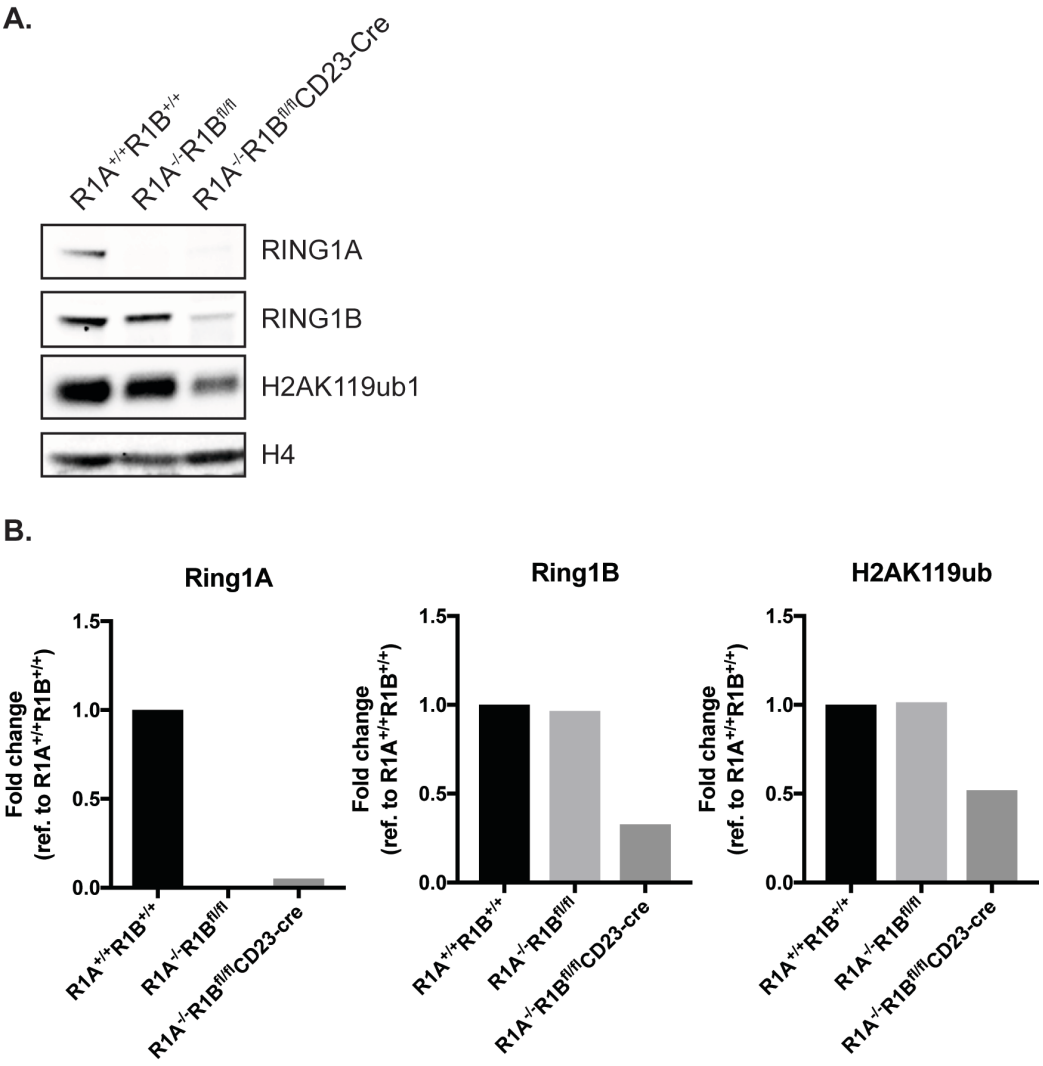

Figure 15. Verification of the mouse model.

A. Immunoblotting analysis and **B.** quantification of RING1A, RING1B protein and H2AK119ub1 histone mark levels in purified CD19^{+} B cells of representative R1A$^{+/+}$R1B$^{+/+}$ control, R1A$^{-/-}$R1B$^{fl/fl}$ and R1A$^{-/-}$R1B$^{fl/fl}$CD23-Cre mutant mice. H4 was used as loading control.

These results indicate that inactivation of PRC1 is achieved in the vast majority of B cells present in the spleen of *Ring1A*$^{-/-}$*; Ring1B*$^{fl/fl}$*; Cd23-Cre* mice. Hereafter the latter animals will be referred to as PRC1$^{-/-}$ mice and will be compared to PRC1$^{+/+}$ control animals, which will carry only the *Cd23-Cre* transgene (Figure 16).

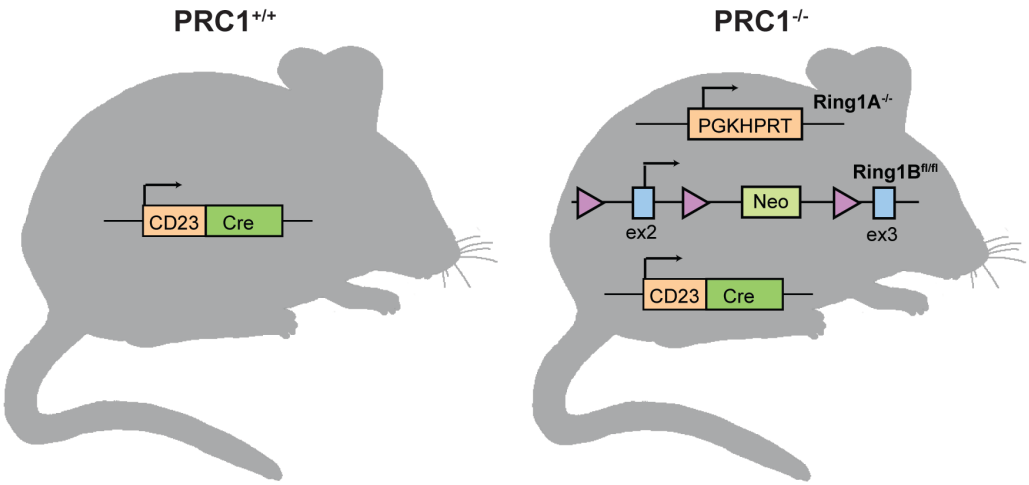

Figure 16. Genetic background of the mice used in the experiments.

Schematic representation of the control (CD23-Cre) and PRC1 mutant mice (Ring1A$^{-/-}$Ring1B$^{fl/fl}$CD23-Cre) used in the experiments. Hereafter, the mice will be referred to as PRC1$^{+/+}$ and PRC1$^{-/-}$, respectively.

5.1.2 PRC1 sustains B cell homeostasis in secondary lymphoid organs

Flow cytometric analysis of cell suspensions retrieved from secondary lymphoid organs (SLOs) revealed lower frequencies and absolute numbers of CD19^{+} B cells in the spleen and in Peyer's patches of PRC1$^{-/-}$ mice when compared to controls (Figure 17). For lymph nodes and peritoneal cavity, CD19^{+} B cells frequencies were reduced, whereas the trend was maintained for absolute numbers although the difference was not significant.

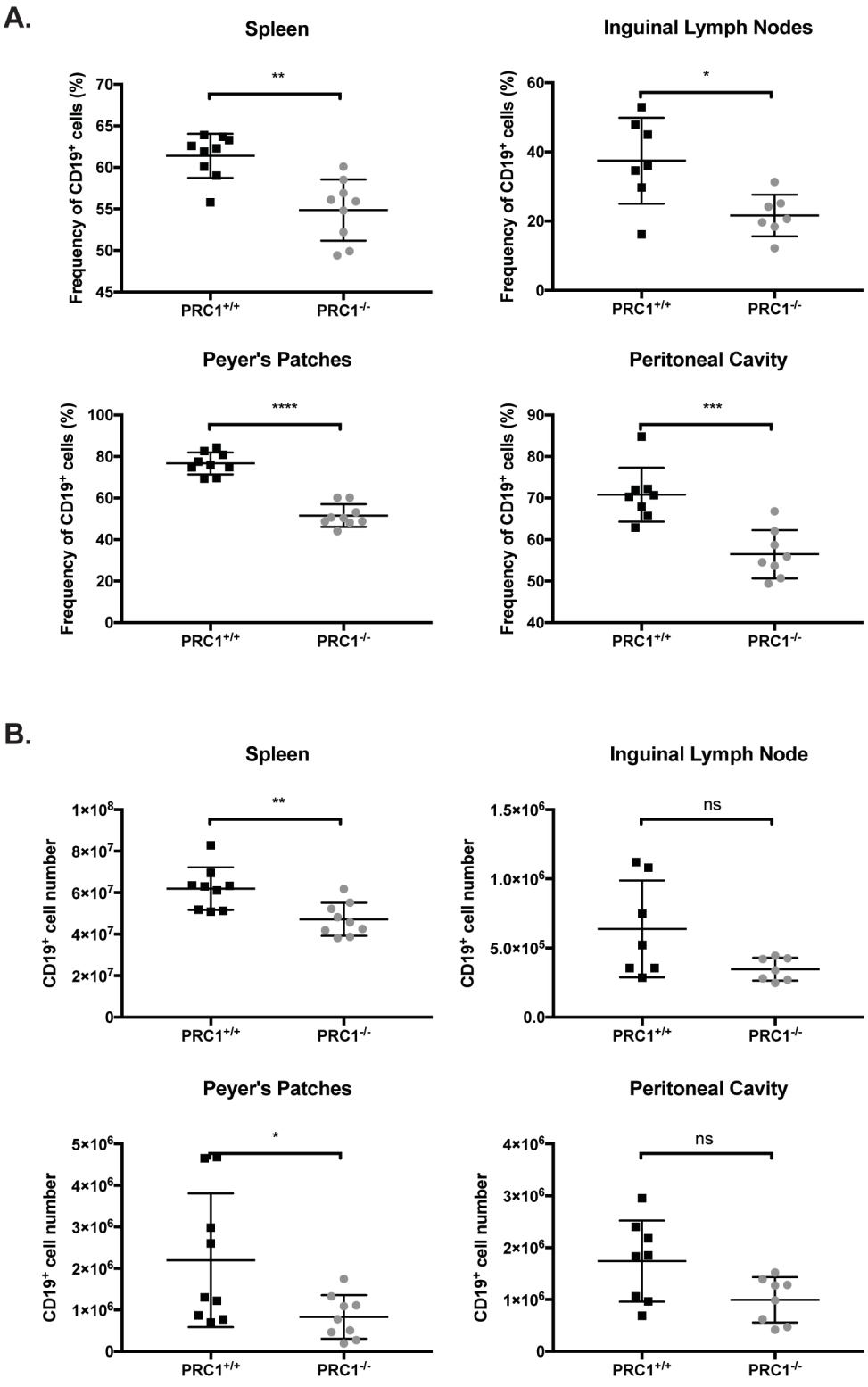

Figure 17. Absolute numbers and frequencies of CD19⁺ B cells in secondary lymphoid organs of control and mutant animals.

A. Frequencies and **B.** absolute numbers of gated CD19⁺ B cells of PRC1$^{+/+}$ control and PRC1$^{-/-}$ mutant mice in animals from 4 to 8-months of age. Bars represent the mean value ± SD. Mann-Whitney non-parametric test: * p<0.05; ** p<0.01; *** p<0.001; **** p<0.0001; ns = not significative.

Instead, in the bone marrow, we failed to score differences between mice of the two PRC1 genotypes, in line with the fact that the Cd23-cre transgene is yet not active in the majority of the B cells residing in these sites (Figure 18).

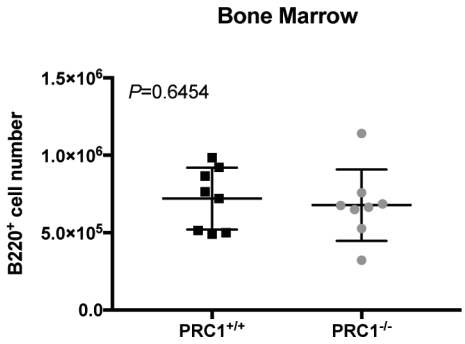

Figure 18. Absolute numbers of B220⁺ B cells are not altered in bone marrow of mutant animals.

Absolute numbers of gated B220⁺ B cells of PRC1$^{+/+}$ control and PRC1$^{-/-}$ mutant mice in animals from 4 to 8-months of age. Bars represent the mean value ± SD. P value is indicated within the plot (Mann-Whitney non-parametric test).

Overall, these data indicate that acute ablation of PRC1 complex starting from late transitional B cells alters their distribution in SLOs.

5.1.3 PRC1 deficiency alters the surface phenotype of peripheral B cells and their full maturation

To obtain a better understanding of the effects of PRC1 inactivation in developing B cells, I performed a comprehensive immunophenotypical analysis, using flow cytometry technology, staining with a combination of fluorescent-labelled antibodies cell suspensions retrieved from several SLOs. In the spleen of PRC1 mutant mice, resting B cells expressed the surface markers CD19, major histocompatibility complex of class II (MHC-II) and BAFF receptor (BAFF-R) to similar levels than their wild-type counterparts (Figure 19A). similar levels of expression were found also for the immature B cell marker HSA/CD24. Surprisingly, the same mutant B cells expressed, however, at higher levels than controls the immature B cell markers CD93/AA4.1 (Figure 19B).

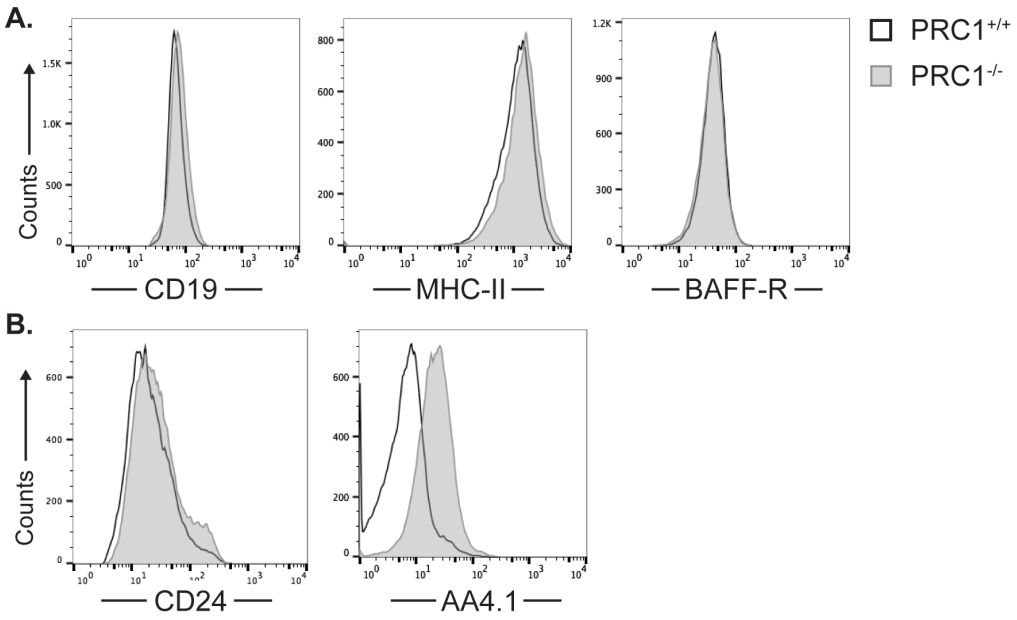

Figure 19. Levels of surface markers associated to mature and immature stages of development in PRC1-proficient and -deficient splenic B cells.

Representative flow cytometric expression of surface markers **A.** CD19, major histocompatibility complex class II (MHC-II) and BAFF receptor (BAFF-R) and **B.** CD24 and AA4.1 on CD19^{+} splenic B cells from PRC1$^{+/+}$ control (dark line) or PRC1$^{-/-}$ mutant animals (light grey line and fill). Data are representative of 9 independent experiments.

Moreover, surface IgM and IgD expression patterns revealed consistent differences between PRC1 control and mutant B cells. Specifically, in PRC1$^{-/-}$ splenic B cells the fraction of IgM^{+} IgD^{+} as well IgM^{+} IgD^{lo} B cells were increased in comparison to control B cells, whereas the more mature IgD^{+} IgM^{lo} B cells were overrepresented in the control B cell population (Figure 20).

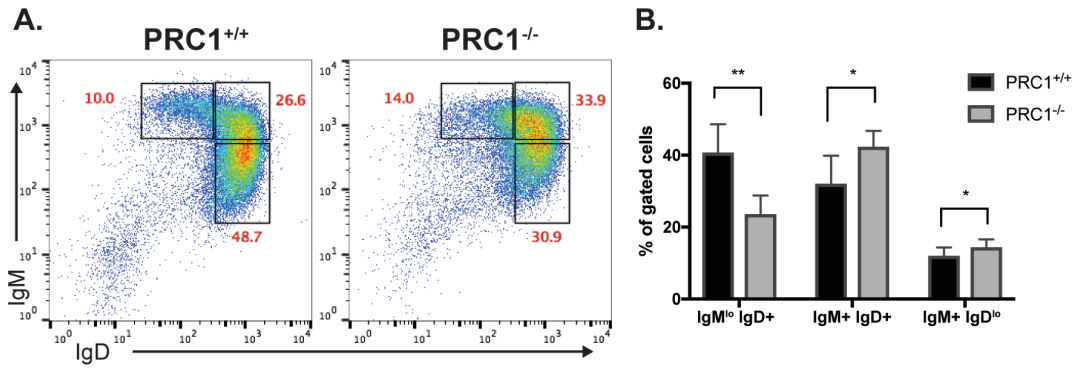

Figure 20. PRC1-deficient animals are characterized by an unbalance between IgM/IgD surface expression.

A. Representative flow cytometric analysis of splenic CD19^{+} B cell subsets from control PRC1$^{+/+}$ (left) and PRC1$^{-/-}$ mutant animals (right). Data are representative of 6

independent experiments. Numbers in red represent the frequencies of gated cells. **B.** Frequencies of IgM^{lo} IgD^{+}, IgM^{+} IgD^{+} and IgM^{+} IgD^{lo} gated CD19^{+} splenic B cells. Bars represent the mean values ± SD. Data are form 6 independent experiments. Mann-Whitney non-parametric test: * $p<0.05$; ** $p<0.01$; ns = not significative.

These observations suggest an overall disturbance imposed by PRC1 inactivation on the expression of the full repertoire of surface markers defining a bona fide mature B cell. Moreover, inactivation of PRC1 appears to prevent a correct temporal regulation in the expression of markers associated to consecutive stages of B cell differentiation, with mutant B cells expressing at the same time both immature and mature B cell markers.

To further explore the molecular basis of the developmental disturbance suffered by PRC1 mutant B cells, I compared RNA-seq data generated from sorted splenic B220^{+} AA4.1^{+} immature and B220^{+} AA4.1^{-} mature control B cells to that of the entire population of CD19^{+} PRC1$^{-/-}$ B cells (most of which express high AA4.1 levels). I performed unsupervised hierarchical clustering analysis on the three RNA-seq datasets, selecting a gene signature distinguishing (q value < 0.05) immature from mature wild-type B cells. Despite clustering closer to mature B cells, PRC1-deficient B cells retained similar expression as immature B cells for a substantial number of genes of the signature (Figure 21).

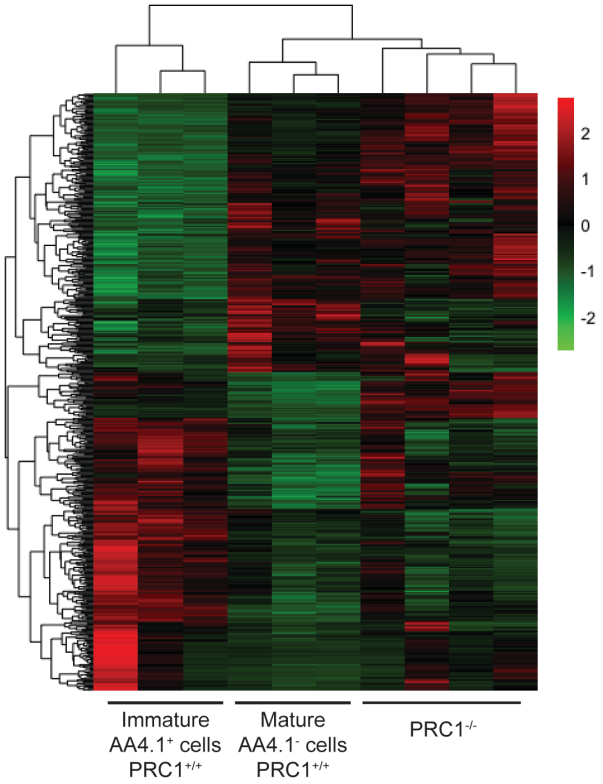

Figure 21. PRC1-deficient B cells show an expression profile in between immature and mature wild-type B cells.

Hierarchical clustering and heat map of 930 genes differentially expressed ($p<0.05$) between $CD19^+B220^+AA4.1^+$ immature and $CD19^+B220^+AA4.1^-$ mature control B cells (n=3) from $PRC1^{+/+}$ animals and of $CD19^+$ splenic B cells (n=4) from $PRC1^{-/-}$ mice. Expression values are relative to the median expression value across all samples (log_2 scale).

These results are coherent with the immunophenotypical analyses and together with the latter data, suggest that late transitional B cells losing PRC1 function can progress to become mature B cells. However, such transition is accompanied with an inefficient repression of transcriptional programs typical of the immature B cells. Interestingly, PRC1 mutant B cells reactivated a substantial set of genes expressed at high levels in embryonic and hematopoietic stem cells (Figure 22). This result points to a role for PRC1 in sustaining the identity of a differentiated somatic cell by ensuring stable repression of gene programs active in pluripotent and/or totipotent stem cells.

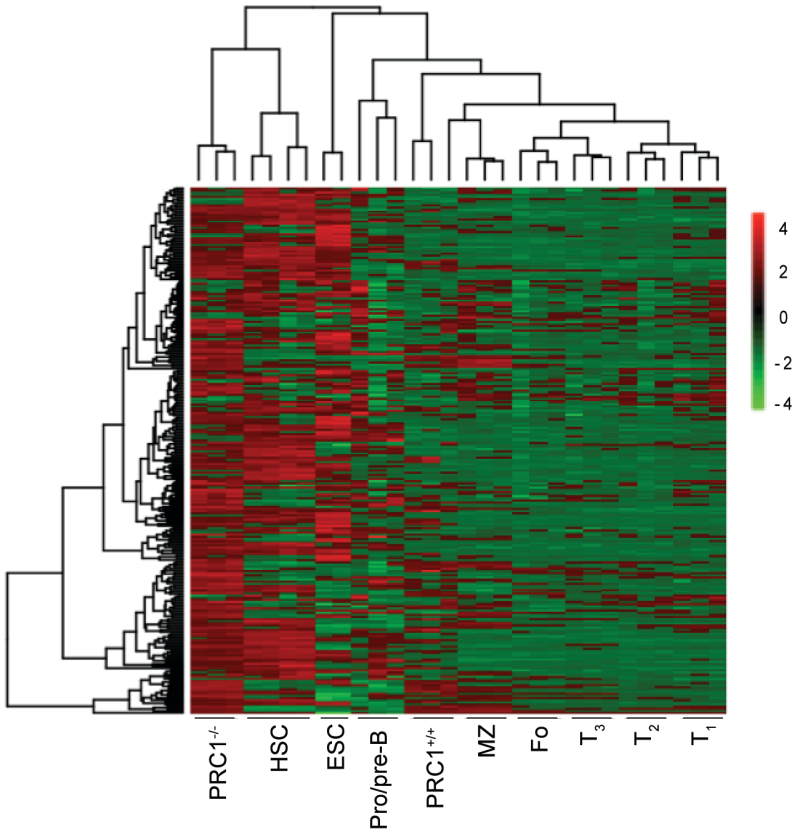

Figure 22. PRC1-deficient B cells up-regulate stem cell genes.

Hierarchical clustering and heat map of up-regulated genes ($p<0.05$, log_2 fold change > 0.25) in $PRC1^{-/-}$ $CD19^+$ cells when compared to $PRC1^{+/+}$ $CD19^+$ cells among

hematopoietic stem cells (HSC), embryonic stem cells (ESC), progenitor B cells (Pro-B $B220^{+}IgM^{-}CD43^{+}CD25^{-}$ and Pre-B $B220^{+}IgM^{-}CD43^{-}$), splenic B cells ($CD19^{+}$), marginal ($CD19^{+}CD23^{lo}CD21^{+}$; MZ) and follicular zone ($CD19^{+}CD23^{hi}CD21^{-}$; Fo) cells and transitional cells (T1 $B220^{+}AA4.1^{+}IgM^{hi}CD23^{-}$; T2 $B220^{+}AA4.1^{+}IgM^{hi}CD23^{+}$; T3 $B220^{+}AA4.1^{+}IgM^{lo}CD23^{+}$). Expression values are relative to the median expression value across all samples (log_2 scale).

5.1.4 PRC1 mutant B cells display altered B220 expression

Together with the atypical co-expression of immature and mature B cell markers, PRC1 mutant B cells displayed aberrant levels of the pan-B cell marker B220. Specifically, in all SLOs of PRC1 mutant mice, $CD19^{+}$ B cells belonged to two major subsets represented respectively by $B220^{+}$ and $B220^{lo}$ cells (Figure 23).

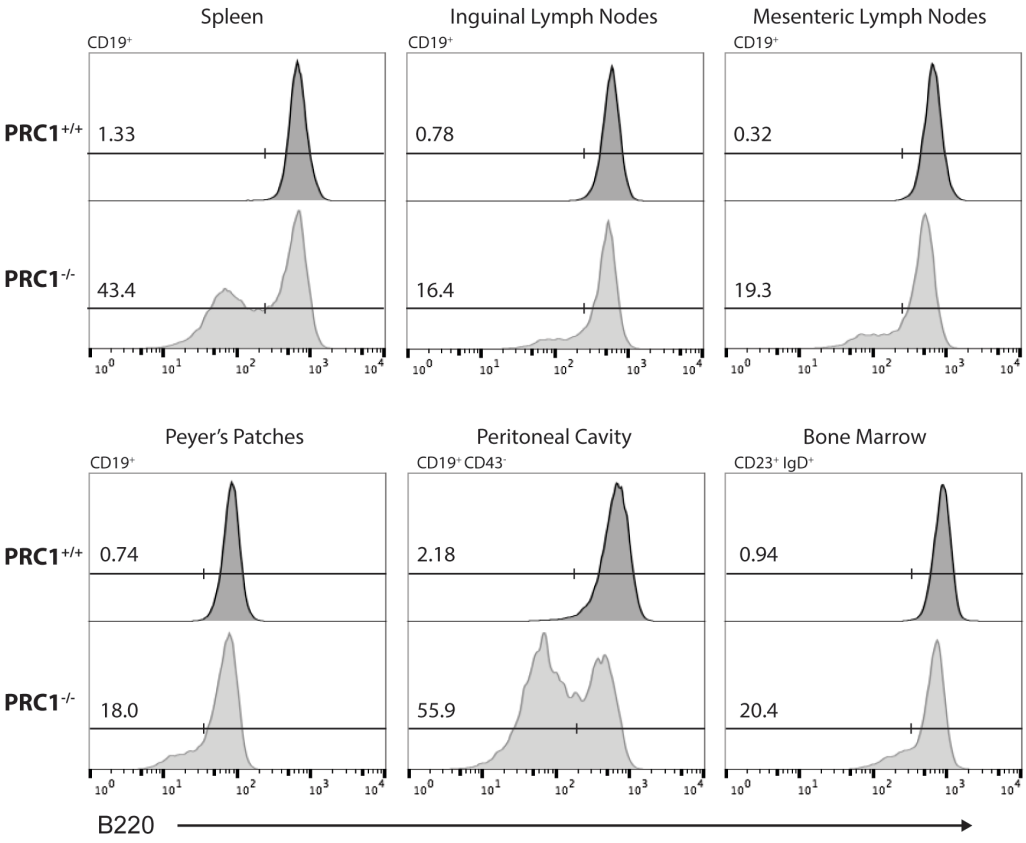

Figure 23. $B220^{lo}$ B cells are present in all secondary lymphoid organs.

Representative flow cytometric expression of the surface marker B220 in gated $CD19^{+}$ cells in spleen, inguinal and mesenteric lymph nodes and Peyer's patches, in $CD19^{+}$ $CD43^{-}$ gated cells in peritoneal cavity and in $CD23^{+}$ IgD^{+} gated cells in the bone marrow. Numbers represent the frequency of $B220^{lo}$ cells in the gated population. Data are representative of 9 independent experiments.

Interestingly, whereas B220^{+} mutant splenic B cells, as their control counterparts, mainly consisted of IgM^{lo} IgD^{+} B cells, PRC1-defective B220^{lo} cells where mostly IgM/IgD double positive B cells (Figure 24). Hence, lower B220 expression in PRC1 mutant B cells correlates with a more immature B cell phenotype.

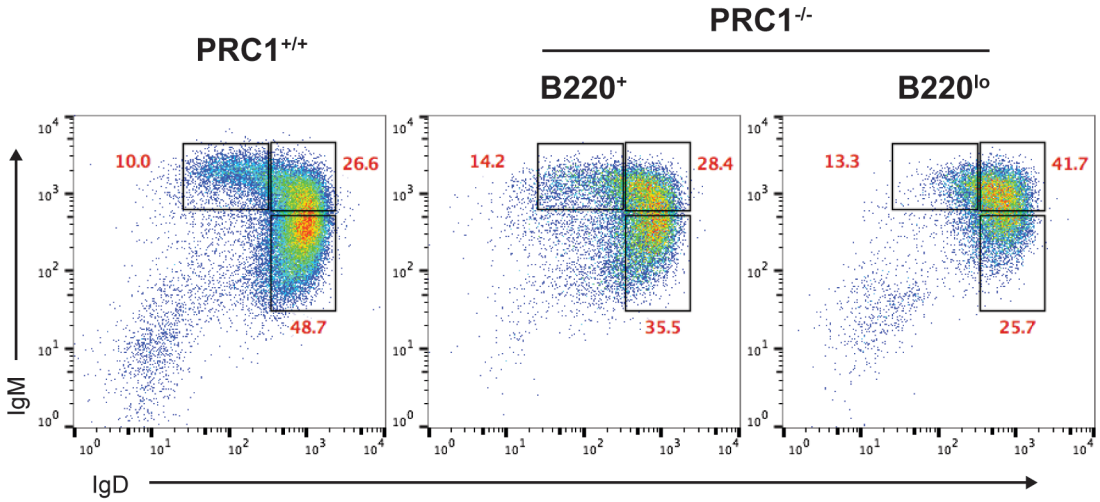

Figure 24. B220^{lo} cells are mainly IgM IgD double positive.

Flow cytometric analysis of IgM and IgD isotype expression on the surface of CD19^{+} cells, sub-gated in B220^{+} (middle) and B220^{lo} (right) in PRC1$^{-/-}$ mutant mice. Numbers indicate the frequency of the gated populations. Data are representative of 6 independent experiments.

To investigate the determinant(s) responsible for the differences in B220 levels seen among PRC1 mutant B cells, the B220^{+} and B220^{lo} subsets were isolated by cell-sorting from the spleen of PRC1 deficient mice, in parallel with the splenic B220^{+} B cell population of controls. From these cells, both genomic DNA and protein lysates were prepared. Quantitative genomic PCR revealed comparable efficiency in Cre-mediated recombination at the *Ring1b*^{fl} locus between the B220^{+} and B220^{lo} subsets of PRC1 mutant B cells (Figure 25A). Instead, immunoblotting analyses revealed a close-to-complete loss of RING1B protein expression and a strong decrease in global H2AK119ub1 levels only in B220^{lo} B cells (Figure 25B, C, D).

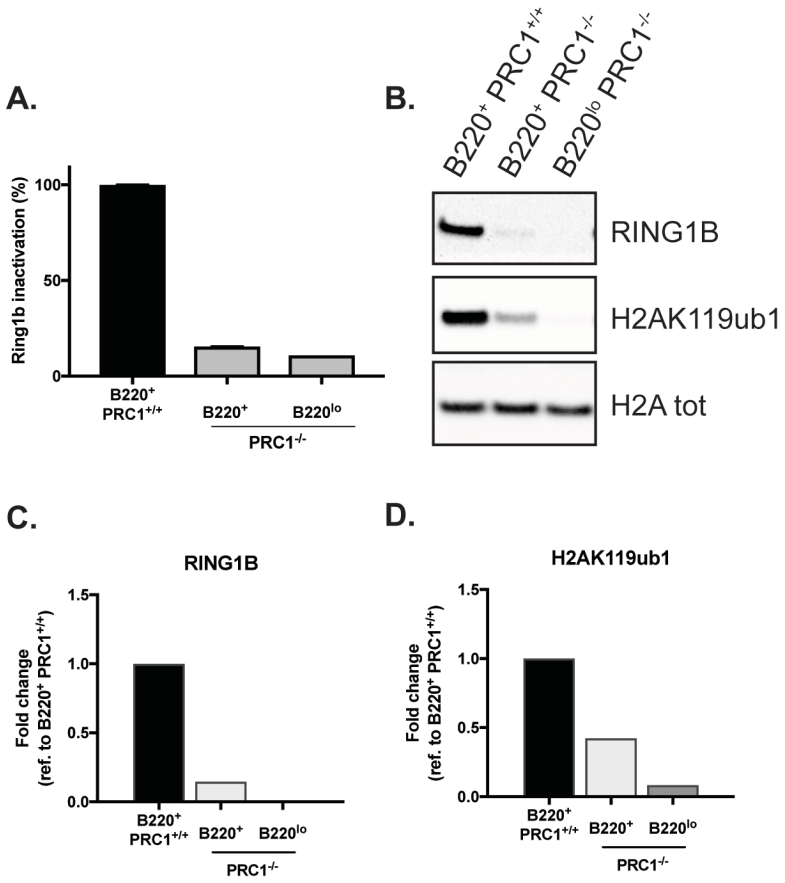

Figure 25. B220^{lo} PRC1$^{-/-}$ B cells are deleted for Ring1B also at the protein level.

A. Genomic qPCR analysis to quantify *Ring1B* gene copy number in CD19^{+} B220^{+} and CD19^{+} B220$^{+/lo}$ splenic B cells sorted from PRC1$^{+/+}$ and PRC1$^{-/-}$ mice, respectively (n=3). Data are normalized to *Gapdh* gene and shown as relative to PRC1$^{+/+}$ control sample. **B.** Immunoblotting analysis and **C-D.** quantification of RING1B protein and H2AK119ub1 histone mark levels in sorted CD19^{+} B cells of representative PRC1$^{+/+}$ control and PRC1$^{-/-}$ mutant mice. H2A was used as loading control. Data are representative of 3 independent experiments.

These results, are compatible with a scenario in which B220^{lo} cells derive from B220^{+} PRC1 mutant B cells as a result of full extinction of RING1B protein expression. In the same two B220 B cell subsets found in PRC1 mutant mice, I also measured by immunoblotting analysis the global levels of H3K27me3 catalyzed by the PRC2 complex. Quantification of the data gave an unexpected result. Indeed, H3K27me3 levels consistently dropped in the B220^{+} fraction of PRC1 mutant B cells when compared to controls. Instead, in the B220^{lo} subset H3K27me3 levels returned more similar to those of control B cells (Figure 26).

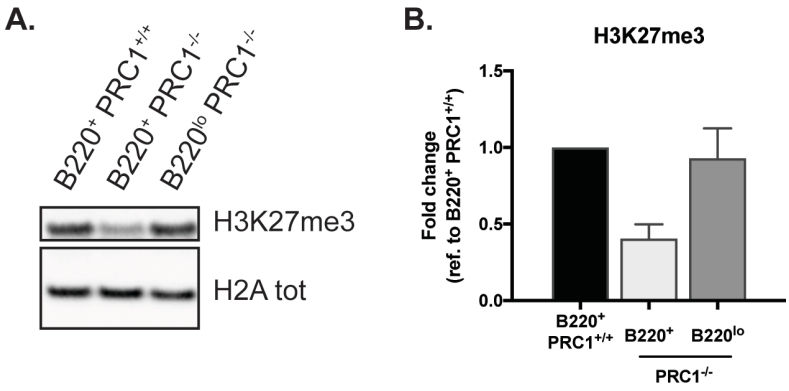

Figure 26. Global H3K27me3 is reduced in B220^{+} cells of PRC1-deficient mice and re-gained in B220^{lo}.

A. Immunoblotting analysis and **B.** quantification of H3K27me3 histone mark levels in sorted CD19^{+} B cells of representative PRC1$^{+/+}$ control and PRC1$^{-/-}$ mutant mice. H2A was used as loading control. Data are representative of 2 independent experiments.

These findings were confirmed by measuring H3K27me3 levels in the various PRC1 control and mutant B cell subsets by intracellular flow cytometric analysis (Figure 27).

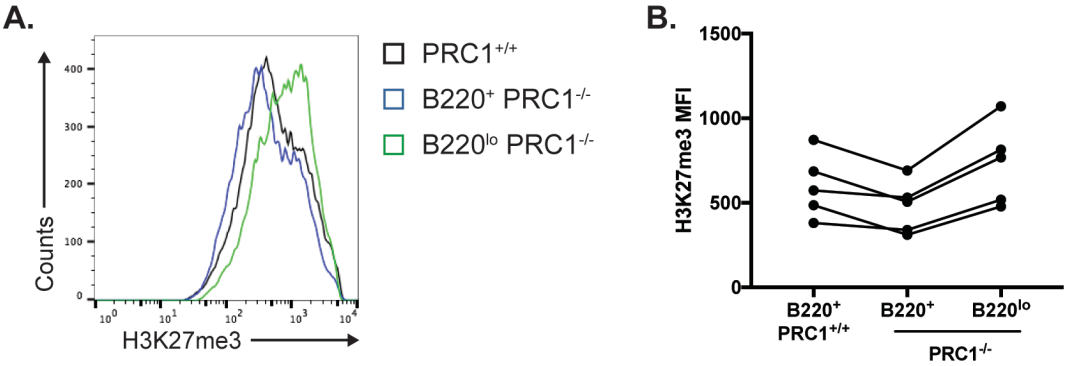

Figure 27. Global H3K27me3 is reduced in B220^{+} cells of PRC1-deficient mice and increased in B220^{lo} compared to controls.

A. Representative flow cytometric expression of H3K27me3 histone mark in gated B220^{+} CD19^{+} splenic B cells from control PRC1$^{+/+}$ mice (black line) or B220$^{+/lo}$ CD19^{+} splenic B cells from PRC1$^{-/-}$ mutant animals (blue and green line, respectively). Data are representative of 5 independent experiments. **B.** Mean fluorescence intensity (MFI) of H3K27me3 histone mark (n=5). Lines join data acquired on the same day by flow cytometry.

These results together with the data on RING1B protein levels suggest that PRC2 activity is transiently reduced in newly generated PRC1 mutant B cells, while it is restored (possibly as a result of a compensatory mechanisms) in PRC1 mutant B cells displaying a more complete inhibition of PRC1 activity.

To investigate in more detail the relationship between B220^{+} and B220^{lo} PRC1 mutant B cells, the latter subsets were purified together with control B cells from the spleen by cell-sorting and cultured *in vitro* for several days in the presence of B-cell activating factor (BAFF) to sustain their survival. Flow cytometric analyses performed on consecutive days of the *in vitro* culture revealed that B220^{+} control B cells as well as B220^{lo} B cells from PRC1 mutant mice retained the same B220 levels. Instead, strikingly, B220^{+} PRC1 mutant B cells showed a gradual decrease in the levels of B220 over the eleven days of *in vitro* culture (Figure 28). These data support the hypothesis that PRC1 mutant B220^{lo} cells derive from their B220^{+} counterparts, whereas the contrary does not likely occur.

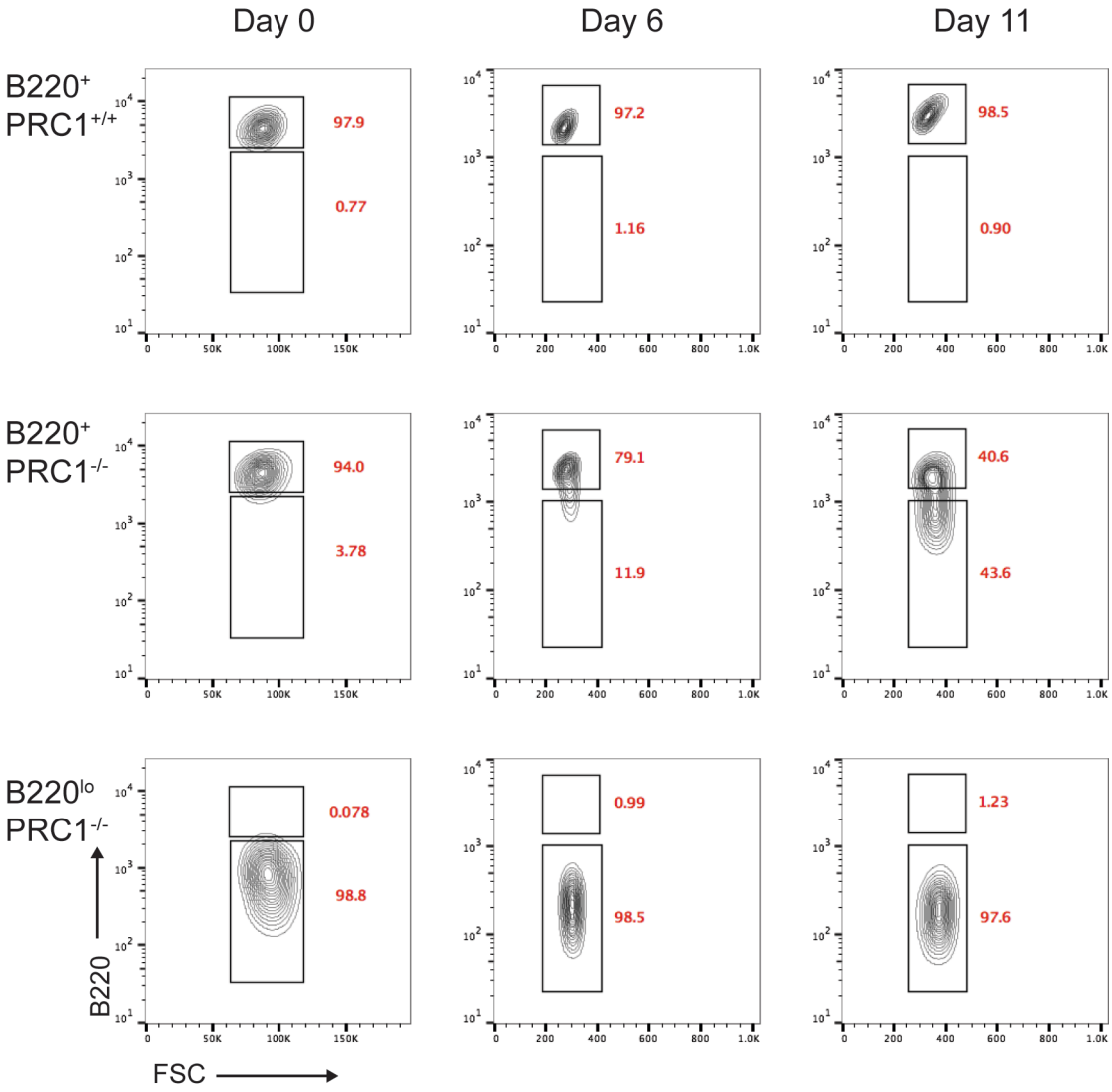

Figure 28. B220^{lo} can derive from B220^{+} of PRC1-deficient animals over time.

Flow cytometric analysis of B220 surface marker expression in sorted B220^{+} B cells from PRC1$^{+/+}$ control animals (n=2) and in sorted B220^{+} and B220^{lo} B cells from PRC1$^{-/-}$ mutant animals (n=2). Cells were cultured *in vitro* with 50 ng/ml of BAFF and

analysed 0, 6 and 11 days after sorting. Numbers represent the frequencies of $B220^{+}$ and $B220^{lo}$ gated cells. Data are representative of 2 independent experiments.

To understand the correlation between the acquisition of a $B220^{lo}$ phenotype and the loss of PRC1, I measured by immunoblotting analysis RING1B and H2AK119ub1 levels in $B220^{+}$ PRC1 mutant B cells, at the onset of the *in vitro* culture and eight days later. For both proteins we observed a clear reduction in the expression levels comparing B cells from day-0 and day-8 of *in vitro* culture (Figure 29). The unperturbed expression of RING1B and H2AK119ub1 in PRC1-proficient B cells cultured for eight days excludes any effect of the *in vitro* culture conditions on RING1B and H2AK119ub1 expression.

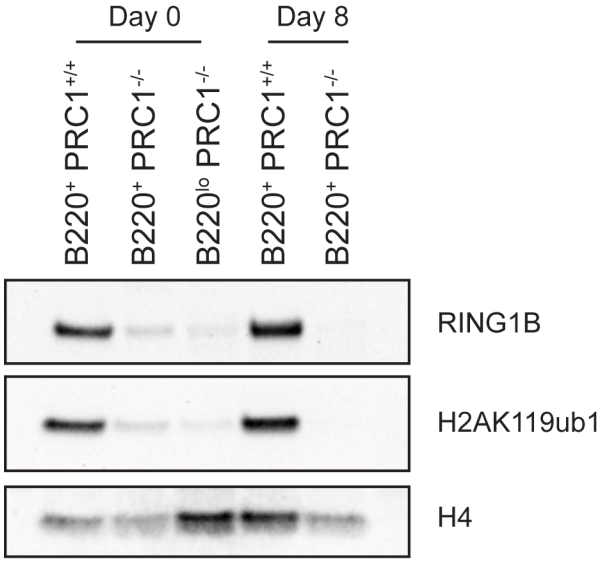

Figure 29. $B220^{+}$ of PRC1-decient animals loose RING1B protein and H2AK119ub1 histone mark over time.

Immunoblotting analysis of RING1B protein and H2AK119ub1 histone mark levels in sorted $B220^{+}$ B cells from $PRC1^{+/+}$ control animals (n=2) and in sorted $B220^{+}$ and $B220^{lo}$ B cells from $PRC1^{-/-}$ mutant animals (n=2). Cells were cultured *in vitro* with 50 ng/ml of BAFF and analysed 0 and 8 days after sorting. Data are representative of 2 independent experiments.

In summary, our data indicate that $B220^{+}$ PRC1 mutant B cells do not represent a steady-state population but rather a subset which continuously evolves into a $B220^{lo}$ derivative with stronger reduction in RING1B and H2AK119ub1 levels, and hence with a higher degree of PRC1 inactivation. The finding that in PRC1 conditional mutant mice, $B220^{+}$ B cells already display a number of immunophenotypic alterations suggests that the developmental defects

resulting from PRC1 inhibition precede the down-regulation of B220 and don't require full extinction of PRC1 activity.

Finally, our findings identify B220 as a useful marker to monitor at single cell resolution the fraction of PRC1 mutant B cells with the strongest inhibition of PRC1 activity.

5.2 Peripheral B cell differentiation in the absence of PRC1

To understand how PRC1 inactivation may affect later peripheral B cell differentiation, we performed an immunophenotypical characterization, by flow cytometry, of the three main mature B cell subsets, namely FO, MZ and B-1 B cells. Whereas FO and MZ B cells were analysed in the spleen of control and mutant animals, B-1 B cells were retrieved from peritoneal cavity lavages. In the spleen of PRC1 mutant mice, we found on $CD19^{+}$ B cells a substantial alteration in the expression levels of the CD23/FcεRII and CD21/CR2 markers. Specifically, PRC1 defective B cells expressed CD23 and CD21 levels lower than FO and MZ B cells, respectively (Figure 30).

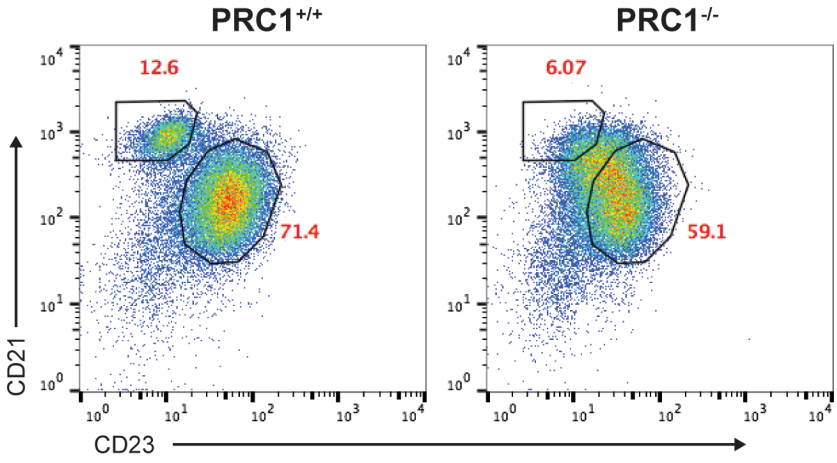

Figure 30. Follicular and marginal zone mature B cells are affected by the lack of PRC1.

Representative flow cytometric analysis of splenic follicular ($CD19^{+}$ $CD23^{+}$ $CD21^{lo}$) and marginal zone ($CD19^{+}$ $CD23^{lo}$ $CD21^{hi}$) B cell subsets from control $PRC1^{+/+}$ (left) and $PRC1^{-/-}$ mutant animals (right). Data are representative of 8 independent experiments. Numbers represent the frequencies of gated cells.

Based on gates set on splenic B cells of PRC1$^{+/+}$ mice, in the spleen of PRC1$^{-/-}$ mice we observed a substantial reduction in the fractions of FO (CD19^{+} CD23^{+} CD21^{lo}) and MZ (CD19^{+} CD23^{lo} CD21^{hi}) B cells (Figure 31A). This decrease, combined with a reduction in the frequency of total CD19^{+} splenic B cells, reveals a detrimental effect of PRC1 inactivation on the size of both the FO and MZ B cell subsets (Figure 31B).

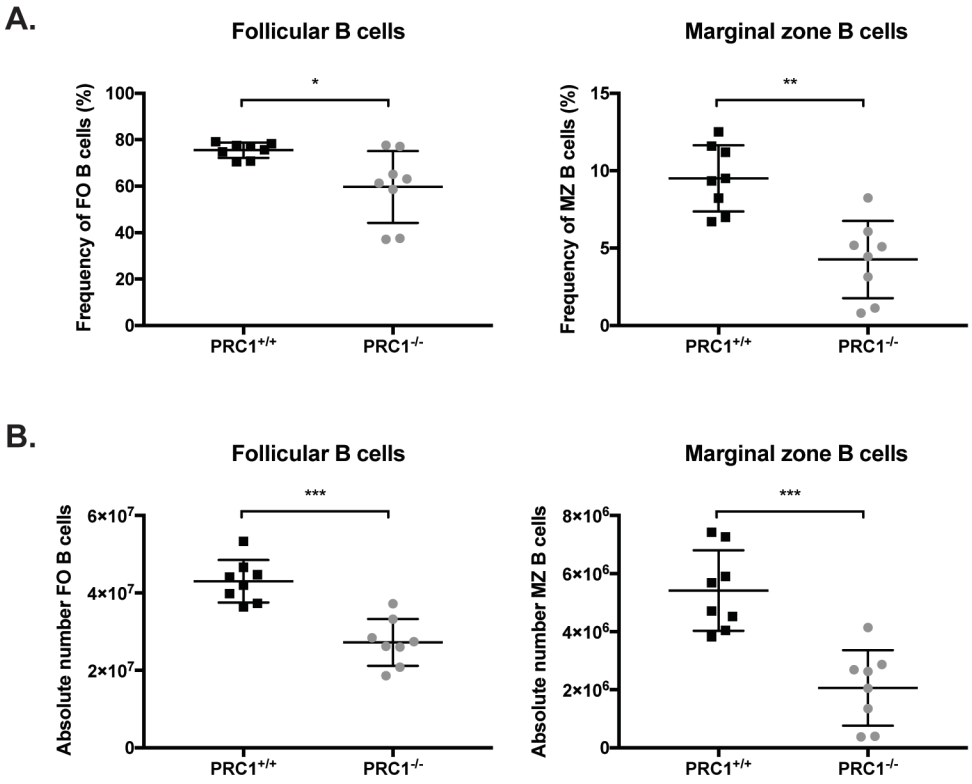

Figure 31. Frequencies and absolute numbers of splenic mature B cells are decreased in PRC1 mutant animals.

A. Frequencies and **B.** absolute numbers of gated follicular (CD19^{+} CD23^{+} CD21^{lo}) and marginal zone (CD19^{+} CD23^{lo} CD21^{hi}) mature B cells of PRC1$^{+/+}$ control and PRC1$^{-/-}$ mutant mice in spleen of animals from 4 to 8-months of age. Bars represent the mean value ± SD. Mann-Whitney non-parametric test: * $p<0.05$; ** $p<0.01$; *** $p<0.001$.

In the peritoneal cavity, CD23 levels in PRC1 mutant B-2 B cells were comparable to those of controls, with frequencies of both B-1 (CD19^{+} CD23^{-}) and B-2 (CD19^{+} CD23^{+}) B cells slightly altered compared to those of PRC1 controls (Figure 32).

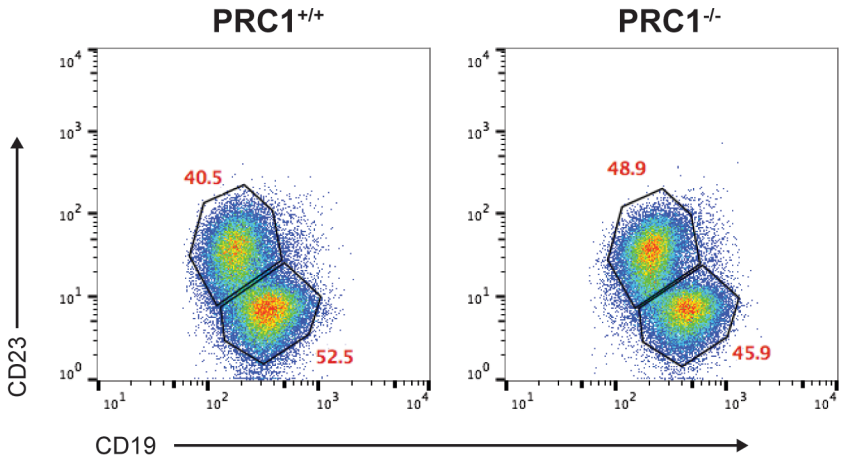

Figure 32. B-1 mature B cells are not affected by the lack of PRC1.

Representative flow cytometric analysis of B-1 ($CD19^+$ $CD23^-$) and B-2 ($CD19^+$ $CD23^+$) B cell subsets in peritoneal cavity from control $PRC1^{+/+}$ (left) and $PRC1^{-/-}$ mutant animals (right). Data are representative of 7 independent experiments. Numbers represent the frequencies of gated cells.

Given the changes in B220 levels suffered by PRC1 mutant B cells, we chose not to use this marker for assigning B cells respectively to the B-1 and B-2 B cell populations in the peritoneum. As shown in Figure 33, the frequency and absolute numbers of B-1 and B-2 B cells in PRC1 mutant mice were reduced, although not significantly.

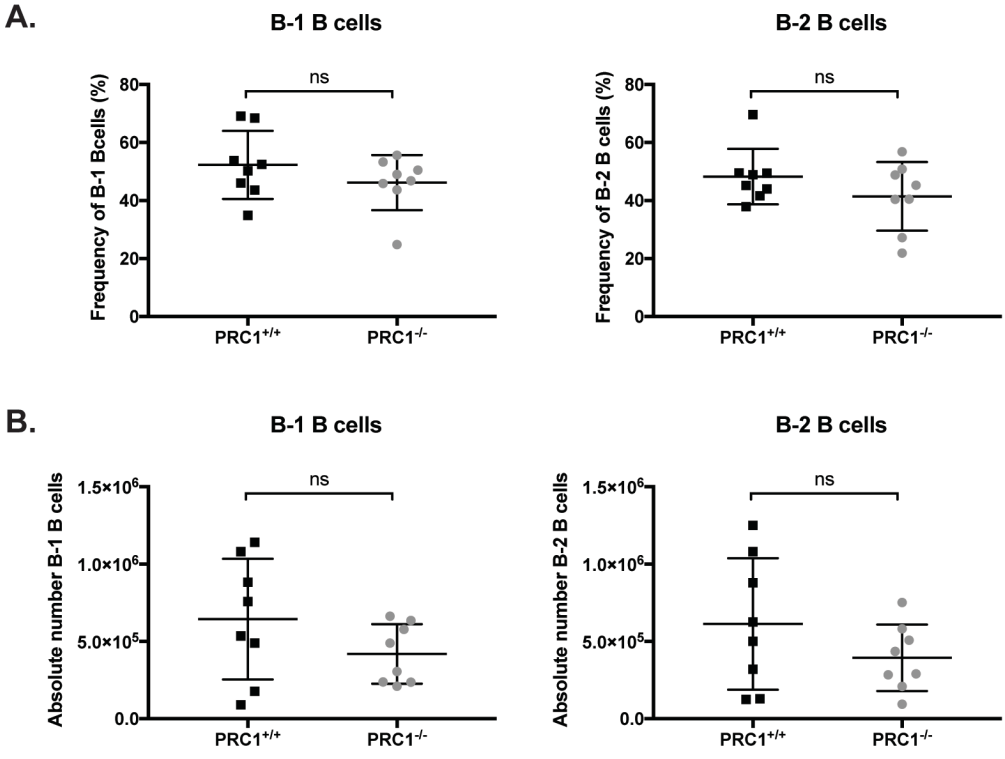

Figure 33. The lack of PRC1 marginally affects B cell development in the peritoneal cavity.

A. Frequencies and **B.** absolute numbers of gated B-1 ($CD19^+$ $CD23^-$) and B-2 ($CD19^+$ $CD23^+$) mature B cells of $PRC1^{+/+}$ control and $PRC1^{-/-}$ mutant mice in peritoneal cavity of animals from 4 to 8-months of age. Bars represent the mean value ± SD. Mann-Whitney non-parametric test: ns = not significative.

B-1 B cells can be classified respectively in B-1a and B-1b B cells according to the levels of CD5 expression. Interestingly, PRC1 mutant mice displayed a higher contribution of B-1a ($CD19^+$ $CD23^-$ $CD5^+$) B cells to the whole population of peritoneal cavity B-1 B cells than the controls (Figure 34 and Figure 35A).

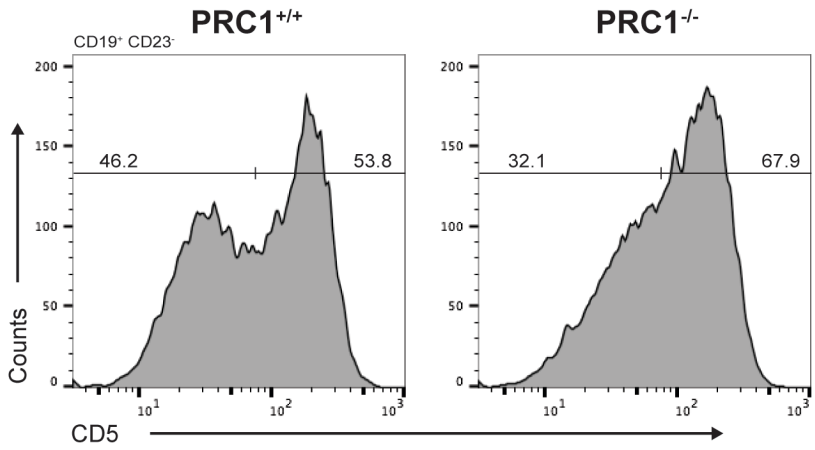

Figure 34. B-1a and B-1b mature B cells are affected by the lack of PRC1.

Representative flow cytometric analysis of B-1a ($CD19^+$ $CD23^-$ $CD5^+$) and B-1b ($CD19^+$ $CD23^-$ $CD5^-$) among B-1 B cells in peritoneal cavity from control $PRC1^{+/+}$ (left) and $PRC1^{-/-}$ mutant animals (right). Cells were pre-gated on $CD19^+$ $CD23^-$ cells. Data are representative of 6 independent experiments. Numbers represent the frequencies of gated cells.

In line with the general reduction of B-1 B cells seen in the peritoneum of PRC1 mutant B cells, the numbers of B-1a and B-1b B cells were reduced when compared to controls, with the B-1b subset suffering from a stronger decrease (Figure 35B).

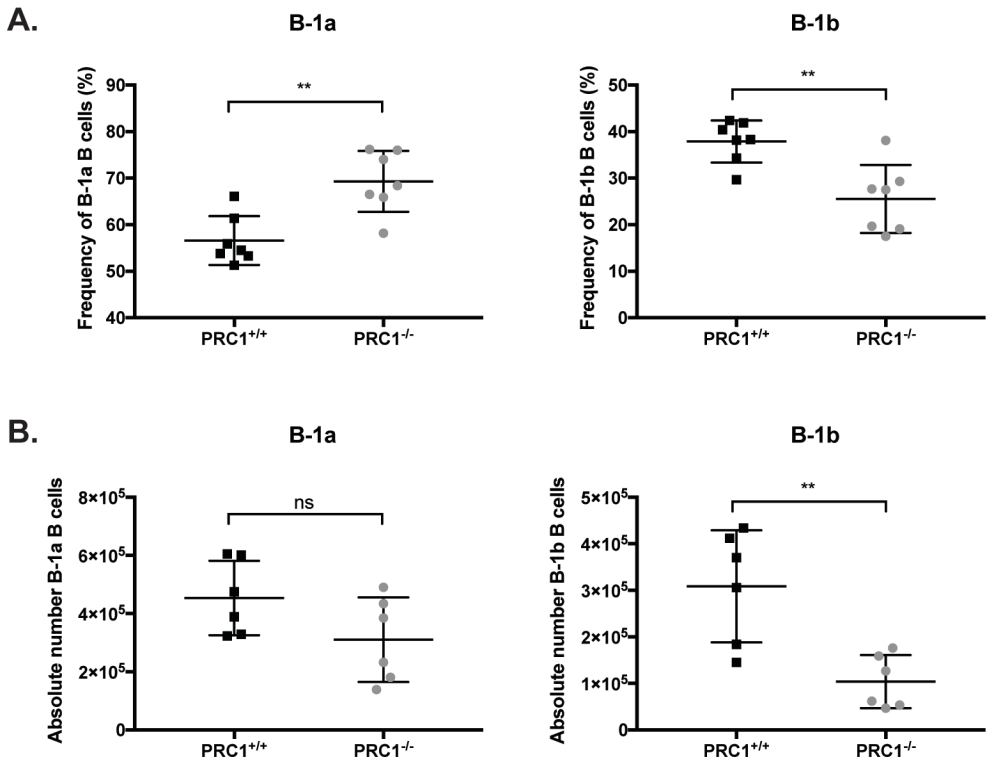

Figure 35. B-1b cells frequencies and absolute numbers are decreased in PRC1 mutant animals.

A. Frequencies and **B.** absolute numbers of gated B-1a ($CD19^+$ $CD23^-$ $CD5^+$) and B-1b ($CD19^+$ $CD23^-$ $CD5^-$) B cells of $PRC1^{+/+}$ control and $PRC1^{-/-}$ mutant mice in animals from 4 to 8-months of age. Bars represent the mean value ± SD. Mann-Whitney non-parametric test: ** $p<0.01$; ns = not significative.

Overall, these results suggest that upon PRC1 inactivation in late immature B cells, their differentiation into the three main mature B cell subsets is substantially disturbed.

5.2.1 Reduced B cells with a marginal zone surface phenotype in PRC1 conditional mutant mice

Among the PRC1 mutant mature B cell subsets, the MZ B population suffered from the strongest impairment. To exclude that the reduction in the MZ B cell subset was due to changes in the expression of the Cr2/CD21 marker, we extended the flow cytometric analysis of MZ B cells assessing the status of the CD1d and CD38 surface markers. As observed for CD21, expression CD1d and CD38 was fairly homogeneous among splenic

PRC1 mutant B cells, reaching levels that were intermediate between those of control FO and MZ B cells (Figure 36).

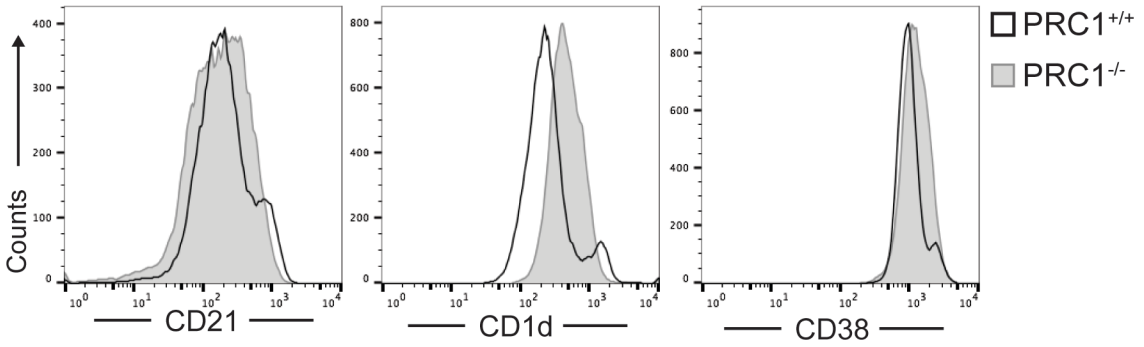

Figure 36. Marginal zone B cell surface marker expression is altered in PRC1-deficient splenic B cells.

Representative flow cytometric expression of the surface markers CD21, CD1d and CD38 on $CD19^+$ splenic B cells from $PRC1^{+/+}$ control (black line) and $PRC1^{-/-}$ mutant mice (light grey line and fill). Data are representative of 9 independent experiments.

When the same type of flow cytometric analysis was performed on $PRC1^{-/-}$ B cells dividing them into the two subsets according to B220 expression, the $B220^+$ fraction resembled more closely FO B cells, whereas the $B220^{lo}$ cells displayed a pattern of CD21, CD1d and CD38 expression that was closer to normal MZ B cells (Figure 37).

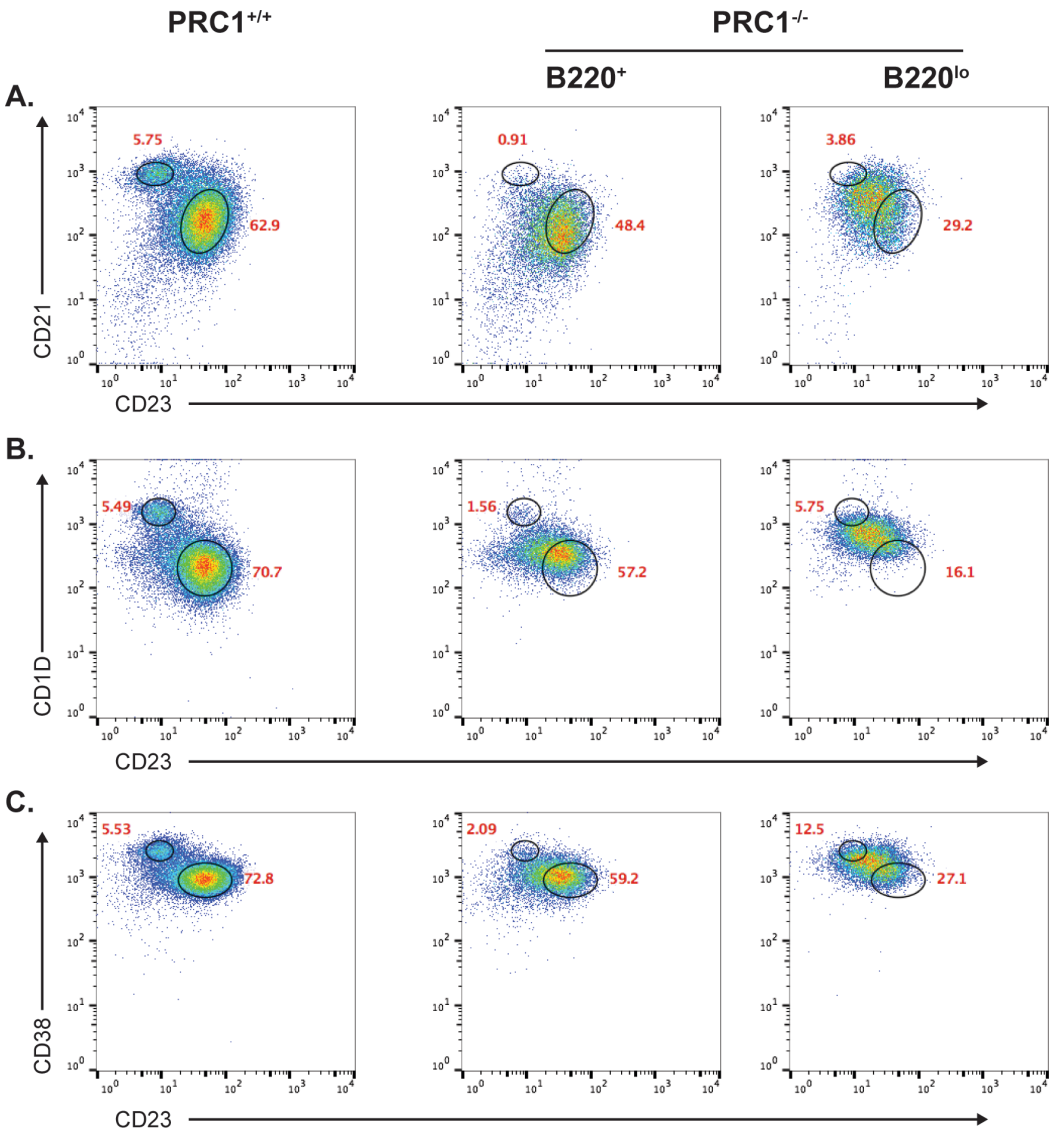

Figure 37. B220^{lo} of PRC1-deficient animals are phenotypically more similar to wild-type marginal zone B cells than their B220^{+} counterpart.

Representative flow cytometric analysis of splenic CD19^{+} B cell subsets from PRC1$^{+/+}$ control (n=9) and PRC1$^{-/-}$ mutant mice (n=9). PRC1-mutat CD19^{+} cells are sub-gated in B220^{+} (middle) and B220^{lo} (right). **A.** Follicular (CD19^{+}CD23^{+}CD21^{lo}) and marginal zone (CD19^{+}CD23^{-}CD21^{hi}) cells are gated. **B.** Follicular (CD19^{+}CD23^{+}CD1d^{lo}) and marginal zone (CD19^{+}CD23^{-}CD1d^{hi}) cells are gated. **C.** Follicular (CD19^{+}CD23^{+}CD38^{lo}) and marginal zone (CD19^{+}CD23^{-}CD38^{hi}) cells are gated. Numbers represent the frequencies of gated cells.

To confirm the reduction in the MZ B cell subset seen in PRC1 mutant mice, I performed immunofluorescence analysis of splenic sections staining for IgM, and using the MOMA-1 antibody to label metallophilic macrophages lining the marginal sinus. As shown in Figure 38, quantification of the data revealed that the average size of the area where MZ B cells reside was significantly reduced in the spleen of PRC1 mutant mice.

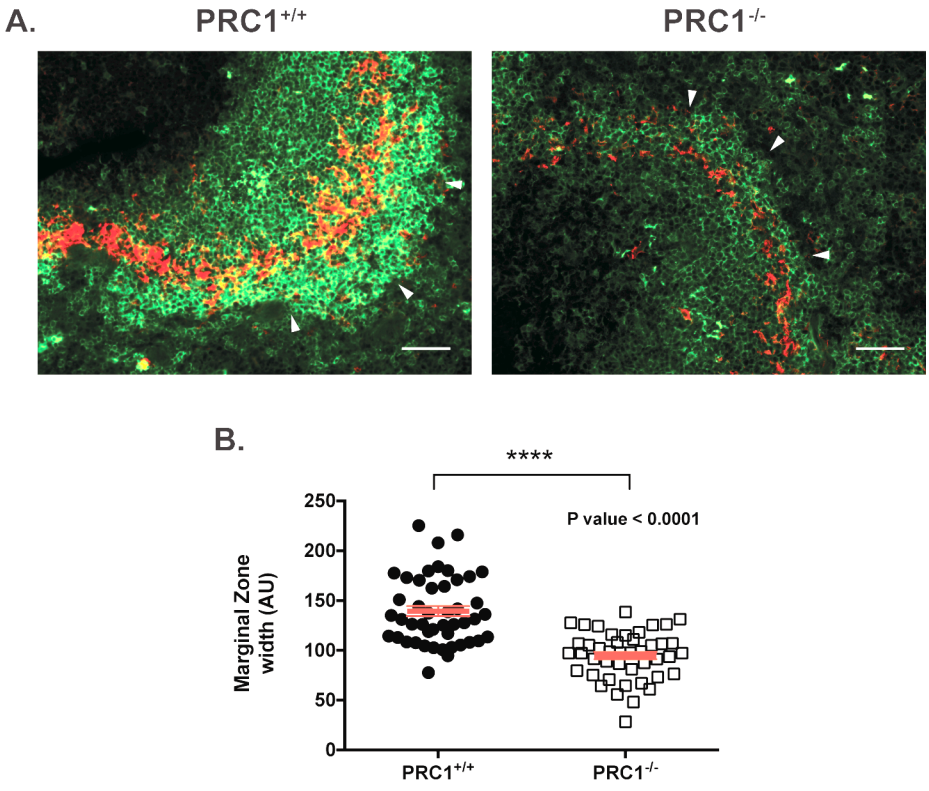

Figure 38. The lack of PRC1 affects marginal zone formation.

A. Representative immunofluorescence analysis and **B.** quantification of MZ width of spleen sections from PRC1$^{+/+}$ control (left; n=3) and PRC1$^{-/-}$ mutant (right; n=3) mice, stained with anti-IgM (green) and anti-CD169 (MOMA-1; red). Original magnification, x10; scale bars, 50 μm. Bars represent the mean value ± SEM. White arrows indicate the marginal zone. Unpaired T test: **** p<0.0001. Data are representative of 3 independent experiments.

The proportion of MOMA-1^{+} metallophilic macrophages appeared also to some extent under-represented in the spleen of PRC1 deficient animals. In contrast, PRC1 inactivation did not prevented B cells from localizing to primary follicles. Together, these data indicate that PRC1 conditional mutant mice suffer from a defect in the formation and/or maintenance of the marginal zone B cell population.

5.2.2 The Notch2 pathway is active in B cells lacking PRC1

Since the Notch2 signalling pathway is crucial for MZ B cell development (Saito et al. 2003), we compared between PRC1 control and mutant splenic B cells *Notch2* transcript levels and those of a representative set of Notch2 target genes. Analysis of RNA-seq data revealed that, whereas *Notch2* gene expression was unaffected, transcripts levels of

Notch2-induced targets *Dtx1* and *Hes1* resulted higher, and Notch2-repressed targets (*Klf2* and *Itgb7*; U. Strobl et al., personal communication) lower in PRC1 mutant B cells, when compared to the bulk of $B220^+$ $AA4.1^-$ mature B cells of control mice (Figure 39).

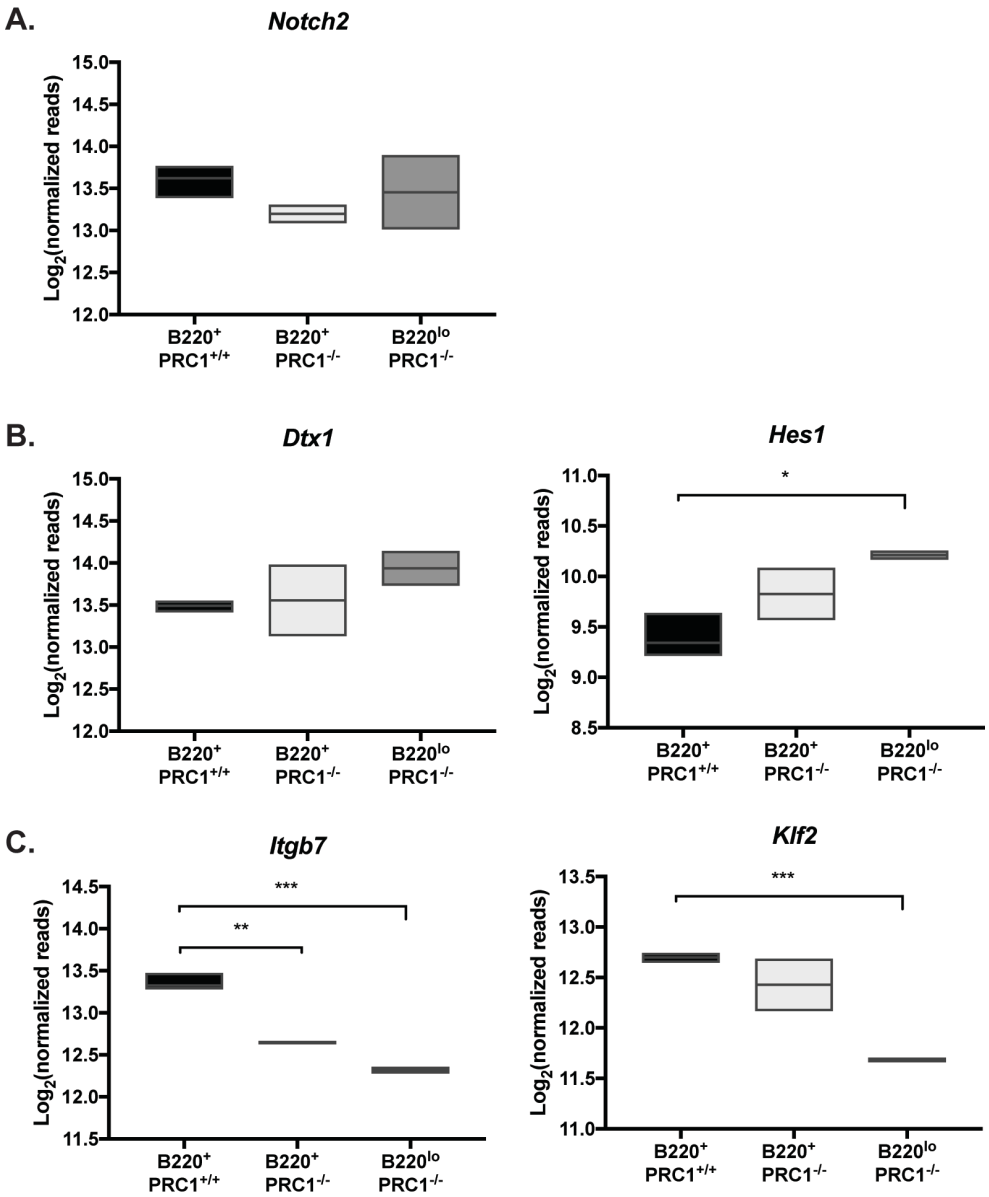

Figure 39. Notch2 positive-target genes are induced in PRC1-deficient B cells, while Notch2 negative-target genes are repressed compared to wild-type follicular B cells.

Floating bar analysis of Notch2 and Notch2-target Log2 normalized reads in $CD19^+$ $B220^+$ B cell from $PRC1^{+/+}$ control (n=3) and in $CD19^+$ $B220^+$ (n=2) and $B220^{lo}$ (n=2) from $PRC1^{-/-}$ mutant mice. **A.** *Notch2* gene. **B.** Notch2 positive-target genes. **C.** Notch2 negative-target genes. Horizontal bars indicate the medians, boxes indicate min and max values. Unpaired t test with Welch's correction: * $p<0.05$; ** $p<0.01$*** $p<0.001$.

The more substantial changes in gene expression were observed in the fraction of $B220^{lo}$ PRC1 mutant B cells, which are highly enriched for PRC1 defective cells. Expression

analysis for a representative set of Notch2 targets was confirmed by quantitative RT-qPCR analysis, comparing their expression in splenic B220^{+} and B220^{lo} mutant B cells to the one of FO and MZ B cells of control mice. Specifically, PRC1 deficient B cells showed *Dtx1* and *Klf2* transcript levels that were intermediate between control FO and MZ B cells. Instead, *Hes1* expression in PRC1 mutant B cells was even higher than that of control MZ B cells (Figure 40).

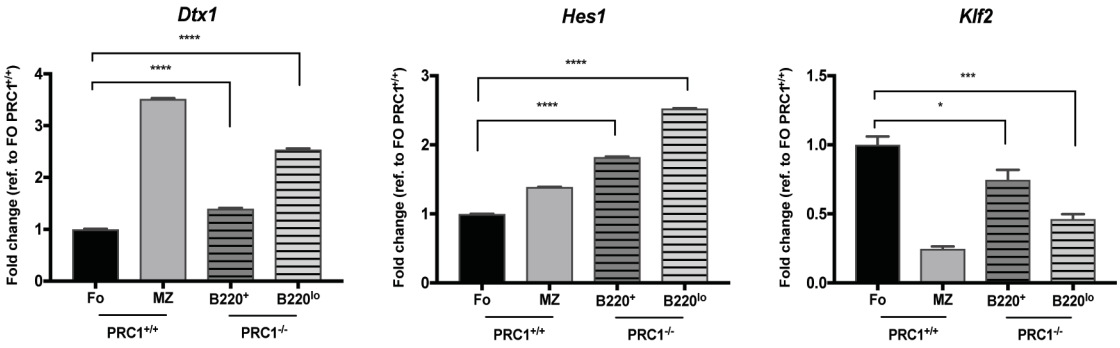

Figure 40. Notch2 signalling pathway is active in PRC1-deficient B cells.

A. RT-qPCR of *Dtx1, Hes1* and *Klf2* genes in CD23^{+}CD21^{lo} Follicular and CD23^{lo}CD21^{+} Marginal Zone CD19^{+} splenic B cells from PRC1$^{+/+}$ control animals and in B220^{+} and B220^{lo} CD19^{+} splenic B cells from PRC1$^{-/-}$ mutant animals. Gene transcript levels were normalized to the housekeeping *Rplp0* gene and to follicular PRC1$^{+/+}$ sample. Data are representative of 2 independent experiments. Unpaired t test with Welch's correction: * p<0.05; *** p<0.001; **** p<0.0001.

To corroborate our results, we extended the transcriptional analyses to PRC1$^{+/+}$ and PRC1$^{-/-}$ B cells isolated from lymph nodes. Under-representation of Notch2 ligands in these sites rendered difficult the detection of transcripts for Notch2 target. Nevertheless, higher expression of Notch2 induced targets were still detectable in B220^{lo} PRC1 mutant B cells when compared to control B cells, which mainly consist of B-2 B cells (Figure 41).

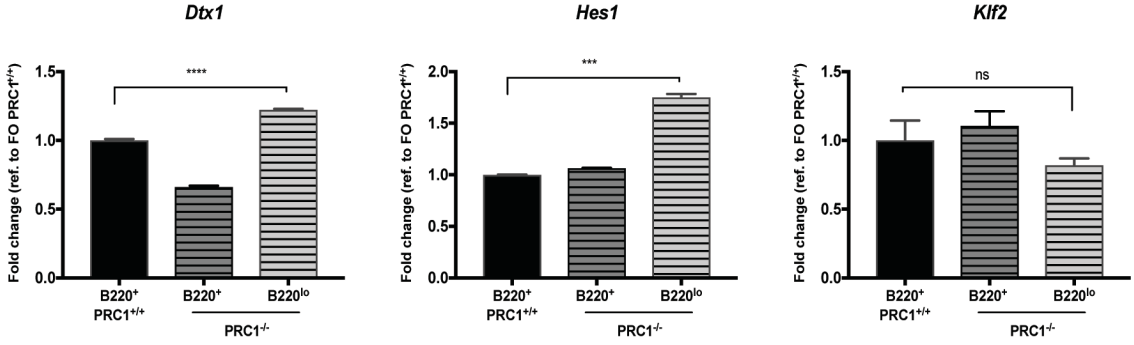

Figure 41. The activation of Notch2 pathway in PRC1-deficient B cells partially requires the presence of Notch2 ligands.

RT-qPCR of *Dtx1, Hes1* and *Klf2* genes in B220^{+} CD19^{+} inguinal lymph nodes B cells from PRC1$^{+/+}$ control animals and in B220^{+} and B220^{lo} CD19^{+} inguinal lymph nodes B cells from PRC1$^{-/-}$ mutant animals. Gene transcript levels were normalized to the housekeeping *Rplp0* gene and to B220^{+} PRC1$^{+/+}$ sample. Data are representative of one independent experiments. Unpaired t test with Welch's correction: *** p<0.001; **** p<0.0001; ns = not significative.

In summary, these results exclude that the reduction in MZ B cells seen in PRC1 mutant mice is due to defects in Notch2 signalling and transcriptional activity. In fact, in line with immunophenotypic data, B220^{lo} PRC1 mutant B cells, which display the strongest PRC1 inhibition, display strong resemblance with control MZ B cells on the basis of Notch2-regulated gene expression.

5.2.3 PRC1 mutant B cells express lower levels of Sphingosine-1-phosphate receptor-1

The integrity of the Notch2 pathway in PRC1 deficient B cells hints that other defects are responsible for the failure of these cells to reach the marginal zone. Given the importance of Sphingosine-1-phosphate receptor-1 (S1pr1) in driving migration of B cells to the marginal zone (Cinamon et al. 2004), I measured *S1pr1* transcript levels in both B220^{+} and B220^{lo} splenic PRC1$^{-/-}$ B cells and compared it to that of control FO and MZ PRC1$^{+/+}$ B cells. Analysis of RT-qPCR data revealed significantly lower *S1pr1* transcripts in PRC1 mutant B cells (Figure 42).

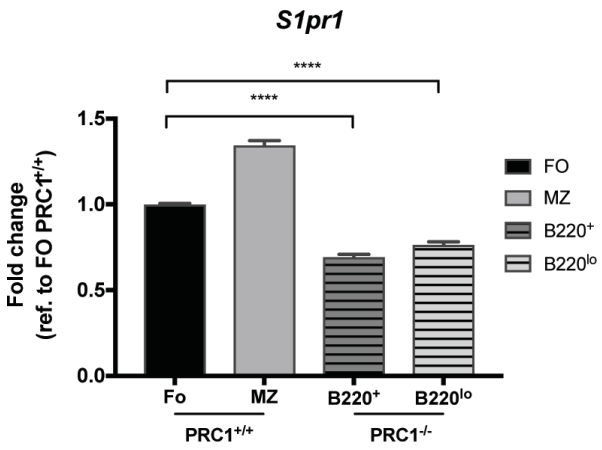

Figure 42. S1pr1 expression is reduced in PRC1-deficient B cells.

RT-qPCR of *S1pr1* gene in CD19^{+} B220^{+} B cells from PRC1$^{+/+}$ control animals and CD19^{+} B220^{+} and CD19^{+} B220^{lo} B cells from PRC1$^{-/-}$ mutant animals. Gene transcript levels were normalized to the housekeeping *Rplp0* gene and to the B220^{+} PRC1$^{-/-}$ sample. Data are representative of 2 independent experiments. Unpaired t test with Welch's correction: **** p<0.0001.

To verify that transcriptional down-regulation of *S1pr1* correlates with a migratory defect of PRC1 mutant B cells, we tested in a transwell assay the chemotactic response of these cells to soluble sphingosine-1-phosphate (S1P). PRC1 inactivation prevented B cells from a vigorous, dose-dependent, migration of mutant B cells towards a gradient of S1P. Indeed, PRC1 mutant B cells migrated similarly to control FO B cells and substantially worse than control MZ B cells (Figure 43).

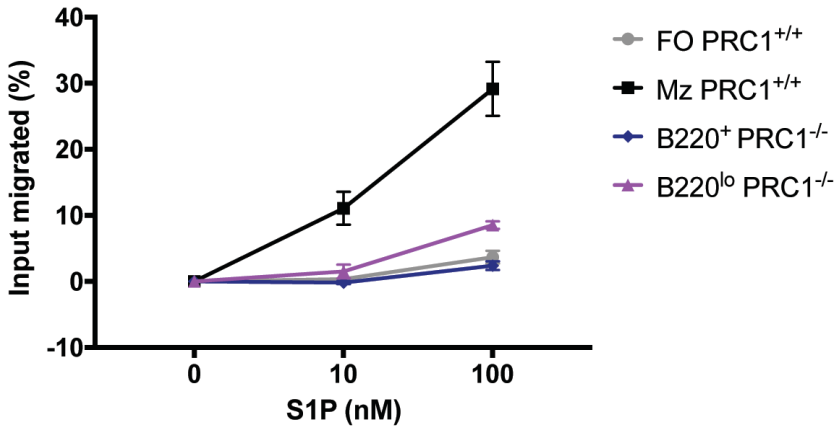

Figure 43. The chemotactic response of PRC1-deficient B cells to S1P is similar to the response of wild-type follicular B cells.

The chemotactic response to S1P chemochine of PRC1$^{+/+}$ and PRC1$^{-/-}$ B cells was determined by enumerating, by flow cytometry, splenic cells transmigrated for 3 hours across the uncoated 5-μm transwell to S1P or media. Transmigrated cells were further analysed for CD19, CD23, CD21 and B220 surface marker expression by flow cytometry. Chemotactic response is shown as the percentage of input cells that transmigrated to the lower chamber. Bars represent the mean value ± SD (n=3). Data are representative of 4 independent experiments.

This result is compatible with a scenario whereby reduced *S1pr1* expression prevents the migration and possibly the transient residence of PRC1 deficient B cells in the MZ (Arnon

and Cyster 2014; Cinamon et al. 2008), thereby preventing the acquisition of a full-blown MZ B cell surface phenotype.

A recent report has identified *S1pr1* as a target of the microRNA miR-125b (Li et al. 2018). Specifically, enforced miR-125b expression in B lineage cell inhibited the egress of immature B cells from the bone marrow through the inhibition of *S1pr1* expression (Allende et al. 2010). Interestingly, expression of miR-125b is negatively controlled by H3K27me3 deposition at the promoter region. To investigate whether miR-125b was induced in PRC1 mutant B cells, levels of its processed form (miR-125b-5p) were quantified in mature $B220^{+}$ $AA4.1^{-}$ control B cells and in $B220^{+}$ and $B220^{lo}$ PRC1 mutant B cells. As shown in Figure 44, miR-125b levels were between 2 and 3-fold increased in B cells lacking PRC1.

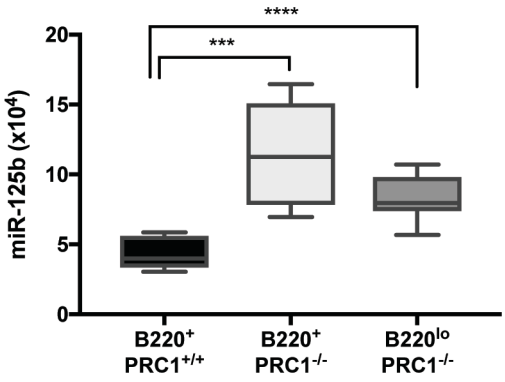

Figure 44. miR-125b expression is increased in PRC1-deficient B cells.

Box-plot analysis of transcript levels of candidate miR-125b gene (relative to sno-135) quantified in $B220^{+}$ B cells from $PRC1^{+/+}$ control animals (n=9) and $B220^{+}$ and $B220^{lo}$ B cells from $PRC1^{-/-}$ mutant animals (n=9). Quantification was performed by TaqMan MicroRNA Assay. In box-plots, horizontal bars indicate the medians, boxes indicate 5th to 95th percentiles. Unpaired Student's t test: *** $p<0.001$; **** $p<0.0001$.

This result suggests that PRC1 participates with PRC2 to the repression of miR-125b gene expression. Once PRC1 is inactivated, PRC2 inhibition of miR-125b is interfered, favouring expression of the miRNA. Future experiments will validate this hypothesis. In summary, in the absence of PRC1, we show that expression of the *S1pr1* gene is reduced leading to a failure of B cells to effectively migrate to the marginal zone attracted by soluble S1P.

5.3 The PRC1 complex sustains mature B cell homeostasis

5.3.1 Reduced *in vivo* turnover and *in vitro* survival of PRC1-deficient B cells

In Figure 17 we show that PRC1 inactivation leads to a reduction in the fraction and absolute number of B cells present in SLOs. To gain more insight into the PRC1-controlled mechanisms that could influence the maintenance of the mature B cell pool, I analysed again bromodeoxyuridine (BrdU) in *vivo* labelling experiments data that were previously generated in our laboratory (Alberghini and Casola, personal communication). For these experiments, control and PRC1 mutant mice had been sacrificed one week after constant administration of BrdU in the drinking water. Flow cytometric assessment of BrdU incorporation indicated that the turnover of $AA4.1^{-}B220^{+}$ mature B cells both in the spleen and bone marrow was increased in PRC1 conditional mutant mice (Figure 45).

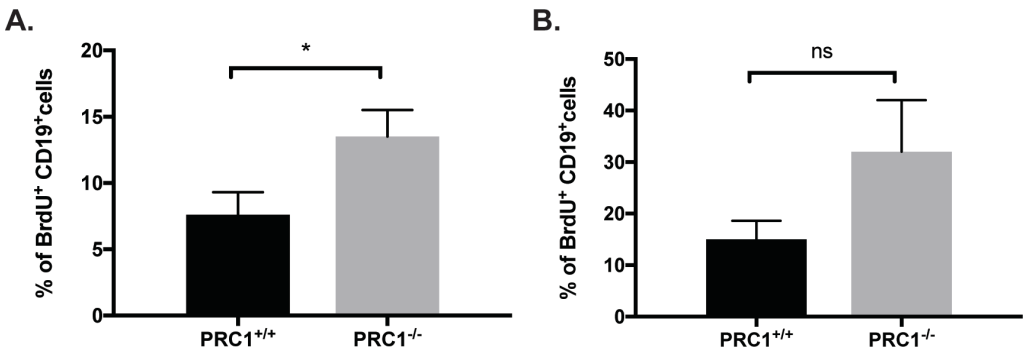

Figure 45. *In vivo* turnover is altered in PRC1-deficient B cells.

A. Percentage of $CD19^{+}$ $BrdU^{+}$ cells in spleen and **B.** bone marrow of $PRC1^{+/+}$ control (n=3) and $PRC1^{-/-}$ mutant mice (n=3) analysed by flow cytometry. Bars represent the mean value ± SD. Unpaired t test with Welch's correction: * $p<0.05$.

Taking advantage of these data, I performed a further analysis looking for possible differences in the extent of BrdU incorporation between $B220^{+}$ and $B220^{lo}$ B cells $PRC1^{-/-}$ B cells. In PRC1 mutant mice the fraction of $BrdU^{+}$ cells was significantly higher in the $B220^{+}$ subset as compared to that of $B220^{lo}$ B cells (Figure 46).

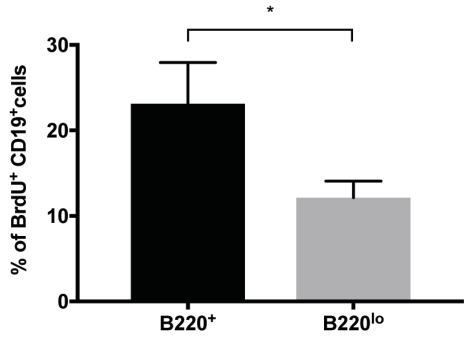

Figure 46. B220^{+} of PRC1-decient animals show increased fraction of BrdU^{+} cells than B220^{lo}.

A. Percentage of CD19^{+} BrdU^{+}-B220^{+} or -B220^{lo} cells in spleen of PRC1-deficient mice (n=3) analysed by flow cytometry. Bars represent the mean value ± SD. Unpaired t test with Welch's correction: * p<0.05.

This result supports previous conclusions, confirming the view that the B220^{lo} subset derives from B220^{+} PRC1 mutant B cells as a result of progressive loss of PRC1 activity through the extinction of RING1B protein.

Overall, the accelerated B cell turnover scored in PRC1 mutant animals, combined with the reduction of the absolute B cell numbers monitored in SLOs, suggests a defect in mature B cell maintenance in these animals. To address this further, we measured the *in vitro* response of PRC1 control and mutant B cells to the survival factor BAFF. Flow cytometric analysis combined with cell counting at different days of the *in vitro* culture revealed a significantly weaker response of PRC1-deficient B cells to BAFF, which was dose-dependent (Figure 47A). In particular, PRC1 mutant B cells suffered from two distinct defects. First, PRC1-deficient B cells underwent a significantly stronger reduction in cell numbers within the first 24 hours of *in vitro* culture (Figure 47A).

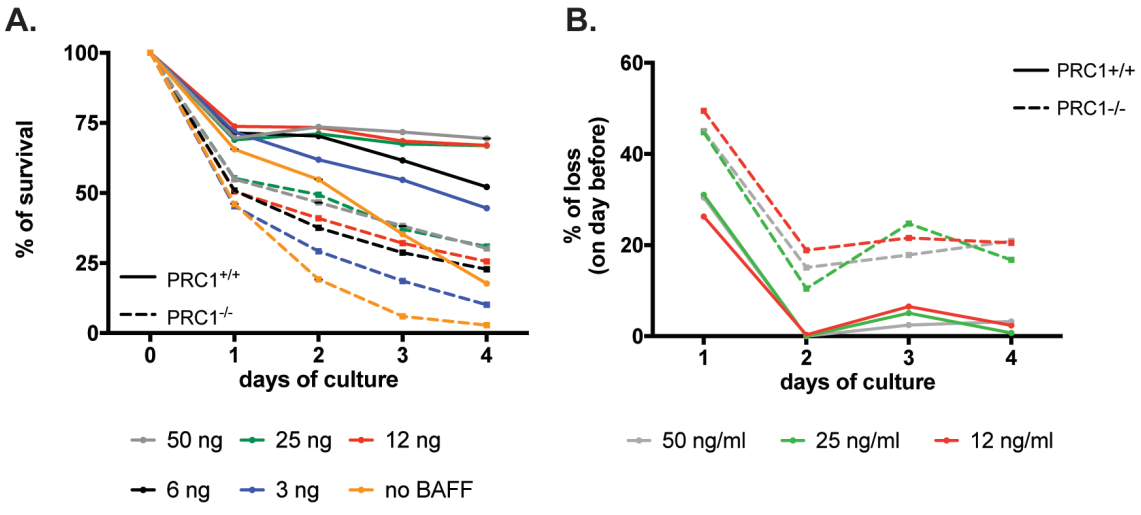

Figure 47. PRC1-deficient B cells show sub-optimal response to BAFF *in vitro*.

In vitro survival curves of CD19^{+} B cells purified from spleen of PRC1$^{+/+}$ control (n=3; continuous line) and PRC1$^{-/-}$ mutant mice (n=3; dashed line), treated without or with BAFF at the indicated concentrations. Markers represent the mean value ± SD. Data shown are representative of 4 independent experiments. **A.** Data are represented as percentage of the number of plated cells at day-0. **B.** Data are represented as percentage of the number of lost cells compared to the day before.

Second, in saturating concentrations of BAFF, the number of control B cells remained relatively stable between day-2 and day-4 of the culture, whereas PRC1 mutant B cells displayed a daily loss of about 20% (Figure 47B). Both observations are suggestive of a defect in the survival of PRC1-deficient B cells.

To test this hypothesis, we first analysed *ex vivo* isolated B cells retrieved from the spleen of PRC1 control and mutant mice, and tested them for the expression of markers of ongoing apoptosis. Specifically, cell suspensions from control and mutant animals were labelled with fluorescent-labelled VAD-FMK (CaspGLOW™) which binds to activated caspases and analysed by flow cytometry. This experiment failed to detect major differences in the fraction of apoptotic cells between PRC1 control and mutant B cells (Figure 48).

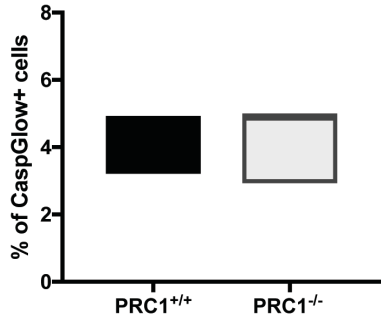

Figure 48. The fraction of apoptotic cells is comparable between control and mutant resting B cells.

Frequencies of Caspase Glow^{+} cells by flow cytometric analysis of PRC1-proficient and -deficient splenic resting CD19^{+} B cells (n=3). Horizontal bars indicate the medians, boxes indicate min and max values.

Consistent with this finding, the expression of apoptotic genes belonging to Bcl-2 family was not altered in resting B cells from PRC1$^{-/-}$ mice (Figure 49).

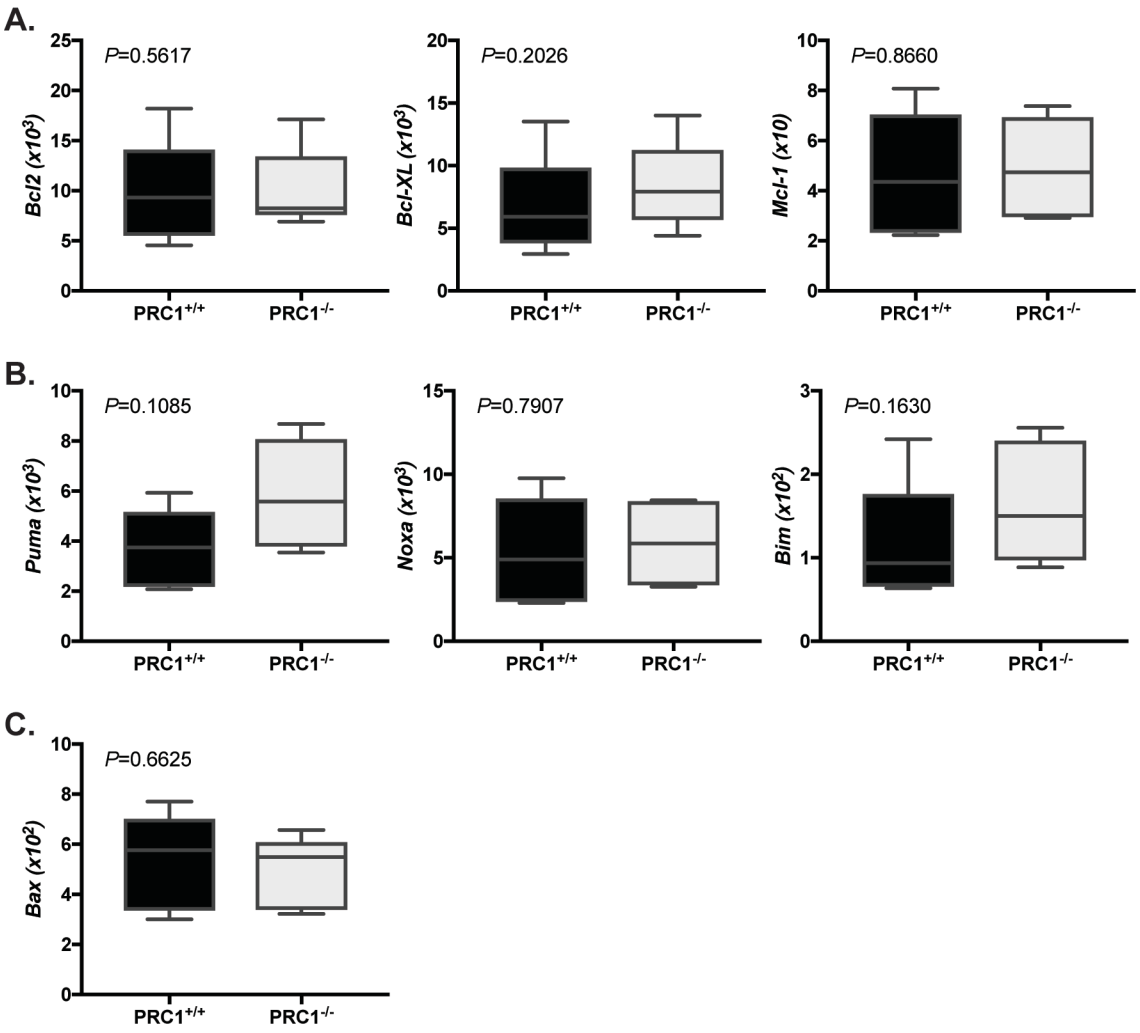

Figure 49. Unaltered expression of apoptotic genes in resting PRC1-deficient B cells.

Box-plot analysis of transcript levels of Bcl2 family apoptotic genes (relative to *Rplp0*) quantified in control PRC1$^{+/+}$ and mutant PRC1$^{-/-}$ resting B cells. **A.** Anti-apoptotic genes. **B.** Apoptotic sensor genes. **C.** Pro-apoptotic gene. *Bcl2, Bcl-$_{XL}$* n=12; *Bim, Bax* n=9; *Mcl-1, Puma, Noxa* n=6. In box-plots, horizontal bars indicate the medians, boxes indicate 5th to 95th percentiles. P values are indicated within each plot (unpaired Student's t test).

Despite the failure to detect changes at the transcriptional level of effectors of the intrinsic apoptotic program, immunoblotting analysis on protein extracts isolated from the same cells revealed a moderate, yet consistent, increase in the expression of the extra-long and

long isoforms of the pro-apoptotic sensor BIM (BIM_{EL} and BIM_L, respectively) (

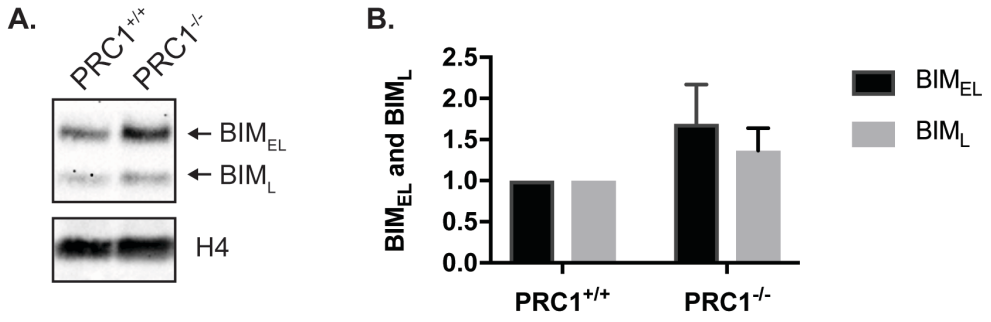

Figure 50).

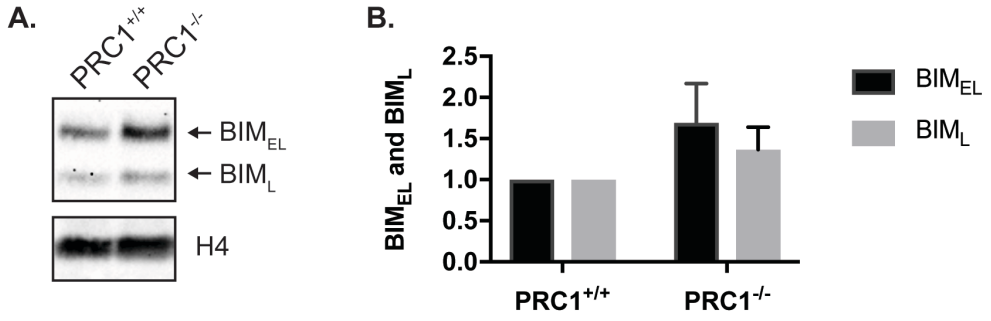

Figure 50. Over-expression of BIM in PRC1-deficient resting B cells.

A. Immunoblotting analysis and **B.** quantification of BIM_{EL} and BIM_L protein levels in purified splenic B cells from $PRC1^{+/+}$ control and $PRC1^{-/-}$ mutant mice. H4 was used as loading control. Data are normalized on values of $PRC1^{+/+}$ resting B cells. Data are representative of 3 independent experiments.

Collectively, these results indicate that PRC1 mutant B cells express in basal conditions higher levels of the pro-apoptotic factor BIM, which, however, under *in vivo* conditions, does not appear to substantially reduce their survival.

We then investigated whether PRC1 mutant B cells suffered from increased susceptibility to undergo apoptosis *in vitro*, under more controlled experimental conditions. Indeed, from monitoring the resistance of *ex vivo* isolated B cells we switched to harsh *in vitro* growth culture conditions, such as keeping B cells in complete B cell medium without soluble BAFF. Under this experimental settings, PRC1 deficient B cells showed a significantly higher fraction of apoptotic cells when compared to controls (Figure 51).

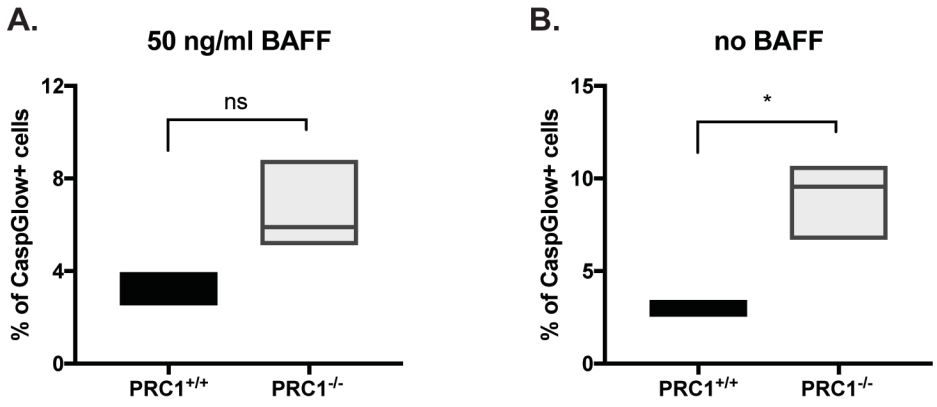

Figure 51. Increased apoptosis upon *in vitro* BAFF stimulation of PRC1-deficient B cells.

Frequencies of Caspase Glow$^+$ cells by flow cytometric analysis of PRC1-proficient and -deficient purified B cells, cultured *in vitro* for 2 days **A.** with 50 ng/ml of BAFF or **B.** without BAFF. Horizontal bars indicate the medians, boxes indicate min and max values. Data are form one experiment. Unpaired t test with Welch's correction: * $p<0.05$; ns = not significative.

Moreover, PRC1 mutant B cells cultured *in vitro* for 48 hours in the presence of BAFF revealed increased expression, when compared to controls, of the pro-apoptotic sensors *Puma*, *Noxa* and *Bim* (Figure 52). Expression of other Bcl-2 family members remained unaffected by PRC1 inactivation (Figure 52).

In line with the data obtained from *ex vivo* isolated B cells, BAFF stimulated PRC1 mutant B cells expressed higher BIM_{EL} and BIM_L protein levels, reaching a 2-fold up-regulation compared to controls when B cells were treated with the lower dose of BAFF (Figure 53).

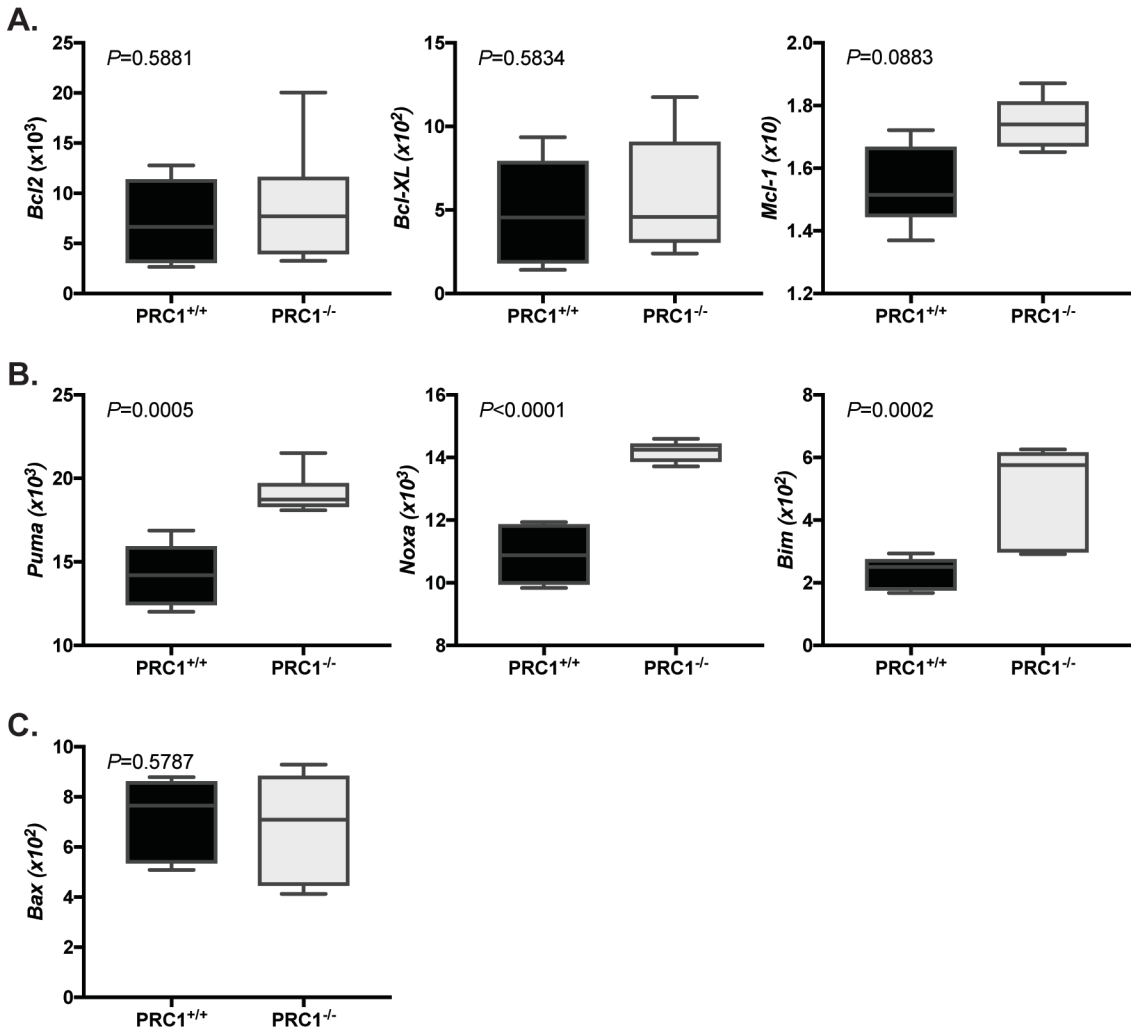

Figure 52. Up-regulation of apoptotic sensors in PRC1-mutant B cells stimulated with BAFF *in vitro*.

Box-plot analysis of transcript levels of Bcl2 family apoptotic genes (relative to *Rplp0*) quantified in control PRC1$^{+/+}$ and mutant PRC1$^{-/-}$ B cells stimulated with 50 ng/ml BAFF *in vitro* for 2 days. **A.** Anti-apoptotic genes. **B.** Apoptotic sensor genes. **C.** Pro-apoptotic gene. *Bcl2, Bcl-$_{XL}$* n=12; *Bim, Bax* n=9; *Mcl-1, Puma, Noxa* n=6. In box-plots, horizontal bars indicate the medians, boxes indicate 5th to 95th percentiles. P values are indicated within each plot (unpaired Student's t test).

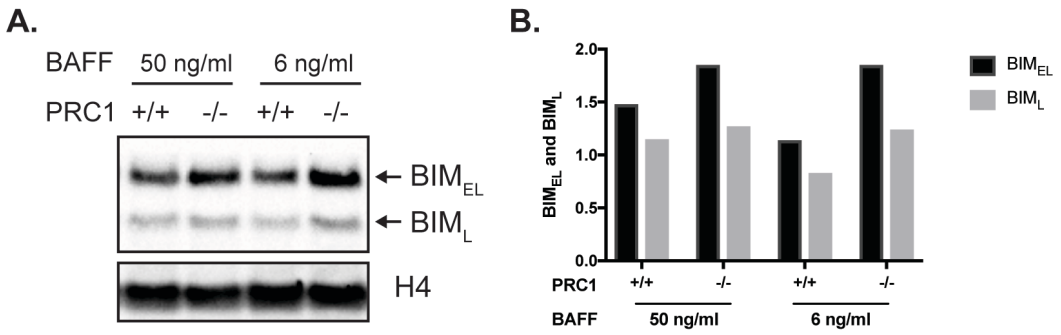

Figure 53. Over-expression of BIM in PRC1-deficient B cells stimulated with BAFF *in vitro*.

A. Immunoblotting analysis and **B.** quantification of BIM_{EL} and BIM_L protein levels in purified splenic B cells from $PRC1^{+/+}$ control and $PRC1^{-/-}$ mutant mice, stimulated with 50 or 6 ng/ml BAFF *in vitro* for 2 days. H4 was used as loading control. Data are representative of 3 independent experiments.

Altogether, these results suggest that B cells lacking a functional PRC1 complex are more sensitive to apoptotic signals due to higher basal expression of the pro-apoptotic factor BIM. Increased susceptibility to death signals may also come from higher expression in PRC1 mutant B cells of the tumor suppressor p21, both in resting conditions and after the stimulation with BAFF (Figure 54).

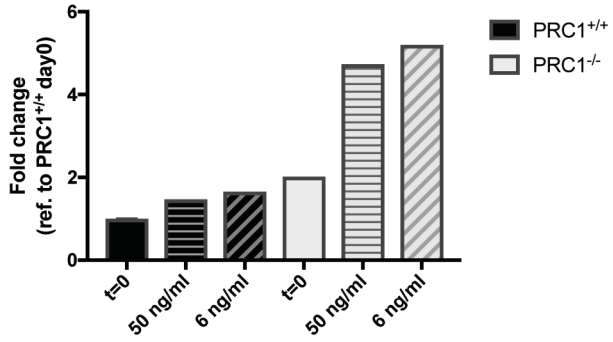

Figure 54. *p21* up-regulation in resting and BAFF-stimulated PRC1-deficient B cells.

RT-qPCR of *p21* gene in B cells from $PRC1^{+/+}$ control and $PRC1^{-/-}$ mutant animals. After purification, B cells were stimulated *in vitro* with 50 or 6 ng/ml BAFF. Gene transcript levels were measured at day-0 and -2 after stimulation. Data were normalized to the housekeeping *Rplp0* gene and to the t=0 $PRC1^{+/+}$ sample. Data are representative of one experiment.

5.3.2 Increased susceptibility to apoptosis correlates with extinction of RING1B protein

To understand whether residual RING1B protein in the bulk of PRC1 mutant B cells could partially protect these cells from apoptosis, we divided $PRC1^{-/-}$ B cells respectively into the $B220^{+}$ and $B220^{lo}$ subsets, with only the latter displaying full extinction of RING1B expression. Both subsets were isolated from the spleen of PRC1 mutant mice and kept shortly in culture with or without BAFF. In both experimental conditions the survival of $B220^{lo}$ was more impaired than that of the $B220^{+}$ counterpart (Figure 55).

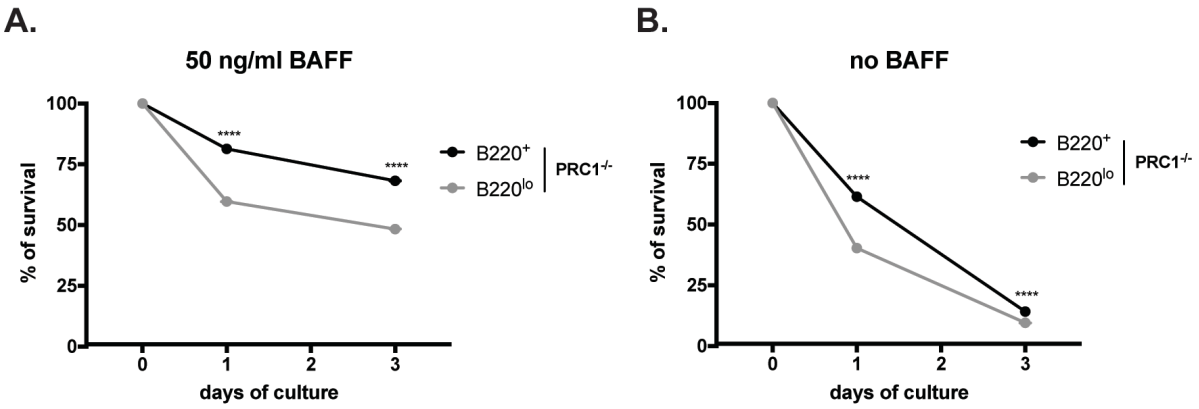

Figure 55. *In vitro* survival of PRC1-deficient B220^{lo} cells is more impaired than the one of PRC1-deficient B220^{+}.

In vitro survival curves of CD19^{+} B220^{+} (black line and dots) and CD19^{+} B220^{lo} (grey line and dots) B cells sorted from the spleen of PRC1$^{-/-}$ mutant mouse and treated **A.** with 50 ng/ml of BAFF or **B.** without BAFF. Markers represent the mean value ± SD. Data shown are representative of 2 independent experiments. Data are represented as percentage of the number of plated cells at day-0. Unpaired Student's t test: **** p<0.0001.

Conversely, the fraction of apoptotic B cells was significantly higher among B220^{lo} B cells, even under conditions of BAFF excess (Figure 56).

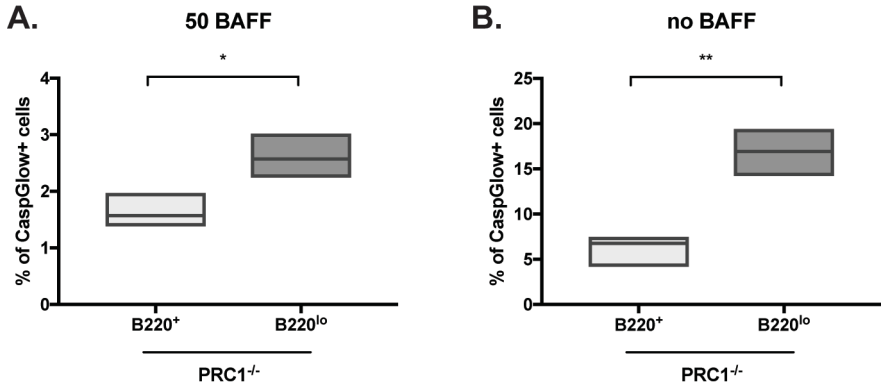

Figure 56. B220^{lo} are more sensitive to apoptosis than B220^{+} cells from PRC1-deficient mice.

Frequencies of Caspase Glow^{+} cells by flow cytometric analysis of B220^{+} or B220^{lo} PRC1$^{-/-}$ purified B cells, cultured *in vitro* for 2 days **A.** with 50 ng/ml of BAFF or **B.** without BAFF. Horizontal bars indicate the medians, boxes indicate min and max values. Data are form one experiment. Unpaired t test with Welch's correction: * p<0.05; ** p<0.01.

Notably, in resting conditions, BIM_{EL} protein levels were higher in B220^{lo} B cells (Figure 57).

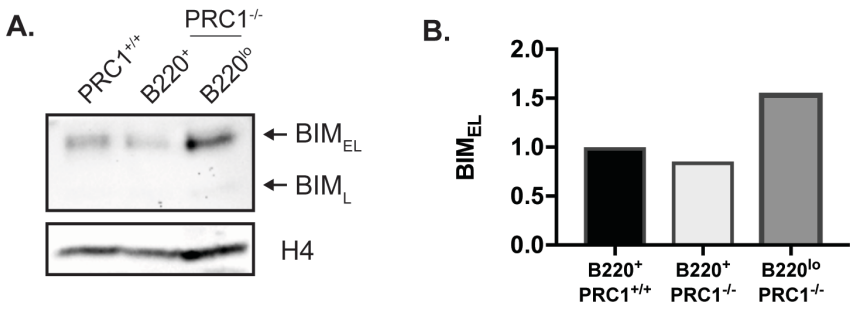

Figure 57. BIM is over-expressed in B220^{lo} of PRC1 deficient animals.

A. Immunoblotting analysis and **B.** quantification of BIM_{EL} protein levels in resting splenic B cells from PRC1$^{+/+}$ control and PRC1$^{-/-}$ mutant mice. H4 was used as loading control. Data are representative of 2 independent experiments.

Together, these data suggest that upon genetic inactivation of PRC1, mutant B cells benefit from a transient phase where they are protected from apoptotic stimuli as a result of residual RING1B protein. Once levels of RING1B fall beyond the limit of detection, PRC1 mutant B cells acquire higher sensitivity to apoptotic stimuli.

5.3.3 PRC1 mutant B cells fail to fully activate AKT in response to BAFF stimulation

We show that B cells lacking PRC1 respond less effectively to the pro-survival factor BAFF. The most important survival pathway activated in B cells by the BAFF receptor is the alternative/non-canonical NF-κB pathway. To test the effect of PRC1 inactivation on this signalling pathway, I measured the levels of NF-κB2/p100 and its cleaved form p52 in *in-vitro* cultured B cells stimulated with BAFF. When compared to controls, PRC1-defective B cells displayed comparable expression and processing of p100, both in resting conditions and after two days of stimulation with two different concentrations of BAFF (Figure 58).

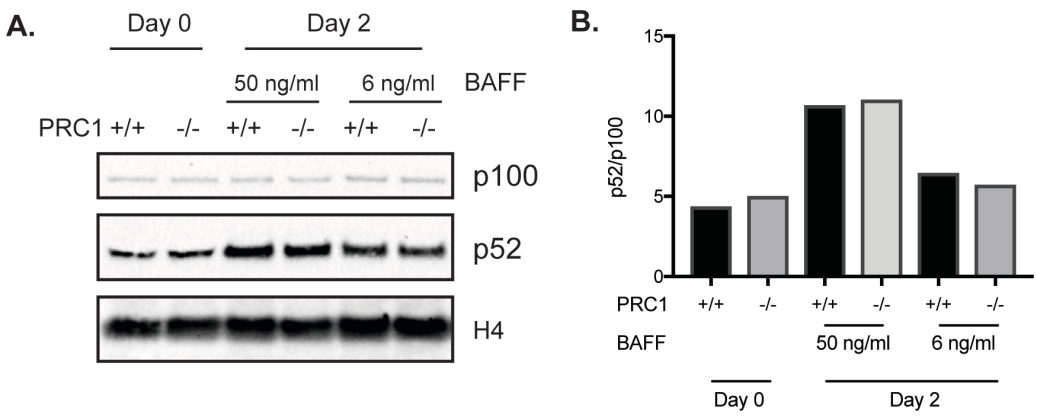

Figure 58. Processing of p100 to p52 of alternative NF-κB signalling pathway is unperturbed in PRC1-deficient B cells.

A. Immunoblotting analysis of p100 and p52 protein levels in PRC1$^{+/+}$ control and PRC1$^{-/-}$ mutant splenic B cells. Cells were cultured *in vitro* with 50 or 6 ng/ml of BAFF and analysed 0 and 2 days after purification. H4 was used as loading control. **B.** Quantification of p52 and p100 protein levels. Data are normalized on H4 protein levels and indicated as ratio of p52/p100, relative to PRC1$^{+/+}$ day-0. Data are representative of 3 independent experiments.

This observation was supported by comparable transcriptional induction of NF-κB target genes in PRC1 control and mutant cells, following two days of BAFF stimulation (Figure 59).

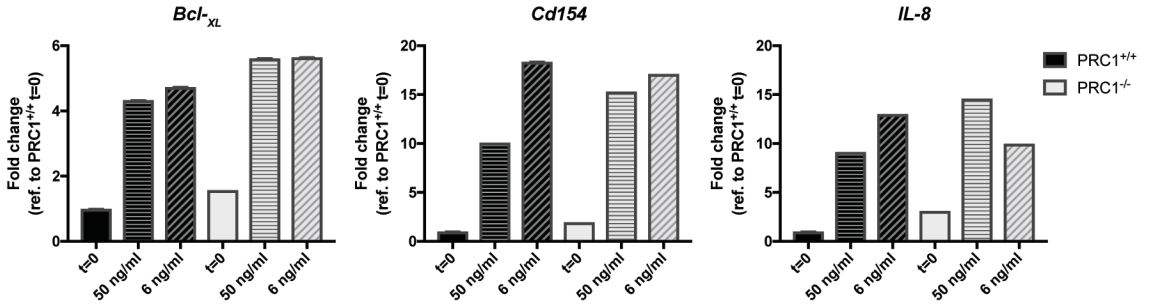

Figure 59. BAFF-target genes are induced comparably in control and mutant B cells.

RT-qPCR of *Bcl-xL, Cd154* and *Il-8* genes in B cells from PRC1$^{+/+}$ control and PRC1$^{-/-}$ mutant animals. After purification, B cells were stimulated *in vitro* with 50 or 6 ng/ml BAFF. Gene transcript levels were measured at day-0 and -2 after stimulation and they were normalized to the housekeeping *Rplp0* gene and to the t=0 PRC1$^{+/+}$ sample. Data are representative of 3 independent experiments.

Since the non-canonical NF-κB pathway is unperturbed in mutant B cells, we sought to identify defects in other pathways triggered by the BAFF receptor (BAFF-R), which are

crucial for cell B survival. In B cells, BAFF-R signalling sustains the activation of the CD19-PI3K-AKT pathway which supports cell survival both *in vivo* and *in vitro* (Jellusova et al. 2013). Hence, we measured in BAFF-stimulated control and PRC1 mutant B cells, AKT phosphorylation on serine-473, which is associated with activation of the kinase. Quantification of immunoblotting data revealed that: 1) total AKT levels were comparable between $PRC1^{+/+}$ and $PRC1^{-/-}$ B cells; 2) p-AKT (Ser-473) levels were reduced in PRC1-deficient B cells (Figure 60).

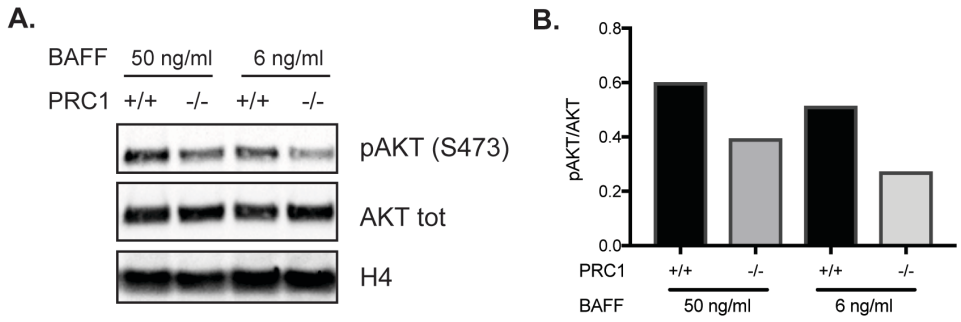

Figure 60. PRC1-deficient B cells show sub-optimal phosphorylation of AKT upon BAFF-R activation.

A. Immunoblotting analysis of AKT serine-473-phosphorylation (pAKT) and of total AKT in $PRC1^{+/+}$ control and $PRC1^{-/-}$ mutant splenic B cells, stimulated with 50 or 6 ng/ml of BAFF *in vitro* for 2 days. H4 was used as loading control. **B.** Quantification of pAKT and AKT protein levels. Data are normalized on H4 protein levels and indicated as ratio of pAKT/AKT. Data are representative of one experiment.

Thus, the lack of PRC1 affects the activation of AKT upon BAFF stimulation. In the same samples, total levels of the AKT downstream target FOXO1 were increased in mutant cells, while the levels of its inhibited form (through phosphorylation on serine-256) were comparable to controls (Figure 61).

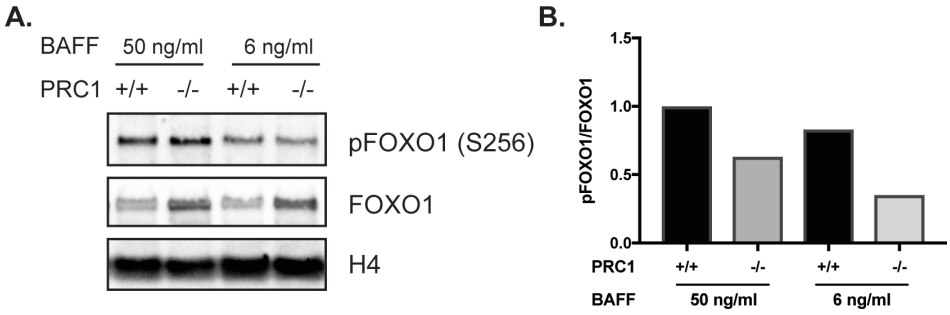

Figure 61. FOXO1 is over-expressed in PRC1-mutant B cells upon BAFF-R activation.

A. Immunoblotting analysis and of FOXO1 serine-256-phosphorylation (pFOXO1) and of total FOXO1 protein levels in PRC1$^{+/+}$ control and PRC1$^{-/-}$ mutant splenic B cells, stimulated with 50 or 6 ng/ml of BAFF *in vitro* for 2 days. H4 was used as loading control. **B.** Quantification of pFOXO1 and FOXO1 protein levels, indicated as ratio of pFOXO1/FOXO1 normalized to control. Data are representative of one experiment.

Therefore, PRC1-deficient B cells stimulated with BAFF are characterized by a reduced pFOXO1/FOXO1 ratio, which could reflect the sub-optimal activation of AKT in response to BAFF stimulation.

In summary, the accelerated turnover of PRC1 mutant B cells *in vivo* is compatible with mutant B cells suffering from an interference with BAFF-induced mature B cell survival. The latter impairment is not caused by disturbances in the alternative NF-κB signalling pathway, but rather by sub-optimal BAFF-dependent activation of the CD19-PI3K-AKT signalling pathway.

5.4 PRC1-deficient B cells are counter selected under a competitive setting

So far, we have shown that PRC1 mutant B cells display: 1) an accelerated turnover *in vivo*, 2) an enhanced sensitivity to apoptotic triggers, and 3) an impaired response to the survival factor BAFF *in vitro*. These behaviours, combined with a general disturbance of development-related transcriptional signatures seen through transcriptomic analyses, could affect the fitness of PRC1-deficient resting mature B cells. To address this point, we performed competitive bone marrow reconstitution experiments. Specifically, we transplanted into B-cell deficient JHT mice bone marrow suspensions from C57BL/6 Ly5.1^{+} congenic mice mixed at 1:1 ratio with those of Ly5.2^{+} mice, respectively proficient (*CD23-cre*) or mutant (*Ring1A$^{-/-}$; Ring1B$^{fl/fl}$; Cd23-cre*) for PRC1 in mature B cells. Hereafter, reconstituted mice will be referred to as PRC1 control and PRC1 mutant chimeras, respectively (Figure 62).

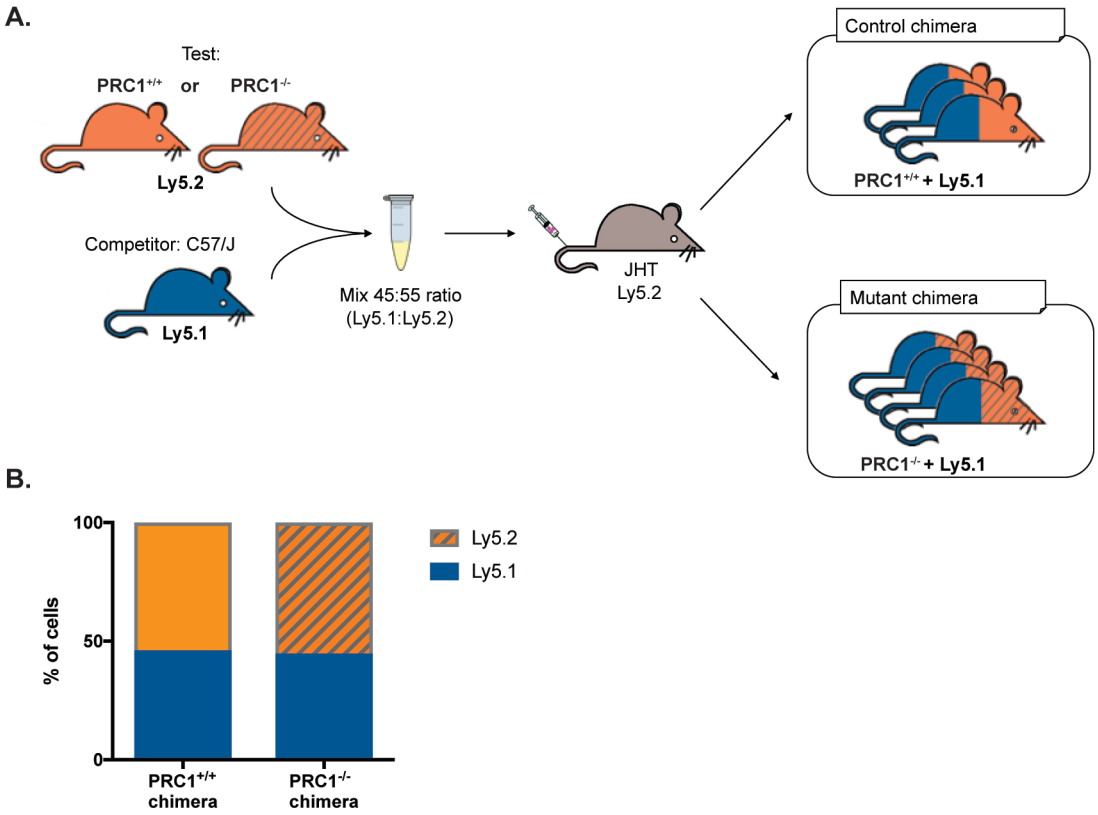

Figure 62. Generation of bone marrow chimera mice.

A. Schematic representation of the procedure to generate bone marrow chimera mice. Recipient mice belong to the JHT strain. Control chimera were transplanted with a mixture of Ly5.1-C57BL/6 cells + Ly5.2-PRC1$^{+/+}$ cells (n=3); mutant chimeras were transplanted with a mixture of Ly5.1-C57BL/6 cells + Ly5.2-PRC1$^{-/-}$ cells (n=4). **B.** Flow cytometric analysis of Ly5.1 and Ly5.2 surface marker expression in C57BL/6-PRC1$^{+/+}$ (left) or C57BL/6-PRC1$^{-/-}$ (right) bone marrow cell mixtures before injection in JHT recipient mice.

Four months after transplantation, we analysed the contribution of the Ly5.1^{+} and Ly5.2^{+} hematopoietic stem cells to the establishment of the peripheral B- and T-cell pools (the latter serving as internal controls). For this, we performed a comprehensive immunophenotypical and histological analysis of the B cell populations residing in the spleen and in the lymph nodes. Control chimeras exhibited Ly5.1/5.2 ratios among B- and T-cell populations that were similar to those detected in the bone marrow donor pools (Figure 63, left columns). Instead, mutant chimeras showed a skewing for Ly5.1^{+} PRC1-proficient B cells, with T-cells being instead equally represented by both Ly5.1^{+} and Ly5.2^{+} cells (Figure 63, right columns).

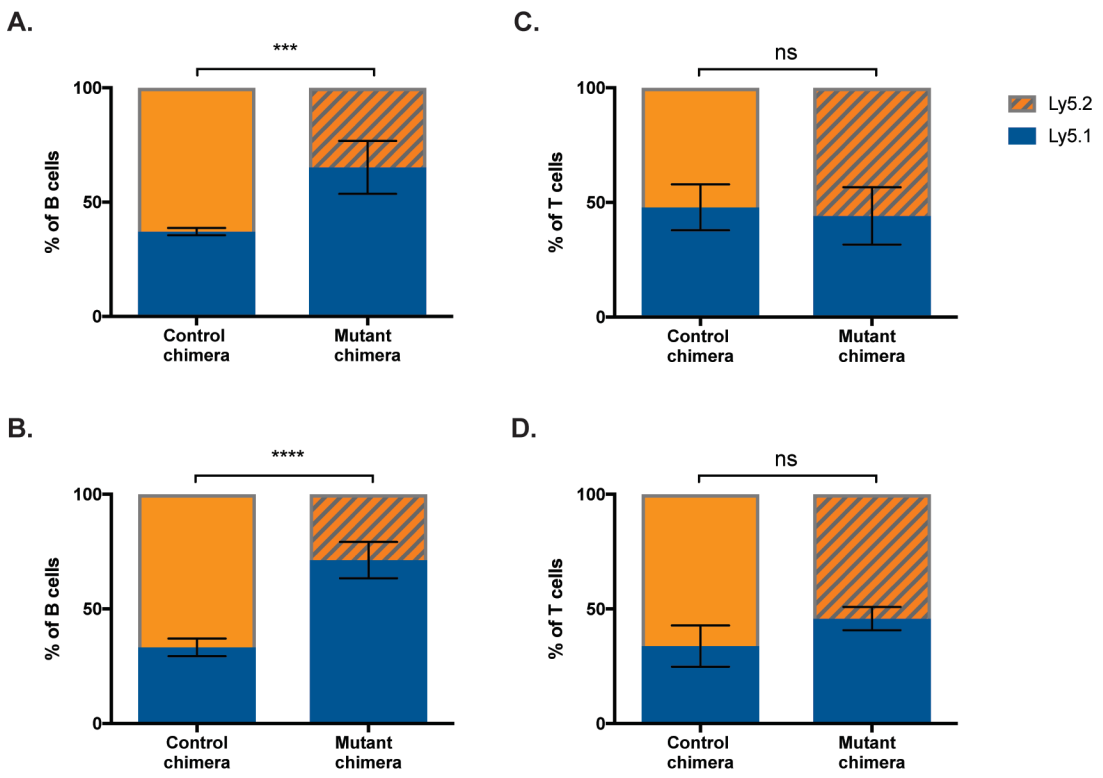

Figure 63. Counter-selection of PRC1-deficient B cells under a competitive setting.

A-B. Flow cytometric analysis of Ly5.1 and Ly5.2 surface marker expression on $CD19^+$ B cells (A.) and $TCR\beta^+$ T cells (A.) in spleens of control (left; n=3) and mutant (right; n=4) bone marrow chimera mice. **C-D.** Flow cytometric analysis of Ly5.1 and Ly5.2 surface marker expression of $CD19^+$ B cells (C.) and $TCR\beta^+$ T cells (D.) in inguinal lymph nodes of control (left; n=3) and mutant (right; n=4) bone marrow chimera mice. **A-D.** Bars represent the mean value ± SD. Chi-squared test: *** $p<0.001$; **** $p<0.0001$.

In mutant chimeras, the identity of PRC1 mutant $Ly5.2^+$ B cells was confirmed by genomic qPCR analysis, revealing a significant reduction in the copy number of functional *Ring1B* alleles (Figure 64).

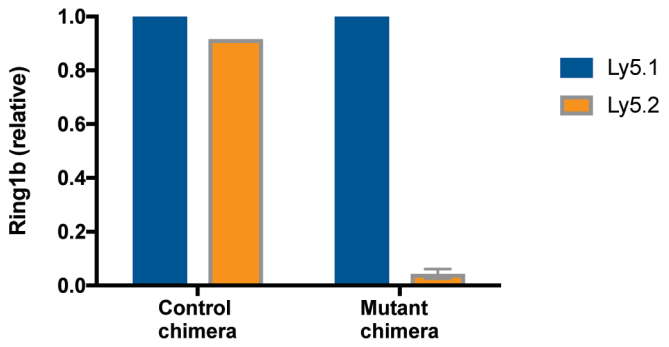

Figure 64. Ring1B allelic deletion in Ly5.2 cells derived from $PRC1^{-/-}$ donors.

Genomic qPCR analysis to quantify *Ring1B* gene copy number in $CD19^+Ly5.1^+$ and $CD19^+Ly5.2^+$ populations sorted from spleens of control (left; n=1) and mutant (right; n=4) bone marrow chimera mice. Data are normalized the *Gapdh* gene and shown as relative to $Ly5.1^+$ cells.

Immunofluorescence analyses of spleen sections from control and mutant chimeras confirmed the under-representation of $Ly5.2^+$ cells in the follicles of mutant chimeras when compared to the control counterparts (Figure 65).

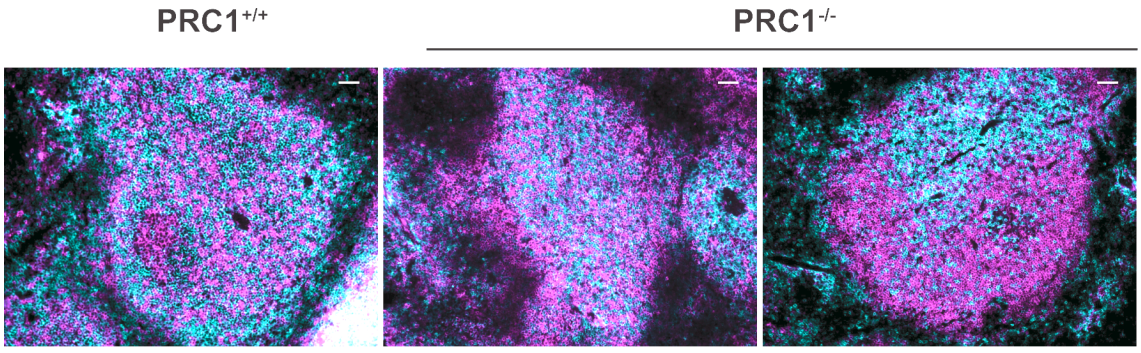

Figure 65. Counter-selection of PRC1-deficient B cells under a competitive setting by immunofluorescence.

Representative immunofluorescence analysis of spleen sections from a control chimera (left) or mutant chimera (middle and right) transplanted mice, stained with anti-Ly5.1 (CD45.1; magenta) and anti-Ly5.2 (CD45.2; cyan). Original magnification, x10; scale bars, 50 μm.

Notably, the remaining $Ly5.2^+$ cells in mutant chimeras were mainly localised in the central part of the follicle, possibly marking the T-cell zone. This observation was confirmed through a quantification of the anti-Ly5.1- and anti-Ly5.2 reactivity seen in the follicular area of control and mutant chimeras with milder phenotype. Specifically, whereas positivity for the Ly5.2 staining was homogeneously distributed in follicular areas of control chimeras, the same reactivity decreased moving from the central arteriole of the follicle (rich in T cells) towards the periphery (rich in B cells) (Figure 66) (Steiniger 2015). Altogether, these findings indicate that PRC1 inactivation in late transitional B cells leads to the generation of a pool of resting bona fide mature B cells with significantly impaired fitness when placed in competition with their PRC1 proficient counterparts.

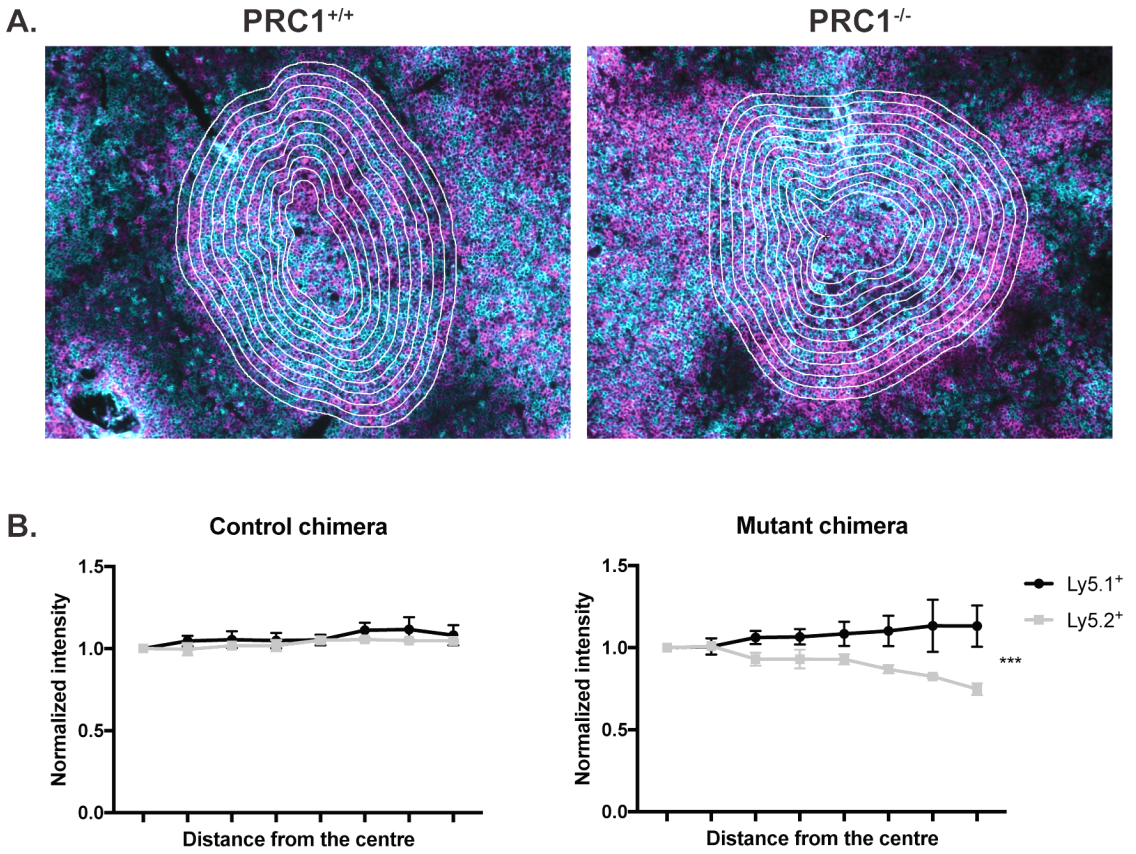

Figure 66. Ly5.2 PRC1-deficient cells localize only in the central area of the follicles.

A. Immunofluorescence analysis of spleen sections from control chimera (left) or mutant chimera (right) transplanted mice, stained with anti-Ly5.1 (CD45.1; magenta) and anti-Ly5.2 (CD45.2; cyan). Images exemplify the strategy used for quantifications. Lines are the edges of concentric sections considered for quantification of Ly5.1 and Ly5.2 signal intensity. **B.** Quantification of Ly5.1 and Ly5.2 signal intensity in splenic sections of control and mutant bone marrow chimeras. Values represent the average of the intensity in each concentric section normalized on the intensity of the central area. Data are represented oriented from the centre of the follicle towards the edges. Welch's t test: *** $p<0.001$.

5.5 Developmental defects of PRC1 mutant B cells are B-cell autonomous

5.5.1 Aberrant surface phenotype of PRC1 mutant B cells is cell intrinsic

The immunophenotypic analysis of B cells from PRC1 deficient mice revealed an aberrant expression of several surface markers. Specifically, PRC1 mutant resting peripheral B cells

could be assigned to two subpopulations on the basis of the expression of B220; furthermore, they expressed higher levels of CD93/AA4.1 and failed to down-regulate IgM expression at the expense of IgD remaining therefore IgM/IgD double positive. To determine whether the changes in marker expression were influenced by Ring1A deficiency in non-B cells, we tested the expression of the same markers in lethally irradiated PRC1 proficient mice reconstituted with bone marrow cells from conditional PRC1 mutant mice. Flow cytometric analysis on cell suspensions retrieved from lymphoid organs of reconstituted animals confirmed the aberrant expression of the B220, IgM, IgD and CD93 markers on the surface of PRC1 mutant B cells (Figure 67).

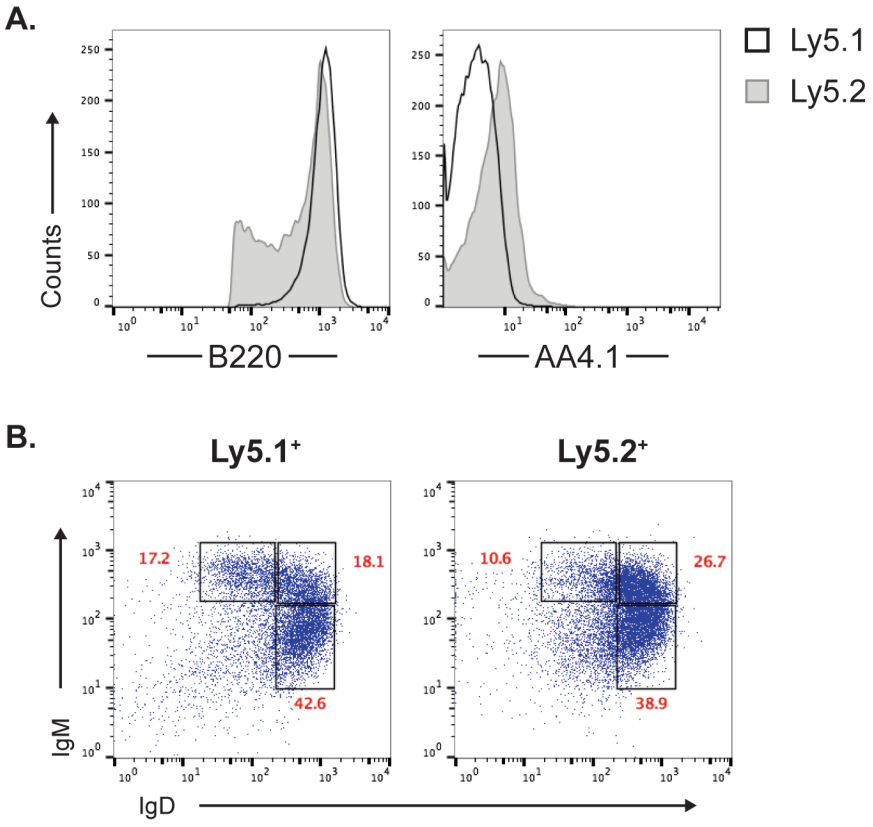

Figure 67. Defects in surface marker expression of B cells lacking PRC1 in bone marrow mutant chimeras.

A. Representative flow cytometric expression of surface markers B220 and AA4.1 on $CD19^+$ $Ly5.1^+$ control (dark line) or $CD19^+$ $Ly5.2^+$ mutant (light grey line and fill) splenic B cells. **B.** Representative dot plot analysis of the combined surface expression of IgM and IgD immunoglobulin isotypes. Data are representative of 4 analysed transplanted mice.

These results indicate that PRC1 inactivation in B cells is sufficient to cause aberrant expression of the B220, IgM, IgD and CD93 markers on the surface of these cells.

5.5.2 The splenic marginal zone is devoid of B cells in mutant bone marrow chimeras

In chapter 5.3, we show that PRC1 mutant B cells display a reduced capacity to reside in the MZ of the spleen. To establish whether PRC1 mutant B cells can home to the MZ under a competitive setting, I analysed, by immunofluorescence and flow cytometric analyses, the identity and distribution of splenic B cells in control and mutant mixed bone marrow chimeras. As shown in Figure 68, $Ly5.2^{+}$ PRC1 mutant B cells were largely undetected in the MZ area of mutant chimeras.

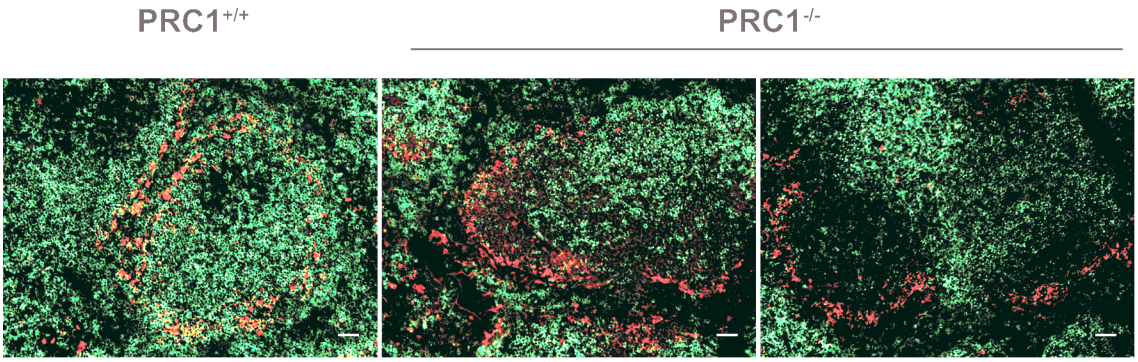

Figure 68. The marginal zone is devoid of Ly5.2 PRC1-deficient B cells.

Representative immunofluorescence analysis of spleen sections from control chimera (left) or mutant chimera (centre and right) transplanted mice, stained with anti-Ly5.2 (CD45.2; green) and anti-CD169 (MOMA-1; red). Original magnification, x10; scale bars, 50 μm.

Moreover, these B cells retained an aberrant surface phenotype, showing levels of the CD21, CD1d and CD38 markers that were intermediate between wild-type FO and MZ B cells, similarly to what was seen in PRC1 deficient mice (Figure 69). Thus, PRC1 deficiency prevents B cells from residing in the MZ in a B-cell autonomous fashion.

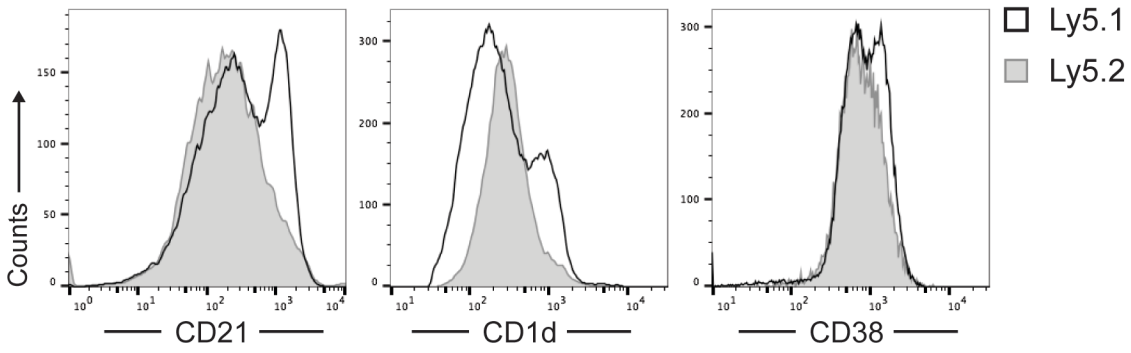

Figure 69. Marginal Zone surface marker expression is altered in PRC1-deficient B cells which develop in a Ring1A-proficient environment.

Representative flow cytometric expression of surface markers CD21, CD1d and CD38 on CD19^{+} Ly5.1^{+} control (dark line) or CD19^{+} Ly5.2^{+} mutant (light grey line and fill) splenic B cells. Data are representative of 4 analysed transplanted mice.

5.6 PRC1 is required to sustain B cell activation

Flow cytometric analysis of cell suspensions from mesenteric lymph nodes and Peyer's patches of PRC1 control and mutant mice revealed a significant reduction of the fraction of CD19^{+} CD95/FAS^{hi} CD38^{lo} germinal centres (GC) B cells in the latter animals (Figure 70).

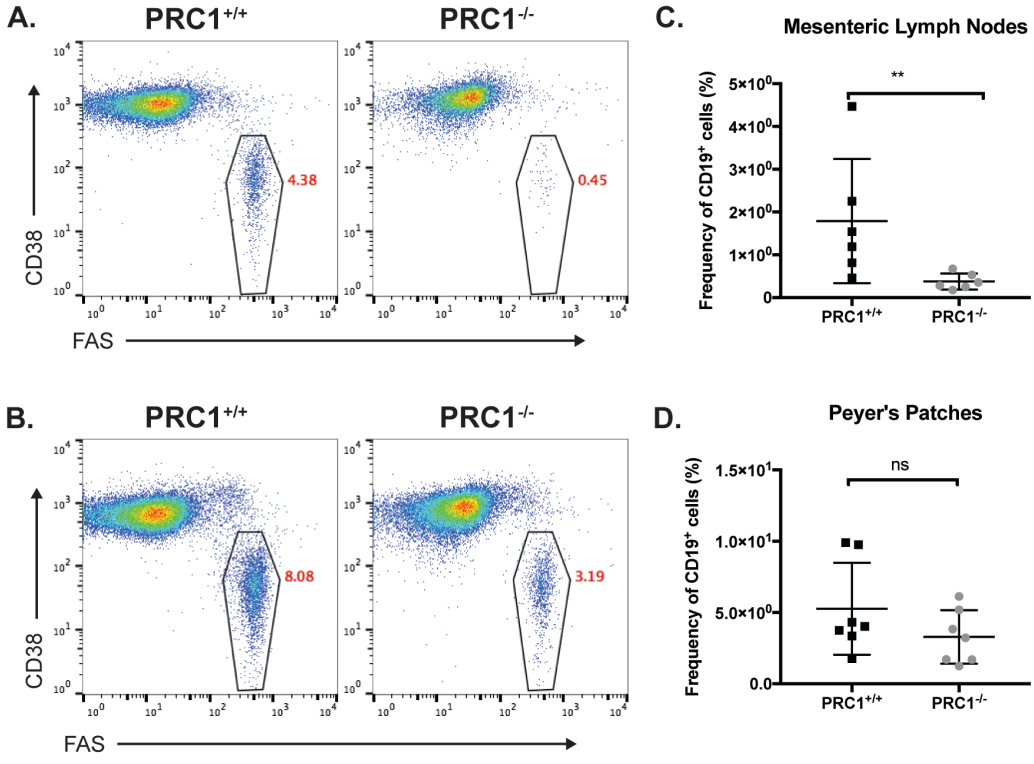

Figure 70. Germinal centres are reduced in lymph nodes of PRC1-deficient animals.

A-B. Representative flow cytometric analysis of gated CD19^{+} CD95/FAS^{hi} CD38^{lo} GC B cell frequencies in the mesenteric lymph nodes (A.) and Peyer's patches (B.) of PRC1$^{+/+}$ control and PRC1$^{-/-}$ mutant mice. **C.** Frequency of gated CD19^{+} Fas^{hi} CD38^{lo} GC in mesenteric lymph nodes in PRC1$^{+/+}$ control (n=6; left) and PRC1$^{-/-}$ mutant mice (n=6; left). Bars represent the mean value ± SEM. Unpaired T test: * p<0.05. **D.** Frequency of gated CD19^{+} Fas^{hi}CD38^{lo} GC in Peyer's patches in PRC1$^{+/+}$ control (n=7; left) and PRC1$^{-/-}$ mutant mice (n=7; left). Bars represent the mean value ± SEM. Mann-Whitney non-parametric test: *** p <0.001; ns = not significative.

Furthermore, previous experiments from our laboratory demonstrated a significant defect in GC formation/maintenance in PRC1 conditional mutant animals upon immunization with the T-cell dependent antigen NP-CGG. Similar defects were observed when PRC1$^{-/-}$ B cells were stimulated *in vitro* with CD40 ligation in the presence of interleukin-4 (IL-4) (Dr. F. Alberghini, PhD thesis work). These observations pointed to a potential problem of PRC1 mutant B cells in getting activated and in proliferating in response to mitogenic stimulation. To get more insight into this, B cells purified from PRC1-proficient and -deficient animals were activated *in vitro* through stimulation with lipopolysaccharide (LPS), which binds to and activates signalling from Toll-like receptor-4 (TLR-4). I added IL-4 to the culture to stimulate B cells to undergo IgG1 and IgE immunoglobulin (Ig) class-switch recombination (CSR). As shown in Figure 71, the growth of PRC1 mutant B cells was significantly delayed until day-2 when compared to control cultures, and was completely stalled at day-3 of stimulation.

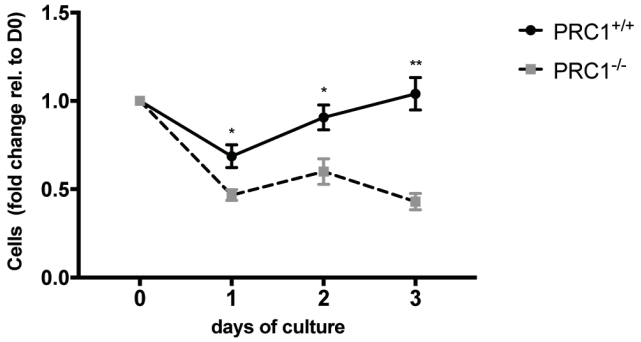

Figure 71. Impairment of cell replication in PRC1-deficient B cells stimulated *in vitro* with LPS and IL-4.

Growth curve of CD19^{+} splenic B cells purified from PRC1$^{+/+}$ control and PRC1$^{-/-}$ mutant mice, stimulated *in vitro* with LPS and IL-4 for 3 days. Markers represent the mean value of three technical replicates ± SD. Unpaired T test: * p<0.05; ** p<0.01. Data shown are representative of 3 independent experiments.

The observed growth inhibition can be attributed to three main causes, namely to proliferation defects, to increased cell death and/or to enhanced terminal differentiation to plasma cells (PC).

5.6.1 PRC1 favours cell-cycle progression ensuring transcriptional repression of CDK inhibitors

To assess the effects of PRC1 inhibition on cell proliferation, I performed cell-cycle distribution analyses. Specifically, I combined pulsed BrdU-labelling with propidium iodide (PI) staining in B cell cultures stimulated with LPS+IL4. Strikingly, both at day-2 and -3, PRC1-deficient B cells accumulated preferentially in the G_0/G_1 phase of the cell cycle with a correspondent reduction of the fraction of cells actively replicating DNA in S-phase (Figure 72).

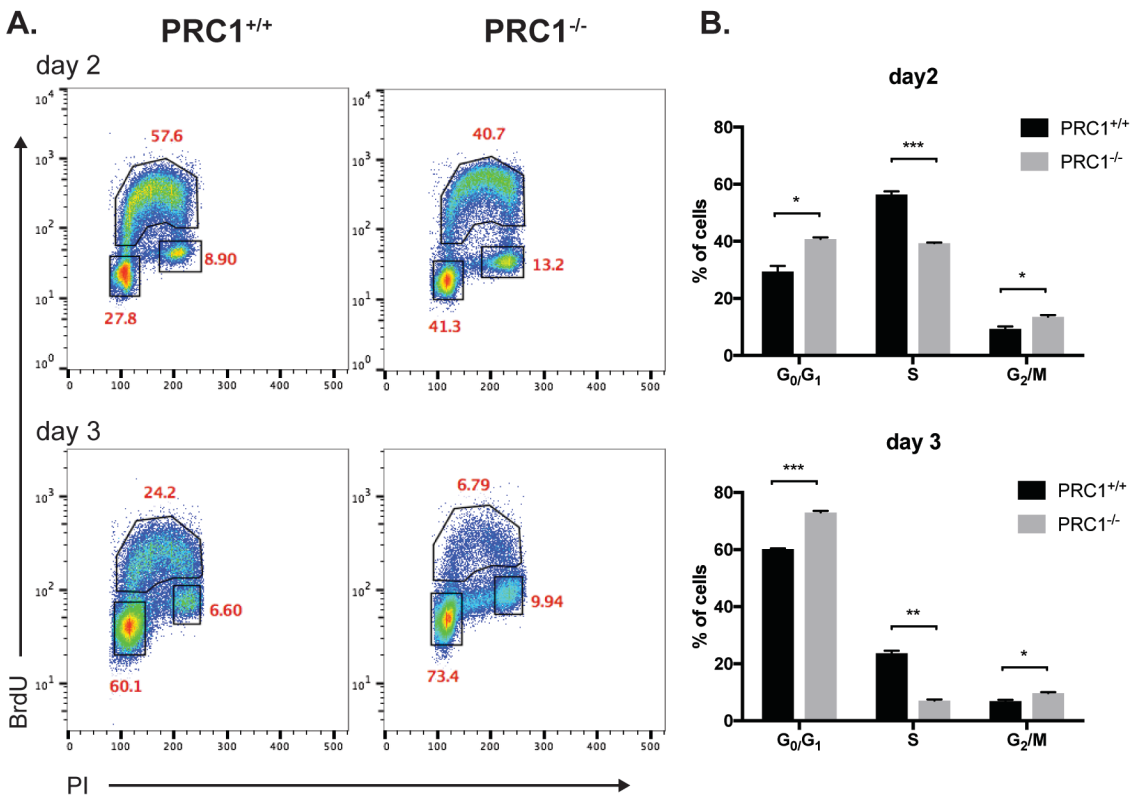

Figure 72. Impairment of cell-cycle progression in PRC1-mutant B cells stimulated *in vitro* with LPS and IL-4.

A. Flow cytometric analysis and **B.** quantification of cell-cycle distribution of $PRC1^{+/+}$ control (left; n=2) and $PRC1^{-/-}$ mutant (right; n=2) B cell cultures, at day-2 and -3 of *in vitro* stimulation with LPS and IL-4. Bars represent the mean value ± SD. Unpaired

Mann-Whitney non-parametric test: * p<0.05; ** p<0.01; *** p<0.001. Data are representative of 2 independent experiments.

The fraction of cells in the G_2-phase was also increased in the mutant B cell cultures. These data point to a strict requirement of PRC1 function in B cells undergoing proliferation in response to mitogens. Expression analyses in resting PRC1 mutant B cells revealed a substantial up-regulation of the Polycomb targets encoding for the cyclin-dependent kinase (CDK) inhibitors *p15*^{Cdkn2b}, *p16*^{INK4a}, *p19*^{ARF}, *p21*^{Cdkn1a} and *p57*^{Kip2} (Figure 73A). Upon LPS+IL4 activation, the latter cells also up-regulated *p18*^{INK4c} and *p27*^{Kip1} which may contribute to the G_1-to-S cell cycle arrest suffered by the inhibition of PRC1 (Figure 73B) (Sauvageau and Sauvageau 2010).

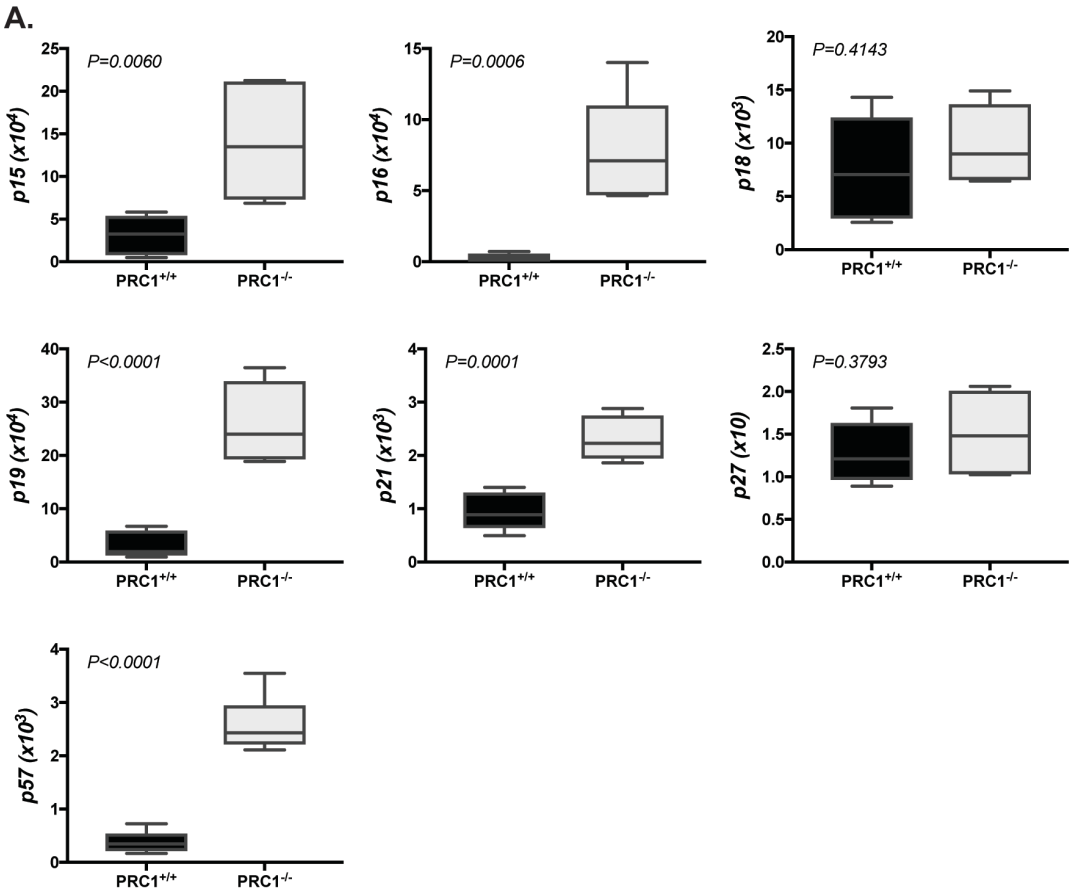

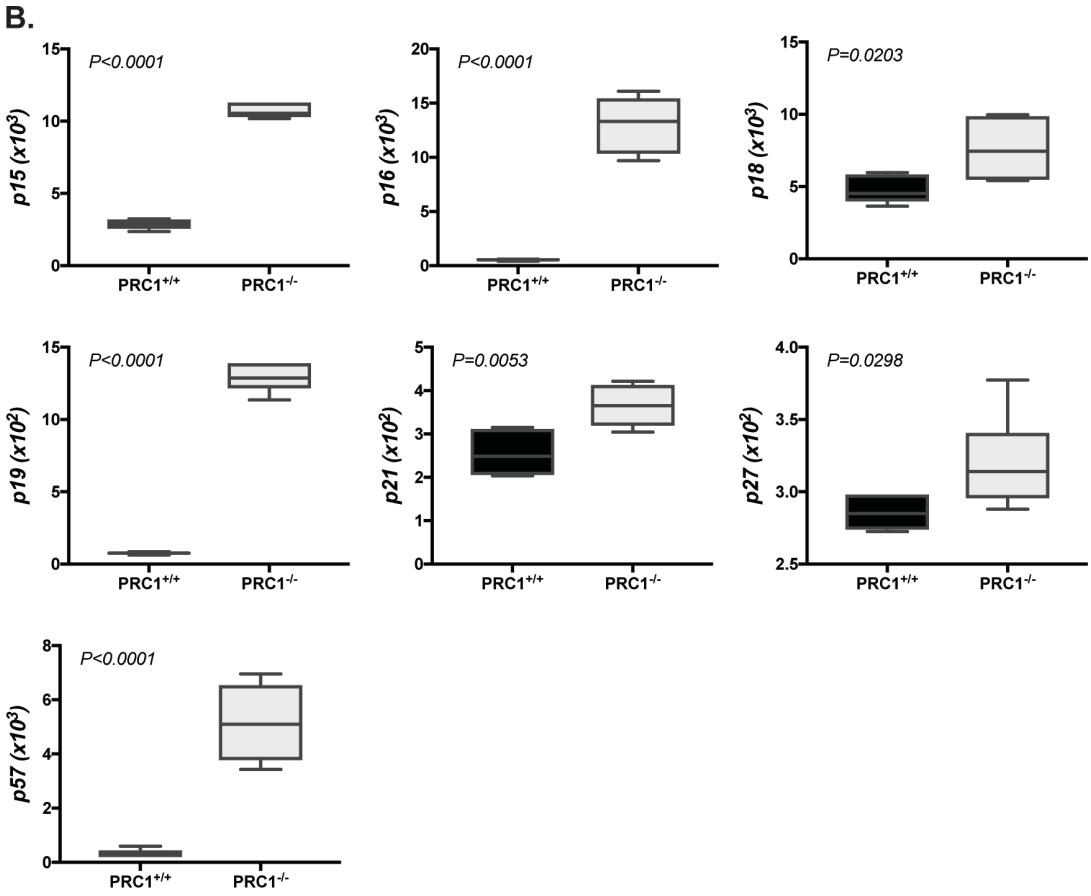

Figure 73. Up-regulation of cyclin-dependent kinase inhibitor transcripts in PRC1-deficient B cells in resting state and upon *in vitro* stimulation with LPS and IL-4.

Box-plot analysis of transcript levels of cyclin-dependent kinase inhibitor genes (relative to *Rplp0*) quantified in control PRC1$^{+/+}$ (n=6) and mutant PRC1$^{-/-}$ (n=6) B cells **A.** in resting state and **B.** after 3 days of *in vitro* stimulation with LPS and IL-4. In box-plots, horizontal bars indicate the medians, boxes indicate 5th to 95th percentiles. P values are indicated within each plot (unpaired Student's t test).

Overall, these results indicate a major inhibition of the G_0/G_1-to-S cell cycle transition in B cells lacking PRC1 caused by a significant up-regulation of CDK inhibitors.

The strong impairment in cell cycle-progression could affect the capacity of LPS+IL-4-stimulated B cells to undergo immunoglobulin isotype switching. To test this hypothesis, *ex vivo* isolated control and PRC1 mutant B cells were first labelled with CFSE followed by their stimulation with LPS + IL-4. Flow cytometric analysis of B cells activated for four days revealed a significant reduction in the proportion of PRC1 mutant B cells that had undergone three or more cell divisions. This defect correlated with a striking reduction in the frequency

of IgG1-expressing B cells (Figure 74A-B). A similar result was observed analysing IgG3-expressing B cells after 4-days of LPS stimulation, although the block in cell-cycle transition was weaker and the difference in the fraction of IgG3-class-switched cells between control and mutant cultures was less remarkable (Figure 74C-D). Altogether, these data highlight the importance of PRC1 in the control of Ig isotype switching, possibly by facilitating the cell-cycle G_1-to-S transition.

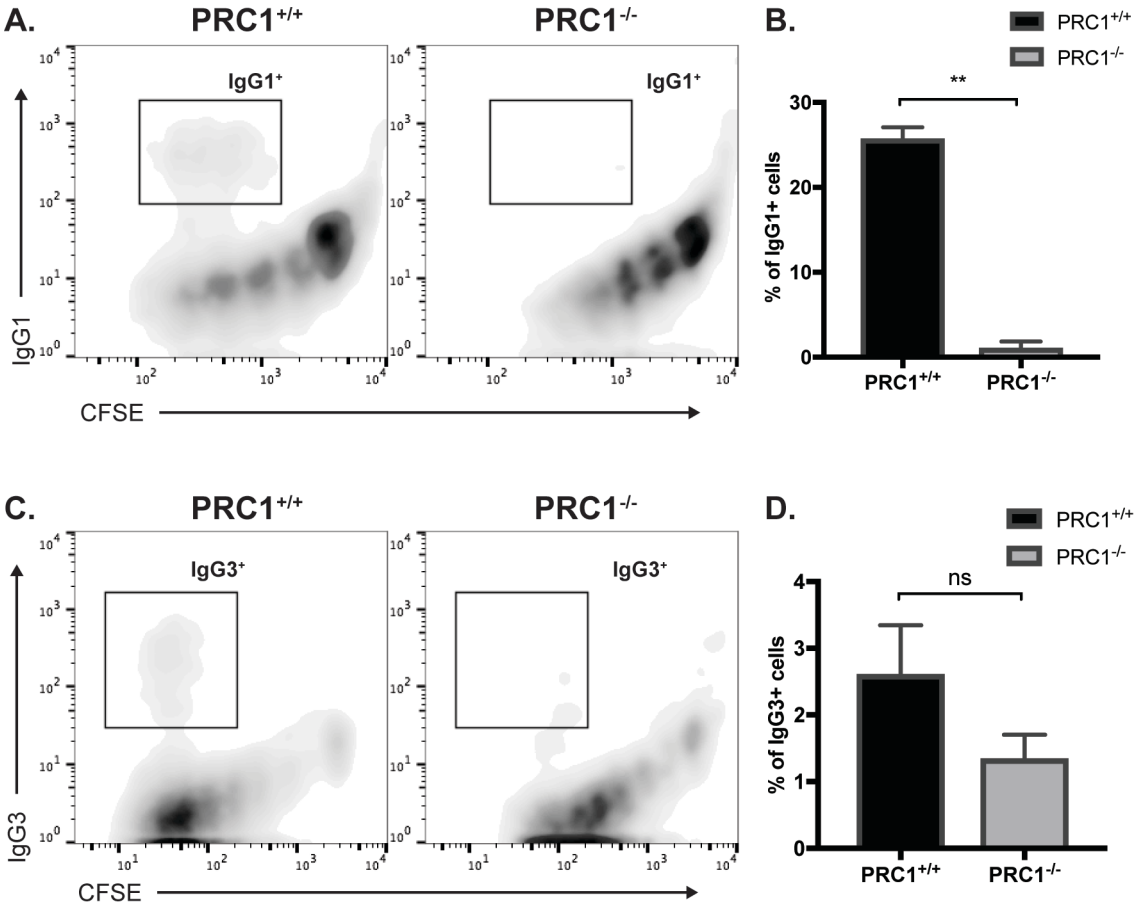

Figure 74. Class switching to IgG1 and IgG3 is defective in PRC1-mutant B cells *in vitro*.

A. Flow cytometric analysis displaying IgG1$^+$ cell frequencies of CFSE-labelled PRC1$^{+/+}$ control (left; n=2) and PRC1$^{-/-}$ mutant (right; n=2) cell cultures, at day-4 of *in vitro* stimulation with LPS and IL-4. **B.** Quantification of class switched IgG1$^+$ cell frequencies in PRC1$^{+/+}$ control (left; n=2) and PRC1$^{-/-}$ mutant (right; n=2) cell cultures, at day-4 of *in vitro* stimulation with LPS and IL-4. **C.** Flow cytometric analysis displaying IgG3$^+$ cell frequencies of CFSE-labelled PRC1$^{+/+}$ control (left; n=2) and PRC1$^{-/-}$ mutant (right; n=2) cell cultures, at day-4 of *in vitro* stimulation with LPS. **D.** Quantification of class switched IgG3$^+$ cell frequencies in PRC1$^{+/+}$ control (left; n=2) and PRC1$^{-/-}$ mutant (right; n=2) cell cultures, at day-4 of *in vitro* stimulation with LPS. Bars represent the mean value ± SD. Unpaired t test with Welch's correction: ** $p<0.01$; ns = not significative. Data are representative of 3 independent experiments.

5.6.2 PRC1 protects B cells from apoptosis and genotoxic DNA damage

To investigate the effect of PRC1 deficiency on cell-death, LPS+IL4 stimulated B cells were labelled with CaspGLOW™, as described previously. By flow cytometry, we scored an over 4-fold increase in the percentage of apoptotic cells in PRC1 mutant B cell cultures relative to controls (Figure 75).

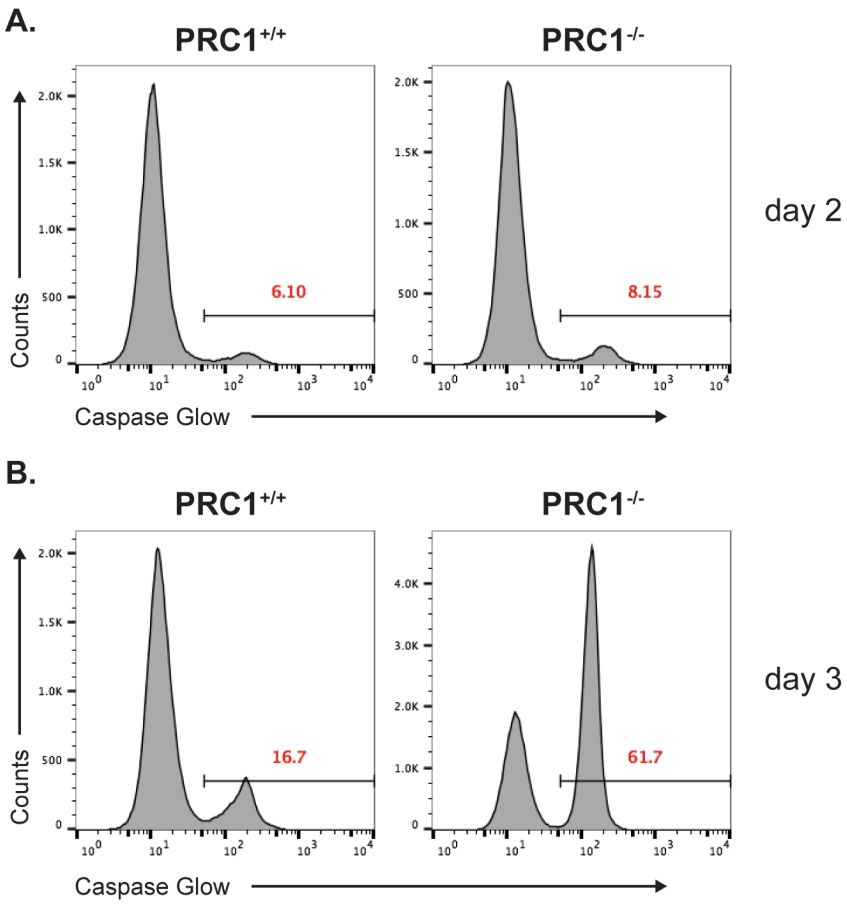

Figure 75. Frequency of apoptotic cells is increased in PRC1-mutant B cells stimulated *in vitro* with LPS and IL-4.

A-B. Flow cytometric analysis of Caspase glow^{+} cells of PRC1$^{+/+}$ control (left; n=2) and PRC1$^{-/-}$ mutant (right; n=2) cell cultures stimulated *in vitro* with LPS and IL-4. Cells were analysed at day-2 (A.) and day-3 (B). Numbers represent the frequency of Caspase Glow^{+} cells. Data are representative of 2 independent experiments.

Consistently with previous observations, after 3-days of stimulation transcripts for the apoptotic sensors *Puma*, *Noxa* and *Bim* were substantially up-regulated, suggesting enhanced sensitivity to apoptotic cell-death of PRC1 mutant B cells (Figure 76).

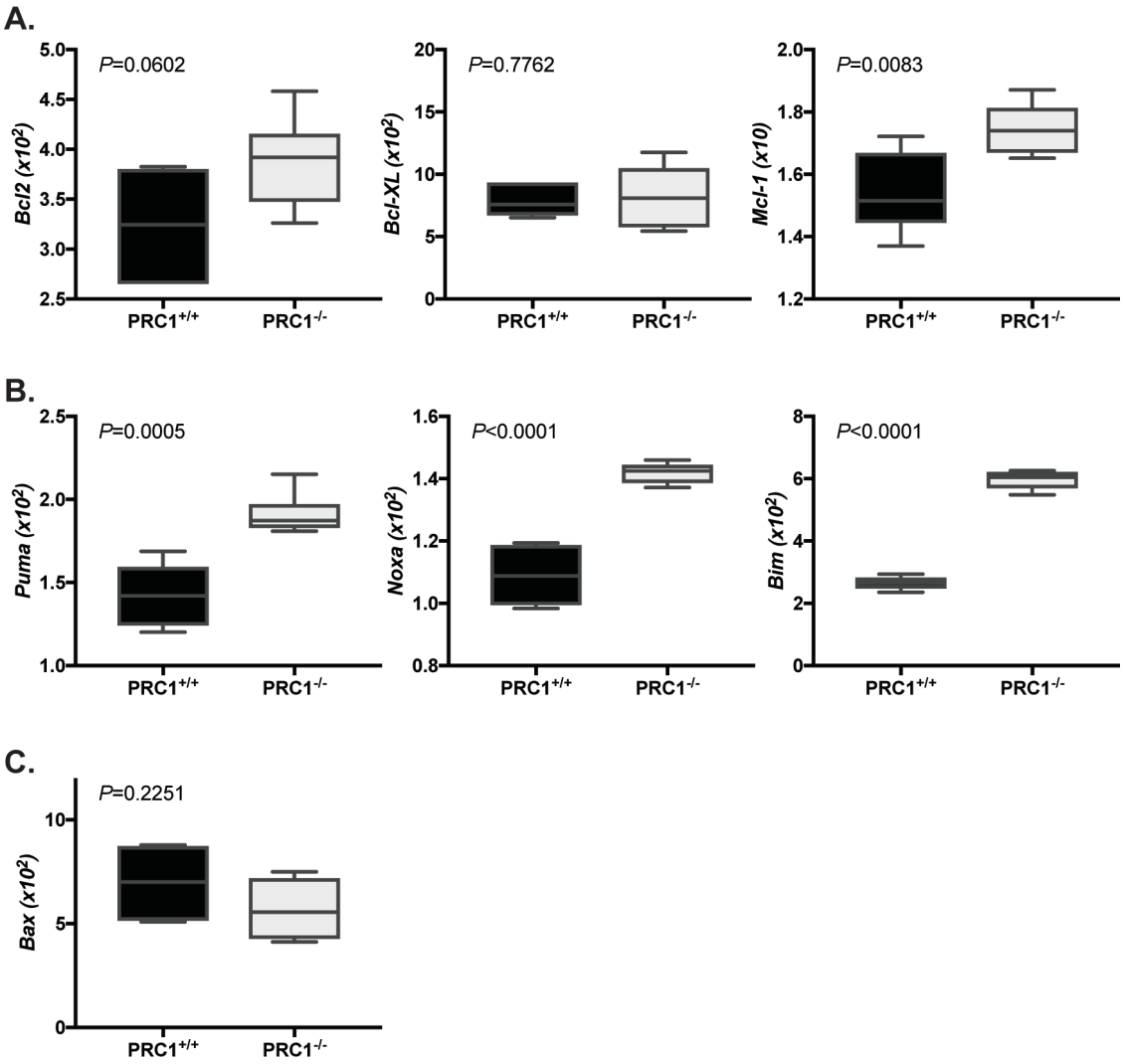

Figure 76. Up-regulation of apoptotic sensors in PRC1-mutant B cells stimulated with LPS and IL-4 *in vitro*.

Box-plot analysis of transcript levels of Bcl2 family apoptotic genes (relative to *Rplp0*) quantified in control PRC1$^{+/+}$ and mutant PRC1$^{-/-}$ B cells stimulated with LPS and IL-4 *in vitro* for 3 days. **A.** Anti-apoptotic genes. **B.** Apoptotic sensor genes. **C.** Pro-apoptotic gene. In box-plots, horizontal bars indicate the medians (n=6), boxes indicate 5th to 95th percentiles. P values are indicated within each plot (unpaired Student's t test).

LPS stimulation triggers the expression of activation-induced cytidine deaminase (AID) (Dedeoglu et al. 2004), which promotes Ig CSR as a result of cytosine deamination at Ig

switch regions, followed by DNA double-strand breaks which ultimately are repaired by the DNA repair machinery leading to the joining of heterologous switch regions. We hypothesized that DNA damage induced in LPS activated B cells by AID (Caganova et al. 2013) and/or other genotoxic processes such as DNA replication (Piunti et al. 2014; Bravo et al. 2015; Klusmann et al. 2018) could be repaired through mechanisms that required PRC1 activity. To investigate this, control and PRC1 mutant B cell cultures, stimulated with LPS+IL4 were assessed by immunofluorescence for the presence of γH2A.X foci, indicating the activation of a DNA damage response counteracting the occurrence of DNA double-strand breaks. To detect ongoing genotoxic damage, we also performed the neutral comet assay (Ostling and Johanson 1984; Lemay and Wood 1999). Both techniques revealed a slight but consistent increase of DNA damage in B cells lacking PRC1. Specifically, while the quantification of γH2A.X foci revealed an increased number of foci per PRC1 mutant cell (Figure 77), for the same cells, the comet assay showed marked DNA tail lengthening relative to control (Figure 78A-B). Additionally, the amount of PRC1 mutant DNA contained in comet tails was significantly higher than in controls (Figure 78C). Altogether, these data suggest an accumulation of DNA damage in LPS-activated B cells lacking PRC1, possibly increasing the sensitivity of these cells to apoptosis.

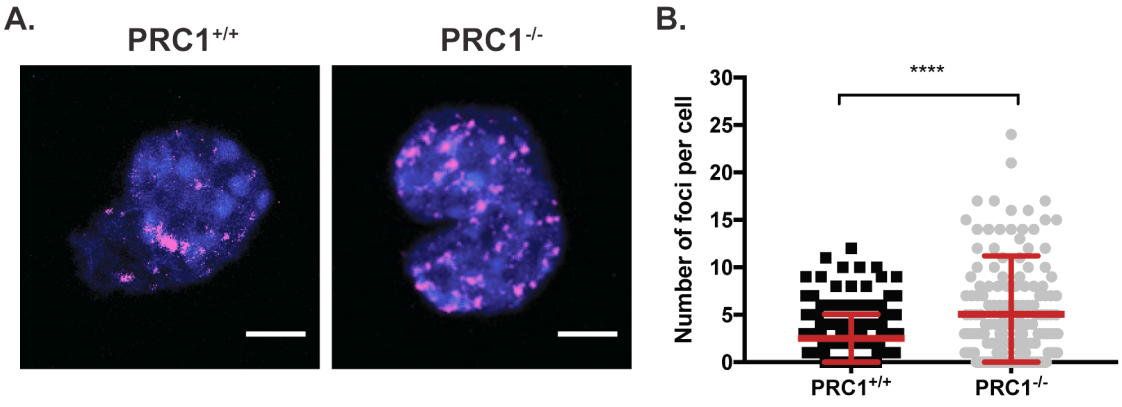

Figure 77. Increased γH2A.X foci in PRC1-deficient B cells stimulated *in vitro* with LPS and IL-4.

A. Representative immunofluorescence staining of cells stained with anti-γH2A.X and **B.** quantification of immunofluorescent γH2A.X foci in PRC1$^{+/+}$ control (left) and PRC1$^{-/-}$ mutant (right) cell cultures, at day-2 of *in vitro* stimulation with LPS and IL-4. Original

magnification, x63; scale bar, 5 μm. Data are representative of 2 independent experiments.

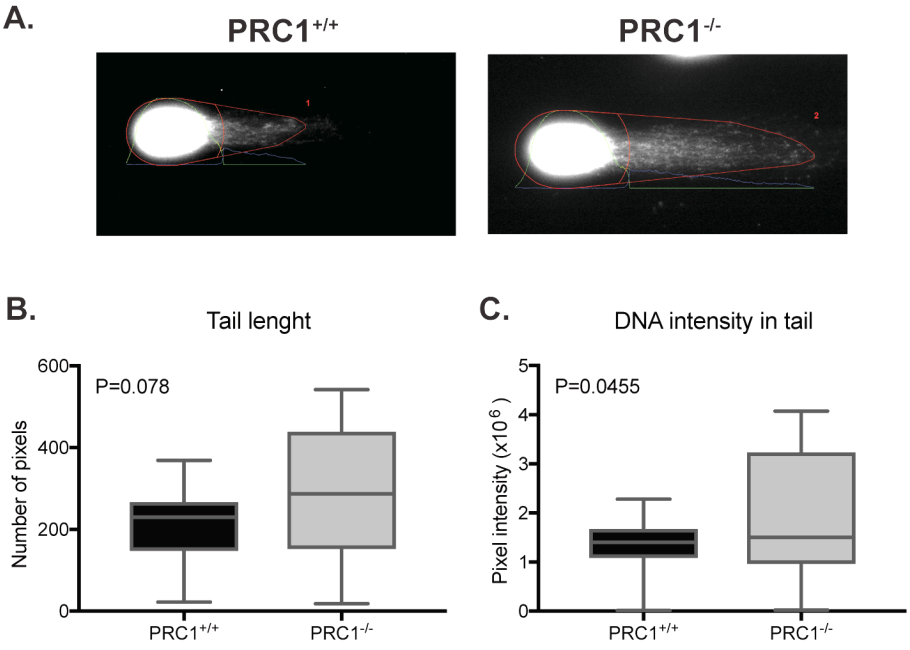

Figure 78. Accumulation of DNA double-strand breaks in PRC1-deficient B cells stimulated *in vitro* with LPS and IL-4.

Neutral comet assay data is shown for PRC1$^{+/+}$ and PRC1$^{-/-}$ purified B cells stimulated *in vitro* with LPS and IL-4 for 2 days. **A.** Representative single cell images used for scoring within the two categories are shown next to the quantitation. **B.** Scoring of the length (pixel) of the comet tails in PRC1$^{+/+}$ sample (n=20) and PRC1$^{-/-}$ sample (n=22). **C.** Scoring of the amount of DNA in the comet tail (pixel intensity) in PRC1$^{+/+}$ sample (n=20) and PRC1$^{-/-}$ sample (n=22). In box-plots, horizontal bars indicate the medians, boxes indicate 5th to 95th percentiles. P values are indicated within each plot (Unpaired t test with Welch's correction). Data are representative of one experiment.

5.6.3 Cell-cycle inhibition and apoptosis are independent from AID induction

Previous work from our group has linked PRC2 to the protection of B cells from genotoxic damage induced by AID (Caganova et al. 2013). To test whether PRC1, as PRC2, confers protection from AID-induced mutagenesis, or rather, contributes to preserve B cells from other sources of DNA damage, we stimulated PRC1 mutant B cells with an agonistic anti-

RP105 antibody. The latter stimulation triggers potent proliferation of the B cells without inducing either AID expression or terminal differentiation (Ogata et al. 2000; Callen et al. 2007). Strikingly, similar to what observed for the LPS stimulation setting, PRC1 mutant B cells displayed severe growth impairment (Figure 79), cell-cycle defects (Figure 80) and increased apoptosis upon anti-RP105 stimulation (Figure 81). These findings indicate that PRC1 deficient B cells, upon mitogenic stimulation, suffer from substantial defects in cell proliferation even in the absence of AID expression.

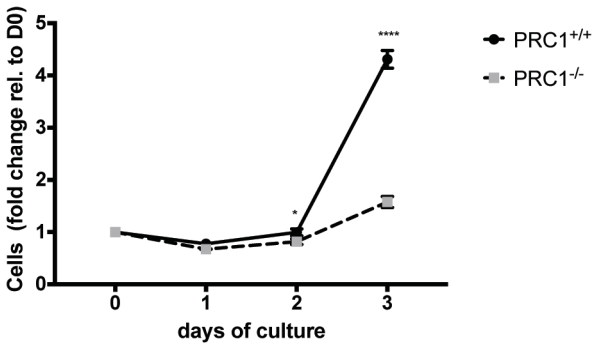

Figure 79. Impairment of cell replication in PRC1-deficient B cells stimulated *in vitro* with anti-RP105.

Growth curve of $CD19^+$ splenic B cells purified from $PRC1^{+/+}$ control and $PRC1^{-/-}$ mutant mice, stimulated *in vitro* with anti-RP105 for 3 days. Markers represent the mean value of three technical replicates ± SD. Unpaired T test: * $p<0.05$; **** $p<0.0001$. Data shown are representative of 3 independent experiments.

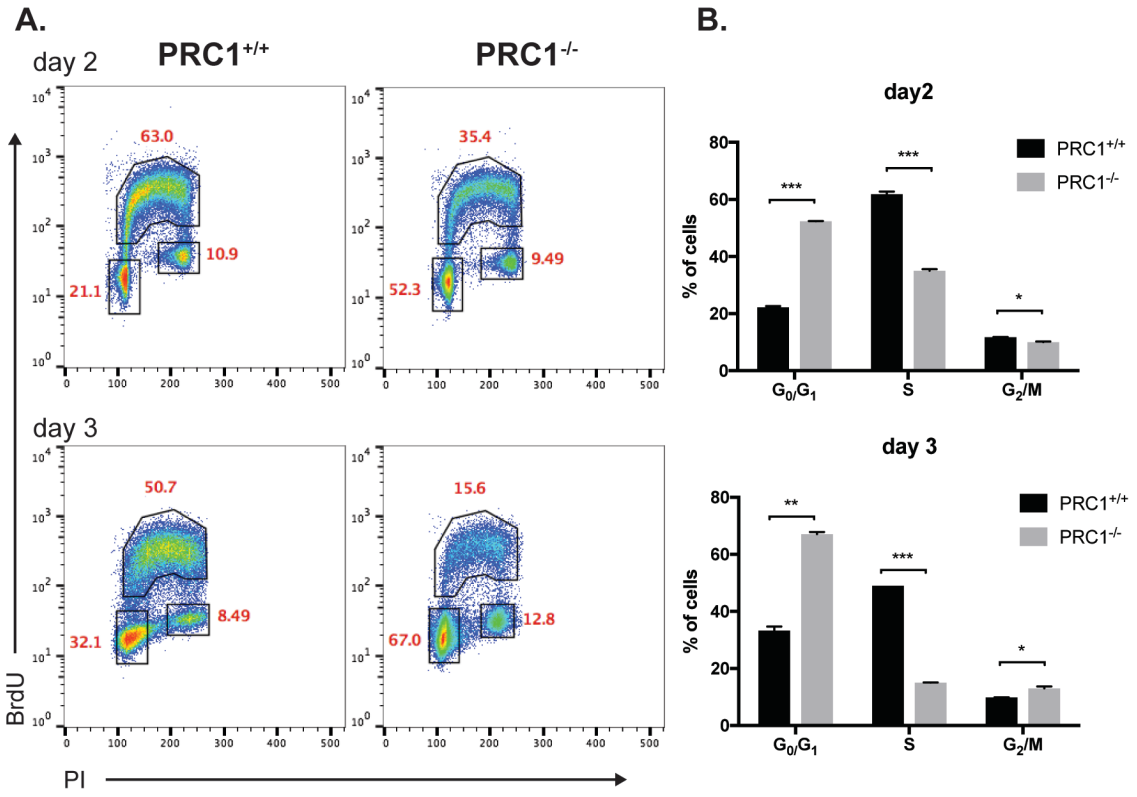

Figure 80. Impairment of cell-cycle progression in PRC1-mutant B cells stimulated *in vitro* with anti-RP105.

A. Flow cytometric analysis and **B.** related quantification of cell-cycle distribution of PRC1$^{+/+}$ control (left; n=2) and PRC1$^{-/-}$ mutant (right; n=2) B cell cultures, at day-2 and -3 of *in vitro* stimulation with anti-RP105. Bars represent the mean value ± SD. Unpaired Mann-Whitney non-parametric test: * p<0.05; ** p<0.01; *** p<0.001. Data are representative of 2 independent experiments.

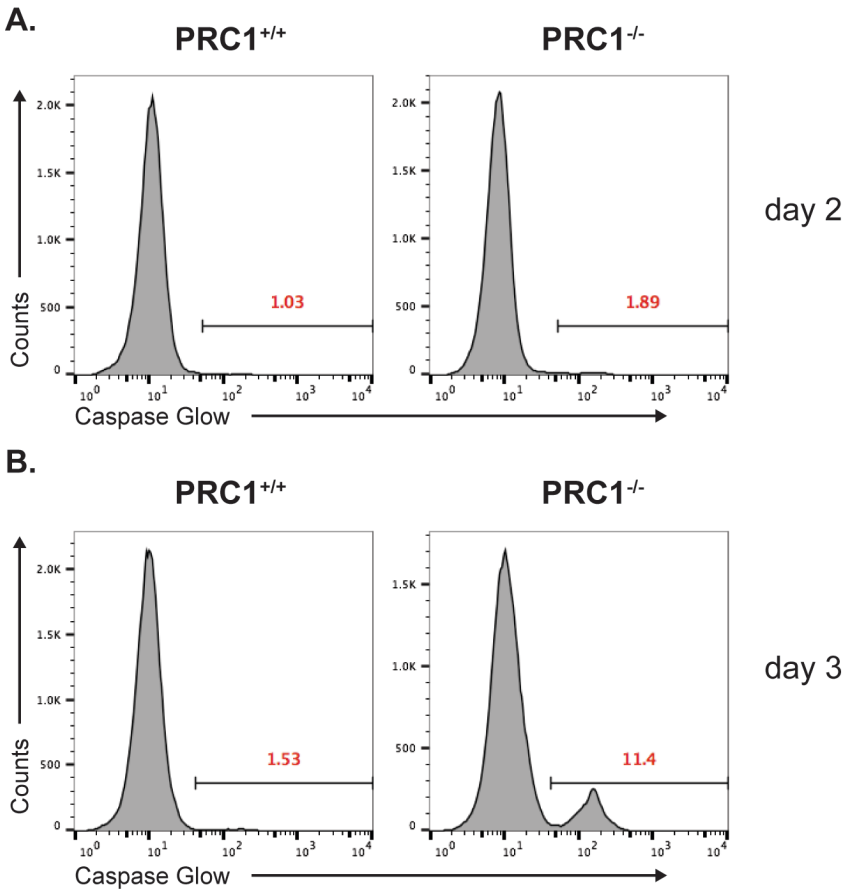

Figure 81. Frequency of apoptotic cells is increased in PRC1-mutant B cells stimulated *in vitro* with anti-RP105.

A-B. Flow cytometric analysis of Caspase glow^{+} cells of PRC1$^{+/+}$ control (left; n=2) and PRC1$^{-/-}$ mutant (right; n=2) cell cultures stimulated *in vitro* with anti-RP105. Cells were analysed at day-2 (A.) and day-3 (B.). Numbers represent the frequency of Caspase Glow^{+} cells. Data are representative of 2 independent experiments.

To understand if heightened cell-cycle arrest and apoptosis in PRC1 mutant B cell cultures stimulated with anti-RP105 correlated with increased genotoxic damage, I measured γH2A.X foci by immunofluorescence analysis. Interestingly, quantification of the data revealed a decrease in the number of γH2A.X foci per cell in PRC1 mutant B cell cultures relative to controls (Figure 82). This difference probably mirrors the different extent of replication-stress suffered respectively by control and mutant B cell cultures, which showed different replication rates.

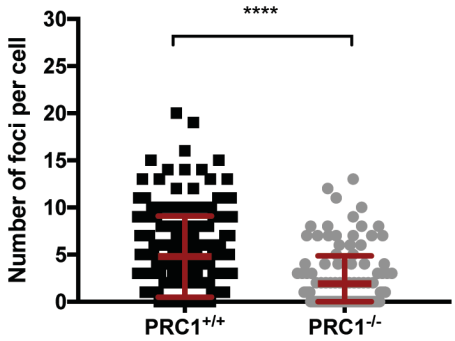

Figure 82. DNA damage is reduced in PRC1 deficient B cells stimulated with anti-RP105.

Quantification of immunofluorescent γH2A.X foci in control (left) and mutant (right) cell cultures, at day-2 of *in vitro* stimulation with anti-RP105. Bars represent the mean value ± SD. Mann-Whitney non-parametric test: **** p<0.0001.

All together these results highlight the property of PRC1 to protect B cells from the genotoxic damage generated during cell proliferation, possibly in relationship to DNA replication.

5.7 PRC1 deficiency facilitates onset of plasma cell differentiation

5.7.1 *In vitro* plasma cell differentiation in the absence of PRC1

Interference with cell proliferation shown by PRC1 mutant B cells stimulated *in vitro* with LPS could result from an acceleration of terminal differentiation. To address this point, B cells stimulated for four days with LPS+IL4 were analysed by flow-cytometry. Despite the marked interference with cell proliferation caused by PRC1 inactivation, the fraction of $IRF4^{hi}$ $CD138^{+}$ bona fide plasma cells (PCs) was comparable between control and $PRC1^{-/-}$ cultures (Figure 83). Moreover, we observed that the PRC1 mutant B cells falling within the $IRF4^{hi}$ $CD138^{-}$ gate established on LPS+IL-4-stimulated control B cells, expressed low, yet detectable, levels of CD138. This result is suggestive of an attempt of PRC1 mutant B cells to complete PC differentiation despite the strong proliferative defect suffered by these cells.

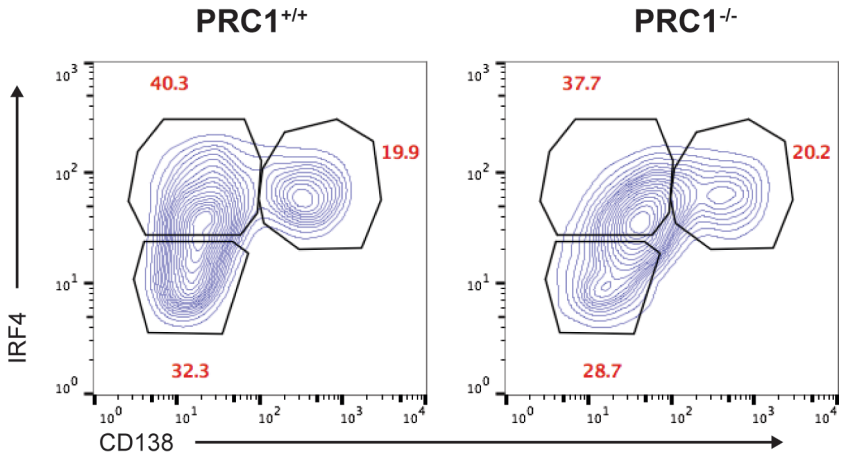

Figure 83. PRC1-deficient B cell differentiation to plasma blasts is comparable to control upon LPS and IL-4 stimulation.

Flow cytometric analysis displaying CD138^{-} IRF4^{lo}, CD138^{-} IRF4^{hi} and CD138^{+} IRF4^{hi} frequencies in PRC1$^{+/+}$ control (left; n=2) and PRC1$^{-/-}$ mutant (right; n=2) cell cultures, at day-4 of *in vitro* stimulation with LPS and IL-4. Data are representative of 3 independent experiments.

We repeated the same experiments stimulating *in vitro* PRC1 control and mutant B cells only with LPS. In these experiments, we observed an even higher proportion of IRF4^{hi} CD138^{+} bona fide PCs in the cultures of PRC1 defective B cells (Figure 84). Conversely, the fraction of IRF4^{hi} CD138^{-} was significantly reduced in PRC1 mutant cultures, consistent with a direct transition of B cells from one resting state to another, which expressed markers of PCs (IRF4^{hi} CD138^{+}).

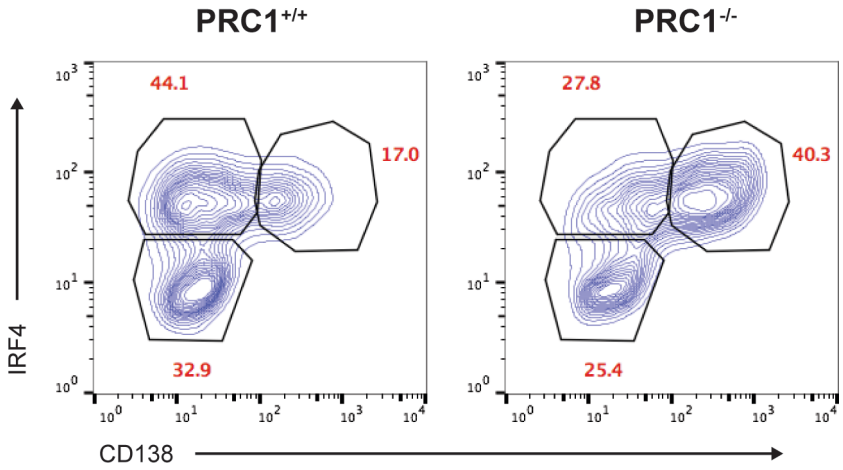

Figure 84. PRC1-deficient B cell differentiation to plasma blasts is enhanced compared to control upon LPS stimulation.

Flow cytometric analysis displaying CD138^{-} IRF4^{lo}, CD138^{-} IRF4^{hi} and CD138^{+} IRF4^{hi} frequencies in PRC1$^{+/+}$ control (left; n=2) and PRC1$^{-/-}$ mutant (right; n=2) cell cultures,

at day-4 of *in vitro* stimulation with LPS. Data are representative of 2 independent experiments.

In support of the idea that PRC1 inactivation facilitates the onset of the PC differentiation program in activated B cells, we found that PRC1 mutant B cells, even when stimulated with agonistic anti-RP105 which fails to induce terminal differentiation (Callen et al. 2007; Ogata et al. 2000), up-regulated the PC marker CD138 (Figure 85).

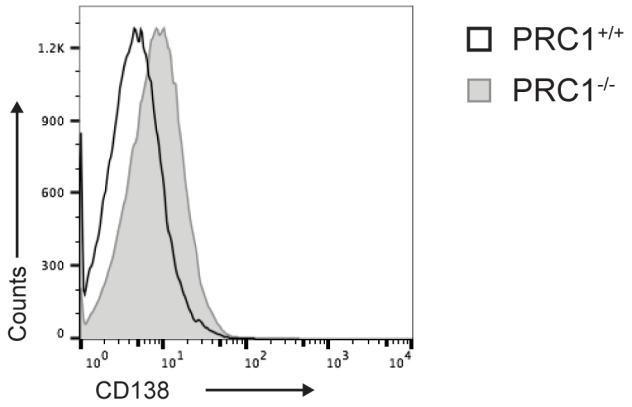

Figure 85. CD138 is over-expressed in PRC1 mutant B cells stimulated with anti-RP105.

Representative flow cytometric expression of the surface marker CD138 in $CD19^+$ B cells from $PRC1^{+/+}$ control (black line) and $PRC1^{-/-}$ mutant animals (grey line and fill) stimulated with anti-RP105 *in vitro* for 4 days. Data are representative of 2 independent experiments.

Together these results indicate that PRC1 plays an important role in delaying onset of terminal differentiation in B cells stimulated with TLR agonists, possibly by ensuring the full epigenetic reprogramming of these cells.

5.7.2 The plasma cell master regulator BLIMP-1 in PRC1 deficient resting and activated B cells

The facilitated generation of CD138-expressing bona fide plasma blasts in *in-vitro* cultures of PRC1 mutant B cells stimulated with LPS hypothesized changes in the expression of the master transcription factor required for PC differentiation, Prdm1/BLIMP-1. To address this point, we performed RT-qPCR measurements of *Prdm1* transcripts in control and PRC1 mutant B cell cultures, before and three days after LPS+IL4 activation. Both control and

PRC1 mutant B cells showed a substantial induction of *Prdm1* in response to LPS+IL4 stimulation (Figure 86), reaching similar levels at the end of the culture period.

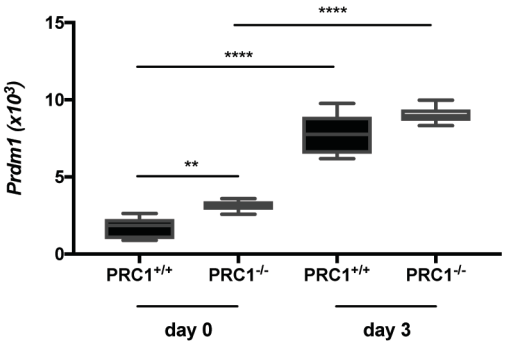

Figure 86. *Prdm1* is induced in PRC1-deficient B cells stimulated *in vitro* with LPS and IL-4.

Box-plot analysis of transcript levels of *Prdm1* gene (relative to *Rplp0*) quantified in PRC1$^{+/+}$ (n=6) and PRC1$^{-/-}$ (n=6) B cell cultures, at day-0 and -3 of *in vitro* stimulation with LPS and IL-4. In box-plots, horizontal bars indicate the medians (n=6), boxes indicate 5th to 95th percentiles. Unpaired Student's t test: ** p<0.01; **** p<0.0001.

These data were confirmed assessing BLIMP-1 protein levels at single cell resolution by flow cytometric analysis (Figure 87).

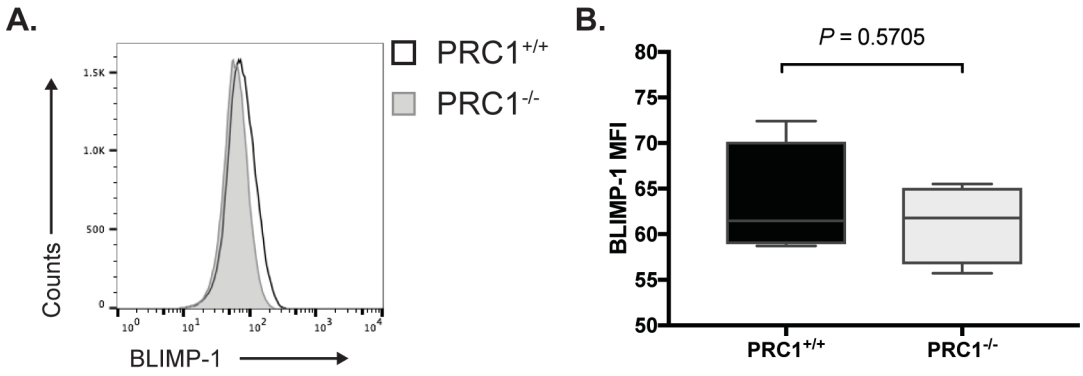

Figure 87. BLIMP-1 is unperturbed in PRC1-deficient *in vitro* stimulated B cells with LPS and IL-4.

A. Representative flow cytometric expression of BLIMP-1 intracellular transcription factor of B cells from PRC1$^{+/+}$ control (black line) or PRC1$^{-/-}$ mutant animals (grey line and fill) at day-4 of *in-vitro* activation with LPS and IL-4. Data are representative of 2 independent experiments. **B.** Mean fluorescence intensity (MFI) of BLIMP-1 protein (n=4). In box-plots, horizontal bars indicate the medians, boxes indicate 5th to 95th percentiles. P value is indicated within the plot (unpaired Student's t test).

Notably, we observed higher *Prdm1* transcript levels in *ex vivo* resting PRC1 mutant B cells in comparison to controls (Figure 86). This result, together with the marked impairment in cell-cycle progression and the comparable induction of *Prdm1* gene expression in response

to LPS stimulation, is suggestive of a scenario in which the lack of PRC1 enhances the differentiation of B cells into terminally differentiated PCs by contributing to create a permissive chromatin state, ensuring rapid and efficient induction of *Prdm1*. Premature expression of Prdm1/BLIMP-1 in activated B cells may also contribute to interfere with the growth of these cells through direct repression of the c-MYC gene (Lin, Wong, and Calame 1997).

5.7.3 Normal expression of IRF4 in PRC1 deficient resting and LPS-activated B cells

Basal increased expression of *Prdm1* was accompanied by a premature induction of CD138 in PRC1 mutant B cells stimulated *in vitro* with LPS. These analyses revealed that also IRF4, the other major transcription factor required for PC differentiation (Sciammas et al. 2006; Ochiai et al. 2013; Klein et al. 2006), followed an atypical induction kinetics after stimulation of the mutant B cells with LPS. Indeed, differently from LPS-activated control B cells, which first up-regulated IRF4 and later induced CD138 expression, PRC1 mutant cultures showed concomitant induction of both proteins (Figure 83 and Figure 84). This result could be explained by the dramatic impairment of LPS-stimulated PRC1 mutant B cells to undergo proliferation, during which IRF4 gets normally up-regulated (Scharer et al. 2018). These results, combined with normal *Irf4* transcript and protein levels detected both in resting (Figure 88) and LPS-activated (Figure 88 and Figure 89) PRC1 mutant B cells, indicate that up-regulation of IRF4 needed to trigger PC differentiation does neither require cell proliferation nor PRC1 activity.

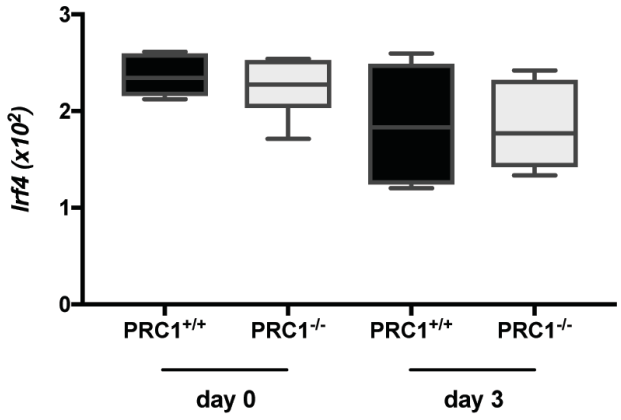

Figure 88. *Irf4* is unperturbed in PRC1-deficient B cells both in resting conditions and upon *in vitro* stimulation with LPS and IL-4.

Box-plot analysis of transcript levels of *Irf4* gene (relative to *Rplp0*) quantified in PRC1$^{+/+}$ (n=6) and PRC1$^{-/-}$ (n=6) B cell cultures, at day-0 and -3 of *in vitro* stimulation with LPS and IL-4. In box-plots, horizontal bars indicate the medians (n=6), boxes indicate 5th to 95th percentiles. Unpaired Student's t test: not significative for all comparisons.

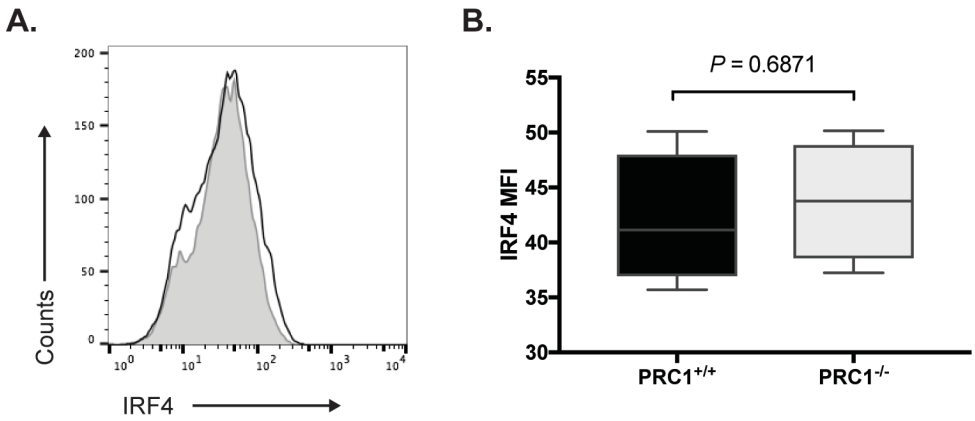

Figure 89. IRF4 is unperturbed in PRC1 mutant B cells stimulated *in vitro* with LPS and IL-4.

A. Representative flow cytometric expression of IRF4 intracellular transcription factor in B cells from PRC1$^{+/+}$ control (black line) or PRC1$^{-/-}$ mutant animals (grey line and fill) activated *in vitro* with LPS and IL-4 for 4 days. Data are representative of 2 independent experiments. **B.** Mean fluorescence intensity (MFI) of IRF4 protein (n=4). In box-plots, horizontal bars indicate the medians, boxes indicate 5th to 95th percentiles. P value is indicated within the plot (unpaired Student's t test).

5.7.4 Blimp1 and PAX-5 are co-expressed in a subset of PRC1 deficient resting B cells *in vivo*

Our studies have unveiled a modest, yet consistent, de-repression of the *Prdm1* locus in PRC1 mutant resting B cells. To confirm this result, trying at the same time to track within the spleen the location of *Prdm1*-expressing resting PRC1 mutant B cells, we performed *in situ* RNA hybridization assays. In control mice, *Prdm1* transcripts were mainly found in the extra-follicular area, in agreement with the localization at these sites of BLIMP-1-expressing PCs. Instead, strikingly, in the spleen of PRC1 mutant mice, *Prdm1* transcripts were detected in a substantial fraction of the cells homing to primary follicles (Figure 90).

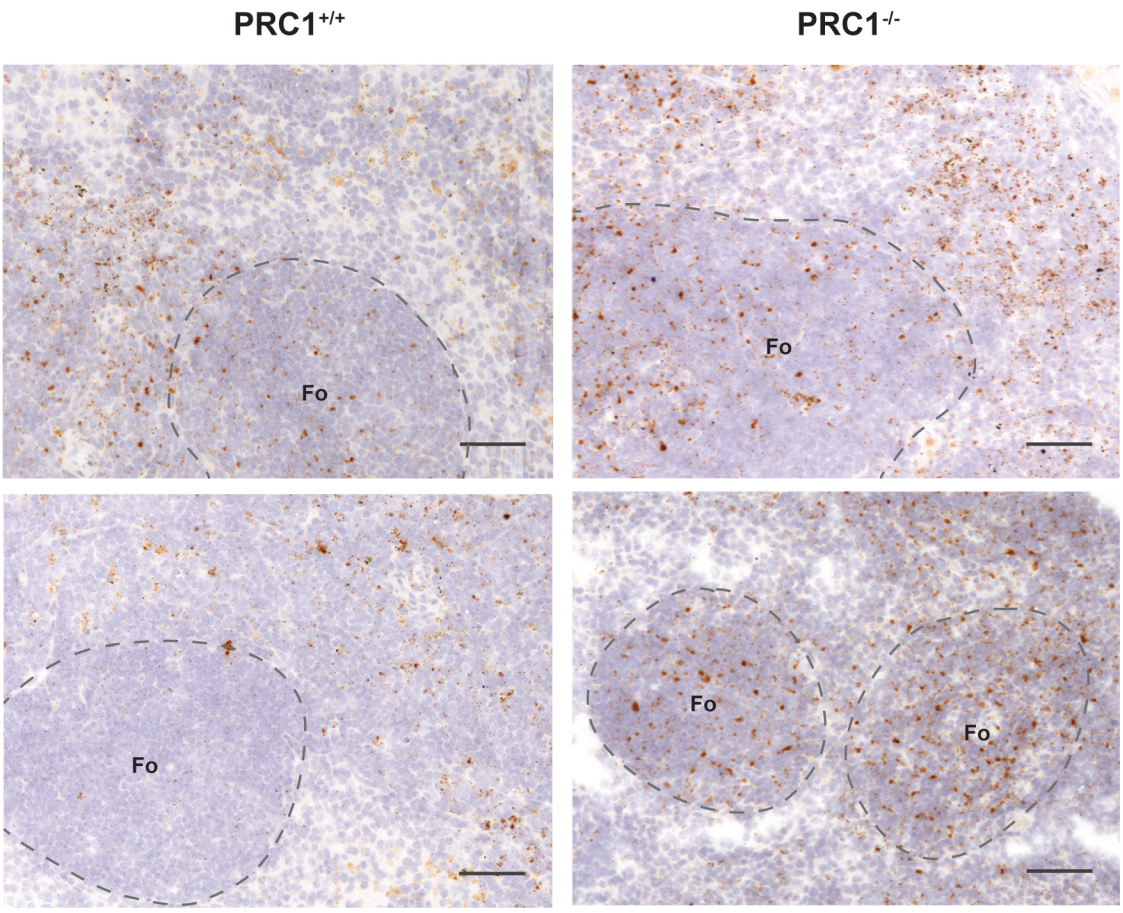

Figure 90. *Prdm1*-positive cells localise also inside the follicles in PRC1-deficient animals.

In situ hybridisation analysis showing the expression of *Prdm1* transcript in splenic sections of PRC1$^{+/+}$ control and PRC1$^{-/-}$ mutant mice. For each genotype, two representative pictures are reported. Prdm1-positive cells are in brown, eosin-positive nuclei in blue. Dashed lines mark the edge of the follicles. Data are representative of 2 independent experiments. Original magnification, x10; scale bars, 50 μm.

Double *in situ* hybridization to concomitantly detect *Prdm1*- and *Pax5*-expressing cells revealed co-expression of the two TFs in a considerable proportion of follicular B cells (Figure 91).

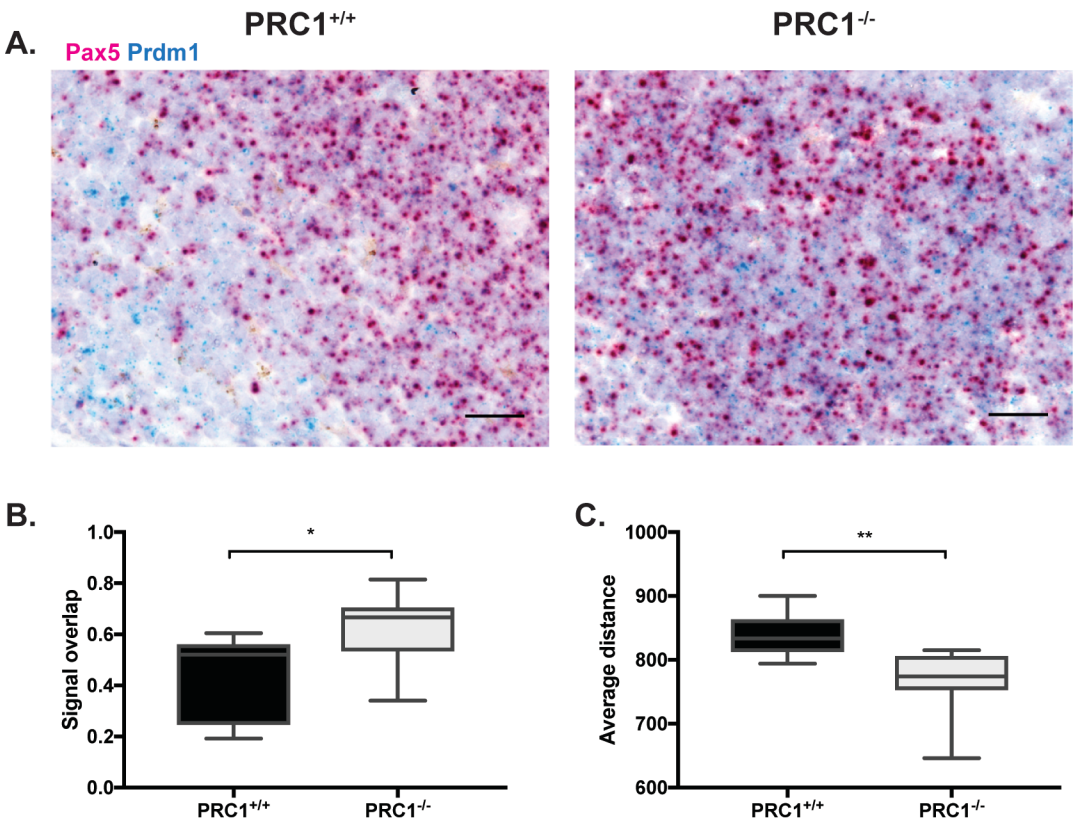

Figure 91. *Pax5* and *Prdm1* signals tend to colocalize in PRC1 deficient spleens.

A. *In situ* hybridisation analysis showing the expression of *Pax5* (magenta) and *Prdm1* (cyan) transcripts in splenic sections of PRC1$^{+/+}$ control and PRC1$^{-/-}$ mutant mice. Nuclei were stained by eosin solution. Data are representative of 2 independent experiments. Original magnification, x20; scale bars, 25 μm. **B.** Quantification of *Pax5* and *Prdm1* signal overlap and **C.** quantification of the average distance between *Pax5* and *Prdm1* signals in control and mutant splenic sections. In box-plots, horizontal bars indicate the medians, boxes indicate 5th to 95th percentiles. Data are representative of 10 measurements per sample type. Unpaired Student's t test: * $p<0.05$; ** $p<0.01$.

Overall, these data highlight the premature *in vivo* expression of *Prdm1*/BLIMP-1 in resting B cells lacking PRC1 activity, which, in turn may facilitate/accelerate the induction of the B cell terminal differentiation program in response to triggering of TLRs and possibly other receptors such as CD40 and BCR.

5.7.5 Pax5 is correctly silenced in LPS-stimulated PRC1 mutant B cells

BLIMP-1 negatively regulates the expression of the PAX5 gene by binding to promoter-proximal regions, where it recruits chromatin-remodeling complexes and PRC2 to induce transcriptional repression (Minnich et al. 2016). To understand whether 1) the expression

of Prdm1 in resting condition could affect the expression of Pax5 and 2) the repression of Pax5 is affected in PRC1 mutant B cells undergoing terminal differentiation, I compared by RT-qPCR analysis the expression of the *Pax5* gene in control and mutant B cell cultures before and three days after the stimulation with LPS and IL-4. Upon triggering of PC differentiation, PRC1 mutant B cells succeeded to down-modulate *Pax5* gene expression, although levels remained slightly higher than those measured in control cultures (Figure 92).

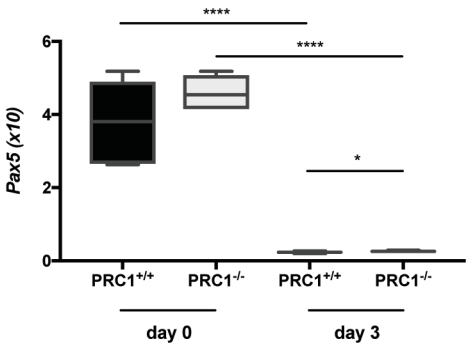

Figure 92. Pax5 is down-regulated in PRC1-deficient B cells stimulated *in vitro* with LPS and IL-4.

Box-plot analysis of transcript levels of *Pax5* gene (relative to *Rplp0*) quantified in $PRC1^{+/+}$ (n=6) and $PRC1^{-/-}$ (n=6) B cell cultures, at day-0 and -3 of *in vitro* stimulation with LPS and IL-4. In box-plots, horizontal bars indicate the medians (n=6), boxes indicate 5th to 95th percentiles. Unpaired Student's t test: * p<0.05; **** p<0.0001.

In resting B cells, PRC1 inactivation did not interfere with either *Pax5* transcript (Figure 92) nor protein (Figure 93) levels, suggesting that the low Prdm1/BLIMP-1 expression measured in these cells is not sufficient to negatively influence Pax5 expression.

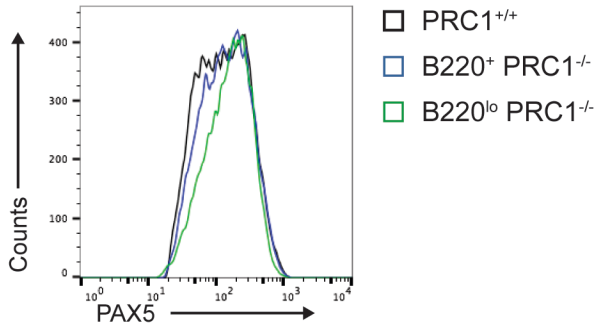

Figure 93. PAX5 expression is comparable between PRC1-proficient and deficient resting B cells.

Representative flow cytometric expression of PAX5 intracellular protein in $CD19^{+}$ splenic B cells from $PRC1^{+/+}$ control ($B220^{+}$ - black line) or $PRC1^{-/-}$ mutant animals

(B220^{+} and B220^{lo} - blue and green line, respectively). Data are representative of 2 independent experiments.

Overall, these results exclude a major contribution of PRC1 in promoting the repression of Pax5 in B cells stimulated to undergo terminal differentiation in response to TLR stimulation.

5.8 PRC1 regulates BCR signalling through modulation of CD45R function

5.8.1 PRC1 is critical for *Ptprc* splicing

PRC1 mutant B cells can be subdivided into two subsets differing in the expression of the B220 surface marker. B220, also defined as CD45R-ABC, corresponds to the CD45R isoform with the highest molecular weight (220 kDa). The expression of CD45R-ABC and the other isoforms of CD45R is controlled at the mRNA level, through alternative splicing of the exons 4-5-6 of *Ptprc* transcript (Figure 94A). Specifically, the inclusion of all exons in the transcript encodes for the CD45R-ABC protein, while the exclusion of one, two or three exons produces lower molecular weight isoforms. In B cells, *Ptprc* splicing is markedly changed at the transition from resting B cells to PCs. Indeed, resting B cells expressing the CD45R-ABC isoform differentiate into PCs which start expressing the shortest isoform CD45R-0, lacking exons 4-5-6, phenotypically resulting in B220^{lo} cells (Jensen et al. 1989; Hathcock et al. 1992). To understand whether, in the absence of PRC1, skipping of exon 4-to-6 of the *Ptprc* gene is anticipated in resting B cells, I amplified by RT-PCR a region of the *Ptprc* cDNA, spanning exon 2 to 7 from control B220^{+} B cells, and PRC1 mutant B220^{+} and B220^{lo} B cell subsets. Interestingly, B220^{lo} mutant B cells expressed two shorter versions of *Ptprc* (hereafter named as fragment A and B), while B220^{+} B cells from control and mutant animals mainly expressed the full-length version of the transcript (Figure 94B). Fragment A was also present in B220^{+} B cells of both controls and mutants, whereas fragment B was detected only in moderate amounts in PRC1 mutant B220^{+} B cells. Based on size estimations, fragments A is supposed to have lost exon 4, while fragment B lacks exon 4 and 6 (Figure 94C).

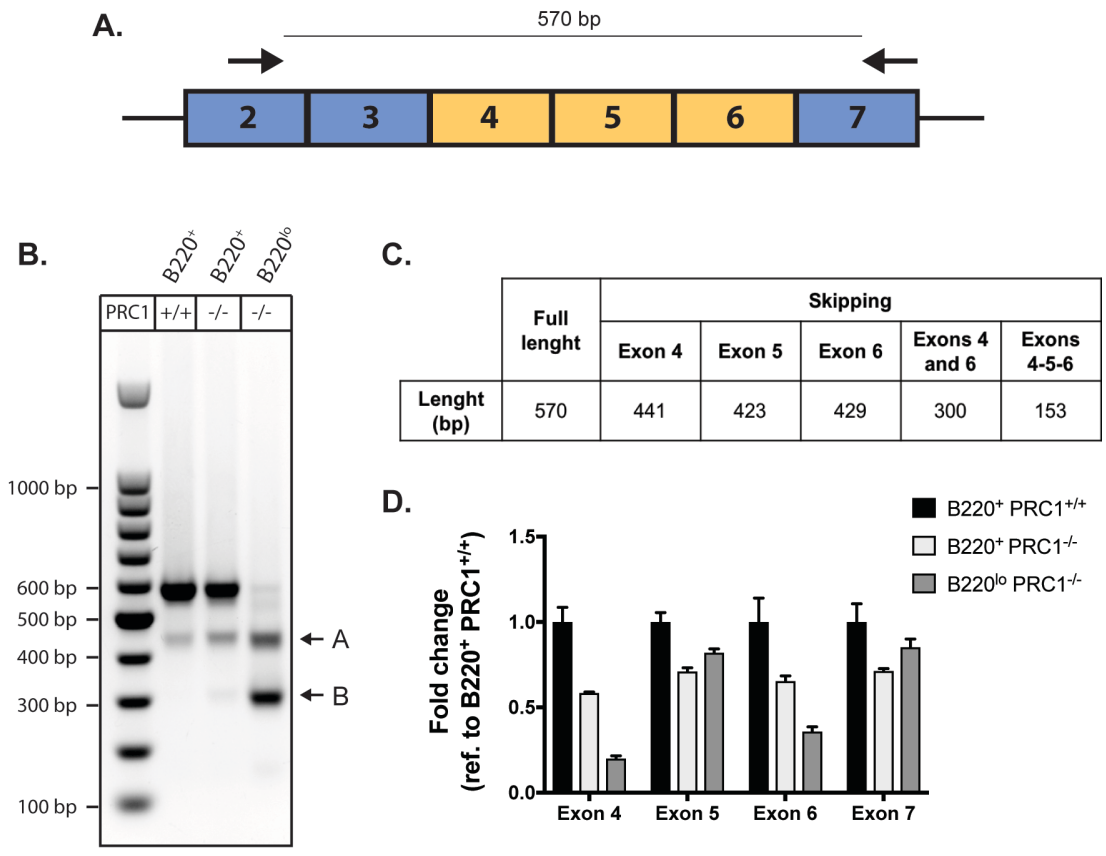

	Full lenght	Skipping				
		Exon 4	Exon 5	Exon 6	Exons 4 and 6	Exons 4-5-6
Lenght (bp)	570	441	423	429	300	153

Figure 94. B220^{lo} of PRC1-deficient mice express aberrant *Ptprc* isoforms, which are splicing variants of the full-length transcript.

A. Schematic view of the first part of *Ptprc* transcript, spanning from exon 2 to exon 7. Exons in yellow (4, 5 and 6) can be alternatively spliced. Primer positions are indicated by arrows. **B.** RT-PCR of *Ptprc* gene using oligonucleotide PCR primers located in exons 2 and 7, amplifying across the region of possibly spliced exons 4, 5 and 6. The reaction was performed on cDNA from sorted B220^{+} B cells from PRC1$^{+/+}$ control animal and B220^{+} and B220^{lo} B cells from PRC1$^{-/-}$ mutant animal. **C.** Table summarizing the predicted length (bp) of the PCR amplicons, according to possible exon skipping. **D.** RT-qPCR of *Ptprc* exons on cDNA from sorted B220^{+} B cells from PRC1$^{+/+}$ control mouse and B220^{+} and B220^{lo} B cells from PRC1$^{-/-}$ mutant mouse. Gene transcript levels were normalized to the housekeeping *Rplp0* gene and to the B220^{+} PRC1$^{+/+}$ sample. Data are representative of one experiment.

This prediction was confirmed by RT-qPCR analysis of *Ptprc* exons, highlighting a strong decrease in the expression of exon 4 and 6 in B220^{lo} cells, and partly also in B220^{+} mutant B cells (Figure 94D). To establish the identity of fragments A and B, we subjected PCR products to Sanger sequencing. As shown in Figure 95, fragment A lacked the sequence corresponding to exon 4 while the fragment B missed sequence information relative to exons 4 and 6.

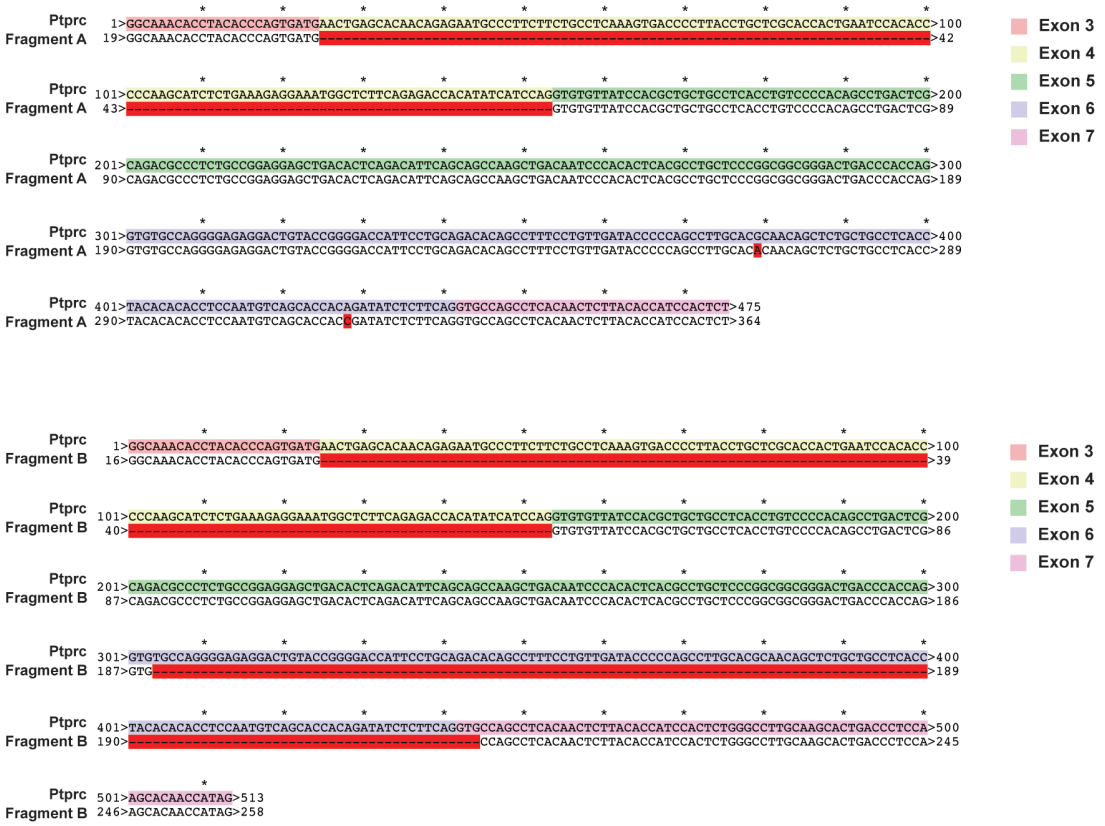

Figure 95. B220^{lo} of PRC1-deficient animals express aberrant splicing variants of *Ptprc* gene, which lack exon 4 or exon 4 and 6.

Sanger sequencing of **A.** fragment A and **B.** fragment B, that were excised from agarose gel. Sequences are aligned to the reference mRNA sequence of *Ptprc* gene. Exons are marked by different colours. Red dashed-stretches represent the missing parts of the sequence.

Sashimi plot analysis of RNA-seq data further confirmed the skipping of exons 4 and 6 in *Ptprc* transcripts derived from PRC1 mutant B cells, in particular in the B220^{lo} subset (Figure 96).

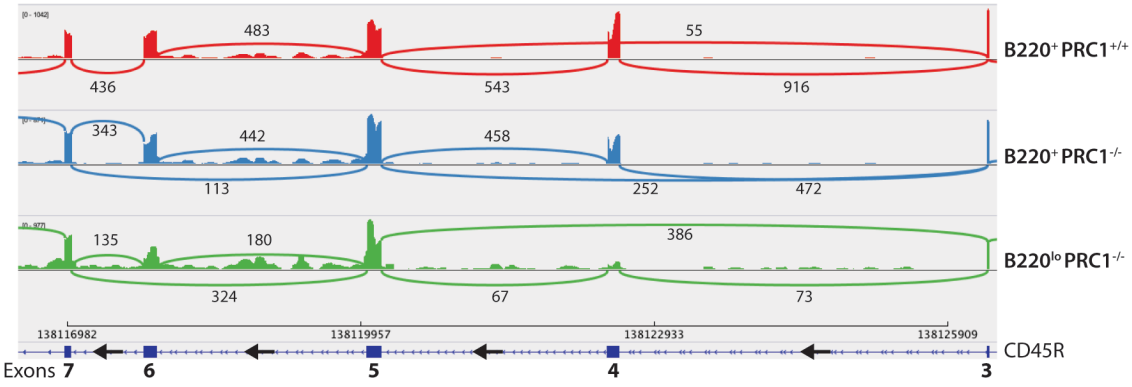

Figure 96. The aberrant splicing of *Prptc* gene in B220^{lo} B cells of PRC1-deficient animals is revealed also by RNA-seq data analysis.

Sashimi plots depict the junctional reads for exons 3, 4, 5, 6 and 7 of *Ptprc* transcript. From top to bottom are sorted B220^{+} B cells from PRC1$^{+/+}$ control animals and B220^{+} and B220^{lo} B cells from PRC1$^{-/-}$ mutant animals. Numbers represent the frequency of exon-to-exon junctions.

Alternative splicing is controlled by a group of RNA binding proteins also termed as heterogeneous nuclear RNA-binding proteins (hnRNPs). Among them, several studies have identified hnRNPLL as a critical regulator of *Prptc* alternative splicing, both in T and B cells (Oberdoerffer et al. 2008; Topp et al. 2008; Wu et al. 2008; Chang, Li, and Rao 2015). To this end, we measured *Hnrnpll* expression by RT-qPCR in PRC1 control and mutant B cells. Importantly, transcripts levels for *Hnrnpll* were more than four-fold increased in the B220^{lo} subset of PRC1 mutant B cells (Figure 97). Together, these data demonstrate that the lack of PRC1 interferes with the correct splicing of the *Ptprc* gene in B cells, possibly as a result of the up-regulation of the splicing factor hnRNPLL.

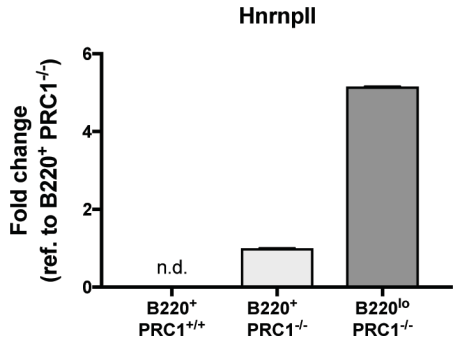

Figure 97. *Hnrnpll* gene is over-expressed in PRC1-deficient B cells.

RT-qPCR of *Hnrnpll* gene in B220^{+} B cells from PRC1$^{+/+}$ control animal and B220^{+} and B220^{lo} B cells from PRC1$^{-/-}$ mutant animal. Gene transcript levels were normalized to the housekeeping *Rplp0* gene and to the B220^{+} PRC1$^{-/-}$ sample. Data are representative of one experiment. n.d. = not detectable.

5.8.2 BCR signalling is interfered in B cells lacking PRC1

Ptprc encodes for a protein tyrosine phosphatase (CD45R), that, in B cells, controls the phosphorylation status of the Src tyrosine kinase LYN (Katagiri et al. 1995). Specifically, CD45R regulates LYN activity by dephosphorylating tyrosine-508 (Y508) (Katagiri et al. 1999; Shrivastava et al. 2004). To date, it is not clear whether different isoforms of CD45R

could have a diverse intracellular activity, in particular towards LYN. To understand whether the alternative splicing of *Ptprc* induced by the lack of PRC1 could influence LYN Y508-phosphorylation, protein lysates of splenic resting B cells from control and PRC1 conditional animals were examined by immunoblotting analysis. Strikingly, I found a consistent increase of phospho-Y508 in PRC1 mutant samples, despite unchanged expression of LYN protein levels (Figure 98).

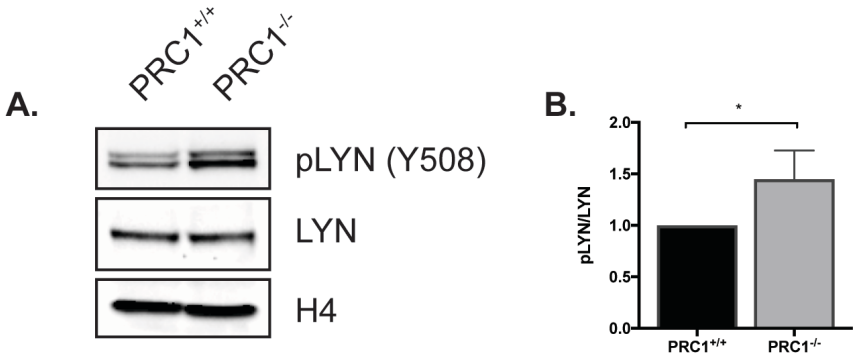

Figure 98. Phosphorylation of LYN on tyrosine-508 is increased in PRC1-deficient B cells.

A. Immunoblotting analysis and **B.** quantification of LYN tyrosine-508-phosphorylation (pLYN) and of total LYN protein levels in $PRC1^{+/+}$ control and $PRC1^{-/-}$ mutant splenic B cells. H4 was used as loading control. Quantifications of pLYN/LYN are relative to control. Data are representative of 3 independent experiments. Unpaired Student's t test: * $p<0.05$.

This result points to a reduced activation of LYN protein in B cells lacking PRC1. To test possible interference of LYN activation in BCR signalling, PRC1-proficient and -deficient B cells were subjected to BCR crosslinking using an anti-Igκ antibody. As readout of BCR signalling we measured the levels of AKT phosphorylation on serine-473 (S473) by immunoblotting analyses, at different time points after Ig cross-linking. In line with a reduced activation of LYN, in PRC1 mutant B cells we found a sub-optimal activation of AKT that was not improved by longer BCR stimulation (Figure 99).

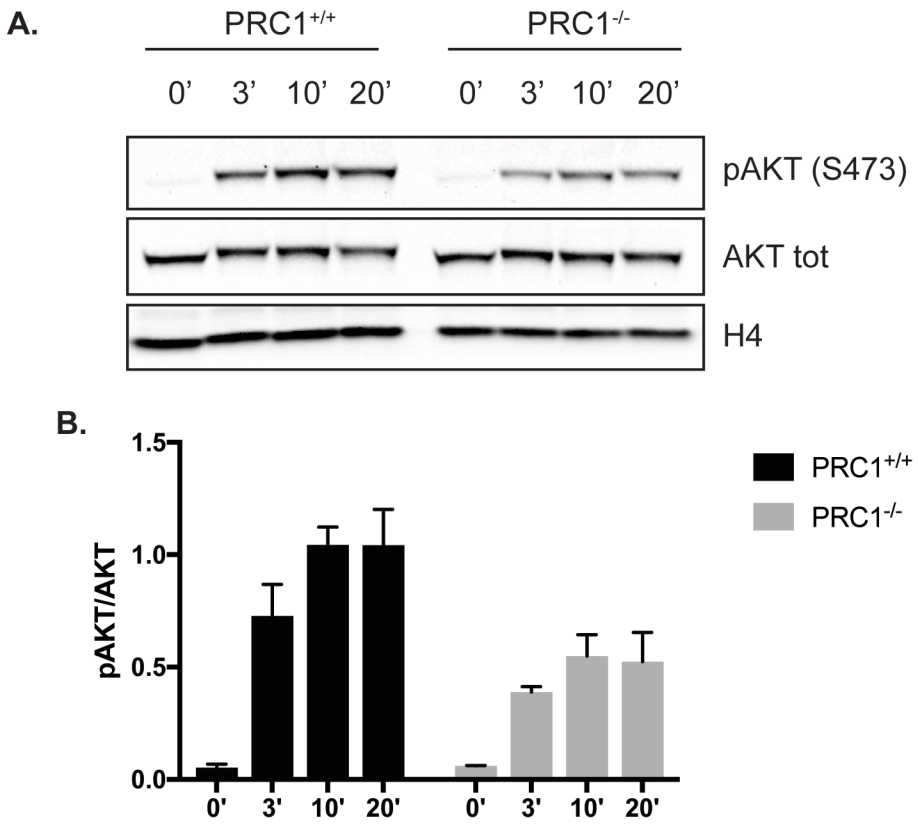

Figure 99. PRC1-deficient B cells show sub-optimal phosphorylation of AKT upon B-cell receptor cross-linking.

A. Immunoblotting analysis and **B.** quantification of AKT serine-473-phosphorylation (pAKT) and of total AKT protein levels in PRC1$^{+/+}$ control and PRC1$^{-/-}$ mutant splenic B cells after 0, 3, 10 and 20 minutes upon B-cell receptor cross-linking with IgK. H4 was used as loading control. Quantifications of pAKT/AKT are relative to control. Data are representative of 2 technical replicates.

Overall, these results suggest that the expression of different isoforms of CD45R in resting B cells lacking PRC1 reduces LYN activity, which consequently dampens the capacity of the cells to effectively signal through the BCR. Notably, the levels of total BTK and GSK3β proteins, two players downstream the BCR, were slightly but consistently increased in PRC1 mutant B cells, suggesting a compensatory mechanism triggered in response to weakened BCR signalling (Figure 100).

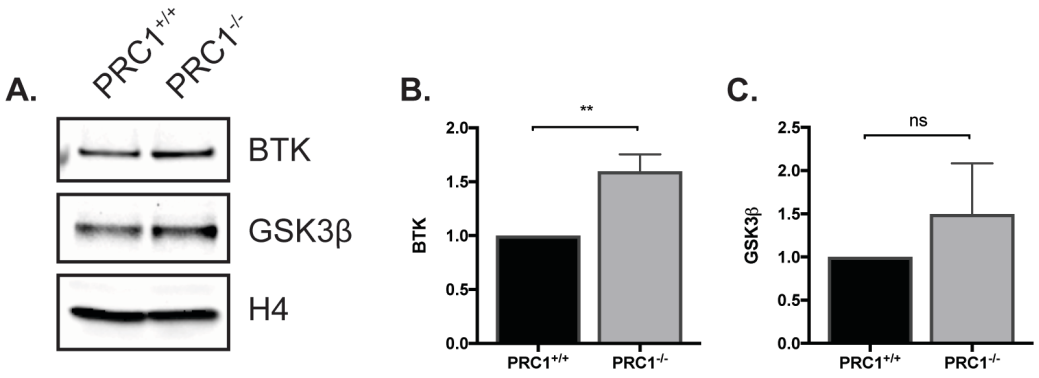

Figure 100. PRC1$^{-/-}$ B cells over-express some B-cell receptor signalling molecules.

A. Immunoblotting analysis and **B-C.** quantification of BTK and GSK3β protein levels in PRC1$^{+/+}$ control and PRC1$^{-/-}$ mutant splenic B cells. H4 was used as loading control. Quantifications of BTK and GSK3β protein levels are relative to control. Data are representative of 3 independent experiments. Unpaired Student's t test: * $p<0.05$; ns = not significative.

5.9 The epigenetic landscape of PRC1 mutant peripheral B cells and its implication on the transcriptional profile of these cells

5.9.1 Transcriptional deregulation of PRC1 deficient B cells is not caused by changes in chromatin accessibility of regulatory regions

In an attempt to identify the molecular mechanisms underlying the developmental defects observed in PRC1 conditional mice, transcriptome analysis of splenic CD19^{+} B cells from control and mutant mice was previously performed in the lab (Dr. F. Alberghini, PhD thesis work). Such analysis revealed an extensive alteration of gene expression in PRC1 mutant B cells, with more than 1000 genes deregulated. In particular, in line with the repressive activity of PRC1, the majority of differentially expressed genes (DEGs) was up-regulated in PRC1 deficient B cells (n=705, 69%), while only one third was down-regulated (n=319, 31%) (Figure 101).

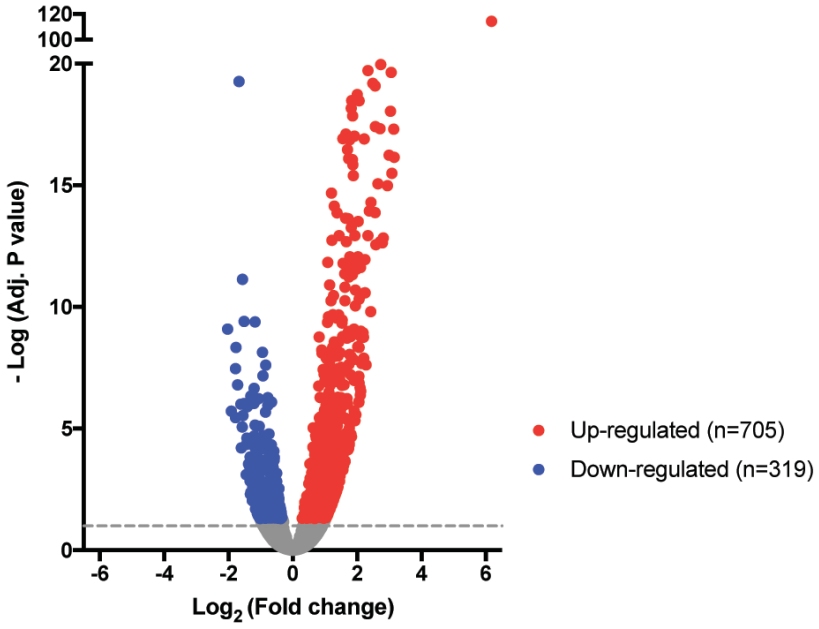

Figure 101. Gene deregulation in PRC1-deficient resting B cells.

Volcano plot displaying differentially expressed genes between $CD19^{+}$ resting B cells from $PRC1^{+/+}$ control (n=3) and $PRC1^{-/-}$ mutant mice (n=2). Red dots represent the significantly up-regulated transcripts (FDR < 0.05, log_2 fold change > +0.25); blue dots represent the significantly down-regulated transcripts (FDR < 0.05, log_2 fold change > -0.25); grey dots represent the transcripts whose expression levels did not reach statistical significance (q > 0.05).

However, the mechanisms causing the transcriptional deregulation were still not understood, neither how the perturbation of gene expression could correlate with the phenotypes exhibited by PRC1 mutant B cells. In order to gain insight into these problems, I studied the profile of open-accessible chromatin regions in control and mutant resting B cells by the assay for transposase-accessible chromatin with high-throughput sequencing (ATAC-seq). The analyses were carried out at the qualitative level, only considering the presence/absence of peaks at different genomic positions. First, we focused the attention on 'accessible' promoters, defined as genomic regions tagged by Tn5 transposase which overlap with annotated transcriptional start sites (TSS). Surprisingly, we found a substantial overlap between the repertoire of active promoters in control and PRC1 mutant B cells (Figure 102).

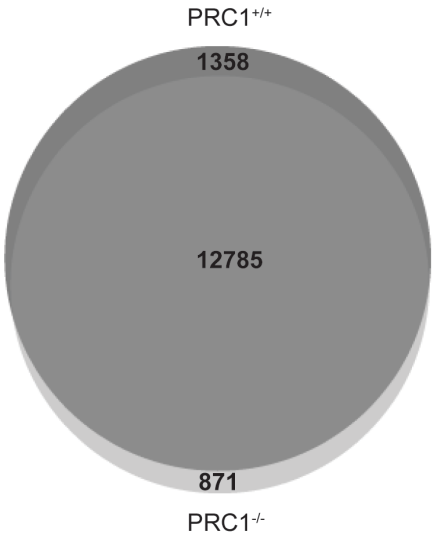

Figure 102. Chromatin accessibility at TSS is comparable between control and mutant resting B cells.

Venn diagram showing the intersection of gene lists with chromatin accessibility at TSS in B cells from $PRC1^{+/+}$ control (n=2) and $PRC1^{-/-}$ mutant mice (n=2). Numbers indicate the number of genes within each category.

Moreover, differentially accessible promoters (DAPs) accounted only for minor fractions of up- and down-regulated genes in PRC1 deficient B cells, which instead were highly enriched for accessible promoters shared between control and mutant cells (Figure 103).

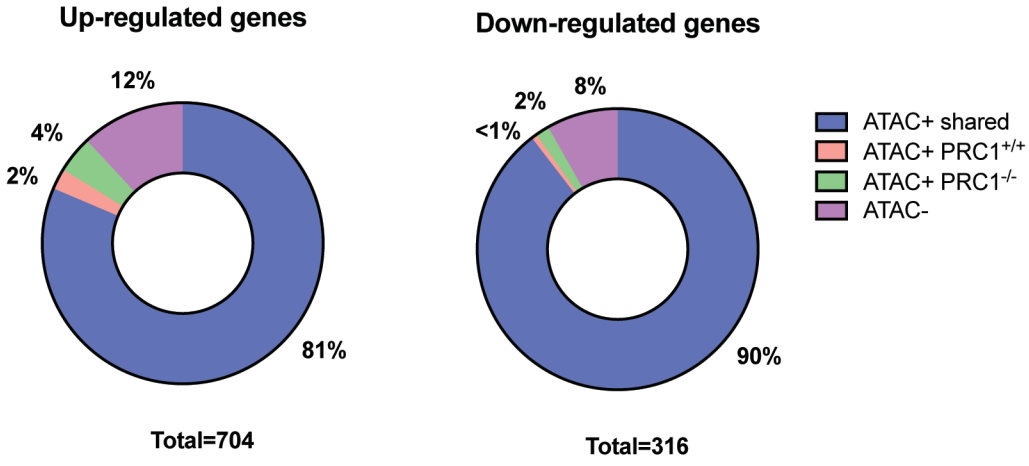

Figure 103. The majority of deregulated genes in PRC1-deficient B cells show no changes in chromatin accessibility at TSS compared to wild-type B cells.

Donut charts displaying the relative enrichment of ATAC peaks at TSS among the genes deregulated upon loss of PRC1 in B cells. ATAC peaks at TSS in control and mutant B cells were intersected, allowing to determine the following categories: $ATAC^{+}$ shared = peak shared between control and mutant B cells; $ATAC^{+}$ $PRC1^{+/+}$ = peak present only in $PRC1^{+/+}$ control B cells; $ATAC^{+}$ $PRC1^{-/-}$ = peak present only in $PRC1^{-/-}$ mutant B cells; $ATAC^{-}$ = peak not present in either control and mutant B cells. These

categories were intersected with the lists of up- and down-regulated genes and the enrichment based on the proportion of genes marked by ATAC+ within each category.

A similar analysis was subsequently performed for enhancer regions, looking for a differential activation possibly induced by the lack of PRC1. Briefly, enhancers were mapped by intersecting ChIP-seq profiles of H3K27ac^{+} and H3K4me1^{+} regions in wild-type resting B cells available in the lab (Sormani and Casola, personal communication) with enhancer regions transcribed in CD19^{+} B cells according to the FANTOM database. Genomic coordinates of enhancer regions were intersected with ATAC-seq profiles of PRC1-proficient and -deficient resting B cells, ultimately defining open/active enhancers in both populations. The comparison between these datasets highlighted a strong overlap, indicating that open/active enhancers are essentially shared between control and mutant cells (Figure 104).

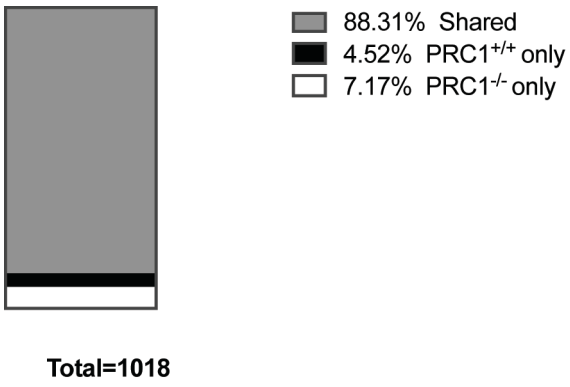

Figure 104. The majority of open-enhancers is in common between PRC1$^{+/+}$ and PRC1$^{-/-}$ B cells.

Stacked column chart displaying the ATAC^{+} enhancer distribution between control and mutant B cells. Enhancers were determined as chromatin region H3K4me1-positive, H3K27ac-positive and having at least one read in CD19^{+} cells in FANTOM database. Enhancer regions were intersected with ATAC^{+} regions of PRC1$^{+/+}$ control and PRC1$^{-/-}$ mutant B cells to generate the final lists of genomic enhancer regions. The two list were further intersected to determine shared enhancers, enhancers active only in PRC1$^{+/+}$ cells and enhancers active only in PRC1$^{-/-}$ cells.

Also in this case, a negative correlation was found between PRC1 DEGs and genes controlled by differentially accessible enhancers (Figure 105).

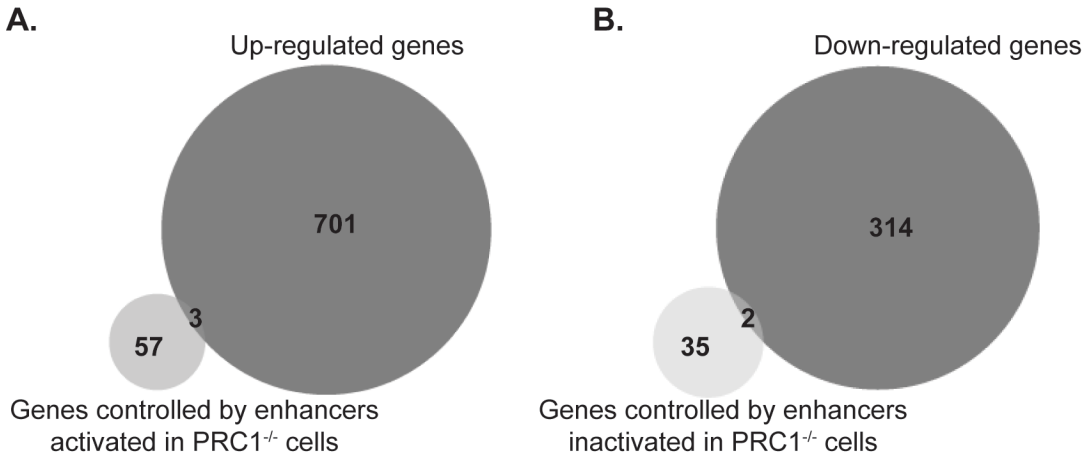

Figure 105. Differentially accessible enhancers do not control DEGs.

Venn diagram showing the intersection of **A.** enhancers active only in PRC1$^{-/-}$ mutant B cells and up-regulated genes and **B.** enhancers inactivated only in PRC1$^{-/-}$ mutant B cells and down-regulated genes. Numbers indicate the number of genes within each category.

Collectively, these data indicate that the alteration of gene expression induced by the absence of PRC1 is not caused by substantial changes in chromatin accessibility both at TSS and enhancer regions, suggesting that transcriptional deregulation is the consequence of subtle, yet functionally relevant, changes in the expression level of selected genes, which include regulators of B cell maturation and peripheral B cell homeostasis. Remarkably, among the genes linked to the phenotypes observed in PRC1 mutant B cells, discussed in the previous chapters, only *Cd93, S1pr1, Hes1* and *Cdkn2a/b* genes were significantly deregulated at the expression level. Instead, important molecular players like miR-125b and *Hnrnpll* were not detected from the bioinformatics analysis of RNA-seq data.

5.9.2 Establishment of a gene classification method based on the epigenetic landscape in resting B cells

So far, we showed that transcriptional deregulation of PRC1-deficient B cells is not associated to major changes in chromatin accessibility in gene regulatory regions. To dissect the possible contribution of histone marks to gene expression deregulation found in PRC1 mutant B cells, I intersected ATAC-seq data with ChIP-seq data profiles of H3K27me3 and of H3K4me3 at TSS in wild-type resting B cells (the latter dataset was

already available in the lab; Carrisi and Casola, personal communication). These ChIP-seq datasets were chosen because the two histone marks correlate with active and repressed transcription, respectively. Hence, different subsets of genes differentially marked by H3K4me3 and H3K27me3 and with accessible or inaccessible promoter were defined (hereafter, the latter are referred to as ATAC$^+$ and ATAC$^-$, respectively) (Figure 106).

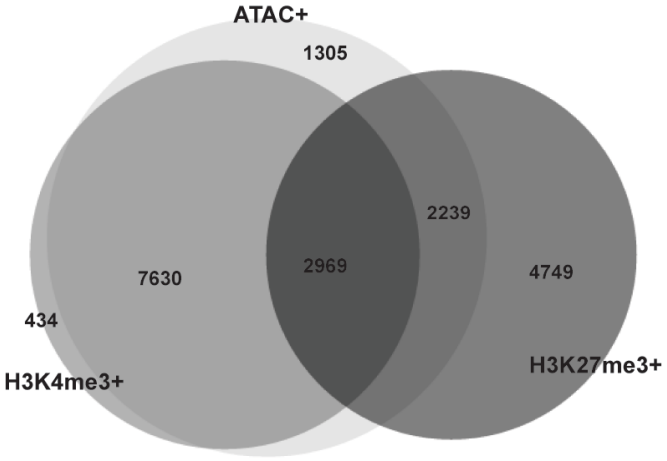

Figure 106. Distribution of ATAC peaks and H3K4me3 and H3K27me3 histone mark peaks at TSS in wild-type B cells.

Venn diagram showing the intersection of a) genes marked by ATAC$^+$ at the TSS; b) genes marked by H3K4me3$^+$ at TSS; c) genes marked by H3K27me3$^+$ at TSS. The three datasets were obtained by ATAC-seq and ChIP-seq on control resting B cells (n=2). Numbers indicate the number of genes within each category.

As expected, the vast majority of promoters marked by H3K4me3 had also open chromatin conformation, compatible with actively transcribed regions (Figure 107A). Instead, genes marked by H3K27me3, which is catalysed by PRC2, fell into two major subsets, according to chromatin accessibility data (Figure 107B).

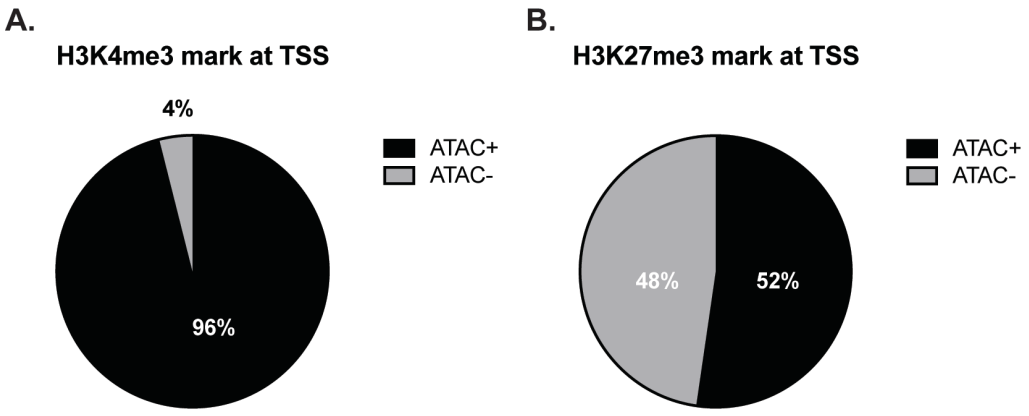

Figure 107. Chromatin accessibility among genes marked by H3K4me3 or H3K27me3 at TSS.

Pie charts displaying the relative enrichment of ATAC$^+$ mark at TSS among genes marked by H3K4me3 and by H3K27me3 in resting wild-type B cells.

Interestingly, among the H3K27me3-marked genes which retained an accessible promoter, about half were also marked by H3K4me3 while the rest were lacking the latter histone mark. These two subsets probably correspond to poised and repressed genes respectively, both still displaying an accessible promoter. To verify that the combinatorial analysis of chromatin accessibility and histone marks was meaningful, we compared the transcription levels of genes belonging to the different categories in wild-type mature B cells. Indeed, expression of gene in ATAC$^+$ categories was higher than the ATAC$^-$ relative counterparts (Figure 108).

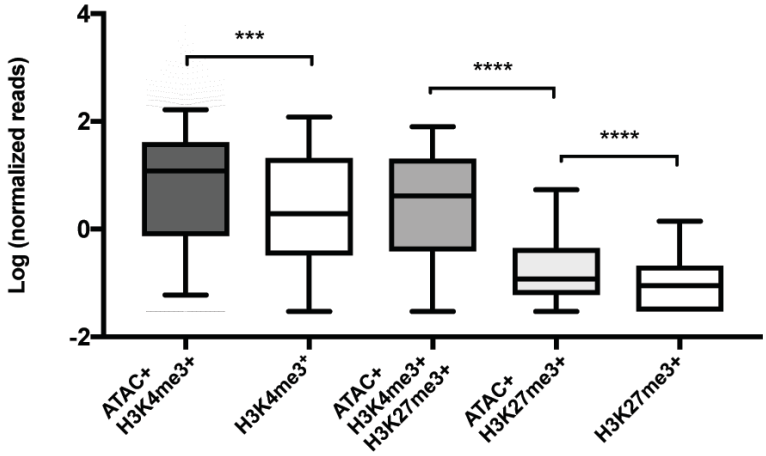

Figure 108. Gene expression is influenced by chromatin accessibility and histone marks at TSS.

Transcriptomic data were divided in different categories according to the presence/absence of ATAC$^+$, H3K4me3$^+$ and H3K27me3$^+$ marks at TSS. Box-plot analyssi show the expression of genes, as log of DeSeq2 normalized reads, within each category. Horizontal bars indicate the medians, boxes indicate 5th to 95th percentiles. Mann-Whitney non-parametric test: *** $p<0.001$; **** $p<0.0001$.

Moreover, among H3K27me3-marked genes, the ones that were also marked by H3K4me3 showed the highest expression levels. Hence, we conclude that the classification of genes based on the combination of chromatin accessibility profiles and histone marks at TSS is a powerful tool for clustering genes according to their expression.

5.9.3 Gene expression is differentially modulated by PRC1 according to the epigenetic landscape

We applied the gene classification method described in 5.9.2 to assess the status of genes respectively up- and down-regulated in PRC1 mutant B cells. As shown in Figure 109 , the analysis showed that down-regulated genes in PRC1 deficient B cells mainly fall within the category of active genes with accessible promoter in wild-type resting B cells (~ 63%). Only minor fractions of genes down-regulated in PRC1 mutant B cells are bivalent (H3K27me3$^+$ H3K4me3$^+$) genes with accessible promoter (~ 15%) or genes in which only promoter accessibility was detected (9%).

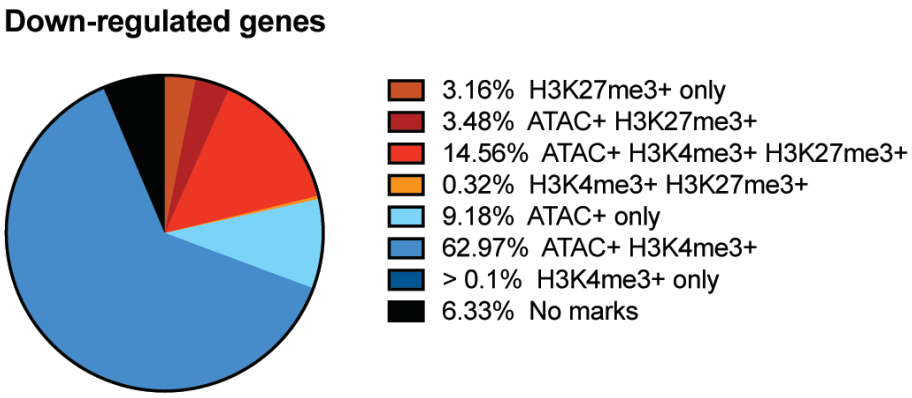

Figure 109. Down-regulated genes are mainly ATAC$^+$ H3K4me3$^+$.

Pie chart displaying the relative enrichment of the categories derived from intersection of ATAC-seq and ChIP-seq data at TSS in down-regulated genes. H3K27me3-positive categories are in shades of red, while H3K27me3-negative in shades of blue. Genes with no ATAC or ChIP-seq mark at TSS are in black.

In summary, these data indicate that PRC1 positively controls the expression of a substantial subset of transcription competent genes in mature B cells. We then subjected ATAC$^+$ H3K4me3$^+$ genes down-regulated in PRC1 mutant B cells to gene ontology (GO) analysis, finding a consistent enrichment in categories related to cell-cycle regulation, especially in mitosis and G_2/M transition, and DNA replication (Figure 110A). Indeed, DEGs belonging to this group are genes encoding DNA polymerases (*PolD1*, *PolH*, *PolE*), factors that act at the replication fork (*Brca1*, *Rad51*), and regulators of the spindle checkpoint (*Plk1*, *Bub1*, *Cdc25*). Categories related to processes which happen in mitosis, namely kinetochore organization and microtubule polymerization and depolymerization, were also

found among H3K4me3^{+} H3K27me3^{+} bivalent genes with accessible promoter (Figure 110B). The latter group was also particularly enriched for genes involved in cholesterol biosynthesis (*Dhcr24*, *Fdft1*, *Sc5d*, *Sqle*), suggesting a possible interference of PRC1 deficiency with lipid metabolism.

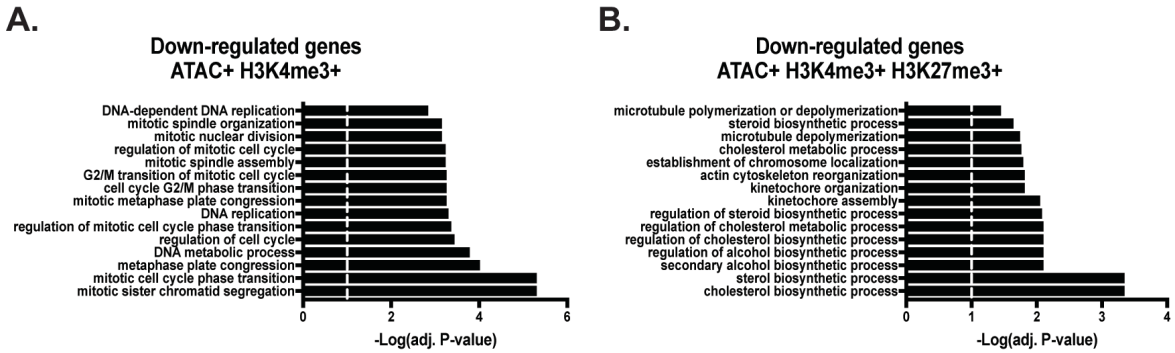

Figure 110. Down-regulated genes in PRC1-deficient B cells belong to cell-cycle and DNA replication GO categories.

Gene ontology analysis of down-regulated genes, **A.** marked ATAC^{+} H3K4me3^{+} and **B.** marked ATAC^{+} H3K4me3^{+} H3K27me3^{+} in control B cells. The first 15 categories of GO Biological Processes are reported.

Notably, down-regulated genes marked by ATAC^{+} H3K4me3^{+} were also enriched for targets of the E2F family transcription factors and FOXM1 TF (Figure 111). Considering the consistent induction of CKI genes upon inactivation of PRC1, it is possible that a fraction of down-regulated genes in PRC1$^{-/-}$ resting B cells is the indirect result of the cell-cycle block experienced by these cells.

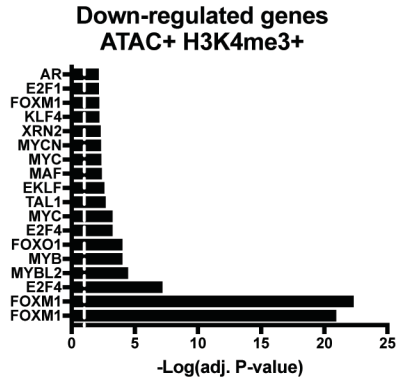

Figure 111. Down-regulated genes in PRC1$^{-/-}$ resting B cells are target of E2F TFs.

ChEA analysis of down-regulated genes in PRC1-deficient B cells and marked by ATAC^{+} H3K4me3^{+} in wild-type resting B cells. The first 18 entries of ChEA are reported.

The most striking data emerging from the analysis of the genes up-regulated in PRC1 mutant B cells is that around two third of them are bona fide PRC2 targets in wild-type B cells (Figure 112).

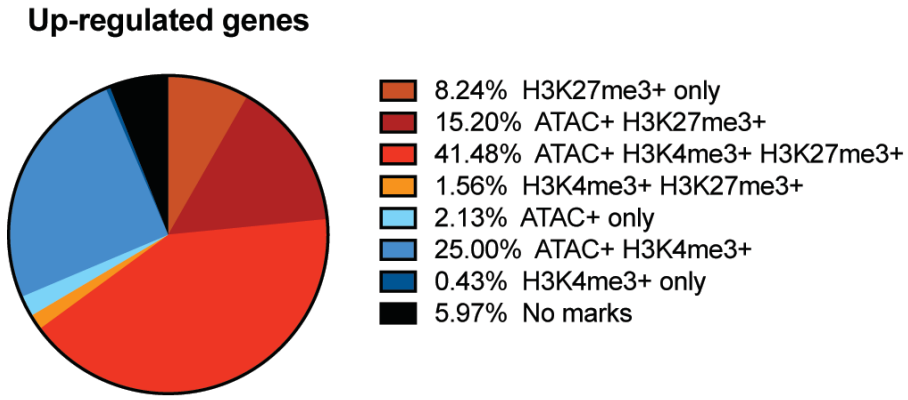

Figure 112. Up-regulated genes are mainly ATAC^{+} H3K4me3^{+} H3K27me3^{+} bivalent genes.

Pie chart displaying the relative enrichment of the categories derived from intersection of ATAC-seq and ChIP-seq data at TSS in up-regulated genes. H3K27me3-positve categories are in shades of red, while H3K27me3-negative in shades of blue. Genes with no ATAC or ChIP-seq mark at TSS are in black.

This enrichment was not detectable among the down-regulated genes in PRC1 defective B cells, where only a minor fraction (22%) was marked with H3K27me3 (Figure 109). These data are coherent with the closely coordinated activity of PRC1 and PRC2 in mediating gene repression. Indeed, the results support a scenario whereby the lack of PRC1 substantially affects the efficiency of PRC2-dependent gene silencing. Indeed, regardless of promoter accessibility status, the genes up-regulated in PRC1 mutant B cells and marked by H3K27me3 alone or in combination with H3K4me3 were preferential targets of PRC2 components (Figure 113).

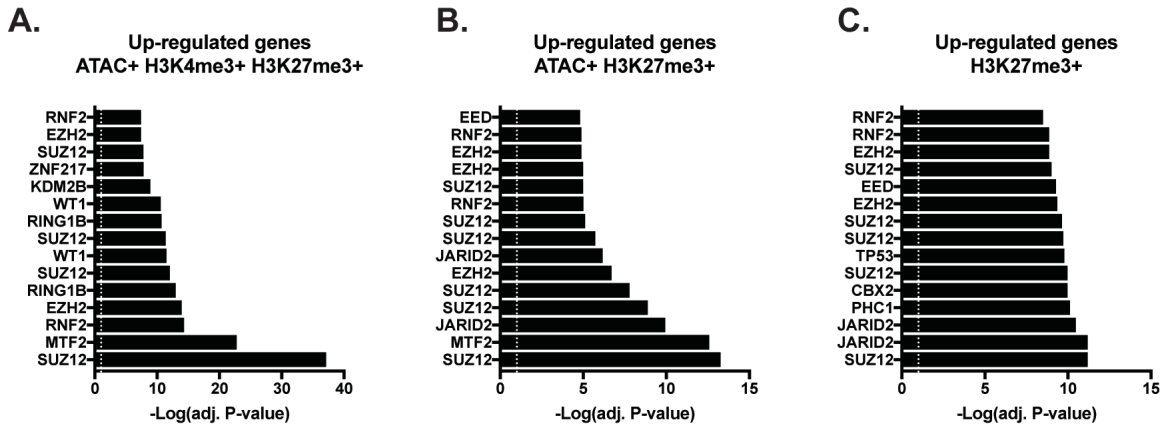

Figure 113. Up-regulated genes marked by H3K27me3 in wild-type cells are target of PcG proteins.

ChEA analysis of up-regulated genes, marked **A.** by ATAC$^+$ H3K4me3$^+$ H3K27me3$^+$ **B.** by ATAC$^+$ H3K27me3$^+$ and **C.** by H3K27me3$^+$ only in control B cells. The first 15 entries of ChEA are reported.

Interestingly, genes up-regulated in PRC1 mutant B cell with accessible promoters and marked at least by H3K27me3 were involved in pathways relevant for embryonic development (Figure 114). In addition to several Hox genes (*Hoxa2-7, 10, 11*, and *13*; *Hoxb3-7*; *Hoxc4-9*), which coordinate the early stages of embryogenesis, we found that PRC1 de-repressed genes belonged to functional categories controlling proliferation and cell-growth, like the Hippo and Wnt signalling.

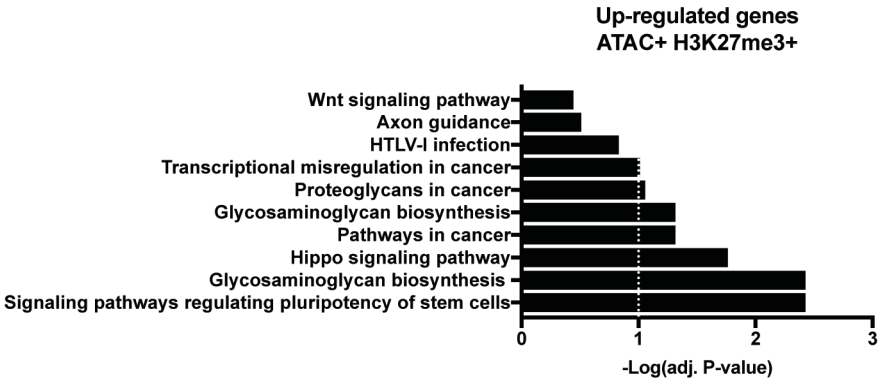

Figure 114. Up-regulated genes marked by H3K27me3 in wild-type cells belongs to pathways active in early stages of development.

KEGG analysis of up-regulated genes, marked by ATAC$^+$ H3K27me3$^+$ regardless the status of H3K4me3 in control B cells. The first 10 entries of KEGG are reported.

The up-regulation in PRC1 mutant B cells of genes lacking H3K27me3 deposition is compatible with PRC2-independent, PRC1-driven gene repression, and/or with the aberrant

activation of one or more transcription factors (TFs). To test the latter hypothesis, since data on the genome-wide occupancy of PRC1 in B cells are, yet, not available, we investigated whether the promoter region of H3K27me3$^-$ genes that were up-regulated in PRC1 mutant B cells was enriched for binding sites for specific transcription factors. This analysis revealed an enrichment for targets of several hematopoietic transcription factors including PU.1, EGR1, MITF, SOX2, MYB and RUNX2 (Figure 115).

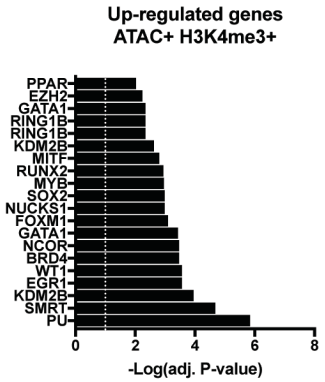

Figure 115. Up-regulated genes not marked by H3K27me3 in wild-type cells are target of transcription factors of macrophages and T cells.

ChEA analysis of up-regulated genes, marked by ATAC$^+$ H3K4me3$^+$ in control B cells. The first 20 entries of ChEA are reported.

The same bioinformatics analysis identified also components of PRC1, including RING1B and KDM2B as significantly enriched at H3K27me3$^-$ genes up-regulated in PRC1 mutant B cells. This result supports the knowledge that PRC1 represses a subset of its target genes in a PRC2-independent fashion.

6. Discussion

The PRC1 complex plays a pivotal role in several cellular processes, including maintenance of cell-identity and cell fate-determination (Di Croce and Helin 2013; Aloia, Di Stefano, and Di Croce 2013; Laugesen and Helin 2014; Ringrose and Paro 2004). In hematopoiesis, PRC1 is crucial for HSC self-renewal and maintenance (Cales et al. 2008; Vidal and Starowicz 2017; Andricovich et al. 2016; Arranz et al. 2012), proliferation of early hematopoietic progenitors including pro/pre-B cells (Park et al. 2003; Cales et al. 2008; van den Boom et al. 2013; Iwama et al. 2004; Rossi et al. 2016), for lineage specification (Andricovich et al. 2016; Oguro et al. 2010) and for T-cell lineage identity (Ikawa et al. 2016). Using a cell-type and stage-specific conditional knock-out approach, we show that PRC1 regulates the maturation and persistence of B cells within SLOs. As a result of PRC1 inactivation starting from late transitional B cells, the pool of peripheral B cells is substantially reduced in numbers and displays an aberrant surface immunophenotype. PRC1 mutant resting B cells suffered from sub-optimal response to BAFF stimulation and BCR signalling. They also showed significantly impaired responses to stimulation with TLR agonists and premature onset of terminal differentiation. The defects suffered by PRC1 mutant B cells were cell intrinsic as indicated by mixed bone marrow reconstitution assays.

6.1 Dynamics of resting peripheral B cells progressively losing PRC1 activity

Following inducible PRC1 inactivation, we identified two major subsets of $CD19^{+}$ B cells in SLOs, differing in the levels of the pan-B cell marker B220. Although both populations showed efficient Cre-mediated recombination of the conditional Ring1B allele, residual levels of RING1B protein and global H2AK119ub1 levels were still detected in the B220-expressing subset, despite being dramatically reduced when compared to controls. Instead, the $B220^{lo}$ subset of PRC1 mutant B cells lacked detectable levels of both RING1B and H2AK119ub1 levels, possibly representing cells that persisted beyond the extinction of RING1B protein expression. In line with this hypothesis, *in vitro* cultures of pure populations of PRC1 mutant $B220^{+}$ B cells revealed their progressive transformation into the $B220^{lo}$

counterparts, which correlated with a loss of residual RING1B protein. Instead, ex vivo isolated B220^{lo} B cells from PRC1 mutant B animals remained stable in their B220 phenotype even after eleven days of *in vitro* culture. Based on these results, we conclude that upon genetic inactivation of PRC1, peripheral B cells undergo a transient stage featured by residual RING1B protein and PRC1 activity. Over time, the residual levels of RING1B protein extinguish and this correlates with the evolution of B220^{+} B cells into its B220^{lo} derivative, which fully lacks PRC1 activity. This scenario is supported by *in vivo* BrdU labelling assays. Indeed, the fraction of splenic B cells that had incorporated BrdU in PRC1 mutant animals was more represented in the B220^{+} B cell subset, consistent with a direct derivation of these cells from newly generated immature B cells.

The proposed model is compatible with a slow turnover of the RING1B protein within resting mature B cells, and an extended latency before PRC1 inactivation causes phenotypic changes of the mutant B cell. Based on BrdU incorporation rates, we estimate that only 2% of the labelled immature B cells become B220^{lo} mature B cells after one week of BrdU labelling, in contrast to the 8 % scored in wild-type mice. We cannot formally exclude that B220^{lo} B cells detected in PRC1 mutant mice derive directly from transitional T2 cells.

6.2 PRC1 in B cell maturation and B cell identity

Regardless of surface B220 levels, PRC1 mutant B cells present in SLOs showed features of incomplete maturation, including concomitant expression of transcriptional signatures and surface markers typical of both immature (eg. *Cd93*, *Sox4*, *Cebpb*) and mature (e.g. *Hcst*, *Pik3r4*, *Cybb*) B cells. In agreement with the repressor activity of PRC1 and PRC2 (Aranda, Mas, and Di Croce 2015), the genes up-regulated in PRC1 knock-out, and marked by H3K27me3 in wild-type B cells, were highly enriched for bona fide targets of RING1B and other PRC1 and PRC2 components. While some of these genes are expressed at higher levels in normal immature B cells when compared to their mature counterparts (e.g. *Serinc5*, *Atpb1*, *Rag1*, *Sox4*, *Cd93*) (Kleiman et al. 2015), others belong to an embryonic/hematopoietic stem cell signature that gets silenced during B-lineage

commitment (e.g. cluster of *Hox* genes, *Fzd4*, *Igf1r*, *Efnb2*) (Ivanova et al. 2002; Painter et al. 2011). Moreover, PRC1-deficient B cells displayed higher expression levels of a group of genes that is not marked by H3K27me3 in wild-type B cells. Interestingly, these genes are enriched for targets of transcription factors such as PU.1, EGR1, MITF, SOX2, MYB and RUNX2 that are (also) expressed by other hematopoietic lineage cells including myeloid cells and T lymphocytes. This result hints to aberrant activation in PRC1 mutant B cells of transcriptional programs typical of other blood cell lineages. However, coherent with findings by Ikawa and colleagues, PRC1 inactivation starting from late transitional immature B cells was insufficient to trans-differentiate these cells into other blood cell lineages and/or for their reprogramming into pluripotent hematopoietic stem cells. This observation is coherent with the demonstration that Ring1A/Ring1B inactivation in differentiating T cells induces the reprogramming to B cells, supporting the idea that the B-cell lineage specification transcriptional program is dominant on other blood-cell lineage specification programs in the lack of PRC1 (Ikawa et al. 2016). Therefore, PRC1 is dispensable to mature B cells to maintain their lineage identity, while it contributes to ensure epigenetic silencing of transcriptional programs active in earlier stages of B cell ontogeny. Besides the general reactivation of genes of early B-cell developmental stages, we found a specific up-regulation of PAX-5-repressed genes. Indeed, despite the normal expression of the B cell master regulator PAX5 in PRC1 mutant B cells, a subset (23 out of 183) of the genes silenced by this transcription factor in mature B cells (Revilla et al. 2012) was up-regulated in the absence of Ring1A/Ring1B expression. Notably, the majority of these genes are normally expressed in progenitor B cells and get silenced during B cell maturation, also by Polycomb repressive proteins. Indeed, 70% of these genes were marked by H3K27me3 in resting wild-type B cells. These observations suggest that PRC1 contributes to maintain the repression of early B-cell lineage developmental genes established by PAX5. Additionally, we also found that up-regulated genes in PRC1 mutant B cells account for 10% of the targets normally repressed by PU.1 in pro-B cells (Batista et al. 2017). Considering that PU.1 has been described to recruit PcG proteins to chromatin (Ridinger-Saison et al. 2013),

it is possible that PRC1 contributes to enforce PU.1 transcriptional repression also in mature B cells.

6.3 Role of PRC1 in mature B cell differentiation

Despite the aberrant transcriptional profile, PRC1 mutant B cells succeeded to transit from short-lived immature B cells to resting mature B cells residing in primary follicles of SLOs. Furthermore, PRC1 mutant follicular B cells succeeded to express IgD and displayed a BrdU incorporation profile closer to that of PRC1 proficient mature B cells, regardless the aberrant expression of markers identifying B-2 B cells, including CD21 and CD23. Follicular B cells were present also in the lymph nodes, and peritoneal cavity, although at reduced numbers. These results suggest that differentiation of short-lived immature B cells into follicular B cells can proceed despite the interference with PRC1 activity. However, given the gradual disappearance of Ring1B protein in developing mature B cells of PRC1 conditional mice discussed in section 6.1 of the Discussion, we cannot exclude that the transition from immature to mature B cell proceeded thanks to residual PRC1 activity.

The lack of PRC1 function had a detrimental effect on the generation of splenic B cells displaying an immunophenotype of MZ B cells on the bases of the CD23, CD21, CD1d and CD38 markers. This result was confirmed performing immunofluorescence analyses on splenic sections, which showed a contraction of the marginal zone area in PRC1 mutant B animals. Given the relevance of Notch2 signalling for the development of MZ B cells (Saito et al. 2003; Pillai and Cariappa 2009), we measured the expression of representative Notch2 target genes in mutant PRC1 B cells. Surprisingly, the Notch2 target genes *Hes1* and *Dtx1* were expressed in PRC1 mutant splenic B cells, especially in the $B220^{lo}$ subpopulation, at levels comparable to those of wild-type MZ B cells. Comparable expression between wild-type MZ B cells and PRC1 mutant splenic B cells was also seen for genes negatively regulated by Notch2 activity, including *Klf2* and *Itgb7* (U. Strobl et al., personal communication). Interestingly, the $B220^{lo}$ splenic B cell subset represented the fraction of PRC1 mutant B cells that resembled more closely MZ B cells in terms of Notch2

target gene regulation (Saito et al. 2003). This observation is in line with the evidence that B220^{lo} cells expressed levels of the MZ B cell markers CD21, CD1d and CD38 that were closer to those of control mice.

The analyses on Notch2 target gene expression were extended to B cells isolated from lymph nodes. Consistent with the modest availability of Notch ligands, the expression of Notch target genes was overall significantly weaker in both PRC1-proficient and -deficient lymph node B cells. However, even in the lymph nodes, B220^{lo} PRC1 mutant B cells displayed stronger expression of Notch2 induced genes. Collectively, these results suggest that PRC1 deficient mature B cells can successfully activate Notch2 signalling which is necessary for the commitment and persistence of B cells within the MZ B cell subset (Saito et al. 2003; Tanigaki et al. 2002; Witt et al. 2003). Despite this, the lack of functional PRC1 activity prevents B cells from populating the MZ area.

A possible explanation for the defect in the homing of PRC1 mutant B cells to the MZ comes from expression analyses indicating lower levels of the transcripts for the Sphingosine-1 phosphate receptor-1 (*S1pr1*) gene measured in PRC1 mutant B cells. The latter receptor is required for the migration of B cells to the splenic MZ and for the shuttling of MZ B cells to the follicular areas (Cinamon et al. 2004; Cinamon et al. 2008). In support for a role of PRC1 in the positive regulation of S1PR1 expression, PRC1 mutant B cells displayed reduced migration towards a gradient of S1P in chemotaxis assays *in vitro*, mirroring the behavior of wild-type FO B cells. The reduced expression of *S1pr1* in B cells lacking PRC1 correlated, in these cells, with the concomitant higher expression of microRNA miR-125b, which directly targets *S1pr1* transcripts, thus interfering with its translation. Interestingly, miR-125b is highly expressed in multipotent progenitors and gets progressively silenced during B-cell development by epigenetic repression, through the acquisition of H3K27me3 and the loss of active histone marks at the promoter region (Li et al. 2018). Hence, the increased expression of miR-125b in PRC1 deficient B cells may be caused by de-repression of the gene due to interfered PRC2 repression of the locus. Future investigations will clarify whether PRC1 targets the miR-125b locus and whether its absence interferes with local recruitment of PRC2.

Similarities between control MZ B cells and B220^{lo} PRC1 mutant B cells in terms of CD21, CD1d and CD38 expression and of comparable activation of Notch2 target genes contrasted with the observation that the same PRC1 mutant B cell subset expressed together with IgM high levels of IgD, which is absent in wild-type MZ B cells. The latter result may be influenced by the substantial rewiring of surface Ig expression and signalling resulting from aberrant splicing of CD45R seen in PRC1 mutant B cells. Indeed, the pattern of IgM/IgD surface staining of B220^{lo} PRC1 mutant B cells is largely reminiscent of the one described for CD45 deficient B cells, displaying a substantial increase of IgM^{+} IgD^{+} double positive cells (Byth et al. 1996).

The inactivation of PRC1 in late transitional B cells was still compatible with the differentiation of these cells into B-1 B cells residing in the peritoneal cavity. However, both frequency and absolute numbers of B-1 B cells in the peritoneum were decreased pointing to a possible interference with their persistence. The CD5^{-} B-1b B cell subset was the main subset of B-1 B cells affected by PRC1 inactivation. The exquisite loss of B-1b B cells consequent to PRC1 inactivation could depend on the different requirements for PRC1 of the two distinct immature B cell type giving rise respectively to B-1a and B-1b B cells (Beaudin et al. 2016; Esplin et al. 2009; Beaudin and Forsberg 2016). The contribution of PRC1 to the developmental path of B-1a and B-1b will be addressed in the future.

All together, these studies have assigned to PRC1 an important role in sustaining the effective homing of developing B cells to the marginal zone, as well as the reaching of multiple lymphoid organs. The changes in the expression pattern of biologically-relevant surface receptors such as IgM and IgD, Cr2/CD21 and of membrane-associated signalling molecules such as CD45 is predicted to have a profound effect on the capacity of the cells to respond to environmental antigens as well as to persist within secondary lymphoid organs as resting mature B cells.

6.4 PRC1 regulation of peripheral B cell maintenance

The reduced percentage and absolute number of B cells in SLOs of PRC1 conditional mutant mice indicated a possible interference with the homeostasis of mature B cells. This hypothesis is supported by *in vivo* BrdU incorporation assays indicating an increased turnover for PRC1 deficient resting mature B cells. Moreover, competitive bone marrow chimera experiments revealed a significant exclusion of PRC1 mutant cells from the pool of mature B cells residing in follicles of SLOs. Altogether these observations are suggestive of an impairment in the fitness/maintenance of PRC1 mutant mature B cells. At least three mechanisms could help to explain the reduced fitness of PRC1 mutant B cells: 1) heightened basal expression of the pro-apoptotic sensor BIM; 2) reduced AKT activation upon BAFF stimulation; 3) sub-optimal BCR signalling.

Ex vivo isolated PRC1 control and mutant resting B cells displayed similar fractions of cells expressing active forms of caspases. In sharp contrast, when PRC1 mutant B cells were isolated *ex vivo* and thereby acutely deprived of survival signals coming from the microenvironment, the fraction of cells activating caspases to undergo apoptosis was significantly higher than in control cultures. Addition of BAFF to the culture medium did not rescued the survival defect observed in PRC1 mutant B cells, as the latter were consistently less represented than their PRC1 proficient counterparts when counted at different days after the initial stimulation. This result could be explained by the higher basal levels of the pro-apoptotic protein BIM expressed by PRC1 mutant B cells. Increased BIM protein levels in PRC1 mutant B mirrors what has been shown for PRC1 deficient T cells (Suzuki et al. 2010). However, in contrast to previous findings (Suzuki et al. 2010) showing a direct negative regulation imposed by PRC1 on *Bim* expression, in preliminary data I could not score by ChIP-qPCR assays significant deposition of both H2AK119ub1 and H3K27me3 repressive marks at the promoter of this gene. Hence our data are suggestive of a regulation by PRC1 on BIM protein levels. In BAFF stimulated PRC1 mutant B cells, the increased expression of BIM was accompanied by higher transcript levels of *Bim* itself and of other pro-apoptotic sensors such as *Puma* and *Noxa* and of the master regulator of apoptosis *p21*. Considered an anti-apoptotic factor for its ability to block cell-cycle progression, p21,

by forming a complex with p53, can also activate the apoptotic pathway by titrating anti-apoptotic proteins away from pro-apoptotic factors (Kim et al. 2017). It is plausible that in non-proliferating mature B cells, *p21* mainly assumes a function of pro-apoptotic factor, thus favouring the activation of programmed cell-death (Karimian, Ahmadi, and Yousefi 2016).

Surprisingly, the survival defect scored in PRC1 mutant B cells stimulated with BAFF was neither due to defects in the activation of the alternative NF-κB pathway (Gardam and Brink 2014), nor to an impairment in BAFF-induced expression of pro-survival genes including *Bcl-$_{XL}$* (Fu et al. 2009). BAFF-R signalling could sustain B cell survival through additional mechanisms, including the stabilization of the anti-apoptotic protein MCL-1 (Maurer et al. 2006) and the activation of the mammalian target of rapamycin complex 1 (mTORC1) kinase (Patke et al. 2006), which favours protein synthesis. Both mechanisms depend on the AKT kinase, whose activation is ensured by the cross-talk between BAFF receptor and BCR signalling (Mackay and Schneider 2009). Indeed, the BCR co-receptor CD19 is required for the activation of the PI3K-AKT pathway by BAFF-R engagement (Jellusova et al. 2013). We found that PRC1 mutant mature B cells exposed to BAFF *in vitro* displayed reduced activation of the AKT kinase, which resulted in a corresponding increase in total FOXO1 levels which are negatively regulated by AKT (Huang and Tindall 2011). These observations suggest that PRC1 inactivation in B cells impairs BAFF-controlled activation of AKT, thereby weakening its pro-survival function. Future studies will be focused on investigating whether PRC1 deficient B cells suffer also from disturbances in MCL-1 protein stabilization and mTORC1 activation.

Another crucial signalling pathway for mature B cell survival is the so-called ‘tonic’ signal emanating from surface BCR. Indeed, ablation of BCR or of its signalling subunit CD79 promotes rapid disappearance *in vivo* of resting mature B cells (Lam, Kuhn, and Rajewsky 1997; Kraus et al. 2004). The BCR-dependent survival signal depends on activation of a PI3K/AKT signalling axis preventing nuclear localization of the Foxo1 transcription factor (Srinivasan et al. 2009; Calamito et al. 2010). To assess the status of the tonic BCR signalling, we tested levels of AKT phosphorylation in unstimulated resting B cells. However, the low basal levels of AKT phosphorylation emanating from the BCR in resting

state were not consistently detected by immunoblotting analyses. Therefore, to investigate the state of AKT activation in PRC1 mutant B cells we stimulated these cells through the BCR using anti-Ig light chain antibodies. These results revealed lower activation state of AKT as assessed by reduced levels of its phosphorylation on serine-473.

Overall, our results point to an interference in the capacity of both the BCR and BAFF to effectively activate the AKT kinase function. This defect could depend on the LYN kinase whose function we found partially inhibited in PRC1 mutant B cells (for further details check section 7 of the Discussion).

The LYN kinase possibly intersects both BCR and BAFF signalling. LYN kinase activity is involved in the initiation of the signalling cascade triggered by the BCR (Yamamoto, Yamanashi, and Toyoshima 1993; Campbell and Sefton 1992). Moreover, LYN directly interact with PI3K, leading to a consistent increase of the PI3K kinase activity (Pleiman, Hertz, and Cambier 1994). Since PI3K is important for both BCR and BAFF signalling and directly activates AKT, it is likely that the increased inhibition of LYN observed in PRC1 mutant B cells affects PI3K and subsequently leads to a dampened AKT activation upon both BCR and BAFF-R triggering. At the moment, however, we cannot exclude alternative mechanisms by which PRC1 inactivation contributes to negatively influence AKT phosphorylation. The elucidation of the molecular mechanisms underlying the sub-optimal activation of AKT will be a topic of our future investigations.

The limited extent of spontaneous apoptosis seen among *ex vivo* isolated PRC1 mutant B cells could depend on the fact that a substantial subset of these cells still retains residual RING1B protein. In support to this reasoning, we observed that BIM protein levels were substantially higher in the $B220^{lo}$ subsets of PRC1 mutant B cells (lacking RING1B protein) when compared to the $B220^{+}$ counterparts (carrying residual RING1B proteins). $B220^{lo}$ PRC1 defective B cells displayed also a remarkably poorer *in vitro* survival response to BAFF when compared to B220-expressing mutant cells. Hence, future experiments aimed to understand the apoptotic signals involved in the killing of PRC1 mutant B cells will focus preferentially on the study of $B220^{lo}$ B cells.

In summary, mature B cells lacking functional PRC1 are more sensitive to pro-apoptotic insults as a result on the one side of heightened expression of pro-apoptotic factor including BIM, *Noxa*, *Puma* and *p21*, and on the other of an impaired capacity to respond to the pro-survival factor BAFF, and possibly to signals emanating from the BCR, due to an interference with AKT activation. These defects may contribute to alter peripheral B cell homeostasis in PRC1 mutant mice.

6.5 PRC1 in B cell activation

The developmental defects associated to PRC1 inactivation may impinge on the ability of mutant mature B cells to respond to mitogenic stimulation. This hypothesis is supported by unpublished work by our laboratory showing impaired GC B cell responses in PRC1 mutant B cells (Dr. F. Alberghini, PhD thesis work). To closely monitor the influence of PRC1 inhibition on B cell activation, we performed a series of *in vitro* stimulations with the TLR agonist lipopolysaccharide. These studies revealed a significant impairment in the growth potential of PRC1-defective B cells. The severe growth retardation seen in PRC1 mutant B cell cultures was linked to a significant arrest of the cells in the G_0/G_1 stage of the cell cycle, reminiscent of previous observations highlighting a crucial control exerted by PRC1 in sustaining G_1-to-S transition of the cell cycle (Gil and Peters 2006; Maertens et al. 2009; Fasano et al. 2007; Bravo et al. 2015; Ohtsubo et al. 2008; Piunti et al. 2014). The established repression operated by PRC1 and PRC2 on the expression of cyclin-dependent kinase inhibitors (CKI) (Gil and Peters 2006; Gong et al. 2006; Fasano et al. 2007; Maertens et al. 2009; Kheradmand Kia et al. 2009; Yang et al. 2009) prompted us to test the levels of different CKIs in PRC1 mutant B cells, under resting conditions and after stimulation with LPS. These experiments revealed a strong and consistent up-regulation in the transcript levels of *Cdkn1a/*$p21^{Cip}$*, Cdkn2a/*$p16^{INK4a}$ and $p19^{INK4d}$*, Cdkn2b/p15*^{INK4b}*, Cdkn1c/*$p57^{Kip2}$ *Cdkn2c/*$p18^{INK4c}$, which was detectable already in PRC1 mutant resting B cells. Moreover, we scored an induction of *Cdkn1b*/$p27^{Kip1}$ gene only in LPS-stimulated PRC1 mutant B cells.

These results are strongly suggestive of a major impairment in cell-cycle progression imposed on B cells by functional PRC1 inactivation.

The impaired proliferation of PRC1 mutant B cells stimulated with LPS and IL-4 could negatively impact on Ig isotype class-switch recombination (CSR). Indeed, it was shown that a minimum of two rounds of cell division are required for IgG and IgA CSR, and perhaps additional rounds for IgE CSR (Hodgkin, Lee, and Lyons 1996; Hasbold et al. 1998; Deenick, Hasbold, and Hodgkin 1999; Rush et al. 2005). We found that *ex vivo* isolated PRC1 mutant splenic B cells displayed a severe reduction in the fraction of IgG1-switched B cells when stimulated with LPS and IL-4. An impairment in IgG3 CSR was also detectable in PRC1 mutant B cell cultures stimulated *in vitro* with LPS alone. These results are in accordance with previous findings by our group showing a defect in IgG1 CSR observed both *in vitro* and *in vivo* analyzing B cells lacking the PRC2 catalytic subunit EZH2 (Caganova et al. 2013). Importantly, however, we cannot exclude that other molecular mechanisms, besides cell-cycle block, could explain the defect in class-switch recombination suffered from PRC1-deficient B cells.

Together with the reduced proliferative potential, causing a severe defect in Ig isotype switching, B cells lacking PRC1 suffered from increased apoptosis after stimulation with LPS and IL-4. In support of this, we observed higher expression in PRC1 mutant B cells cultures stimulated with LPS of genes encoding for the pro-apoptotic proteins *Puma*, *Noxa* and *Bim*. This phenotype was associated to a significant increase in the genotoxic damage suffered by B cells lacking PRC1, when compared to the proficient counterparts.

The accumulation of DNA damage in PRC1 mutant B cells is possibly contributed by Activation Induced cytidine Deaminase (AID), as it was substantially reduced when the same cells were stimulated with an agonistic anti-RP105 antibody, which triggers vigorous B cell proliferation without inducing AID expression (Callen et al. 2007). Defective repair resulting from DNA replication-associated DNA damage could represent another mechanism contributing to increased apoptosis of PRC1 mutant B cells (Piunti et al. 2014; Bravo et al. 2015; Klusmann et al. 2018), as suggested by the higher fraction of cells expressing activated caspases after stimulation with anti-RP105.

Overall, our results are compatible with a scenario whereby the absence of PRC1 precludes/limits B cells from transiting from the G_0/G_1 to the S-phase of the cell cycle upon mitogenic activation. This effect is likely mediated by de-repression of several CDK inhibitors in the absence of PRC1. Such condition could prolong the exposure of mutant B cells to the action of AID (Wang et al. 2017), increasing the genotoxic damage caused by its action. Prolonged exposure to AID could ultimately favour the death of PRC1 mutant B cells, which is in line with the substantial reduction in the fraction of GC B cells seen when either PRC1 or PRC2 are specifically inactivated in GC B cells (Caganova et al. 2013 and Dr. F. Alberghini, PhD thesis work).

On the other hand, PRC1 mutant B cells succeeding to enter into S-phase upon LPS or CD40L stimulation may suffer from genotoxic damage associated to DNA replication, which could in turn contribute to the apoptotic response or to growth inhibition by activating an intra-S phase and/or a G_2/M cell-cycle checkpoint.

6.6 PRC1 and terminal B cell differentiation

Activation of B cells through the TLR 4-ligand LPS ultimately triggers a transcriptional network promoting terminal B cell differentiation. This process is accompanied by changes in the surface marker repertoire of the cells and the secretion of immunoglobulins. These changes are orchestrated by a transcriptional network centered around two transcription factors, IRF4 and BLIMP-1 whose expression is strongly increased upon LPS stimulation. Strikingly, the strong cell-cycle inhibition caused by PRC1 inactivation correlated with highly efficient generation of plasmablasts that succeeded to up-regulate IRF4 expression and to induce the expression of the plasma cell surface marker CD138/Syndecan-1. Hence, considering the dramatic reduction in the total output of B cells generated *in vitro* over the four days of LPS stimulation, the proportion of $CD138^+$ plasmablasts produced by PRC1 mutant cultures was greatly enhanced when compared to control cultures. In line with this result, we observed that PRC1 mutant B cells induced expression of CD138, even after stimulation with anti-RP105, which does not induce terminal differentiation (Ogata et al.

2000; Callen et al. 2007). Altogether, these observations indicate that upon PRC1 inhibition, B cells more efficiently activate the developmental program leading to plasma cell differentiation.

Enhanced *in vitro* generation of bona fide PCs after LPS stimulation could be the consequence of two non-mutually exclusive processes induced by the lack of PRC1 in B cells: 1) the premature exit from the cell-cycle and 2) improved up-regulation of the PC master regulator BLIMP-1.

Inhibition of cell proliferation has been linked to PC differentiation previously. In particular, the up-regulation of the CKI gene $p18^{INK4c}$ is required for activated-B cells to stop the proliferation and to undergo differentiation into Ig-secreting PCs (Tourigny et al. 2002). The significant induction of all CKI genes, including $p18^{INK4c}$, experienced by LPS-activated PRC1 mutant B cells could therefore contribute to the premature triggering of the PC differentiation program. Measurements of *Prdm1*/*Blimp-1* transcripts in sorted PRC1 mutant resting B cells present in the spleen revealed consistently higher levels as compared to control B cells. Tracking individual Prdm1-expressing cells using RNA *in situ* hybridization on splenic sections confirmed the existence of a substantial portion of FO B cells that expressed at the same time *Pax5* and *Prdm1* in PRC1 mutant B cells. This result contrasted sharply with the mutually exclusive pattern of *Pax5* and *Prdm1* expression seen respectively in FO B cells and extra follicular PCs present in the spleen of control mice. Altogether, our data are consistent with a pre-mature de-repression of the *Prdm1/Blimp-1* locus in resting B cells, in the absence of PRC1. The levels of *Prdm1* in these cells were significantly lower than those measured in wild-type and PRC1 mutant PCs, pointing to the need of environmental antigens to trigger B cells for the full-blown activation of the terminal differentiation program. A possible direct control exerted by PRC1 on the *Prdm1* locus is suggested by previous work from different laboratories, including ours, indicating that PRC2 directly binds to and represses the *Prdm1* gene (Caganova et al. 2013; Beguelin et al. 2013; Scharer et al. 2018). Our work suggests that *Prdm1* repression operated by the Polycomb axis strictly requires also the activity of PRC1. In support of the latter statement, in PRC1

deficient resting B cells we scored a reduction of H2AK119ub1 histone mark at the *Prdm1* promoter by preliminary ChIP-qPCR assay.

The premature expression of *Prdm1* in PRC1 mutant resting B cells, combined with the normal expression of *Irf4*, could anticipate in these cells the acquisition of, at least some, PC phenotypes. For instance, the $B220^{lo}$ B cell subset of PRC1 mutant B cells displayed a significant increase in the expression of the *Hnrnpll* gene, which is in common with terminally differentiated PCs. In these cells as in others, including T cells, Hnrnpll plays a crucial role in the regulation of alternative splicing (Chang, Li, and Rao 2015) (Oberdoerffer et al. 2008). According to the Immgen database (www.immgen.org), in B lineage cells *Hnrnpll* is transiently expressed in pro-B cells before getting silenced throughout the later stages of B cell lymphopoiesis. The expression of *Hnrnpll* is strongly induced upon triggering of plasma cell differentiation (data obtained from the Immgen database, www.immgen.org), where it contributes to modulate the splicing of thousands of different types of transcripts including *Irf4* (Chang, Li, and Rao 2015), the IgH chain (Peng et al. 2017) and the membrane-bound *Ptprc* phosphatase, also called CD45R (Oberdoerffer et al. 2008; Preussner et al. 2012). Specifically, *Hnrnpll* leads to the skipping of exons 4 and 6 of the *Ptprc* transcript, promoting the expression of alternative isoforms, which are no further recognized by the anti-B220 antibody. The premature induction of *Hnrnpll* in PRC1 mutant resting B cells is likely the cause for the reduced reactivity of these cells to the anti-B220 antibody. In support of this result, RT-qPCR analyses revealed that PRC1 mutant B cells expressed *Ptprc* transcripts lacking either exon-4, or exon-4 and -6. The results were confirmed applying dedicated bioinformatic tools to RNA-seq data to reconstruct the expression of alternatively spliced transcripts respectively in control and PRC1 mutant $B220^{lo}$ B cells.

By using the same tool, we discovered that, similarly to PCs (Chang, Li, and Rao 2015), PRC1 deficient resting B cells displayed the skipping of exon 8 of the *Irf4* transcript, further supporting a premature expression of *Hnrnpll* and the induction of PC transcriptional/splicing features.

Collectively, our results indicate that, in resting B cells, the mild de-repression of the *Prdm1* locus has two consequences. First, resting B cells lacking PRC1 aberrantly acquire phenotypical and molecular traits of PCs, which correlate with the premature activation of the splicing factor hnRNPLL. Second, PRC1 mutant B cells are facilitated to undergo terminal differentiation upon stimulation with TLR ligands.

Although PRC1 mutant B cells are more prone to trigger the PC differentiation program, the failure to accompany this process with an intermediate phase of cell proliferation, may impair the full implementation of this developmental transition. In particular, cell division preceding PC differentiation appears to be crucial for the full epigenetic reprogramming needed to enforce the transcriptional program sustaining the identity and function of terminally differentiated B cells.

In particular, during the first cell divisions following B cell activation, the progressive loss of DNA-methylation at critical enhancers is needed to sustain the transcriptional changes accompanying terminal differentiation (Barwick et al. 2016). Additionally, in later cell divisions, PBs undergo a consistent change in the repertoire of chromatin accessible regions featuring promoter-proximal and -distal regulatory regions, induced by the concerted action of a new set of TFs and genome wide redistribution of chromatin factors including PRC2 (Scharer et al. 2018).

Considering the substantial impairment in B cell proliferation caused by PRC1 inactivation in response to LPS stimulation, it is very likely that under these conditions, epigenetic reprogramming of terminally differentiated plasma cells is incomplete. This condition may ultimately impair the secretory capacity of the PCs lacking PRC1. In support of this, previous work in our laboratory could show that PRC1 mutant mice suffer from lower basal Ig serum titers (including IgM) and, upon immunization with the T-cell dependent antigen NP-CGG, these animals were unable to produce both low and high-affinity antigen-specific IgM and IgG1 antibodies (Dr. F. Alberghini, PhD thesis work).

The triggering of the PC differentiation program requires at the same time the induction of the PC-associated transcription factor Prdm1/BLIMP-1, and the silencing of the B-cell identity PAX5 transcription factor. Given the importance of PRC2 in supporting the

repressive activity of BLIMP-1 on its targets (Minnich et al. 2016), and given that PAX5 is repressed by BLIMP-1 (Lin et al. 2002), we asked whether PRC1 mutant B cells could still silence PAX5 upon LPS stimulation. qRT-PCR determination of Pax5 transcripts revealed a down-regulation of the gene in LPS-activated B cells despite the absence of PRC1 activity. This data excludes a major contribution of PRC1 in the active repression of the *Pax5* gene when B cells are triggered to undergo PC differentiation in response to LPS stimulation. Whether PRC1 catalytic activity is needed for stable silencing of at least a subset of BLIMP-1 repressed genes will represent a major focus of our future investigations.

6.7 *Hnrnpll*, CD45R and B cell signalling

The interference with normal regulation of *Hnrnpll* expression in mature B cells in response to PRC1 inactivation represents a major finding of our investigations. This defect could have a major impact both on normal B cell homeostasis, as well as on the triggering of terminal B cell differentiation. How is PRC1 regulating *Hnrnpll* expression? Preliminary data based on ChIP-qPCR experiments discourage a direct regulation of *Hnrnpll* expression by PRC1 and/or PRC2. Specifically, I did not score changes in H3K27me3 levels at the promoter of the *Hnrnpll* gene after PRC1 inactivation, whereas H2AK119ub1 levels were barely detected in the same genomic region even in control B cells. A candidate TF to control *Hnrnpll* expression is BLIMP1. Indeed, transcriptional analyses of B-lymphoma cells in which the BLIMP-1 expression was induced by retroviral complementation, or LPS stimulation revealed induction of *Hnrnpll* expression (Sciammas and Davis 2004). However, *Hnrnpll* was not included in the list of genes directly bound by BLIMP-1 at the promoter region in LPS-stimulated plasmablasts constitutively expressing *Prdm1* in a recent investigation (Minnich et al. 2016). Hence, BLIMP-1 favours *Hnrnpll* expression either indirectly or by binding to *Hnrnpll* distal regulatory regions. The latter hypothesis is supported by the observation that half of the identified BLIMP-1 binding sites in the chromatin of LPS-stimulated plasmablasts are located in putative enhancers (Minnich et al. 2016).

In PRC1 mutant B cells, the premature induction of *Hnrnpll* correlated with alternative splicing of *Ptprc*-specific transcripts, encoding for the CD45 receptor (CD45R). CD45R is a transmembrane protein endowed with tyrosine phosphatase activity. It regulates intracellular signalling pathways by activating Src family kinases (Hermiston, Zikherman, and Zhu 2009). Src-like kinases expressed in B cells include LYN, FYN and BLK (Saijo et al. 2003). The splicing induced by *Hnrnpll* promotes the expression of shorter CD45R isoforms, alternative to CD45R-ABC which is recognized by the anti-B220 antibody (Hathcock et al. 1992; Oberdoerffer et al. 2008). Importantly, different CD45R isoforms show diverse capacity to dimerize, with the shorter isoforms displaying the strongest dimerization potential (Xu and Weiss 2002). In its dimeric form, the intracellular protein tyrosine phosphatase (PTP) activity of CD45R is inhibited, probably due to steric inhibition of the PTP catalytic domain (Majeti et al. 1998). Additionally, a recent study suggested that the activity of the CD45R isoforms is further modulated by their capacity to be recruited into membrane lipid rafts (Zheng et al. 2015). Indeed, whereas CD45R-O isoform is preferentially recruited to lipid rafts upon IL-6 stimulation, CD45R-A remains outside of the lipid rafts. It has been proposed that the different localization in the plasma membrane of CD45R isoforms influences their recruitment into specific signalling cascades (Zheng et al. 2015). In line with these evidences, we found that the expression of shorter isoforms of CD45R in $B220^{lo}$ B cells from PRC1 mutant animals correlated with an accumulation of the inhibited, Y508-phosphorylated, form of the LYN tyrosine kinase. LYN plays a crucial role in positively regulating the initial steps of BCR signalling, through the phosphorylation of the ITAM motifs of the Igα /Igβ heterodimer. ITAM phosphorylation, in turn, allows the recruitment of the SYK kinase and the activation of the downstream BCR signalling cascade. Moreover, LYN interacts with and enhance the kinase activity of the PI3K enzyme, which plays also a role in the BCR signalling pathway (Pleiman, Hertz, and Cambier 1994). An increase in the pool of inhibited LYN, as detected in PRC1 mutant B cells, is expected to negatively interfere with BCR signalling. Indeed, we found that upon BCR cross-linking, the levels of the activated form of the AKT kinase, phosphorylated on serine-473, were reduced in PRC1 mutant B cells.

Combined, our results suggest that PRC1 inactivation leads to increased expression of the splicing factor *Hnrnpll*, which promotes alternative *Ptprc* splicing. This condition causes the expression on the cell surface of PRC1 mutant B cells of the shorter CD45R-BC and CD45R-B isoforms (Figure 116).

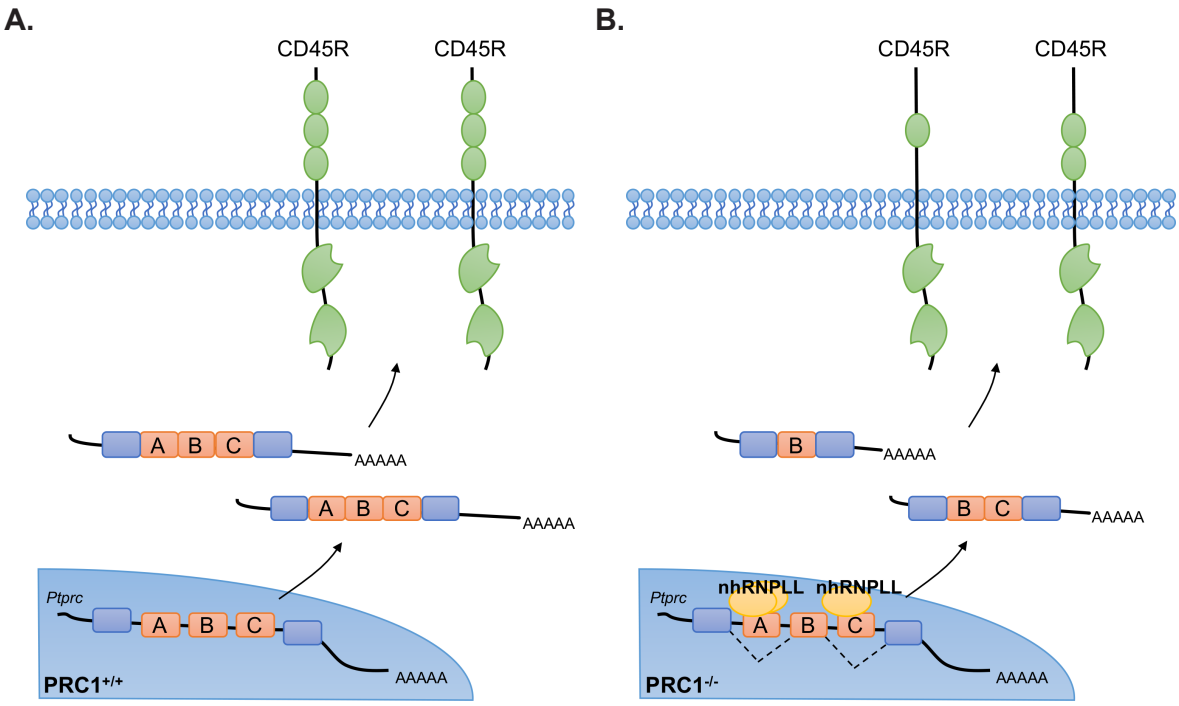

Figure 116. Alternative splicing of the *Ptprc* transcript in PRC1$^{+/+}$ and PRC1$^{-/-}$ B cells.

A. In resting PRC1 proficient B cells, the *Ptprc*-specific mRNA retains exons A, B and C. This transcript encodes for the longest version of CD45R, named CD45R-ABC, which is recognized by the anti-B220 antibody. **B.** In PRC1 mutant resting B cells, the expression of hnRNPLL favours alternative splicing of the *Ptprc* transcript, leading to the expression of shorter transcripts lacking respectively exon 4 and exon-4 and-6. The latter transcripts encode for shorter versions of CD45R, namely CD45R-B and CD45R-BC, respectively.

Improved dimerization of the latter isoforms leads to a reduction in overall phosphatase activity delivered by CD45R towards LYN. Hyper-phosphorylated LYN keeps the protein in a closed conformation preventing effective phosphorylation of the ITAM motifs of the BCR signalling components Igα and Igβ and the enhancement of PI3K activity. Finally, reduced phosphorylation of the Igα/Igβ ITAMs weakens the capacity of B cells to get activated in response to BCR engagement (Figure 117). Reduced LYN activity in resting PRC1 mutant B cells may also impair tonic BCR signalling, increasing the susceptibility of these cells to undergo apoptosis.

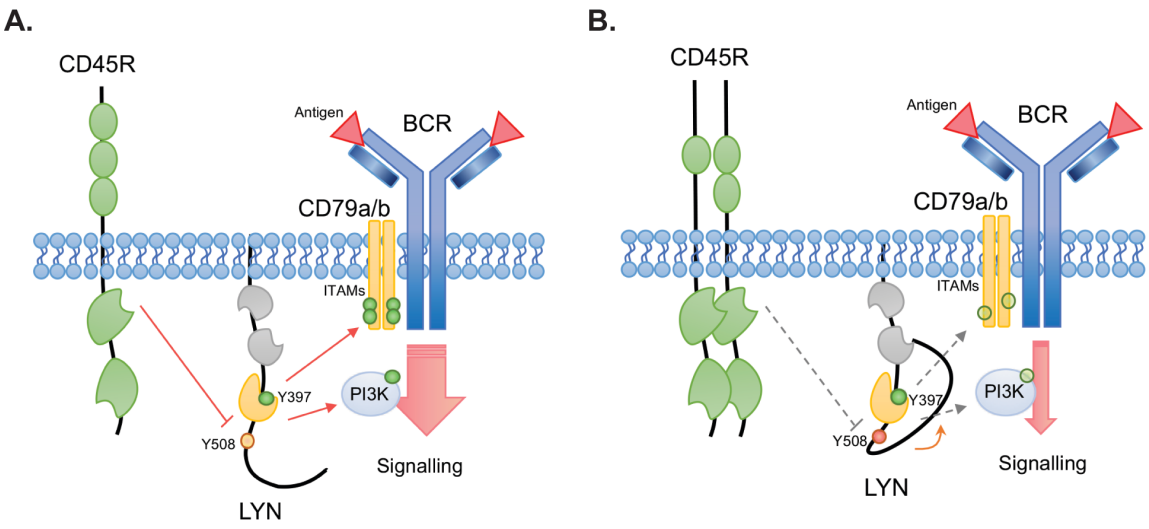

Figure 117. Differential regulation of LYN and BCR signalling by alternative CD45R isoforms.

A. Full-length CD45R-ABC transcripts expressed in resting wild-type B cells encode for the CD45R isoform equipped with the capacity to dephosphorylate the Src-like kinase LYN on tyrosine-508 (Y508). Once dephosphorylated, LYN binds and phosphorylates tyrosine residues within the ITAM motifs of the Igα and Igβ components of the BCR complex, favouring, thereby, the activation of downstream signalling events. **B.** In PRC1 mutant B cells, the expression of the shorter isoforms CD45R-B or CD45R-BC, at the expense of full length CD45R-ABC, favours CD45R dimerization, which inhibits its phosphatase activity. Under these conditions, the pool of inactive Y508-phosphorylated LYN increases preventing effective activation of the BCR signalling cascade.

6.8 Transcriptional deregulation in PRC1 deficient B cells: how is it working?

Transcriptomic analyses have indicated that inactivation of PRC1 in resting B cells leads to deregulation of a generous subset of genes. The transcriptional alterations monitored in PRC1 mutant B cells did not reflect qualitative global changes in chromatin accessibility status at promoter-proximal and -distal regulatory regions, excluding major rewiring of the epigenetic landscape of the B cells.

Since we proved that the overall chromatin accessibility is not responsible for the observed transcriptional mis-regulation, the two most likely scenarios were local and fine-tuned

histone modifications changes and/or aberrant activation of promoter specific TFs induced by PRC1 inactivation.

Genes significantly up-regulated in PRC1 mutant resting B cells accounted for more than two third of all deregulated genes. The majority of these genes (65%) is marked by tri-methylation of H3K27 in wild-type mature B cells, suggesting a co-occupancy of these loci by PRC1 and PRC2. Indeed, this subset of genes was highly enriched for targets of both PRC1 and PRC2 subunits identified in different cell types and experimental conditions. Our data indicate that inactivation of the sole PRC1 is sufficient to de-repress the expression of genes that are targeted also by PRC2. This observation is coherent with evidences highlighting the strict requirement for PRC1-induced chromatin compaction to ensure stable PcG-dependent gene silencing (Shao et al. 1999; Francis, Kingston, and Woodcock 2004; King et al. 2018). Recently published experiments of PRC1-artificial targeting to specific genomic loci have shown that PRC1-linked mono-ubiquitilyation of histone H2A is sufficient to recruit PRC2 with subsequent deposition of H3K27me3 histone mark (Blackledge et al. 2014; Cooper et al. 2014). Based on experimental data (Kalb et al. 2014), Kalb and co-workers have recently proposed a model of PRC2 recruitment to target genes, which requires previous H2AK119 mono-ubiquitylation at these sites. Moreover, studies on non-canonical PRC1 have revealed the property of these complexes to recruit PRC2 at selected genomic sites (Blackledge et al. 2014; Rose et al. 2016).

In line with these evidences, we report lower global H3K27me3 levels in the $B220^{+}$ B cell subset of PRC1 mutant mice, suggestive of an impairment of PRC2 to catalyze deposition of H3K27me3 at target sites when PRC1 activity is acutely eliminated. Notably, global levels of H3K27me3 are restored in $B220^{lo}$ PRC1 mutant cells that have experienced a longer time without PRC1 function. Whether this reflects a redistribution of the PRC2 complex on chromatin, or, instead, a gradual restoration of PRC2 recruitment at physiological sites, will require dedicated investigations comparing the genome wide H3K27me3 distribution status in control B cells and in the $B220^{+}$ and $B220^{lo}$ subsets of PRC1 defective B cells.

Among the genes up-regulated in PRC1 mutant B cells, we also found sites not yet described to be marked by H3K27me3 in resting wild-type B cells. For this subset of genes,

we therefore excluded a participation of PRC2 in the transcriptional regulation. The up-regulation of these genes might depend on the loss of PRC1 recruitment to these sites and/or on the aberrant activation of selected TFs, which in turn positively modulate their expression. Indeed, a subset of the genes up-regulated in PRC1 mutant B cells was enriched for targets of the ncPRC1 subunit KDM2B and the catalytic subunit RING1B, pointing to a ncPRC1-dependent and PRC2-independent mechanism of gene silencing. Another group of genes whose expression was increased upon PRC1 inhibition in B cells, where enriched for bona fide targets of a selected set of TFs including for instance PU.1, SMRT, EGR1, MYB, GATA1. However, RNA-seq data failed to detect and effective increase the expression of these TFs in PRC1 mutant mature B cells, rendering unlikely the hypothesis that they are positively controlling the expression of a subset of mis-regulated genes.

In conclusion, our data suggest that the genes up-regulated in PRC1 deficient B cells and lacking the H3K27me3 mark in wild-type B cells may get activated by the loss of PRC1 recruitment to these sites. Importantly, we exclude that these genes are transcriptionally activated by the aberrant induction of selected TFs.

PRC1 inactivation in resting B cells caused also a subset of genes to be significantly down-regulated. As predicted, most of the down-regulated genes in mutant B cells is not marked by H3K27me3 at the promoter region, which is instead was in an accessible chromatin conformation and was marked by H3K4me3. Recent evidences have suggested that PRC1 may also favour active gene transcription through its binding to either Aurora B Kinase or cohesins (Frangini et al. 2013; Schaaf et al. 2013). Therefore, we investigated whether the genes down-regulated in PRC1 defective B cells, overlapped with those described to be positively controlled by RING1B (Frangini et al. 2013; Schaaf et al. 2013). The investigations failed to reveal a major intersection between the gene lists, excluding a direct positive regulation of RING1B on the expression of these genes.

Genes down-regulated in PRC1 mutant B cells are enriched for functional categories related to cell-cycle progression and DNA synthesis. Hence, their down-regulation could be linked to functional interference of E2F and FOXM1 transcription factors which control most of

their expression, as a result of the potent cell-cycle arrest suffered by PRC1 mutant B cells (Cobrinik 2005; Ji and Dyson 2010).

Together, the data presented in this PhD thesis indicate that PRC1 plays a critical role at multiple stages of B cell differentiation, influencing the biology of both resting and activated B cells. The transcriptional regulation ensured by PRC1 in these cells is critical to control molecular processes central to B cell maturation and fitness, peripheral B cell homeostasis and terminal differentiation. Our data support a model whereby PRC1 and PRC2 are both essential in the regulation of shared targets. Nevertheless, we also highlight the importance of the sole PRC1 in the transcriptional regulation of a selected subset of its targets.

7. Acknowledgments

I thank all the people that actively contributed to this work:

Federica Alberghini for having performed the initial part of this project;

Our collaborator Claudio Tripodo for the *in situ* hybridization experiments and analyses and for the scientific support;

Emanuele Martini for developing the ImageJ plugin to quantify signal intensity in splenic follicles;

Federica Zanardi for the bioinformatic analyses and support.

I thank all the people that gave me technical help:

Federica Pisati for teaching me how to perform immunofluorescent stainings;

Martina Sormani, Laura Perucho-Aznar and Valentina Petrocelli for help in bone marrow chimera transplantation;

Giulia Mazzucco and Ylli Doksani for γH2A.X staining protocol;

Fabio Pessina for DNA damage quantification and comet assay;

Chiara Bruckman for sharing the anti-BIM antibody;

Marta Milan and Mahshid Rahmat for the suggestions for the ATAC-sequencing set-up.

I thank the people from the IFOM-IEO Campus facilities, who support every day's work with their skill and expertise:

Cell culture facility (Ilaria Rancati, Stefania Lavore, Laura Carmignani)

DNA sequencing facility (Milena Ficarazzi)

Genomic facility (Mirko Riboni, Simone Minardi)

Imaging facility (Dario Parazzoli, Francesca Casagrande, Ilaria Costa, Sara Barozzi)

Animal facility (Alberto Gobbi, Manuela Capillo)

Real Time PCR facility (Valentina Dall'Olio, Laura Tizzoni)

Sorting facility past and present members (Simona Ronzoni, Mariagrazia Totaro, Serena Magni)

I thank all the SCAs for their invaluable support, for their help and for making our lab life so pleasant. Thank you Laura Perucho-Aznar, Martina Sormani, Federica Greco, Daniel Segura Garzon, Federica Mainoldi and Marianna Ossorio. Thank also to the past members Valentina Petrocelli and Federica Zanardi.

I also thank my advisors Dr. Diego Pasini and Dr. Cristina Rada for useful help and suggestions and my examiners Dr. Francesco Nicassio and Dr. Ulf Klein for reading my thesis, for their evaluations and comments.

I thank my former supervisor Dr. Svend Petersen-Mahrt for teaching me how to work in a high-quality scientific environment. The technical preparation I acquired by working in his laboratory during the first two years of my PhD is absolutely priceless.

I would like to express my sincere gratitude to my supervisor Dr. Stefano Casola for his enthusiasm, for his scientific curiosity and rigor. Thank for welcoming me in your laboratory at the beginning of the third year of my PhD and for believing in me since the beginning. Thank for our scientific discussion that laid the foundation of this work.

Finally, I would like to thank my family for supporting me during these four year of my career and my life. I thank my parents for being my stable point of reference, for sustaining me in every moment and situation. I thank Fabio, my personal advisor in science and in life, for sharing with me good and bad moments of this PhD, I wish they will be the firsts of a long list.

I wish to dedicate all the effort I put in this work to my grandparents, my everlasting source of inspiration.

8. Reference list

Adams, B., P. Dorfler, A. Aguzzi, Z. Kozmik, P. Urbanek, I. Maurer-Fogy, and M. Busslinger. 1992. 'Pax-5 encodes the transcription factor BSAP and is expressed in B lymphocytes, the developing CNS, and adult testis', *Genes Dev*, 6: 1589-607.

Adolfsson, J., O. J. Borge, D. Bryder, K. Theilgaard-Monch, I. Astrand-Grundstrom, E. Sitnicka, Y. Sasaki, and S. E. Jacobsen. 2001. 'Upregulation of Flt3 expression within the bone marrow Lin(-)Sca1(+)c-kit(+) stem cell compartment is accompanied by loss of self-renewal capacity', *Immunity*, 15: 659-69.

Adolfsson, J., R. Mansson, N. Buza-Vidas, A. Hultquist, K. Liuba, C. T. Jensen, D. Bryder, L. Yang, O. J. Borge, L. A. Thoren, K. Anderson, E. Sitnicka, Y. Sasaki, M. Sigvardsson, and S. E. Jacobsen. 2005. 'Identification of Flt3+ lympho-myeloid stem cells lacking erythro-megakaryocytic potential a revised road map for adult blood lineage commitment', *Cell*, 121: 295-306.

Aguilo, F., M. M. Zhou, and M. J. Walsh. 2011. 'Long noncoding RNA, polycomb, and the ghosts haunting INK4b-ARF-INK4a expression', *Cancer Res*, 71: 5365-9.

Akasaka, T., K. Tsuji, H. Kawahira, M. Kanno, K. Harigaya, L. Hu, Y. Ebihara, T. Nakahata, O. Tetsu, M. Taniguchi, and H. Koseki. 1997. 'The role of mel-18, a mammalian Polycomb group gene, during IL-7-dependent proliferation of lymphocyte precursors', *Immunity*, 7: 135-46.

Akashi, K., D. Traver, T. Miyamoto, and I. L. Weissman. 2000. 'A clonogenic common myeloid progenitor that gives rise to all myeloid lineages', *Nature*, 404: 193-7.

Akira, S., and K. Takeda. 2004. 'Toll-like receptor signalling', *Nat Rev Immunol*, 4: 499-511.

Allende, M. L., G. Tuymetova, B. G. Lee, E. Bonifacino, Y. P. Wu, and R. L. Proia. 2010. 'S1P1 receptor directs the release of immature B cells from bone marrow into blood', *J Exp Med*, 207: 1113-24.

Allman, D., R. C. Lindsley, W. DeMuth, K. Rudd, S. A. Shinton, and R. R. Hardy. 2001. 'Resolution of Three Nonproliferative Immature Splenic B Cell Subsets Reveals Multiple Selection Points During Peripheral B Cell Maturation', *The Journal of Immunology*, 167: 6834-40.

Allman, D. M., S. E. Ferguson, and M. P. Cancro. 1992. 'Peripheral B cell maturation. I. Immature peripheral B cells in adults are heat-stable antigenhi and exhibit unique signaling characteristics', *J Immunol*, 149: 2533-40.

Allman, D. M., S. E. Ferguson, V. M. Lentz, and M. P. Cancro. 1993. 'Peripheral B cell maturation. II. Heat-stable antigen(hi) splenic B cells are an immature developmental intermediate in the production of long-lived marrow-derived B cells', *J Immunol*, 151: 4431-44.

Allman, D., and S. Pillai. 2008. 'Peripheral B cell subsets', *Curr Opin Immunol*, 20: 149-57.

Aloia, L., B. Di Stefano, and L. Di Croce. 2013. 'Polycomb complexes in stem cells and embryonic development', *Development*, 140: 2525-34.

Alugupalli, K. R., J. M. Leong, R. T. Woodland, M. Muramatsu, T. Honjo, and R. M. Gerstein. 2004. 'B1b lymphocytes confer T cell-independent long-lasting immunity', *Immunity*, 21: 379-90.

Amin, R. H., and M. S. Schlissel. 2008. 'Foxo1 directly regulates the transcription of recombination-activating genes during B cell development', *Nat Immunol*, 9: 613-22.

Anders, S., P. T. Pyl, and W. Huber. 2015. 'HTSeq--a Python framework to work with high-throughput sequencing data', *Bioinformatics*, 31: 166-9.

Andricovich, J., Y. Kai, W. Peng, A. Foudi, and A. Tzatsos. 2016. 'Histone demethylase KDM2B regulates lineage commitment in normal and malignant hematopoiesis', *J Clin Invest*, 126: 905-20.

Angelin-Duclos, C., G. Cattoretti, K. I. Lin, and K. Calame. 2000. 'Commitment of B lymphocytes to a plasma cell fate is associated with Blimp-1 expression in vivo', *J Immunol*, 165: 5462-71.

Aranda, S., G. Mas, and L. Di Croce. 2015. 'Regulation of gene transcription by Polycomb proteins', *Sci Adv*, 1: e1500737.

Arnold, P., A. Scholer, M. Pachkov, P. J. Balwierz, H. Jorgensen, M. B. Stadler, E. van Nimwegen, and D. Schubeler. 2013. 'Modeling of epigenome dynamics identifies transcription factors that mediate Polycomb targeting', *Genome Res*, 23: 60-73.

Arnon, T. I., and J. G. Cyster. 2014. 'Blood, sphingosine-1-phosphate and lymphocyte migration dynamics in the spleen', *Curr Top Microbiol Immunol*, 378: 107-28.

Arnon, T. I., Y. Xu, C. Lo, T. Pham, J. An, S. Coughlin, G. W. Dorn, and J. G. Cyster. 2011. 'GRK2-dependent S1PR1 desensitization is required for lymphocytes to overcome their attraction to blood', *Science*, 333: 1898-903.

Arranz, L., A. Herrera-Merchan, J. M. Ligos, A. de Molina, O. Dominguez, and S. Gonzalez. 2012. 'Bmi1 is critical to prevent Ikaros-mediated lymphoid priming in hematopoietic stem cells', *Cell Cycle*, 11: 65-78.

Attanavanich, K., and J. F. Kearney. 2004. 'Marginal zone, but not follicular B cells, are potent activators of naive CD4 T cells', *J Immunol*, 172: 803-11.

Banaszynski, L. A., D. Wen, S. Dewell, S. J. Whitcomb, M. Lin, N. Diaz, S. J. Elsasser, A. Chapgier, A. D. Goldberg, E. Canaani, S. Rafii, D. Zheng, and C. D. Allis. 2013. 'Hira-dependent histone H3.3 deposition facilitates PRC2 recruitment at developmental loci in ES cells', *Cell*, 155: 107-20.

Bartocci, C., J. K. Diedrich, I. Ouzounov, J. Li, A. Piunti, D. Pasini, J. R. Yates, 3rd, and E. Lazzerini Denchi. 2014. 'Isolation of chromatin from dysfunctional telomeres reveals an important role for Ring1b in NHEJ-mediated chromosome fusions', *Cell Rep*, 7: 1320-32.

Barwick, B. G., C. D. Scharer, A. P. R. Bally, and J. M. Boss. 2016. 'Plasma cell differentiation is coupled to division-dependent DNA hypomethylation and gene regulation', *Nat Immunol*, 17: 1216-25.

Basso, K., and R. Dalla-Favera. 2015. 'Germinal centres and B cell lymphomagenesis', *Nat Rev Immunol*, 15: 172-84.

Batista, C. R., S. K. Li, L. S. Xu, L. A. Solomon, and R. P. DeKoter. 2017. 'PU.1 Regulates Ig Light Chain Transcription and Rearrangement in Pre-B Cells during B Cell Development', *J Immunol*, 198: 1565-74.

Baumgarth, N. 2017. 'A Hard(y) Look at B-1 Cell Development and Function', *J Immunol*, 199: 3387-94.

Bea, S., F. Tort, M. Pinyol, X. Puig, L. Hernandez, S. Hernandez, P. L. Fernandez, M. van Lohuizen, D. Colomer, and E. Campo. 2001. 'BMI-1 gene amplification and overexpression in hematological malignancies occur mainly in mantle cell lymphomas', *Cancer Res*, 61: 2409-12.

Beaudin, A. E., S. W. Boyer, J. Perez-Cunningham, G. E. Hernandez, S. C. Derderian, C. Jujjavarapu, E. Aaserude, T. MacKenzie, and E. C. Forsberg. 2016. 'A Transient Developmental Hematopoietic Stem Cell Gives Rise to Innate-like B and T Cells', *Cell Stem Cell*, 19: 768-83.

Beaudin, A. E., and E. C. Forsberg. 2016. 'To B1a or not to B1a: do hematopoietic stem cells contribute to tissue-resident immune cells?', *Blood*, 128: 2765-69.

Beck, S., B. K. Lee, C. Rhee, J. Song, A. J. Woo, and J. Kim. 2014. 'CpG island-mediated global gene regulatory modes in mouse embryonic stem cells', *Nat Commun*, 5: 5490.

Beguelin, W., R. Popovic, M. Teater, Y. Jiang, K. L. Bunting, M. Rosen, H. Shen, S. N. Yang, L. Wang, T. Ezponda, E. Martinez-Garcia, H. Zhang, Y. Zheng, S. K. Verma, M. T. McCabe, H. M. Ott, G. S. Van Aller, R. G. Kruger, Y. Liu, C. F. McHugh, D. W. Scott, Y. R. Chung, N. Kelleher, R. Shaknovich, C. L. Creasy, R. D. Gascoyne, K. K. Wong, L. Cerchietti, R. L. Levine, O. Abdel-Wahab, J. D. Licht, O. Elemento, and A. M. Melnick. 2013. 'EZH2 is required for germinal center formation and somatic EZH2 mutations promote lymphoid transformation', *Cancer Cell*, 23: 677-92.

Beguelin, W., M. Teater, M. D. Gearhart, M. T. Calvo Fernandez, R. L. Goldstein, M. G. Cardenas, K. Hatzi, M. Rosen, H. Shen, C. M. Corcoran, M. Y. Hamline, R. D. Gascoyne, R. L. Levine, O. Abdel-Wahab, J. D. Licht, R. Shaknovich, O. Elemento, V. J. Bardwell, and A. M. Melnick. 2016. 'EZH2 and BCL6 Cooperate to Assemble CBX8-BCOR Complex to Repress Bivalent Promoters, Mediate Germinal Center Formation and Lymphomagenesis', *Cancer Cell*, 30: 197-213.

Bell, O., M. Schwaiger, E. J. Oakeley, F. Lienert, C. Beisel, M. B. Stadler, and D. Schubeler. 2010. 'Accessibility of the Drosophila genome discriminates PcG repression, H4K16 acetylation and replication timing', *Nat Struct Mol Biol*, 17: 894-900.

Berberich, S., R. Forster, and O. Pabst. 2007. 'The peritoneal micromilieu commits B cells to home to body cavities and the small intestine', *Blood*, 109: 4627-34.

Berland, R., and H. H. Wortis. 2003. 'Normal B-1a cell development requires B cell-intrinsic NFATc1 activity', *Proc Natl Acad Sci U S A*, 100: 13459-64.

Bernstein, B. E., T. S. Mikkelsen, X. Xie, M. Kamal, D. J. Huebert, J. Cuff, B. Fry, A. Meissner, M. Wernig, K. Plath, R. Jaenisch, A. Wagschal, R. Feil, S. L. Schreiber, and E. S. Lander. 2006. 'A bivalent chromatin structure marks key developmental genes in embryonic stem cells', *Cell*, 125: 315-26.

Bevington, S., and J. Boyes. 2013. 'Transcription-coupled eviction of histones H2A/H2B governs V(D)J recombination', *EMBO J*, 32: 1381-92.

Bhatnagar, S., C. Gazin, L. Chamberlain, J. Ou, X. Zhu, J. S. Tushir, C. M. Virbasius, L. Lin, L. J. Zhu, N. Wajapeyee, and M. R. Green. 2014. 'TRIM37 is a new histone H2A ubiquitin ligase and breast cancer oncoprotein', *Nature*, 516: 116-20.

Bilwes, A. M., J. den Hertog, T. Hunter, and J. P. Noel. 1996. 'Structural basis for inhibition of receptor protein-tyrosine phosphatase-alpha by dimerization', *Nature*, 382: 555-9.

Biswas, S., and C. M. Rao. 2018. 'Epigenetic tools (The Writers, The Readers and The Erasers) and their implications in cancer therapy', *Eur J Pharmacol*, 837: 8-24.

Blackledge, N. P., A. M. Farcas, T. Kondo, H. W. King, J. F. McGouran, L. L. Hanssen, S. Ito, S. Cooper, K. Kondo, Y. Koseki, T. Ishikura, H. K. Long, T. W. Sheahan, N. Brockdorff, B. M. Kessler, H. Koseki, and R. J. Klose. 2014. 'Variant PRC1 complex-dependent H2A ubiquitylation drives PRC2 recruitment and polycomb domain formation', *Cell*, 157: 1445-59.

Bonizzi, G., M. Bebien, D. C. Otero, K. E. Johnson-Vroom, Y. Cao, D. Vu, A. G. Jegga, B. J. Aronow, G. Ghosh, R. C. Rickert, and M. Karin. 2004. 'Activation of IKKalpha target genes depends on recognition of specific kappaB binding sites by RelB:p52 dimers', *EMBO J*, 23: 4202-10.

Bonizzi, G., and M. Karin. 2004. 'The two NF-kappaB activation pathways and their role in innate and adaptive immunity', *Trends Immunol*, 25: 280-8.

Bossen, C., and P. Schneider. 2006. 'BAFF, APRIL and their receptors: structure, function and signaling', *Semin Immunol*, 18: 263-75.

Boyer, L. A., K. Plath, J. Zeitlinger, T. Brambrink, L. A. Medeiros, T. I. Lee, S. S. Levine, M. Wernig, A. Tajonar, M. K. Ray, G. W. Bell, A. P. Otte, M. Vidal, D. K. Gifford, R. A. Young, and R. Jaenisch. 2006. 'Polycomb complexes repress developmental regulators in murine embryonic stem cells', *Nature*, 441: 349-53.

Brass, A. L., A. Q. Zhu, and H. Singh. 1999. 'Assembly requirements of PU.1-Pip (IRF-4) activator complexes: inhibiting function in vivo using fused dimers', *EMBO J*, 18: 977-91.

Bravo, M., F. Nicolini, K. Starowicz, S. Barroso, C. Cales, A. Aguilera, and M. Vidal. 2015. 'Polycomb RING1A- and RING1B-dependent histone H2A monoubiquitylation at pericentromeric regions promotes S-phase progression', *J Cell Sci*, 128: 3660-71.

Brookes, E., I. de Santiago, D. Hebenstreit, K. J. Morris, T. Carroll, S. Q. Xie, J. K. Stock, M. Heidemann, D. Eick, N. Nozaki, H. Kimura, J. Ragoussis, S. A. Teichmann, and A. Pombo. 2012. 'Polycomb associates genome-wide with a specific RNA polymerase II variant, and regulates metabolic genes in ESCs', *Cell Stem Cell*, 10: 157-70.

Buenrostro, J. D., B. Wu, H. Y. Chang, and W. J. Greenleaf. 2015. 'ATAC-seq: A Method for Assaying Chromatin Accessibility Genome-Wide', *Curr Protoc Mol Biol*, 109: 21 29 1-9.

Busslinger, M. 2004. 'Transcriptional control of early B cell development', *Annu Rev Immunol*, 22: 55-79.

Byth, K. F., L. A. Conroy, S. Howlett, A. J. Smith, J. May, D. R. Alexander, and N. Holmes. 1996. 'CD45-null transgenic mice reveal a positive regulatory role for CD45 in early thymocyte development, in the selection of CD4+CD8+ thymocytes, and B cell maturation', *J Exp Med*, 183: 1707-18.

Caamano, J. H., C. A. Rizzo, S. K. Durham, D. S. Barton, C. Raventos-Suarez, C. M. Snapper, and R. Bravo. 1998. 'Nuclear factor (NF)-kappa B2 (p100/p52) is required for normal splenic microarchitecture and B cell-mediated immune responses', *J Exp Med*, 187: 185-96.

Cadera, E. J., F. Wan, R. H. Amin, H. Nolla, M. J. Lenardo, and M. S. Schlissel. 2009. 'NF-kappaB activity marks cells engaged in receptor editing', *J Exp Med*, 206: 1803-16.

Caganova, M., C. Carrisi, G. Varano, F. Mainoldi, F. Zanardi, P. L. Germain, L. George, F. Alberghini, L. Ferrarini, A. K. Talukder, M. Ponzoni, G. Testa, T. Nojima, C. Doglioni, D. Kitamura, K. M. Toellner, I. H. Su, and S. Casola. 2013. 'Germinal center dysregulation by histone methyltransferase EZH2 promotes lymphomagenesis', *J Clin Invest*, 123: 5009-22.

Calabrese, J. M., W. Sun, L. Song, J. W. Mugford, L. Williams, D. Yee, J. Starmer, P. Mieczkowski, G. E. Crawford, and T. Magnuson. 2012. 'Site-specific silencing of regulatory elements as a mechanism of X inactivation', *Cell*, 151: 951-63.

Calamito, M., M. M. Juntilla, M. Thomas, D. L. Northrup, J. Rathmell, M. J. Birnbaum, G. Koretzky, and D. Allman. 2010. 'Akt1 and Akt2 promote peripheral B-cell maturation and survival', *Blood*, 115: 4043-50.

Cales, C., L. Pavon, K. Starowicz, C. Perez, M. Bravo, T. Ikawa, H. Koseki, and M. Vidal. 2015. 'Role of Polycomb RYBP in Maintaining the B-1-to-B-2 B-Cell Lineage Switch in Adult Hematopoiesis', *Mol Cell Biol*, 36: 900-12.

Cales, C., M. Roman-Trufero, L. Pavon, I. Serrano, T. Melgar, M. Endoh, C. Perez, H. Koseki, and M. Vidal. 2008. 'Inactivation of the polycomb group protein Ring1B unveils an antiproliferative role in hematopoietic cell expansion and cooperation with tumorigenesis associated with Ink4a deletion', *Mol Cell Biol*, 28: 1018-28.

Callen, E., M. Jankovic, S. Difilippantonio, J. A. Daniel, H. T. Chen, A. Celeste, M. Pellegrini, K. McBride, D. Wangsa, A. L. Bredemeyer, B. P. Sleckman, T. Ried, M. Nussenzweig, and A. Nussenzweig. 2007. 'ATM prevents the persistence and propagation of chromosome breaks in lymphocytes', *Cell*, 130: 63-75.

Calnan, D. R., and A. Brunet. 2008. 'The FoxO code', *Oncogene*, 27: 2276-88.

Campbell, M. A., and B. M. Sefton. 1992. 'Association between B-lymphocyte membrane immunoglobulin and multiple members of the Src family of protein tyrosine kinases', *Mol Cell Biol*, 12: 2315-21.

Campbell, S., I. H. Ismail, L. C. Young, G. G. Poirier, and M. J. Hendzel. 2013. 'Polycomb repressive complex 2 contributes to DNA double-strand break repair', *Cell Cycle*, 12: 2675-83.

Cao, Q., X. Wang, M. Zhao, R. Yang, R. Malik, Y. Qiao, A. Poliakov, A. K. Yocum, Y. Li, W. Chen, X. Cao, X. Jiang, A. Dahiya, C. Harris, F. Y. Feng, S. Kalantry, Z. S. Qin, S. M. Dhanasekaran, and A. M. Chinnaiyan. 2014. 'The central role of EED in the orchestration of polycomb group complexes', *Nat Commun*, 5: 3127.

Cao, R., L. Wang, H. Wang, L. Xia, H. Erdjument-Bromage, P. Tempst, R. S. Jones, and Y. Zhang. 2002. 'Role of histone H3 lysine 27 methylation in Polycomb-group silencing', *Science*, 298: 1039-43.

Cariappa, A., C. Chase, H. Liu, P. Russell, and S. Pillai. 2007. 'Naive recirculating B cells mature simultaneously in the spleen and bone marrow', *Blood*, 109: 2339-45.

Cariappa, A., H. C. Liou, B. H. Horwitz, and S. Pillai. 2000. 'Nuclear factor kappa B is required for the development of marginal zone B lymphocytes', *J Exp Med*, 192: 1175-82.

Casola, S. 2007. 'Control of peripheral B-cell development', *Curr Opin Immunol*, 19: 143-9.

Casola, S., K. L. Otipoby, M. Alimzhanov, S. Humme, N. Uyttersprot, J. L. Kutok, M. C. Carroll, and K. Rajewsky. 2004. 'B cell receptor signal strength determines B cell fate', *Nat Immunol*, 5: 317-27.

Chamberlain, S. J., D. Yee, and T. Magnuson. 2008. 'Polycomb repressive complex 2 is dispensable for maintenance of embryonic stem cell pluripotency', *Stem Cells*, 26: 1496-505.

Chan, V. W., C. A. Lowell, and A. L. DeFranco. 1998. 'Defective negative regulation of antigen receptor signaling in Lyn-deficient B lymphocytes', *Curr Biol*, 8: 545-53.

Chang, S. K., B. K. Arendt, J. R. Darce, X. Wu, and D. F. Jelinek. 2006. 'A role for BLyS in the activation of innate immune cells', *Blood*, 108: 2687-94.

Chang, S. K., S. A. Mihalcik, and D. F. Jelinek. 2008. 'B lymphocyte stimulator regulates adaptive immune responses by directly promoting dendritic cell maturation', *J Immunol*, 180: 7394-403.
Chang, X., B. Li, and A. Rao. 2015. 'RNA-binding protein hnRNPLL regulates mRNA splicing and stability during B-cell to plasma-cell differentiation', *Proc Natl Acad Sci U S A*, 112: E1888-97.
Chen, E. Y., C. M. Tan, Y. Kou, Q. Duan, Z. Wang, G. V. Meirelles, N. R. Clark, and A. Ma'ayan. 2013. 'Enrichr: interactive and collaborative HTML5 gene list enrichment analysis tool', *BMC Bioinformatics*, 14: 128.
Chen, H., and P. C. Boutros. 2011. 'VennDiagram: a package for the generation of highly-customizable Venn and Euler diagrams in R', *BMC Bioinformatics*, 12: 35.
Chen, I. J., H. L. Chen, and M. Demetriou. 2007. 'Lateral compartmentalization of T cell receptor versus CD45 by galectin-N-glycan binding and microfilaments coordinate basal and activation signaling', *J Biol Chem*, 282: 35361-72.
Chen, J., J. J. Limon, C. Blanc, S. L. Peng, and D. A. Fruman. 2010. 'Foxo1 regulates marginal zone B-cell development', *Eur J Immunol*, 40: 1890-6.
Chen, S., J. Ma, F. Wu, L. J. Xiong, H. Ma, W. Xu, R. Lv, X. Li, J. Villen, S. P. Gygi, X. S. Liu, and Y. Shi. 2012. 'The histone H3 Lys 27 demethylase JMJD3 regulates gene expression by impacting transcriptional elongation', *Genes Dev*, 26: 1364-75.
Chitale, S., and H. Richly. 2017. 'Nuclear organization of nucleotide excision repair is mediated by RING1B dependent H2A-ubiquitylation', *Oncotarget*, 8: 30870-87.
Cho, V., Y. Mei, A. Sanny, S. Chan, A. Enders, E. M. Bertram, A. Tan, C. C. Goodnow, and T. D. Andrews. 2014. 'The RNA-binding protein hnRNPLL induces a T cell alternative splicing program delineated by differential intron retention in polyadenylated RNA', *Genome Biol*, 15: R26.
Chopra, V. S., D. A. Hendrix, L. J. Core, C. Tsui, J. T. Lis, and M. Levine. 2011. 'The polycomb group mutant esc leads to augmented levels of paused Pol II in the Drosophila embryo', *Mol Cell*, 42: 837-44.
Chou, D. M., B. Adamson, N. E. Dephoure, X. Tan, A. C. Nottke, K. E. Hurov, S. P. Gygi, M. P. Colaiacovo, and S. J. Elledge. 2010. 'A chromatin localization screen reveals poly (ADP ribose)-regulated recruitment of the repressive polycomb and NuRD complexes to sites of DNA damage', *Proc Natl Acad Sci U S A*, 107: 18475-80.
Chu, C., K. Qu, F. L. Zhong, S. E. Artandi, and H. Y. Chang. 2011. 'Genomic maps of long noncoding RNA occupancy reveal principles of RNA-chromatin interactions', *Mol Cell*, 44: 667-78.
Chung, J. B., M. Silverman, and J. G. Monroe. 2003. 'Transitional B cells: step by step towards immune competence', *Trends Immunol*, 24: 343-9.
Ciccia, A., and S. J. Elledge. 2010. 'The DNA damage response: making it safe to play with knives', *Mol Cell*, 40: 179-204.
Cinamon, G., M. Matloubian, M. J. Lesneski, Y. Xu, C. Low, T. Lu, R. L. Proia, and J. G. Cyster. 2004. 'Sphingosine 1-phosphate receptor 1 promotes B cell localization in the splenic marginal zone', *Nat Immunol*, 5: 713-20.
Cinamon, G., M. A. Zachariah, O. M. Lam, F. W. Foss, Jr., and J. G. Cyster. 2008. 'Follicular shuttling of marginal zone B cells facilitates antigen transport', *Nat Immunol*, 9: 54-62.
Claudio, E., K. Brown, S. Park, H. Wang, and U. Siebenlist. 2002. 'BAFF-induced NEMO-independent processing of NF-kappa B2 in maturing B cells', *Nat Immunol*, 3: 958-65.
Cobaleda, C., A. Schebesta, A. Delogu, and M. Busslinger. 2007. 'Pax5: the guardian of B cell identity and function', *Nat Immunol*, 8: 463-70.
Cobrinik, D. 2005. 'Pocket proteins and cell cycle control', *Oncogene*, 24: 2796-809.
Cooper, S., M. Dienstbier, R. Hassan, L. Schermelleh, J. Sharif, N. P. Blackledge, V. De Marco, S. Elderkin, H. Koseki, R. Klose, A. Heger, and N. Brockdorff. 2014. 'Targeting polycomb to pericentric heterochromatin in embryonic stem cells reveals a role for H2AK119u1 in PRC2 recruitment', *Cell Rep*, 7: 1456-70.
Creppe, C., A. Palau, R. Malinverni, V. Valero, and M. Buschbeck. 2014. 'A Cbx8-containing polycomb complex facilitates the transition to gene activation during ES cell differentiation', *PLoS Genet*, 10: e1004851.

Creyghton, M. P., S. Markoulaki, S. S. Levine, J. Hanna, M. A. Lodato, K. Sha, R. A. Young, R. Jaenisch, and L. A. Boyer. 2008. 'H2AZ is enriched at polycomb complex target genes in ES cells and is necessary for lineage commitment', *Cell*, 135: 649-61.

Croker, B. A., D. M. Tarlinton, L. A. Cluse, A. J. Tuxen, A. Light, F. C. Yang, D. A. Williams, and A. W. Roberts. 2002. 'The Rac2 guanosine triphosphatase regulates B lymphocyte antigen receptor responses and chemotaxis and is required for establishment of B-1a and marginal zone B lymphocytes', *J Immunol*, 168: 3376-86.

Cross, D. A., D. R. Alessi, P. Cohen, M. Andjelkovich, and B. A. Hemmings. 1995. 'Inhibition of glycogen synthase kinase-3 by insulin mediated by protein kinase B', *Nature*, 378: 785-9.

Crowley, J. E., J. L. Scholz, W. J. Quinn, 3rd, J. E. Stadanlick, J. F. Treml, L. S. Treml, Y. Hao, R. Goenka, P. J. O'Neill, A. H. Matthews, R. F. Parsons, and M. P. Cancro. 2008. 'Homeostatic control of B lymphocyte subsets', *Immunol Res*, 42: 75-83.

Davidovich, C., X. Wang, C. Cifuentes-Rojas, K. J. Goodrich, A. R. Gooding, J. T. Lee, and T. R. Cech. 2015. 'Toward a consensus on the binding specificity and promiscuity of PRC2 for RNA', *Mol Cell*, 57: 552-8.

de Napoles, M., J. E. Mermoud, R. Wakao, Y. A. Tang, M. Endoh, R. Appanah, T. B. Nesterova, J. Silva, A. P. Otte, M. Vidal, H. Koseki, and N. Brockdorff. 2004. 'Polycomb group proteins Ring1A/B link ubiquitylation of histone H2A to heritable gene silencing and X inactivation', *Dev Cell*, 7: 663-76.

De Silva, N. S., K. Silva, M. M. Anderson, G. Bhagat, and U. Klein. 2016. 'Impairment of Mature B Cell Maintenance upon Combined Deletion of the Alternative NF-kappaB Transcription Factors RELB and NF-kappaB2 in B Cells', *J Immunol*, 196: 2591-601.

De Silva, N. S., G. Simonetti, N. Heise, and U. Klein. 2012. 'The diverse roles of IRF4 in late germinal center B-cell differentiation', *Immunol Rev*, 247: 73-92.

Deaton, A. M., M. Gomez-Rodriguez, J. Mieczkowski, M. Y. Tolstorukov, S. Kundu, R. I. Sadreyev, L. E. Jansen, and R. E. Kingston. 2016. 'Enhancer regions show high histone H3.3 turnover that changes during differentiation', *Elife*, 5.

Dedeoglu, F., B. Horwitz, J. Chaudhuri, F. W. Alt, and R. S. Geha. 2004. 'Induction of activation-induced cytidine deaminase gene expression by IL-4 and CD40 ligation is dependent on STAT6 and NFkappaB', *Int Immunol*, 16: 395-404.

Deenick, E. K., J. Hasbold, and P. D. Hodgkin. 1999. 'Switching to IgG3, IgG2b, and IgA is division linked and independent, revealing a stochastic framework for describing differentiation', *J Immunol*, 163: 4707-14.

del Mar Lorente, M., C. Marcos-Gutierrez, C. Perez, J. Schoorlemmer, A. Ramirez, T. Magin, and M. Vidal. 2000. 'Loss- and gain-of-function mutations show a polycomb group function for Ring1A in mice', *Development*, 127: 5093-100.

Dengler, H. S., G. V. Baracho, S. A. Omori, S. Bruckner, K. C. Arden, D. H. Castrillon, R. A. DePinho, and R. C. Rickert. 2008. 'Distinct functions for the transcription factor Foxo1 at various stages of B cell differentiation', *Nat Immunol*, 9: 1388-98.

Di Croce, L., and K. Helin. 2013. 'Transcriptional regulation by Polycomb group proteins', *Nat Struct Mol Biol*, 20: 1147-55.

Dietrich, N., M. Lerdrup, E. Landt, S. Agrawal-Singh, M. Bak, N. Tommerup, J. Rappsilber, E. Sodersten, and K. Hansen. 2012. 'REST-mediated recruitment of polycomb repressor complexes in mammalian cells', *PLoS Genet*, 8: e1002494.

Difilippantonio, M. J., J. Zhu, H. T. Chen, E. Meffre, M. C. Nussenzweig, E. E. Max, T. Ried, and A. Nussenzweig. 2000. 'DNA repair protein Ku80 suppresses chromosomal aberrations and malignant transformation', *Nature*, 404: 510-4.

Dolmetsch, R. E., R. S. Lewis, C. C. Goodnow, and J. I. Healy. 1997. 'Differential activation of transcription factors induced by Ca2+ response amplitude and duration', *Nature*, 386: 855-8.

Dominguez-Sola, D., J. Kung, A. B. Holmes, V. A. Wells, T. Mo, K. Basso, and R. Dalla-Favera. 2015. 'The FOXO1 Transcription Factor Instructs the Germinal Center Dark Zone Program', *Immunity*, 43: 1064-74.

Earl, L. A., and L. G. Baum. 2008. 'CD45 glycosylation controls T-cell life and death', *Immunol Cell Biol*, 86: 608-15.

Eastman, Q. M., T. M. Leu, and D. G. Schatz. 1996. 'Initiation of V(D)J recombination in vitro obeying the 12/23 rule', *Nature*, 380: 85-8.

El Chartouni, C., L. Schwarzfischer, and M. Rehli. 2010. 'Interleukin-4 induced interferon regulatory factor (Irf) 4 participates in the regulation of alternative macrophage priming', *Immunobiology*, 215: 821-5.
Elledge, S. J. 1996. 'Cell cycle checkpoints: preventing an identity crisis', *Science*, 274: 1664-72.
Endoh, M., T. A. Endo, T. Endoh, K. Isono, J. Sharif, O. Ohara, T. Toyoda, T. Ito, R. Eskeland, W. A. Bickmore, M. Vidal, B. E. Bernstein, and H. Koseki. 2012. 'Histone H2A mono-ubiquitination is a crucial step to mediate PRC1-dependent repression of developmental genes to maintain ES cell identity', *PLoS Genet*, 8: e1002774.
Esplin, B. L., R. S. Welner, Q. Zhang, L. A. Borghesi, and P. W. Kincade. 2009. 'A differentiation pathway for B1 cells in adult bone marrow', *Proc Natl Acad Sci U S A*, 106: 5773-8.
Facchino, S., M. Abdouh, W. Chatoo, and G. Bernier. 2010. 'BMI1 confers radioresistance to normal and cancerous neural stem cells through recruitment of the DNA damage response machinery', *J Neurosci*, 30: 10096-111.
Fagarasan, S., and T. Honjo. 2003. 'Intestinal IgA synthesis: regulation of front-line body defences', *Nat Rev Immunol*, 3: 63-72.
Farcas, A. M., N. P. Blackledge, I. Sudbery, H. K. Long, J. F. McGouran, N. R. Rose, S. Lee, D. Sims, A. Cerase, T. W. Sheahan, H. Koseki, N. Brockdorff, C. P. Ponting, B. M. Kessler, and R. J. Klose. 2012. 'KDM2B links the Polycomb Repressive Complex 1 (PRC1) to recognition of CpG islands', *Elife*, 1: e00205.
Fasano, C. A., J. T. Dimos, N. B. Ivanova, N. Lowry, I. R. Lemischka, and S. Temple. 2007. 'shRNA knockdown of Bmi-1 reveals a critical role for p21-Rb pathway in NSC self-renewal during development', *Cell Stem Cell*, 1: 87-99.
Fitzgerald, D. P., and W. Bender. 2001. 'Polycomb group repression reduces DNA accessibility', *Mol Cell Biol*, 21: 6585-97.
Forster, R., A. E. Mattis, E. Kremmer, E. Wolf, G. Brem, and M. Lipp. 1996. 'A putative chemokine receptor, BLR1, directs B cell migration to defined lymphoid organs and specific anatomic compartments of the spleen', *Cell*, 87: 1037-47.
Francis, N. J., R. E. Kingston, and C. L. Woodcock. 2004. 'Chromatin compaction by a polycomb group protein complex', *Science*, 306: 1574-7.
Frangini, A., M. Sjoberg, M. Roman-Trufero, G. Dharmalingam, V. Haberle, T. Bartke, B. Lenhard, M. Malumbres, M. Vidal, and N. Dillon. 2013. 'The aurora B kinase and the polycomb protein ring1B combine to regulate active promoters in quiescent lymphocytes', *Mol Cell*, 51: 647-61.
Franzoso, G., L. Carlson, L. Xing, L. Poljak, E. W. Shores, K. D. Brown, A. Leonardi, T. Tran, B. F. Boyce, and U. Siebenlist. 1997. 'Requirement for NF-kappaB in osteoclast and B-cell development', *Genes Dev*, 11: 3482-96.
Fu, L., Y. C. Lin-Lee, L. V. Pham, A. T. Tamayo, L. C. Yoshimura, and R. J. Ford. 2009. 'BAFF-R promotes cell proliferation and survival through interaction with IKKbeta and NF-kappaB/c-Rel in the nucleus of normal and neoplastic B-lymphoid cells', *Blood*, 113: 4627-36.
Fujita, N., D. L. Jaye, C. Geigerman, A. Akyildiz, M. R. Mooney, J. M. Boss, and P. A. Wade. 2004. 'MTA3 and the Mi-2/NuRD complex regulate cell fate during B lymphocyte differentiation', *Cell*, 119: 75-86.
Fukui, Y., O. Hashimoto, T. Sanui, T. Oono, H. Koga, M. Abe, A. Inayoshi, M. Noda, M. Oike, T. Shirai, and T. Sasazuki. 2001. 'Haematopoietic cell-specific CDM family protein DOCK2 is essential for lymphocyte migration', *Nature*, 412: 826-31.
Fuxa, M., J. Skok, A. Souabni, G. Salvagiotto, E. Roldan, and M. Busslinger. 2004. 'Pax5 induces V-to-DJ rearrangements and locus contraction of the immunoglobulin heavy-chain gene', *Genes Dev*, 18: 411-22.
Fyodorov, D. V., B. R. Zhou, A. I. Skoultchi, and Y. Bai. 2018. 'Emerging roles of linker histones in regulating chromatin structure and function', *Nat Rev Mol Cell Biol*, 19: 192-206.
Gao, Z., J. Zhang, R. Bonasio, F. Strino, A. Sawai, F. Parisi, Y. Kluger, and D. Reinberg. 2012. 'PCGF homologs, CBX proteins, and RYBP define functionally distinct PRC1 family complexes', *Mol Cell*, 45: 344-56.

Gardam, S., and R. Brink. 2014. 'Non-Canonical NF-kappaB Signaling Initiated by BAFF Influences B Cell Biology at Multiple Junctures', *Front Immunol*, 4: 509.
Gerondakis, S., R. Grumont, R. Gugasyan, L. Wong, I. Isomura, W. Ho, and A. Banerjee. 2006. 'Unravelling the complexities of the NF-kappaB signalling pathway using mouse knockout and transgenic models', *Oncogene*, 25: 6781-99.
Ghosh, S., M. J. May, and E. B. Kopp. 1998. 'NF-kappa B and Rel proteins: evolutionarily conserved mediators of immune responses', *Annu Rev Immunol*, 16: 225-60.
Gieni, R. S., I. H. Ismail, S. Campbell, and M. J. Hendzel. 2011. 'Polycomb group proteins in the DNA damage response: a link between radiation resistance and "stemness"', *Cell Cycle*, 10: 883-94.
Gil, J., and G. Peters. 2006. 'Regulation of the INK4b-ARF-INK4a tumour suppressor locus: all for one or one for all', *Nat Rev Mol Cell Biol*, 7: 667-77.
Ginjala, V., K. Nacerddine, A. Kulkarni, J. Oza, S. J. Hill, M. Yao, E. Citterio, M. van Lohuizen, and S. Ganesan. 2011. 'BMI1 is recruited to DNA breaks and contributes to DNA damage-induced H2A ubiquitination and repair', *Mol Cell Biol*, 31: 1972-82.
Girkontaite, I., K. Missy, V. Sakk, A. Harenberg, K. Tedford, T. Potzel, K. Pfeffer, and K. D. Fischer. 2001. 'Lsc is required for marginal zone B cells, regulation of lymphocyte motility and immune responses', *Nat Immunol*, 2: 855-62.
Glasmacher, E., S. Agrawal, A. B. Chang, T. L. Murphy, W. Zeng, B. Vander Lugt, A. A. Khan, M. Ciofani, C. J. Spooner, S. Rutz, J. Hackney, R. Nurieva, C. R. Escalante, W. Ouyang, D. R. Littman, K. M. Murphy, and H. Singh. 2012. 'A genomic regulatory element that directs assembly and function of immune-specific AP-1-IRF complexes', *Science*, 338: 975-80.
Gong, Y., J. Yue, X. Wu, X. Wang, J. Wen, L. Lu, X. Peng, B. Qiang, and J. Yuan. 2006. 'NSPc1 is a cell growth regulator that acts as a transcriptional repressor of p21Waf1/Cip1 via the RARE element', *Nucleic Acids Res*, 34: 6158-69.
Grau, D. J., B. A. Chapman, J. D. Garlick, M. Borowsky, N. J. Francis, and R. E. Kingston. 2011. 'Compaction of chromatin by diverse Polycomb group proteins requires localized regions of high charge', *Genes Dev*, 25: 2210-21.
Grossmann, M., L. A. O'Reilly, R. Gugasyan, A. Strasser, J. M. Adams, and S. Gerondakis. 2000. 'The anti-apoptotic activities of Rel and RelA required during B-cell maturation involve the regulation of Bcl-2 expression', *EMBO J*, 19: 6351-60.
Guinamard, R., M. Okigaki, J. Schlessinger, and J. V. Ravetch. 2000. 'Absence of marginal zone B cells in Pyk-2-deficient mice defines their role in the humoral response', *Nat Immunol*, 1: 31-6.
Guo, F., D. Weih, E. Meier, and F. Weih. 2007. 'Constitutive alternative NF-kappaB signaling promotes marginal zone B-cell development but disrupts the marginal sinus and induces HEV-like structures in the spleen', *Blood*, 110: 2381-9.
Gupta, R. A., N. Shah, K. C. Wang, J. Kim, H. M. Horlings, D. J. Wong, M. C. Tsai, T. Hung, P. Argani, J. L. Rinn, Y. Wang, P. Brzoska, B. Kong, R. Li, R. B. West, M. J. van de Vijver, S. Sukumar, and H. Y. Chang. 2010. 'Long non-coding RNA HOTAIR reprograms chromatin state to promote cancer metastasis', *Nature*, 464: 1071-6.
Gupta, S., M. Jiang, A. Anthony, and A. B. Pernis. 1999. 'Lineage-specific modulation of interleukin 4 signaling by interferon regulatory factor 4', *J Exp Med*, 190: 1837-48.
Gyory, I., J. Wu, G. Fejer, E. Seto, and K. L. Wright. 2004. 'PRDI-BF1 recruits the histone H3 methyltransferase G9a in transcriptional silencing', *Nat Immunol*, 5: 299-308.
Haas, K. M., J. C. Poe, D. A. Steeber, and T. F. Tedder. 2005. 'B-1a and B-1b cells exhibit distinct developmental requirements and have unique functional roles in innate and adaptive immunity to S. pneumoniae', *Immunity*, 23: 7-18.
Hagman, J., and K. Lukin. 2006. 'Transcription factors drive B cell development', *Curr Opin Immunol*, 18: 127-34.
Hansen, K. H., A. P. Bracken, D. Pasini, N. Dietrich, S. S. Gehani, A. Monrad, J. Rappsilber, M. Lerdrup, and K. Helin. 2008. 'A model for transmission of the H3K27me3 epigenetic mark', *Nat Cell Biol*, 10: 1291-300.
Hao, Z., and K. Rajewsky. 2001. 'Homeostasis of peripheral B cells in the absence of B cell influx from the bone marrow', *J Exp Med*, 194: 1151-64.
Hardy, R. R. 2006. 'B-1 B cell development', *J Immunol*, 177: 2749-54.

Hart, G. T., S. L. Peery, S. E. Hamilton, and S. C. Jameson. 2012. 'Cutting edge: Kruppel-like factor 2 is required for phenotypic maintenance but not development of B1 B cells', *J Immunol*, 189: 3293-7.
Hart, G. T., X. Wang, K. A. Hogquist, and S. C. Jameson. 2011. 'Kruppel-like factor 2 (KLF2) regulates B-cell reactivity, subset differentiation, and trafficking molecule expression', *Proc Natl Acad Sci U S A*, 108: 716-21.
Hasbold, J., A. B. Lyons, M. R. Kehry, and P. D. Hodgkin. 1998. 'Cell division number regulates IgG1 and IgE switching of B cells following stimulation by CD40 ligand and IL-4', *Eur J Immunol*, 28: 1040-51.
Hastings, W. D., J. R. Tumang, T. W. Behrens, and T. L. Rothstein. 2006. 'Peritoneal B-2 cells comprise a distinct B-2 cell population with B-1b-like characteristics', *Eur J Immunol*, 36: 1114-23.
Hathcock, K. S., H. Hirano, S. Murakami, and R. J. Hodes. 1992. 'CD45 expression by B cells. Expression of different CD45 isoforms by subpopulations of activated B cells', *J Immunol*, 149: 2286-94.
He, J., A. T. Nguyen, and Y. Zhang. 2011. 'KDM2b/JHDM1b, an H3K36me2-specific demethylase, is required for initiation and maintenance of acute myeloid leukemia', *Blood*, 117: 3869-80.
Healy, J. I., R. E. Dolmetsch, L. A. Timmerman, J. G. Cyster, M. L. Thomas, G. R. Crabtree, R. S. Lewis, and C. C. Goodnow. 1997. 'Different nuclear signals are activated by the B cell receptor during positive versus negative signaling', *Immunity*, 6: 419-28.
Hermiston, M. L., Z. Xu, and A. Weiss. 2003. 'CD45: a critical regulator of signaling thresholds in immune cells', *Annu Rev Immunol*, 21: 107-37.
Hermiston, M. L., J. Zikherman, and J. W. Zhu. 2009. 'CD45, CD148, and Lyp/Pep: critical phosphatases regulating Src family kinase signaling networks in immune cells', *Immunol Rev*, 228: 288-311.
Hernandez, J. D., J. Klein, S. J. Van Dyken, J. D. Marth, and L. G. Baum. 2007. 'T-cell activation results in microheterogeneous changes in glycosylation of CD45', *Int Immunol*, 19: 847-56.
Herranz, N., D. Pasini, V. M. Diaz, C. Franci, A. Gutierrez, N. Dave, M. Escriva, I. Hernandez-Munoz, L. Di Croce, K. Helin, A. Garcia de Herreros, and S. Peiro. 2008. 'Polycomb complex 2 is required for E-cadherin repression by the Snail1 transcription factor', *Mol Cell Biol*, 28: 4772-81.
Hibbs, M. L., K. W. Harder, J. Armes, N. Kountouri, C. Quilici, F. Casagranda, A. R. Dunn, and D. M. Tarlinton. 2002. 'Sustained activation of Lyn tyrosine kinase in vivo leads to autoimmunity', *J Exp Med*, 196: 1593-604.
Hibbs, M. L., D. M. Tarlinton, J. Armes, D. Grail, G. Hodgson, R. Maglitto, S. A. Stacker, and A. R. Dunn. 1995. 'Multiple defects in the immune system of Lyn-deficient mice, culminating in autoimmune disease', *Cell*, 83: 301-11.
Ho, S. N., D. J. Thomas, L. A. Timmerman, X. Li, U. Francke, and G. R. Crabtree. 1995. 'NFATc3, a lymphoid-specific NFATc family member that is calcium-regulated and exhibits distinct DNA binding specificity', *J Biol Chem*, 270: 19898-907.
Hodgkin, P. D., J. H. Lee, and A. B. Lyons. 1996. 'B cell differentiation and isotype switching is related to division cycle number', *J Exp Med*, 184: 277-81.
Holmes, M. L., S. Carotta, L. M. Corcoran, and S. L. Nutt. 2006. 'Repression of Flt3 by Pax5 is crucial for B-cell lineage commitment', *Genes Dev*, 20: 933-8.
Hong, Z., J. Jiang, L. Lan, S. Nakajima, S. Kanno, H. Koseki, and A. Yasui. 2008. 'A polycomb group protein, PHF1, is involved in the response to DNA double-strand breaks in human cell', *Nucleic Acids Res*, 36: 2939-47.
Honma, K., H. Udono, T. Kohno, K. Yamamoto, A. Ogawa, T. Takemori, A. Kumatori, S. Suzuki, T. Matsuyama, and K. Yui. 2005. 'Interferon regulatory factor 4 negatively regulates the production of proinflammatory cytokines by macrophages in response to LPS', *Proc Natl Acad Sci U S A*, 102: 16001-6.
Horcher, M., A. Souabni, and M. Busslinger. 2001. 'Pax5/BSAP maintains the identity of B cells in late B lymphopoiesis', *Immunity*, 14: 779-90.
Hozumi, K., N. Negishi, D. Suzuki, N. Abe, Y. Sotomaru, N. Tamaoki, C. Mailhos, D. Ish-Horowicz, S. Habu, and M. J. Owen. 2004. 'Delta-like 1 is necessary for the generation of marginal zone B cells but not T cells in vivo', *Nat Immunol*, 5: 638-44.

Huang, H., and D. J. Tindall. 2011. 'Regulation of FOXO protein stability via ubiquitination and proteasome degradation', *Biochim Biophys Acta*, 1813: 1961-4.
Hurlin, P. J., E. Steingrimsson, N. G. Copeland, N. A. Jenkins, and R. N. Eisenman. 1999. 'Mga, a dual-specificity transcription factor that interacts with Max and contains a T-domain DNA-binding motif', *EMBO J*, 18: 7019-28.
Ikawa, T., K. Masuda, T. A. Endo, M. Endo, K. Isono, Y. Koseki, R. Nakagawa, K. Kometani, J. Takano, Y. Agata, Y. Katsura, T. Kurosaki, M. Vidal, H. Koseki, and H. Kawamoto. 2016. 'Conversion of T cells to B cells by inactivation of polycomb-mediated epigenetic suppression of the B-lineage program', *Genes Dev*, 30: 2475-85.
Illingworth, R. S., C. H. Botting, G. R. Grimes, W. A. Bickmore, and R. Eskeland. 2012. 'PRC1 and PRC2 are not required for targeting of H2A.Z to developmental genes in embryonic stem cells', *PLoS One*, 7: e34848.
Ismail, I. H., C. Andrin, D. McDonald, and M. J. Hendzel. 2010. 'BMI1-mediated histone ubiquitylation promotes DNA double-strand break repair', *J Cell Biol*, 191: 45-60.
Ivanova, N. B., J. T. Dimos, C. Schaniel, J. A. Hackney, K. A. Moore, and I. R. Lemischka. 2002. 'A stem cell molecular signature', *Science*, 298: 601-4.
Iwama, A., H. Oguro, M. Negishi, Y. Kato, Y. Morita, H. Tsukui, H. Ema, T. Kamijo, Y. Katoh-Fukui, H. Koseki, M. van Lohuizen, and H. Nakauchi. 2004. 'Enhanced self-renewal of hematopoietic stem cells mediated by the polycomb gene product Bmi-1', *Immunity*, 21: 843-51.
Jacobs, J. J., B. Scheijen, J. W. Voncken, K. Kieboom, A. Berns, and M. van Lohuizen. 1999. 'Bmi-1 collaborates with c-Myc in tumorigenesis by inhibiting c-Myc-induced apoptosis via INK4a/ARF', *Genes Dev*, 13: 2678-90.
Jellusova, J., A. V. Miletic, M. H. Cato, W. W. Lin, Y. Hu, G. A. Bishop, M. J. Shlomchik, and R. C. Rickert. 2013. 'Context-specific BAFF-R signaling by the NF-kappaB and PI3K pathways', *Cell Rep*, 5: 1022-35.
Jensen, G. S., S. Poppema, M. J. Mant, and L. M. Pilarski. 1989. 'Transition in CD45 isoform expression during differentiation of normal and abnormal B cells', *Int Immunol*, 1: 229-36.
Ji, Jun-Yuan, and Nicholas J. Dyson. 2010. 'Interplay Between Cyclin-Dependent Kinases and E2F-Dependent Transcription.' in Greg H. Enders (ed.), *Cell Cycle Deregulation in Cancer* (Springer New York: New York, NY).
Jiang, X. X., Q. Nguyen, Y. Chou, T. Wang, V. Nandakumar, P. Yates, L. Jones, L. Wang, H. Won, H. R. Lee, J. U. Jung, M. Muschen, X. F. Huang, and S. Y. Chen. 2011. 'Control of B cell development by the histone H2A deubiquitinase MYSM1', *Immunity*, 35: 883-96.
Jung, Y. S., Y. Qian, and X. Chen. 2010. 'Examination of the expanding pathways for the regulation of p21 expression and activity', *Cell Signal*, 22: 1003-12.
Kajiume, T., Y. Ninomiya, H. Ishihara, R. Kanno, and M. Kanno. 2004. 'Polycomb group gene mel-18 modulates the self-renewal activity and cell cycle status of hematopoietic stem cells', *Exp Hematol*, 32: 571-8.
Kalb, R., S. Latwiel, H. I. Baymaz, P. W. Jansen, C. W. Muller, M. Vermeulen, and J. Muller. 2014. 'Histone H2A monoubiquitination promotes histone H3 methylation in Polycomb repression', *Nat Struct Mol Biol*, 21: 569-71.
Kallies, A., J. Hasbold, K. Fairfax, C. Pridans, D. Emslie, B. S. McKenzie, A. M. Lew, L. M. Corcoran, P. D. Hodgkin, D. M. Tarlinton, and S. L. Nutt. 2007. 'Initiation of plasma-cell differentiation is independent of the transcription factor Blimp-1', *Immunity*, 26: 555-66.
Kallies, A., J. Hasbold, D. M. Tarlinton, W. Dietrich, L. M. Corcoran, P. D. Hodgkin, and S. L. Nutt. 2004. 'Plasma cell ontogeny defined by quantitative changes in blimp-1 expression', *J Exp Med*, 200: 967-77.
Kamijo, T., J. D. Weber, G. Zambetti, F. Zindy, M. F. Roussel, and C. J. Sherr. 1998. 'Functional and physical interactions of the ARF tumor suppressor with p53 and Mdm2', *Proc Natl Acad Sci U S A*, 95: 8292-7.
Kamminga, L. M., L. V. Bystrykh, A. de Boer, S. Houwer, J. Douma, E. Weersing, B. Dontje, and G. de Haan. 2006. 'The Polycomb group gene Ezh2 prevents hematopoietic stem cell exhaustion', *Blood*, 107: 2170-9.

Karimian, A., Y. Ahmadi, and B. Yousefi. 2016. 'Multiple functions of p21 in cell cycle, apoptosis and transcriptional regulation after DNA damage', *DNA Repair (Amst)*, 42: 63-71.
Karin, M., and Y. Ben-Neriah. 2000. 'Phosphorylation meets ubiquitination: the control of NF-[kappa]B activity', *Annu Rev Immunol*, 18: 621-63.
Katagiri, T., M. Ogimoto, K. Hasegawa, Y. Arimura, K. Mitomo, M. Okada, M. R. Clark, K. Mizuno, and H. Yakura. 1999. 'CD45 negatively regulates lyn activity by dephosphorylating both positive and negative regulatory tyrosine residues in immature B cells', *J Immunol*, 163: 1321-6.
Katagiri, T., M. Ogimoto, K. Hasegawa, K. Mizuno, and H. Yakura. 1995. 'Selective regulation of Lyn tyrosine kinase by CD45 in immature B cells', *J Biol Chem*, 270: 27987-90.
Kaustov, L., H. Ouyang, M. Amaya, A. Lemak, N. Nady, S. Duan, G. A. Wasney, Z. Li, M. Vedadi, M. Schapira, J. Min, and C. H. Arrowsmith. 2011. 'Recognition and specificity determinants of the human cbx chromodomains', *J Biol Chem*, 286: 521-9.
Kawabe, T., T. Naka, K. Yoshida, T. Tanaka, H. Fujiwara, S. Suematsu, N. Yoshida, T. Kishimoto, and H. Kikutani. 1994. 'The immune responses in CD40-deficient mice: impaired immunoglobulin class switching and germinal center formation', *Immunity*, 1: 167-78.
Kelly, T. K., Y. Liu, F. D. Lay, G. Liang, B. P. Berman, and P. A. Jones. 2012. 'Genome-wide mapping of nucleosome positioning and DNA methylation within individual DNA molecules', *Genome Res*, 22: 2497-506.
Ketting, René F. 2010. 'microRNA Biogenesis and Function.' in Helge Großhans (ed.), *Regulation of microRNAs* (Springer US: New York, NY).
Kheradmand Kia, S., P. Solaimani Kartalaei, E. Farahbakhshian, F. Pourfarzad, M. von Lindern, and C. P. Verrijzer. 2009. 'EZH2-dependent chromatin looping controls INK4a and INK4b, but not ARF, during human progenitor cell differentiation and cellular senescence', *Epigenetics Chromatin*, 2: 16.
Kim, E. M., C. H. Jung, J. Kim, S. G. Hwang, J. K. Park, and H. D. Um. 2017. 'The p53/p21 Complex Regulates Cancer Cell Invasion and Apoptosis by Targeting Bcl-2 Family Proteins', *Cancer Res*, 77: 3092-100.
Kim, J. K., M. Samaranayake, and S. Pradhan. 2009. 'Epigenetic mechanisms in mammals', *Cell Mol Life Sci*, 66: 596-612.
King, H. W., N. A. Fursova, N. P. Blackledge, and R. J. Klose. 2018. 'Polycomb repressive complex 1 shapes the nucleosome landscape but not accessibility at target genes', *Genome Res*, 28: 1494-507.
Klauke, K., V. Radulovic, M. Broekhuis, E. Weersing, E. Zwart, S. Olthof, M. Ritsema, S. Bruggeman, X. Wu, K. Helin, L. Bystrykh, and G. de Haan. 2013. 'Polycomb Cbx family members mediate the balance between haematopoietic stem cell self-renewal and differentiation', *Nat Cell Biol*, 15: 353-62.
Kleiman, E., D. Salyakina, M. De Heusch, K. L. Hoek, J. M. Llanes, I. Castro, J. A. Wright, E. S. Clark, D. M. Dykxhoorn, E. Capobianco, A. Takeda, J. C. Renauld, and W. N. Khan. 2015. 'Distinct Transcriptomic Features are Associated with Transitional and Mature B-Cell Populations in the Mouse Spleen', *Front Immunol*, 6: 30.
Klein, U., S. Casola, G. Cattoretti, Q. Shen, M. Lia, T. Mo, T. Ludwig, K. Rajewsky, and R. Dalla-Favera. 2006. 'Transcription factor IRF4 controls plasma cell differentiation and class-switch recombination', *Nat Immunol*, 7: 773-82.
Klein, U., and R. Dalla-Favera. 2008. 'Germinal centres: role in B-cell physiology and malignancy', *Nat Rev Immunol*, 8: 22-33.
Klusmann, I., K. Wohlberedt, A. Magerhans, F. Teloni, J. O. Korbel, M. Altmeyer, and M. Dobbelstein. 2018. 'Chromatin modifiers Mdm2 and RNF2 prevent RNA:DNA hybrids that impair DNA replication', *Proc Natl Acad Sci U S A*.
Kondo, M., I. L. Weissman, and K. Akashi. 1997. 'Identification of clonogenic common lymphoid progenitors in mouse bone marrow', *Cell*, 91: 661-72.
Kondo, T., K. Isono, K. Kondo, T. A. Endo, S. Itohara, M. Vidal, and H. Koseki. 2014. 'Polycomb potentiates meis2 activation in midbrain by mediating interaction of the promoter with a tissue-specific enhancer', *Dev Cell*, 28: 94-101.

Kouzarides, T. 2007. 'Chromatin modifications and their function', *Cell*, 128: 693-705.
Kozmik, Z., S. Wang, P. Dorfler, B. Adams, and M. Busslinger. 1992. 'The promoter of the CD19 gene is a target for the B-cell-specific transcription factor BSAP', *Mol Cell Biol*, 12: 2662-72.
Kraus, M., M. B. Alimzhanov, N. Rajewsky, and K. Rajewsky. 2004. 'Survival of resting mature B lymphocytes depends on BCR signaling via the Igalpha/beta heterodimer', *Cell*, 117: 787-800.
Ku, M., R. P. Koche, E. Rheinbay, E. M. Mendenhall, M. Endoh, T. S. Mikkelsen, A. Presser, C. Nusbaum, X. Xie, A. S. Chi, M. Adli, S. Kasif, L. M. Ptaszek, C. A. Cowan, E. S. Lander, H. Koseki, and B. E. Bernstein. 2008. 'Genomewide analysis of PRC1 and PRC2 occupancy identifies two classes of bivalent domains', *PLoS Genet*, 4: e1000242.
Kuleshov, M. V., M. R. Jones, A. D. Rouillard, N. F. Fernandez, Q. Duan, Z. Wang, S. Koplev, S. L. Jenkins, K. M. Jagodnik, A. Lachmann, M. G. McDermott, C. D. Monteiro, G. W. Gundersen, and A. Ma'ayan. 2016. 'Enrichr: a comprehensive gene set enrichment analysis web server 2016 update', *Nucleic Acids Res*, 44: W90-7.
Kumararatne, D. S., R. F. Gagnon, and Y. Smart. 1980. 'Selective loss of large lymphocytes from the marginal zone of the white pulp in rat spleens following a single dose of cyclophosphamide. A study using quantitative histological methods', *Immunology*, 40: 123-31.
Kunisawa, J., Y. Kurashima, M. Gohda, M. Higuchi, I. Ishikawa, F. Miura, I. Ogahara, and H. Kiyono. 2007. 'Sphingosine 1-phosphate regulates peritoneal B-cell trafficking for subsequent intestinal IgA production', *Blood*, 109: 3749-56.
Kuroda, K., H. Han, S. Tani, K. Tanigaki, T. Tun, T. Furukawa, Y. Taniguchi, H. Kurooka, Y. Hamada, S. Toyokuni, and T. Honjo. 2003. 'Regulation of marginal zone B cell development by MINT, a suppressor of Notch/RBP-J signaling pathway', *Immunity*, 18: 301-12.
Kurosaki, T. 2011. 'Regulation of BCR signaling', *Mol Immunol*, 48: 1287-91.
Kwon, H., D. Thierry-Mieg, J. Thierry-Mieg, H. P. Kim, J. Oh, C. Tunyaplin, S. Carotta, C. E. Donovan, M. L. Goldman, P. Tailor, K. Ozato, D. E. Levy, S. L. Nutt, K. Calame, and W. J. Leonard. 2009. 'Analysis of interleukin-21-induced Prdm1 gene regulation reveals functional cooperation of STAT3 and IRF4 transcription factors', *Immunity*, 31: 941-52.
Kwon, K., C. Hutter, Q. Sun, I. Bilic, C. Cobaleda, S. Malin, and M. Busslinger. 2008. 'Instructive role of the transcription factor E2A in early B lymphopoiesis and germinal center B cell development', *Immunity*, 28: 751-62.
Lam, K. P., R. Kuhn, and K. Rajewsky. 1997. 'In vivo ablation of surface immunoglobulin on mature B cells by inducible gene targeting results in rapid cell death', *Cell*, 90: 1073-83.
Langmead, B., and S. L. Salzberg. 2012. 'Fast gapped-read alignment with Bowtie 2', *Nat Methods*, 9: 357-9.
Laugesen, A., and K. Helin. 2014. 'Chromatin repressive complexes in stem cells, development, and cancer', *Cell Stem Cell*, 14: 735-51.
Lee, T. I., R. G. Jenner, L. A. Boyer, M. G. Guenther, S. S. Levine, R. M. Kumar, B. Chevalier, S. E. Johnstone, M. F. Cole, K. Isono, H. Koseki, T. Fuchikami, K. Abe, H. L. Murray, J. P. Zucker, B. Yuan, G. W. Bell, E. Herbolsheimer, N. M. Hannett, K. Sun, D. T. Odom, A. P. Otte, T. L. Volkert, D. P. Bartel, D. A. Melton, D. K. Gifford, R. Jaenisch, and R. A. Young. 2006. 'Control of developmental regulators by Polycomb in human embryonic stem cells', *Cell*, 125: 301-13.
Leeb, M., D. Pasini, M. Novatchkova, M. Jaritz, K. Helin, and A. Wutz. 2010. 'Polycomb complexes act redundantly to repress genomic repeats and genes', *Genes Dev*, 24: 265-76.
Leeb, M., and A. Wutz. 2007. 'Ring1B is crucial for the regulation of developmental control genes and PRC1 proteins but not X inactivation in embryonic cells', *J Cell Biol*, 178: 219-29.
Lemay, M., and K. A. Wood. 1999. 'Detection of DNA damage and identification of UV-induced photoproducts using the CometAssay kit', *Biotechniques*, 27: 846-51.

Lewis, E. B. 1978. 'A gene complex controlling segmentation in Drosophila', *Nature*, 276: 565-70.
Li, G., A. Y. So, R. Sookram, S. Wong, J. K. Wang, Y. Ouyang, P. He, Y. Su, R. Casellas, and D. Baltimore. 2018. 'Epigenetic silencing of miR-125b is required for normal B-cell development', *Blood*, 131: 1920-30.
Li, L., B. Liu, O. L. Wapinski, M. C. Tsai, K. Qu, J. Zhang, J. C. Carlson, M. Lin, F. Fang, R. A. Gupta, J. A. Helms, and H. Y. Chang. 2013. 'Targeted disruption of Hotair leads to homeotic transformation and gene derepression', *Cell Rep*, 5: 3-12.
Li, X., K. Su, C. Ji, A. J. Szalai, J. Wu, Y. Zhang, T. Zhou, R. P. Kimberly, and J. C. Edberg. 2008. 'Immune opsonins modulate BLyS/BAFF release in a receptor-specific fashion', *J Immunol*, 181: 1012-8.
Li, Z., T. Otevrel, Y. Gao, H. L. Cheng, B. Seed, T. D. Stamato, G. E. Taccioli, and F. W. Alt. 1995. 'The XRCC4 gene encodes a novel protein involved in DNA double-strand break repair and V(D)J recombination', *Cell*, 83: 1079-89.
Lin, K. I., C. Angelin-Duclos, T. C. Kuo, and K. Calame. 2002. 'Blimp-1-dependent repression of Pax-5 is required for differentiation of B cells to immunoglobulin M-secreting plasma cells', *Mol Cell Biol*, 22: 4771-80.
Lin, Y. C., S. Jhunjhunwala, C. Benner, S. Heinz, E. Welinder, R. Mansson, M. Sigvardsson, J. Hagman, C. A. Espinoza, J. Dutkowski, T. Ideker, C. K. Glass, and C. Murre. 2010. 'A global network of transcription factors, involving E2A, EBF1 and Foxo1, that orchestrates B cell fate', *Nat Immunol*, 11: 635-43.
Lin, Y., K. Wong, and K. Calame. 1997. 'Repression of c-myc transcription by Blimp-1, an inducer of terminal B cell differentiation', *Science*, 276: 596-9.
Liu, J., L. Cao, J. Chen, S. Song, I. H. Lee, C. Quijano, H. Liu, K. Keyvanfar, H. Chen, L. Y. Cao, B. H. Ahn, N. G. Kumar, Rovira, II, X. L. Xu, M. van Lohuizen, N. Motoyama, C. X. Deng, and T. Finkel. 2009. 'Bmi1 regulates mitochondrial function and the DNA damage response pathway', *Nature*, 459: 387-92.
Liu, Y. J. 1997. 'Sites of B lymphocyte selection, activation, and tolerance in spleen', *J Exp Med*, 186: 625-9.
Lizio, Marina, Jayson Harshbarger, Hisashi Shimoji, Jessica Severin, Takeya Kasukawa, Serkan Sahin, Imad Abugessaisa, Shiro Fukuda, Fumi Hori, Sachi Ishikawa-Kato, Christopher J. Mungall, Erik Arner, J. Kenneth Baillie, Nicolas Bertin, Hidemasa Bono, Michiel de Hoon, Alexander D. Diehl, Emmanuel Dimont, Tom C. Freeman, Kaori Fujieda, Winston Hide, Rajaram Kaliyaperumal, Toshiaki Katayama, Timo Lassmann, Terrence F. Meehan, Koro Nishikata, Hiromasa Ono, Michael Rehli, Albin Sandelin, Erik A. Schultes, Peter A. C. ‘t Hoen, Zuotian Tatum, Mark Thompson, Tetsuro Toyoda, Derek W. Wright, Carsten O. Daub, Masayoshi Itoh, Piero Carninci, Yoshihide Hayashizaki, Alistair R. R. Forrest, Hideya Kawaji, and Fantom consortium the. 2015. 'Gateways to the FANTOM5 promoter level mammalian expression atlas', *Genome Biology*, 16: 22.
Lo, C. G., T. T. Lu, and J. G. Cyster. 2003. 'Integrin-dependence of lymphocyte entry into the splenic white pulp', *J Exp Med*, 197: 353-61.
Loder, F., B. Mutschler, R. J. Ray, C. J. Paige, P. Sideras, R. Torres, M. C. Lamers, and R. Carsetti. 1999. 'B cell development in the spleen takes place in discrete steps and is determined by the quality of B cell receptor-derived signals', *J Exp Med*, 190: 75-89.
Lodish, H. F., B. Zhou, G. Liu, and C. Z. Chen. 2008. 'Micromanagement of the immune system by microRNAs', *Nat Rev Immunol*, 8: 120-30.
Love, M. I., W. Huber, and S. Anders. 2014. 'Moderated estimation of fold change and dispersion for RNA-seq data with DESeq2', *Genome Biol*, 15: 550.
Lowell, C. A. 2004. 'Src-family kinases: rheostats of immune cell signaling', *Mol Immunol*, 41: 631-43.
Lu, R., K. L. Medina, D. W. Lancki, and H. Singh. 2003. 'IRF-4,8 orchestrate the pre-B-to-B transition in lymphocyte development', *Genes Dev*, 17: 1703-8.
Mackay, F., and C. Ambrose. 2003. 'The TNF family members BAFF and APRIL: the growing complexity', *Cytokine Growth Factor Rev*, 14: 311-24.
Mackay, F., and H. Leung. 2006. 'The role of the BAFF/APRIL system on T cell function', *Semin Immunol*, 18: 284-9.

Mackay, F., and P. Schneider. 2009. 'Cracking the BAFF code', *Nat Rev Immunol*, 9: 491-502.
Maertens, G. N., S. El Messaoudi-Aubert, T. Racek, J. K. Stock, J. Nicholls, M. Rodriguez-Niedenfuhr, J. Gil, and G. Peters. 2009. 'Several distinct polycomb complexes regulate and co-localize on the INK4a tumor suppressor locus', *PLoS One*, 4: e6380.
Majeti, R., A. M. Bilwes, J. P. Noel, T. Hunter, and A. Weiss. 1998. 'Dimerization-induced inhibition of receptor protein tyrosine phosphatase function through an inhibitory wedge', *Science*, 279: 88-91.
Majewski, I. J., M. E. Blewitt, C. A. de Graaf, E. J. McManus, M. Bahlo, A. A. Hilton, C. D. Hyland, G. K. Smyth, J. E. Corbin, D. Metcalf, W. S. Alexander, and D. J. Hilton. 2008. 'Polycomb repressive complex 2 (PRC2) restricts hematopoietic stem cell activity', *PLoS Biol*, 6: e93.
Manz, R. A., A. Thiel, and A. Radbruch. 1997. 'Lifetime of plasma cells in the bone marrow', *Nature*, 388: 133-4.
Margueron, R., N. Justin, K. Ohno, M. L. Sharpe, J. Son, W. J. Drury, 3rd, P. Voigt, S. R. Martin, W. R. Taylor, V. De Marco, V. Pirrotta, D. Reinberg, and S. J. Gamblin. 2009. 'Role of the polycomb protein EED in the propagation of repressive histone marks', *Nature*, 461: 762-7.
Martin, F., and J. F. Kearney. 2002. 'Marginal-zone B cells', *Nat Rev Immunol*, 2: 323-35.
Matsuzaki, H., H. Daitoku, M. Hatta, K. Tanaka, and A. Fukamizu. 2003. 'Insulin-induced phosphorylation of FKHR (Foxo1) targets to proteasomal degradation', *Proc Natl Acad Sci U S A*, 100: 11285-90.
Maurer, U., C. Charvet, A. S. Wagman, E. Dejardin, and D. R. Green. 2006. 'Glycogen synthase kinase-3 regulates mitochondrial outer membrane permeabilization and apoptosis by destabilization of MCL-1', *Mol Cell*, 21: 749-60.
May, M. J., and S. Ghosh. 1997. 'Rel/NF-kappa B and I kappa B proteins: an overview', *Semin Cancer Biol*, 8: 63-73.
McBlane, J. F., D. C. van Gent, D. A. Ramsden, C. Romeo, C. A. Cuomo, M. Gellert, and M. A. Oettinger. 1995. 'Cleavage at a V(D)J recombination signal requires only RAG1 and RAG2 proteins and occurs in two steps', *Cell*, 83: 387-95.
McCabe, M. T., H. M. Ott, G. Ganji, S. Korenchuk, C. Thompson, G. S. Van Aller, Y. Liu, A. P. Graves, A. Della Pietra, 3rd, E. Diaz, L. V. LaFrance, M. Mellinger, C. Duquenne, X. Tian, R. G. Kruger, C. F. McHugh, M. Brandt, W. H. Miller, D. Dhanak, S. K. Verma, P. J. Tummino, and C. L. Creasy. 2012. 'EZH2 inhibition as a therapeutic strategy for lymphoma with EZH2-activating mutations', *Nature*, 492: 108-12.
McCall, K., and W. Bender. 1996. 'Probes of chromatin accessibility in the Drosophila bithorax complex respond differently to Polycomb-mediated repression', *EMBO J*, 15: 569-80.
McManus, S., A. Ebert, G. Salvagiotto, J. Medvedovic, Q. Sun, I. Tamir, M. Jaritz, H. Tagoh, and M. Busslinger. 2011. 'The transcription factor Pax5 regulates its target genes by recruiting chromatin-modifying proteins in committed B cells', *EMBO J*, 30: 2388-404.
Medina, K. L., J. M. Pongubala, K. L. Reddy, D. W. Lancki, R. Dekoter, M. Kieslinger, R. Grosschedl, and H. Singh. 2004. 'Assembling a gene regulatory network for specification of the B cell fate', *Dev Cell*, 7: 607-17.
Medvedovic, J., A. Ebert, H. Tagoh, and M. Busslinger. 2011. 'Pax5: a master regulator of B cell development and leukemogenesis', *Adv Immunol*, 111: 179-206.
Melek, M., M. Gellert, and D. C. van Gent. 1998. 'Rejoining of DNA by the RAG1 and RAG2 proteins', *Science*, 280: 301-3.
Mendenhall, E. M., R. P. Koche, T. Truong, V. W. Zhou, B. Issac, A. S. Chi, M. Ku, and B. E. Bernstein. 2010. 'GC-rich sequence elements recruit PRC2 in mammalian ES cells', *PLoS Genet*, 6: e1001244.
Merino, D., S. W. Lok, J. E. Visvader, and G. J. Lindeman. 2016. 'Targeting BCL-2 to enhance vulnerability to therapy in estrogen receptor-positive breast cancer', *Oncogene*, 35: 1877-87.
Mikkelsen, T. S., M. Ku, D. B. Jaffe, B. Issac, E. Lieberman, G. Giannoukos, P. Alvarez, W. Brockman, T. K. Kim, R. P. Koche, W. Lee, E. Mendenhall, A. O'Donovan, A. Presser, C. Russ, X. Xie, A. Meissner, M. Wernig, R. Jaenisch, C. Nusbaum, E. S.

Lander, and B. E. Bernstein. 2007. 'Genome-wide maps of chromatin state in pluripotent and lineage-committed cells', *Nature*, 448: 553-60.
Milanovic, M., N. Heise, N. S. De Silva, M. M. Anderson, K. Silva, A. Carette, F. Orelli, G. Bhagat, and U. Klein. 2017. 'Differential requirements for the canonical NF-kappaB transcription factors c-REL and RELA during the generation and activation of mature B cells', *Immunol Cell Biol*, 95: 261-71.
Minnich, M., H. Tagoh, P. Bonelt, E. Axelsson, M. Fischer, B. Cebolla, A. Tarakhovsky, S. L. Nutt, M. Jaritz, and M. Busslinger. 2016. 'Multifunctional role of the transcription factor Blimp-1 in coordinating plasma cell differentiation', *Nat Immunol*, 17: 331-43.
Mittrucker, H. W., T. Matsuyama, A. Grossman, T. M. Kundig, J. Potter, A. Shahinian, A. Wakeham, B. Patterson, P. S. Ohashi, and T. W. Mak. 1997. 'Requirement for the transcription factor LSIRF/IRF4 for mature B and T lymphocyte function', *Science*, 275: 540-3.
Morey, L., L. Aloia, L. Cozzuto, S. A. Benitah, and L. Di Croce. 2013. 'RYBP and Cbx7 define specific biological functions of polycomb complexes in mouse embryonic stem cells', *Cell Rep*, 3: 60-9.
Morey, L., C. Brenner, F. Fazi, R. Villa, A. Gutierrez, M. Buschbeck, C. Nervi, S. Minucci, F. Fuks, and L. Di Croce. 2008. 'MBD3, a component of the NuRD complex, facilitates chromatin alteration and deposition of epigenetic marks', *Mol Cell Biol*, 28: 5912-23.
Morin, R. D., N. A. Johnson, T. M. Severson, A. J. Mungall, J. An, R. Goya, J. E. Paul, M. Boyle, B. W. Woolcock, F. Kuchenbauer, D. Yap, R. K. Humphries, O. L. Griffith, S. Shah, H. Zhu, M. Kimbara, P. Shashkin, J. F. Charlot, M. Tcherpakov, R. Corbett, A. Tam, R. Varhol, D. Smailus, M. Moksa, Y. Zhao, A. Delaney, H. Qian, I. Birol, J. Schein, R. Moore, R. Holt, D. E. Horsman, J. M. Connors, S. Jones, S. Aparicio, M. Hirst, R. D. Gascoyne, and M. A. Marra. 2010. 'Somatic mutations altering EZH2 (Tyr641) in follicular and diffuse large B-cell lymphomas of germinal-center origin', *Nat Genet*, 42: 181-5.
Mozzetta, C., J. Pontis, L. Fritsch, P. Robin, M. Portoso, C. Proux, R. Margueron, and S. Ait-Si-Ali. 2014. 'The histone H3 lysine 9 methyltransferases G9a and GLP regulate polycomb repressive complex 2-mediated gene silencing', *Mol Cell*, 53: 277-89.
Muramatsu, M., K. Kinoshita, S. Fagarasan, S. Yamada, Y. Shinkai, and T. Honjo. 2000. 'Class switch recombination and hypermutation require activation-induced cytidine deaminase (AID), a potential RNA editing enzyme', *Cell*, 102: 553-63.
Neff, T., A. U. Sinha, M. J. Kluk, N. Zhu, M. H. Khattab, L. Stein, H. Xie, S. H. Orkin, and S. A. Armstrong. 2012. 'Polycomb repressive complex 2 is required for MLL-AF9 leukemia', *Proc Natl Acad Sci U S A*, 109: 5028-33.
Negre, N., J. Hennetin, L. V. Sun, S. Lavrov, M. Bellis, K. P. White, and G. Cavalli. 2006. 'Chromosomal distribution of PcG proteins during Drosophila development', *PLoS Biol*, 4: e170.
Neri, F., D. Incarnato, A. Krepelova, S. Rapelli, A. Pagnani, R. Zecchina, C. Parlato, and S. Oliviero. 2013. 'Genome-wide analysis identifies a functional association of Tet1 and Polycomb repressive complex 2 in mouse embryonic stem cells', *Genome Biol*, 14: R91.
Nevins, J. R. 2001. 'The Rb/E2F pathway and cancer', *Hum Mol Genet*, 10: 699-703.
Newman, R., H. Ahlfors, A. Saveliev, A. Galloway, D. J. Hodson, R. Williams, G. S. Besra, C. N. Cook, A. F. Cunningham, S. E. Bell, and M. Turner. 2017. 'Maintenance of the marginal-zone B cell compartment specifically requires the RNA-binding protein ZFP36L1', *Nat Immunol*, 18: 683-93.
Novack, D. V., L. Yin, A. Hagen-Stapleton, R. D. Schreiber, D. V. Goeddel, F. P. Ross, and S. L. Teitelbaum. 2003. 'The IkappaB function of NF-kappaB2 p100 controls stimulated osteoclastogenesis', *J Exp Med*, 198: 771-81.
Nutt, S. L., and B. L. Kee. 2007. 'The transcriptional regulation of B cell lineage commitment', *Immunity*, 26: 715-25.
Nutt, S. L., A. M. Morrison, P. Dorfler, A. Rolink, and M. Busslinger. 1998. 'Identification of BSAP (Pax-5) target genes in early B-cell development by loss- and gain-of-function experiments', *EMBO J*, 17: 2319-33.

O'Loghlen, A., A. M. Munoz-Cabello, A. Gaspar-Maia, H. A. Wu, A. Banito, N. Kunowska, T. Racek, H. N. Pemberton, P. Beolchi, F. Lavial, O. Masui, M. Vermeulen, T. Carroll, J. Graumann, E. Heard, N. Dillon, V. Azuara, A. P. Snijders, G. Peters, E. Bernstein, and J. Gil. 2012. 'MicroRNA regulation of Cbx7 mediates a switch of Polycomb orthologs during ESC differentiation', *Cell Stem Cell*, 10: 33-46.

Oberdoerffer, S., L. F. Moita, D. Neems, R. P. Freitas, N. Hacohen, and A. Rao. 2008. 'Regulation of CD45 alternative splicing by heterogeneous ribonucleoprotein, hnRNPLL', *Science*, 321: 686-91.

Ochiai, K., M. Maienschein-Cline, M. Mandal, J. R. Triggs, E. Bertolino, R. Sciammas, A. R. Dinner, M. R. Clark, and H. Singh. 2012. 'A self-reinforcing regulatory network triggered by limiting IL-7 activates pre-BCR signaling and differentiation', *Nat Immunol*, 13: 300-7.

Ochiai, K., M. Maienschein-Cline, G. Simonetti, J. Chen, R. Rosenthal, R. Brink, A. S. Chong, U. Klein, A. R. Dinner, H. Singh, and R. Sciammas. 2013. 'Transcriptional regulation of germinal center B and plasma cell fates by dynamical control of IRF4', *Immunity*, 38: 918-29.

Ogata, H., I. Su, K. Miyake, Y. Nagai, S. Akashi, I. Mecklenbrauker, K. Rajewsky, M. Kimoto, and A. Tarakhovsky. 2000. 'The toll-like receptor protein RP105 regulates lipopolysaccharide signaling in B cells', *J Exp Med*, 192: 23-9.

Oguro, H., J. Yuan, H. Ichikawa, T. Ikawa, S. Yamazaki, H. Kawamoto, H. Nakauchi, and A. Iwama. 2010. 'Poised lineage specification in multipotential hematopoietic stem and progenitor cells by the polycomb protein Bmi1', *Cell Stem Cell*, 6: 279-86.

Ohtsubo, M., S. Yasunaga, Y. Ohno, M. Tsumura, S. Okada, N. Ishikawa, K. Shirao, A. Kikuchi, H. Nishitani, M. Kobayashi, and Y. Takihara. 2008. 'Polycomb-group complex 1 acts as an E3 ubiquitin ligase for Geminin to sustain hematopoietic stem cell activity', *Proc Natl Acad Sci U S A*, 105: 10396-401.

Okada, T., A. Maeda, A. Iwamatsu, K. Gotoh, and T. Kurosaki. 2000. 'BCAP: the tyrosine kinase substrate that connects B cell receptor to phosphoinositide 3-kinase activation', *Immunity*, 13: 817-27.

Oo, M. L., S. Thangada, M. T. Wu, C. H. Liu, T. L. Macdonald, K. R. Lynch, C. Y. Lin, and T. Hla. 2007. 'Immunosuppressive and anti-angiogenic sphingosine 1-phosphate receptor-1 agonists induce ubiquitinylation and proteasomal degradation of the receptor', *J Biol Chem*, 282: 9082-9.

Ostling, O., and K. J. Johanson. 1984. 'Microelectrophoretic study of radiation-induced DNA damages in individual mammalian cells', *Biochem Biophys Res Commun*, 123: 291-8.

Otipoby, K. L., A. Waisman, E. Derudder, L. Srinivasan, A. Franklin, and K. Rajewsky. 2015. 'The B-cell antigen receptor integrates adaptive and innate immune signals', *Proc Natl Acad Sci U S A*, 112: 12145-50.

Painter, M. W., S. Davis, R. R. Hardy, D. Mathis, C. Benoist, and Consortium Immunological Genome Project. 2011. 'Transcriptomes of the B and T lineages compared by multiplatform microarray profiling', *J Immunol*, 186: 3047-57.

Palacios, E. H., and A. Weiss. 2004. 'Function of the Src-family kinases, Lck and Fyn, in T-cell development and activation', *Oncogene*, 23: 7990-8000.

Pan, G., S. Tian, J. Nie, C. Yang, V. Ruotti, H. Wei, G. A. Jonsdottir, R. Stewart, and J. A. Thomson. 2007. 'Whole-genome analysis of histone H3 lysine 4 and lysine 27 methylation in human embryonic stem cells', *Cell Stem Cell*, 1: 299-312.

Pan, M. R., G. Peng, W. C. Hung, and S. Y. Lin. 2011. 'Monoubiquitination of H2AX protein regulates DNA damage response signaling', *J Biol Chem*, 286: 28599-607.

Park, I. K., D. Qian, M. Kiel, M. W. Becker, M. Pihalja, I. L. Weissman, S. J. Morrison, and M. F. Clarke. 2003. 'Bmi-1 is required for maintenance of adult self-renewing haematopoietic stem cells', *Nature*, 423: 302-5.

Pasini, D., A. P. Bracken, J. B. Hansen, M. Capillo, and K. Helin. 2007. 'The polycomb group protein Suz12 is required for embryonic stem cell differentiation', *Mol Cell Biol*, 27: 3769-79.

Pasparakis, M., M. Schmidt-Supprian, and K. Rajewsky. 2002. 'IkappaB kinase signaling is essential for maintenance of mature B cells', *J Exp Med*, 196: 743-52.

Pathak, S., S. Ma, L. Trinh, and R. Lu. 2008. 'A role for interferon regulatory factor 4 in receptor editing', *Mol Cell Biol*, 28: 2815-24.
Patke, A., I. Mecklenbrauker, H. Erdjument-Bromage, P. Tempst, and A. Tarakhovsky. 2006. 'BAFF controls B cell metabolic fitness through a PKC beta- and Akt-dependent mechanism', *J Exp Med*, 203: 2551-62.
Peng, Y., J. Yuan, Z. Zhang, and X. Chang. 2017. 'Cytoplasmic poly(A)-binding protein 1 (PABPC1) interacts with the RNA-binding protein hnRNPLL and thereby regulates immunoglobulin secretion in plasma cells', *J Biol Chem*, 292: 12285-95.
Pengelly, A. R., R. Kalb, K. Finkl, and J. Muller. 2015. 'Transcriptional repression by PRC1 in the absence of H2A monoubiquitylation', *Genes Dev*, 29: 1487-92.
Petro, J. B., R. M. Gerstein, J. Lowe, R. S. Carter, N. Shinners, and W. N. Khan. 2002. 'Transitional type 1 and 2 B lymphocyte subsets are differentially responsive to antigen receptor signaling', *J Biol Chem*, 277: 48009-19.
Pherson, M., Z. Misulovin, M. Gause, K. Mihindukulasuriya, A. Swain, and D. Dorsett. 2017. 'Polycomb repressive complex 1 modifies transcription of active genes', *Sci Adv*, 3: e1700944.
Pillai, S., and A. Cariappa. 2009. 'The follicular versus marginal zone B lymphocyte cell fate decision', *Nat Rev Immunol*, 9: 767-77.
Piunti, A., A. Rossi, A. Cerutti, M. Albert, S. Jammula, A. Scelfo, L. Cedrone, G. Fragola, L. Olsson, H. Koseki, G. Testa, S. Casola, K. Helin, F. d'Adda di Fagagna, and D. Pasini. 2014. 'Polycomb proteins control proliferation and transformation independently of cell cycle checkpoints by regulating DNA replication', *Nat Commun*, 5: 3649.
Plath, K., J. Fang, S. K. Mlynarczyk-Evans, R. Cao, K. A. Worringer, H. Wang, C. C. de la Cruz, A. P. Otte, B. Panning, and Y. Zhang. 2003. 'Role of histone H3 lysine 27 methylation in X inactivation', *Science*, 300: 131-5.
Pleiman, C. M., W. M. Hertz, and J. C. Cambier. 1994. 'Activation of phosphatidylinositol-3' kinase by Src-family kinase SH3 binding to the p85 subunit', *Science*, 263: 1609-12.
Pohl, T., R. Gugasyan, R. J. Grumont, A. Strasser, D. Metcalf, D. Tarlinton, W. Sha, D. Baltimore, and S. Gerondakis. 2002. 'The combined absence of NF-kappa B1 and c-Rel reveals that overlapping roles for these transcription factors in the B cell lineage are restricted to the activation and function of mature cells', *Proc Natl Acad Sci U S A*, 99: 4514-9.
Pomerantz, J., N. Schreiber-Agus, N. J. Liegeois, A. Silverman, L. Alland, L. Chin, J. Potes, K. Chen, I. Orlow, H. W. Lee, C. Cordon-Cardo, and R. A. DePinho. 1998. 'The Ink4a tumor suppressor gene product, p19Arf, interacts with MDM2 and neutralizes MDM2's inhibition of p53', *Cell*, 92: 713-23.
Pone, E. J., H. Zan, J. Zhang, A. Al-Qahtani, Z. Xu, and P. Casali. 2010. 'Toll-like receptors and B-cell receptors synergize to induce immunoglobulin class-switch DNA recombination: relevance to microbial antibody responses', *Crit Rev Immunol*, 30: 1-29.
Pone, E. J., J. Zhang, T. Mai, C. A. White, G. Li, J. K. Sakakura, P. J. Patel, A. Al-Qahtani, H. Zan, Z. Xu, and P. Casali. 2012. 'BCR-signalling synergizes with TLR-signalling for induction of AID and immunoglobulin class-switching through the non-canonical NF-kappaB pathway', *Nat Commun*, 3: 767.
Posfai, E., R. Kunzmann, V. Brochard, J. Salvaing, E. Cabuy, T. C. Roloff, Z. Liu, M. Tardat, M. van Lohuizen, M. Vidal, N. Beaujean, and A. H. Peters. 2012. 'Polycomb function during oogenesis is required for mouse embryonic development', *Genes Dev*, 26: 920-32.
Preussner, M., S. Schreiner, L. H. Hung, M. Porstner, H. M. Jack, V. Benes, G. Ratsch, and A. Bindereif. 2012. 'HnRNP L and L-like cooperate in multiple-exon regulation of CD45 alternative splicing', *Nucleic Acids Res*, 40: 5666-78.
Pridans, C., M. L. Holmes, M. Polli, J. M. Wettenhall, A. Dakic, L. M. Corcoran, G. K. Smyth, and S. L. Nutt. 2008. 'Identification of Pax5 target genes in early B cell differentiation', *J Immunol*, 180: 1719-28.
Qin, J., W. A. Whyte, E. Anderssen, E. Apostolou, H. H. Chen, S. Akbarian, R. T. Bronson, K. Hochedlinger, S. Ramaswamy, R. A. Young, and H. Hock. 2012. 'The polycomb

group protein L3mbtl2 assembles an atypical PRC1-family complex that is essential in pluripotent stem cells and early development', *Cell Stem Cell*, 11: 319-32.
Quinlan, A. R., and I. M. Hall. 2010. 'BEDTools: a flexible suite of utilities for comparing genomic features', *Bioinformatics*, 26: 841-2.
Raaphorst, F. M., F. J. van Kemenade, T. Blokzijl, E. Fieret, K. M. Hamer, D. P. Satijn, A. P. Otte, and C. J. Meijer. 2000. 'Coexpression of BMI-1 and EZH2 polycomb group genes in Reed-Sternberg cells of Hodgkin's disease', *Am J Pathol*, 157: 709-15.
Raaphorst, F. M., F. J. van Kemenade, E. Fieret, K. M. Hamer, D. P. E. Satijn, A. P. Otte, and C. J. L. M. Meijer. 2000. 'Cutting Edge: Polycomb Gene Expression Patterns Reflect Distinct B Cell Differentiation Stages in Human Germinal Centers', *The Journal of Immunology*, 164: 1-4.
Radtke, F., A. Wilson, S. J. Mancini, and H. R. MacDonald. 2004. 'Notch regulation of lymphocyte development and function', *Nat Immunol*, 5: 247-53.
Rajewsky, K. 1996. 'Clonal selection and learning in the antibody system', *Nature*, 381: 751-8.
Rammensee, H. G., T. Friede, and S. Stevanoviic. 1995. 'MHC ligands and peptide motifs: first listing', *Immunogenetics*, 41: 178-228.
Reddington, J. P., S. M. Perricone, C. E. Nestor, J. Reichmann, N. A. Youngson, M. Suzuki, D. Reinhardt, D. S. Dunican, J. G. Prendergast, H. Mjoseng, B. H. Ramsahoye, E. Whitelaw, J. M. Greally, I. R. Adams, W. A. Bickmore, and R. R. Meehan. 2013. 'Redistribution of H3K27me3 upon DNA hypomethylation results in de-repression of Polycomb target genes', *Genome Biol*, 14: R25.
Reif, K., E. H. Ekland, L. Ohl, H. Nakano, M. Lipp, R. Forster, and J. G. Cyster. 2002. 'Balanced responsiveness to chemoattractants from adjacent zones determines B-cell position', *Nature*, 416: 94-9.
Ren, X., and T. K. Kerppola. 2011. 'REST interacts with Cbx proteins and regulates polycomb repressive complex 1 occupancy at RE1 elements', *Mol Cell Biol*, 31: 2100-10.
Rengarajan, J., K. A. Mowen, K. D. McBride, E. D. Smith, H. Singh, and L. H. Glimcher. 2002. 'Interferon regulatory factor 4 (IRF4) interacts with NFATc2 to modulate interleukin 4 gene expression', *J Exp Med*, 195: 1003-12.
Revilla, I. Domingo R., I. Bilic, B. Vilagos, H. Tagoh, A. Ebert, I. M. Tamir, L. Smeenk, J. Trupke, A. Sommer, M. Jaritz, and M. Busslinger. 2012. 'The B-cell identity factor Pax5 regulates distinct transcriptional programmes in early and late B lymphopoiesis', *EMBO J*, 31: 3130-46.
Reynolds, N., M. Salmon-Divon, H. Dvinge, A. Hynes-Allen, G. Balasooriya, D. Leaford, A. Behrens, P. Bertone, and B. Hendrich. 2012. 'NuRD-mediated deacetylation of H3K27 facilitates recruitment of Polycomb Repressive Complex 2 to direct gene repression', *EMBO J*, 31: 593-605.
Rickert, R. C., K. Rajewsky, and J. Roes. 1995. 'Impairment of T-cell-dependent B-cell responses and B-1 cell development in CD19-deficient mice', *Nature*, 376: 352-5.
Ridinger-Saison, M., E. Evanno, I. Gallais, P. Rimmele, D. Selimoglu-Buet, E. Sapharikas, F. Moreau-Gachelin, and C. Guillouf. 2013. 'Epigenetic silencing of Bim transcription by Spi-1/PU.1 promotes apoptosis resistance in leukaemia', *Cell Death Differ*, 20: 1268-78.
Riising, E. M., I. Comet, B. Leblanc, X. Wu, J. V. Johansen, and K. Helin. 2014. 'Gene silencing triggers polycomb repressive complex 2 recruitment to CpG islands genome wide', *Mol Cell*, 55: 347-60.
Ringrose, L., and R. Paro. 2004. 'Epigenetic regulation of cellular memory by the Polycomb and Trithorax group proteins', *Annu Rev Genet*, 38: 413-43.
Rinn, J. L., M. Kertesz, J. K. Wang, S. L. Squazzo, X. Xu, S. A. Brugmann, L. H. Goodnough, J. A. Helms, P. J. Farnham, E. Segal, and H. Y. Chang. 2007. 'Functional demarcation of active and silent chromatin domains in human HOX loci by noncoding RNAs', *Cell*, 129: 1311-23.
Roman-Trufero, M., H. R. Mendez-Gomez, C. Perez, A. Hijikata, Y. Fujimura, T. Endo, H. Koseki, C. Vicario-Abejon, and M. Vidal. 2009. 'Maintenance of undifferentiated state and self-renewal of embryonic neural stem cells by Polycomb protein Ring1B', *Stem Cells*, 27: 1559-70.

Rose, N. R., H. W. King, N. P. Blackledge, N. A. Fursova, K. J. Ember, R. Fischer, B. M. Kessler, and R. J. Klose. 2016. 'RYBP stimulates PRC1 to shape chromatin-based communication between Polycomb repressive complexes', *Elife*, 5.

Rossi, A., K. J. Ferrari, A. Piunti, S. Jammula, F. Chiacchiera, L. Mazzarella, A. Scelfo, P. G. Pelicci, and D. Pasini. 2016. 'Maintenance of leukemic cell identity by the activity of the Polycomb complex PRC1 in mice', *Sci Adv*, 2: e1600972.

Rouleau, M., D. McDonald, P. Gagne, M. E. Ouellet, A. Droit, J. M. Hunter, S. Dutertre, C. Prigent, M. J. Hendzel, and G. G. Poirier. 2007. 'PARP-3 associates with polycomb group bodies and with components of the DNA damage repair machinery', *J Cell Biochem*, 100: 385-401.

Rush, J. S., M. Liu, V. H. Odegard, S. Unniraman, and D. G. Schatz. 2005. 'Expression of activation-induced cytidine deaminase is regulated by cell division, providing a mechanistic basis for division-linked class switch recombination', *Proc Natl Acad Sci U S A*, 102: 13242-7.

Saijo, K., C. Schmedt, I. H. Su, H. Karasuyama, C. A. Lowell, M. Reth, T. Adachi, A. Patke, A. Santana, and A. Tarakhovsky. 2003. 'Essential role of Src-family protein tyrosine kinases in NF-kappaB activation during B cell development', *Nat Immunol*, 4: 274-9.

Saito, T., S. Chiba, M. Ichikawa, A. Kunisato, T. Asai, K. Shimizu, T. Yamaguchi, G. Yamamoto, S. Seo, K. Kumano, E. Nakagami-Yamaguchi, Y. Hamada, S. Aizawa, and H. Hirai. 2003. 'Notch2 is preferentially expressed in mature B cells and indispensable for marginal zone B lineage development', *Immunity*, 18: 675-85.

Sander, S., V. T. Chu, T. Yasuda, A. Franklin, R. Graf, D. P. Calado, S. Li, K. Imami, M. Selbach, M. Di Virgilio, L. Bullinger, and K. Rajewsky. 2015. 'PI3 Kinase and FOXO1 Transcription Factor Activity Differentially Control B Cells in the Germinal Center Light and Dark Zones', *Immunity*, 43: 1075-86.

Sanui, T., A. Inayoshi, M. Noda, E. Iwata, J. V. Stein, T. Sasazuki, and Y. Fukui. 2003. 'DOCK2 regulates Rac activation and cytoskeletal reorganization through interaction with ELMO1', *Blood*, 102: 2948-50.

Sauvageau, M., and G. Sauvageau. 2010. 'Polycomb group proteins: multi-faceted regulators of somatic stem cells and cancer', *Cell Stem Cell*, 7: 299-313.

Sayegh, C. E., S. Jhunjhunwala, R. Riblet, and C. Murre. 2005. 'Visualization of looping involving the immunoglobulin heavy-chain locus in developing B cells', *Genes Dev*, 19: 322-7.

Schaaf, C. A., Z. Misulovin, M. Gause, A. Koenig, D. W. Gohara, A. Watson, and D. Dorsett. 2013. 'Cohesin and polycomb proteins functionally interact to control transcription at silenced and active genes', *PLoS Genet*, 9: e1003560.

Scharer, C. D., B. G. Barwick, M. Guo, A. P. R. Bally, and J. M. Boss. 2018. 'Plasma cell differentiation is controlled by multiple cell division-coupled epigenetic programs', *Nat Commun*, 9: 1698.

Schebesta, A., S. McManus, G. Salvagiotto, A. Delogu, G. A. Busslinger, and M. Busslinger. 2007. 'Transcription factor Pax5 activates the chromatin of key genes involved in B cell signaling, adhesion, migration, and immune function', *Immunity*, 27: 49-63.

Schebesta, M., P. L. Pfeffer, and M. Busslinger. 2002. 'Control of pre-BCR signaling by Pax5-dependent activation of the BLNK gene', *Immunity*, 17: 473-85.

Schiemann, B., J. L. Gommerman, K. Vora, T. G. Cachero, S. Shulga-Morskaya, M. Dobles, E. Frew, and M. L. Scott. 2001. 'An essential role for BAFF in the normal development of B cells through a BCMA-independent pathway', *Science*, 293: 2111-4.

Schneider, P., H. Takatsuka, A. Wilson, F. Mackay, A. Tardivel, S. Lens, T. G. Cachero, D. Finke, F. Beermann, and J. Tschopp. 2001. 'Maturation of marginal zone and follicular B cells requires B cell activating factor of the tumor necrosis factor family and is independent of B cell maturation antigen', *J Exp Med*, 194: 1691-7.

Schoeftner, S., A. K. Sengupta, S. Kubicek, K. Mechtler, L. Spahn, H. Koseki, T. Jenuwein, and A. Wutz. 2006. 'Recruitment of PRC1 function at the initiation of X inactivation independent of PRC2 and silencing', *EMBO J*, 25: 3110-22.

Scholz, J. L., J. E. Crowley, M. M. Tomayko, N. Steinel, P. J. O'Neill, W. J. Quinn, 3rd, R. Goenka, J. P. Miller, Y. H. Cho, V. Long, C. Ward, T. S. Migone, M. J. Shlomchik,

and M. P. Cancro. 2008. 'BLyS inhibition eliminates primary B cells but leaves natural and acquired humoral immunity intact', *Proc Natl Acad Sci U S A*, 105: 15517-22.
Schwartz, Y. B., T. G. Kahn, D. A. Nix, X. Y. Li, R. Bourgon, M. Biggin, and V. Pirrotta. 2006. 'Genome-wide analysis of Polycomb targets in Drosophila melanogaster', *Nat Genet*, 38: 700-5.
Sciammas, R., and M. M. Davis. 2004. 'Modular nature of Blimp-1 in the regulation of gene expression during B cell maturation', *J Immunol*, 172: 5427-40.
Sciammas, R., A. L. Shaffer, J. H. Schatz, H. Zhao, L. M. Staudt, and H. Singh. 2006. 'Graded expression of interferon regulatory factor-4 coordinates isotype switching with plasma cell differentiation', *Immunity*, 25: 225-36.
Sciortino, G., D. Tegolo, and C. Valenti. 2017. 'Automatic detection and measurement of nuchal translucency', *Comput Biol Med*, 82: 12-20.
Seenundun, S., S. Rampalli, Q. C. Liu, A. Aziz, C. Palii, S. Hong, A. Blais, M. Brand, K. Ge, and F. J. Dilworth. 2010. 'UTX mediates demethylation of H3K27me3 at muscle-specific genes during myogenesis', *EMBO J*, 29: 1401-11.
Senftleben, U., Y. Cao, G. Xiao, F. R. Greten, G. Krahn, G. Bonizzi, Y. Chen, Y. Hu, A. Fong, S. C. Sun, and M. Karin. 2001. 'Activation by IKKalpha of a second, evolutionary conserved, NF-kappa B signaling pathway', *Science*, 293: 1495-9.
Shaffer, A. L., K. I. Lin, T. C. Kuo, X. Yu, E. M. Hurt, A. Rosenwald, J. M. Giltnane, L. Yang, H. Zhao, K. Calame, and L. M. Staudt. 2002. 'Blimp-1 orchestrates plasma cell differentiation by extinguishing the mature B cell gene expression program', *Immunity*, 17: 51-62.
Shao, Z., F. Raible, R. Mollaaghababa, J. R. Guyon, C. T. Wu, W. Bender, and R. E. Kingston. 1999. 'Stabilization of chromatin structure by PRC1, a Polycomb complex', *Cell*, 98: 37-46.
Shapiro-Shelef, M., K. I. Lin, L. J. McHeyzer-Williams, J. Liao, M. G. McHeyzer-Williams, and K. Calame. 2003. 'Blimp-1 is required for the formation of immunoglobulin secreting plasma cells and pre-plasma memory B cells', *Immunity*, 19: 607-20.
Shen, J., P. Li, X. Shao, Y. Yang, X. Liu, M. Feng, Q. Yu, R. Hu, and Z. Wang. 2018. 'The E3 Ligase RING1 Targets p53 for Degradation and Promotes Cancer Cell Proliferation and Survival', *Cancer Res*, 78: 359-71.
Shen, X., Y. Liu, Y. J. Hsu, Y. Fujiwara, J. Kim, X. Mao, G. C. Yuan, and S. H. Orkin. 2008. 'EZH1 mediates methylation on histone H3 lysine 27 and complements EZH2 in maintaining stem cell identity and executing pluripotency', *Mol Cell*, 32: 491-502.
Sherr, C. J., and J. M. Roberts. 1999. 'CDK inhibitors: positive and negative regulators of G1-phase progression', *Genes Dev*, 13: 1501-12.
Shimizu, K., S. Chiba, N. Hosoya, K. Kumano, T. Saito, M. Kurokawa, Y. Kanda, Y. Hamada, and H. Hirai. 2000. 'Binding of Delta1, Jagged1, and Jagged2 to Notch2 rapidly induces cleavage, nuclear translocation, and hyperphosphorylation of Notch2', *Mol Cell Biol*, 20: 6913-22.
Shin, I., F. M. Yakes, F. Rojo, N. Y. Shin, A. V. Bakin, J. Baselga, and C. L. Arteaga. 2002. 'PKB/Akt mediates cell-cycle progression by phosphorylation of p27(Kip1) at threonine 157 and modulation of its cellular localization', *Nat Med*, 8: 1145-52.
Shrivastava, P., T. Katagiri, M. Ogimoto, K. Mizuno, and H. Yakura. 2004. 'Dynamic regulation of Src-family kinases by CD45 in B cells', *Blood*, 103: 1425-32.
Shukla, S., E. Kavak, M. Gregory, M. Imashimizu, B. Shutinoski, M. Kashlev, P. Oberdoerffer, R. Sandberg, and S. Oberdoerffer. 2011. 'CTCF-promoted RNA polymerase II pausing links DNA methylation to splicing', *Nature*, 479: 74-9.
Siebenlist, U., K. Brown, and E. Claudio. 2005. 'Control of lymphocyte development by nuclear factor-kappaB', *Nat Rev Immunol*, 5: 435-45.
Simonetti, G., A. Carette, K. Silva, H. Wang, N. S. De Silva, N. Heise, C. W. Siebel, M. J. Shlomchik, and U. Klein. 2013. 'IRF4 controls the positioning of mature B cells in the lymphoid microenvironments by regulating NOTCH2 expression and activity', *J Exp Med*, 210: 2887-902.
Sing, A., D. Pannell, A. Karaiskakis, K. Sturgeon, M. Djabali, J. Ellis, H. D. Lipshitz, and S. P. Cordes. 2009. 'A vertebrate Polycomb response element governs segmentation of the posterior hindbrain', *Cell*, 138: 885-97.

Smith, K. G., T. D. Hewitson, G. J. Nossal, and D. M. Tarlinton. 1996. 'The phenotype and fate of the antibody-forming cells of the splenic foci', *Eur J Immunol*, 26: 444-8.
Song, H., and J. Cerny. 2003. 'Functional heterogeneity of marginal zone B cells revealed by their ability to generate both early antibody-forming cells and germinal centers with hypermutation and memory in response to a T-dependent antigen', *J Exp Med*, 198: 1923-35.
Soria, G., and V. Gottifredi. 2010. 'PCNA-coupled p21 degradation after DNA damage: The exception that confirms the rule?', *DNA Repair (Amst)*, 9: 358-64.
Srinivasan, L., Y. Sasaki, D. P. Calado, B. Zhang, J. H. Paik, R. A. DePinho, J. L. Kutok, J. F. Kearney, K. L. Otipoby, and K. Rajewsky. 2009. 'PI3 kinase signals BCR-dependent mature B cell survival', *Cell*, 139: 573-86.
Stall, A. M., S. Adams, L. A. Herzenberg, and A. B. Kantor. 1992. 'Characteristics and development of the murine B-1b (Ly-1 B sister) cell population', *Ann N Y Acad Sci*, 651: 33-43.
Steiniger, B. S. 2015. 'Human spleen microanatomy: why mice do not suffice', *Immunology*, 145: 334-46.
Stock, J. K., S. Giadrossi, M. Casanova, E. Brookes, M. Vidal, H. Koseki, N. Brockdorff, A. G. Fisher, and A. Pombo. 2007. 'Ring1-mediated ubiquitination of H2A restrains poised RNA polymerase II at bivalent genes in mouse ES cells', *Nat Cell Biol*, 9: 1428-35.
Su, I. H., A. Basavaraj, A. N. Krutchinsky, O. Hobert, A. Ullrich, B. T. Chait, and A. Tarakhovsky. 2003. 'Ezh2 controls B cell development through histone H3 methylation and Igh rearrangement', *Nat Immunol*, 4: 124-31.
Su, S. T., H. Y. Ying, Y. K. Chiu, F. R. Lin, M. Y. Chen, and K. I. Lin. 2009. 'Involvement of histone demethylase LSD1 in Blimp-1-mediated gene repression during plasma cell differentiation', *Mol Cell Biol*, 29: 1421-31.
Su, T. T., and D. J. Rawlings. 2002. 'Transitional B lymphocyte subsets operate as distinct checkpoints in murine splenic B cell development', *J Immunol*, 168: 2101-10.
Su, W. J., J. S. Fang, F. Cheng, C. Liu, F. Zhou, and J. Zhang. 2013. 'RNF2/Ring1b negatively regulates p53 expression in selective cancer cell types to promote tumor development', *Proc Natl Acad Sci U S A*, 110: 1720-5.
Suzuki, A., C. Iwamura, K. Shinoda, D. J. Tumes, M. Y. Kimura, H. Hosokawa, Y. Endo, S. Horiuchi, K. Tokoyoda, H. Koseki, M. Yamashita, and T. Nakayama. 2010. 'Polycomb group gene product Ring1B regulates Th2-driven airway inflammation through the inhibition of Bim-mediated apoptosis of effector Th2 cells in the lung', *J Immunol*, 184: 4510-20.
Tan-Pertel, H. T., L. Walker, D. Browning, A. Miyamoto, G. Weinmaster, and J. C. Gasson. 2000. 'Notch signaling enhances survival and alters differentiation of 32D myeloblasts', *J Immunol*, 165: 4428-36.
Tanaka, S., S. Miyagi, G. Sashida, T. Chiba, J. Yuan, M. Mochizuki-Kashio, Y. Suzuki, S. Sugano, C. Nakaseko, K. Yokote, H. Koseki, and A. Iwama. 2012. 'Ezh2 augments leukemogenicity by reinforcing differentiation blockage in acute myeloid leukemia', *Blood*, 120: 1107-17.
Tanigaki, K., H. Han, N. Yamamoto, K. Tashiro, M. Ikegawa, K. Kuroda, A. Suzuki, T. Nakano, and T. Honjo. 2002. 'Notch-RBP-J signaling is involved in cell fate determination of marginal zone B cells', *Nat Immunol*, 3: 443-50.
Tavares, L., E. Dimitrova, D. Oxley, J. Webster, R. Poot, J. Demmers, K. Bezstarosti, S. Taylor, H. Ura, H. Koide, A. Wutz, M. Vidal, S. Elderkin, and N. Brockdorff. 2012. 'RYBP-PRC1 complexes mediate H2A ubiquitylation at polycomb target sites independently of PRC2 and H3K27me3', *Cell*, 148: 664-78.
Tellier, J., and S. L. Nutt. 2017. 'Standing out from the crowd: How to identify plasma cells', *Eur J Immunol*, 47: 1276-79.
———. 2018. 'Plasma cells: The programming of an antibody-secreting machine', *Eur J Immunol*.
Tellier, J., W. Shi, M. Minnich, Y. Liao, S. Crawford, G. K. Smyth, A. Kallies, M. Busslinger, and S. L. Nutt. 2016. 'Blimp-1 controls plasma cell function through the regulation of immunoglobulin secretion and the unfolded protein response', *Nat Immunol*, 17: 323-30.

Tetsu, O., H. Ishihara, R. Kanno, M. Kamiyasu, H. Inoue, T. Tokuhisa, M. Taniguchi, and M. Kanno. 1998. 'mel-18 negatively regulates cell cycle progression upon B cell antigen receptor stimulation through a cascade leading to c-myc/cdc25', *Immunity*, 9: 439-48.

Thomas, M. L. 1989. 'The leukocyte common antigen family', *Annu Rev Immunol*, 7: 339-69.

Thomas, M. L., and L. Lefrancois. 1988. 'Differential expression of the leucocyte-common antigen family', *Immunol Today*, 9: 320-6.

Thompson, J. S., S. A. Bixler, F. Qian, K. Vora, M. L. Scott, T. G. Cachero, C. Hession, P. Schneider, I. D. Sizing, C. Mullen, K. Strauch, M. Zafari, C. D. Benjamin, J. Tschopp, J. L. Browning, and C. Ambrose. 2001. 'BAFF-R, a newly identified TNF receptor that specifically interacts with BAFF', *Science*, 293: 2108-11.

Timmerman, L. A., J. I. Healy, S. N. Ho, L. Chen, C. C. Goodnow, and G. R. Crabtree. 1997. 'Redundant expression but selective utilization of nuclear factor of activated T cells family members', *J Immunol*, 159: 2735-40.

Tokimasa, S., H. Ohta, A. Sawada, Y. Matsuda, J. Y. Kim, S. Nishiguchi, J. Hara, and Y. Takihara. 2001. 'Lack of the Polycomb-group gene rae28 causes maturation arrest at the early B-cell developmental stage', *Exp Hematol*, 29: 93-103.

Tolhuis, B., E. de Wit, I. Muijrers, H. Teunissen, W. Talhout, B. van Steensel, and M. van Lohuizen. 2006. 'Genome-wide profiling of PRC1 and PRC2 Polycomb chromatin binding in Drosophila melanogaster', *Nat Genet*, 38: 694-9.

Tonegawa, S. 1983. 'Somatic generation of antibody diversity', *Nature*, 302: 575-81.

Topp, J. D., J. Jackson, A. A. Melton, and K. W. Lynch. 2008. 'A cell-based screen for splicing regulators identifies hnRNP LL as a distinct signal-induced repressor of CD45 variable exon 4', *RNA*, 14: 2038-49.

Tourigny, M. R., J. Ursini-Siegel, H. Lee, K. M. Toellner, A. F. Cunningham, D. S. Franklin, S. Ely, M. Chen, X. F. Qin, Y. Xiong, I. C. MacLennan, and S. Chen-Kiang. 2002. 'CDK inhibitor p18(INK4c) is required for the generation of functional plasma cells', *Immunity*, 17: 179-89.

Trapnell, C., L. Pachter, and S. L. Salzberg. 2009. 'TopHat: discovering splice junctions with RNA-Seq', *Bioinformatics*, 25: 1105-11.

Trojer, P., A. R. Cao, Z. Gao, Y. Li, J. Zhang, X. Xu, G. Li, R. Losson, H. Erdjument-Bromage, P. Tempst, P. J. Farnham, and D. Reinberg. 2011. 'L3MBTL2 protein acts in concert with PcG protein-mediated monoubiquitination of H2A to establish a repressive chromatin structure', *Mol Cell*, 42: 438-50.

Tsai, M. C., O. Manor, Y. Wan, N. Mosammaparast, J. K. Wang, F. Lan, Y. Shi, E. Segal, and H. Y. Chang. 2010. 'Long noncoding RNA as modular scaffold of histone modification complexes', *Science*, 329: 689-93.

Tucker, E., K. O'Donnell, M. Fuchsberger, A. A. Hilton, D. Metcalf, K. Greig, N. A. Sims, J. M. Quinn, W. S. Alexander, D. J. Hilton, B. T. Kile, D. M. Tarlinton, and R. Starr. 2007. 'A novel mutation in the Nfkb2 gene generates an NF-kappa B2 "super repressor"', *J Immunol*, 179: 7514-22.

Tunyaplin, C., A. L. Shaffer, C. D. Angelin-Duclos, X. Yu, L. M. Staudt, and K. L. Calame. 2004. 'Direct repression of prdm1 by Bcl-6 inhibits plasmacytic differentiation', *J Immunol*, 173: 1158-65.

Turner, C. A., Jr., D. H. Mack, and M. M. Davis. 1994. 'Blimp-1, a novel zinc finger-containing protein that can drive the maturation of B lymphocytes into immunoglobulin-secreting cells', *Cell*, 77: 297-306.

Ushmorov, A., and T. Wirth. 2018. 'FOXO in B-cell lymphopoiesis and B cell neoplasia', *Semin Cancer Biol*, 50: 132-41.

van den Boom, V., M. Rozenveld-Geugien, F. Bonardi, D. Malanga, D. van Gosliga, A. M. Heijink, G. Viglietto, G. Morrone, F. Fusetti, E. Vellenga, and J. J. Schuringa. 2013. 'Nonredundant and locus-specific gene repression functions of PRC1 paralog family members in human hematopoietic stem/progenitor cells', *Blood*, 121: 2452-61.

van der Lugt, N. M., J. Domen, K. Linders, M. van Roon, E. Robanus-Maandag, H. te Riele, M. van der Valk, J. Deschamps, M. Sofroniew, M. van Lohuizen, and et al. 1994. 'Posterior transformation, neurological abnormalities, and severe hematopoietic

defects in mice with a targeted deletion of the bmi-1 proto-oncogene', *Genes Dev*, 8: 757-69.
van der Stoop, P., E. A. Boutsma, D. Hulsman, S. Noback, M. Heimerikx, R. M. Kerkhoven, J. W. Voncken, L. F. Wessels, and M. van Lohuizen. 2008. 'Ubiquitin E3 ligase Ring1b/Rnf2 of polycomb repressive complex 1 contributes to stable maintenance of mouse embryonic stem cells', *PLoS One*, 3: e2235.
van Gent, D. C., J. F. McBlane, D. A. Ramsden, M. J. Sadofsky, J. E. Hesse, and M. Gellert. 1995. 'Initiation of V(D)J recombination in a cell-free system', *Cell*, 81: 925-34.
van Kemenade, F. J., F. M. Raaphorst, T. Blokzijl, E. Fieret, K. M. Hamer, D. P. Satijn, A. P. Otte, and C. J. Meijer. 2001. 'Coexpression of BMI-1 and EZH2 polycomb-group proteins is associated with cycling cells and degree of malignancy in B-cell non-Hodgkin lymphoma', *Blood*, 97: 3896-901.
van Vliet, S. J., S. I. Gringhuis, T. B. Geijtenbeek, and Y. van Kooyk. 2006. 'Regulation of effector T cells by antigen-presenting cells via interaction of the C-type lectin MGL with CD45', *Nat Immunol*, 7: 1200-8.
Vella, P., I. Barozzi, A. Cuomo, T. Bonaldi, and D. Pasini. 2012. 'Yin Yang 1 extends the Myc-related transcription factors network in embryonic stem cells', *Nucleic Acids Res*, 40: 3403-18.
Venkataraman, L., D. A. Francis, Z. Wang, J. Liu, T. L. Rothstein, and R. Sen. 1994. 'Cyclosporin-A sensitive induction of NF-AT in murine B cells', *Immunity*, 1: 189-96.
Verma, I. M., J. K. Stevenson, E. M. Schwarz, D. Van Antwerp, and S. Miyamoto. 1995. 'Rel/NF-kappa B/I kappa B family: intimate tales of association and dissociation', *Genes Dev*, 9: 2723-35.
Verweij, C. L., C. Guidos, and G. R. Crabtree. 1990. 'Cell type specificity and activation requirements for NFAT-1 (nuclear factor of activated T-cells) transcriptional activity determined by a new method using transgenic mice to assay transcriptional activity of an individual nuclear factor', *J Biol Chem*, 265: 15788-95.
Victora, G. D., D. Dominguez-Sola, A. B. Holmes, S. Deroubaix, R. Dalla-Favera, and M. C. Nussenzweig. 2012. 'Identification of human germinal center light and dark zone cells and their relationship to human B-cell lymphomas', *Blood*, 120: 2240-8.
Victora, G. D., and M. C. Nussenzweig. 2012. 'Germinal centers', *Annu Rev Immunol*, 30: 429-57.
Vidal, M., and K. Starowicz. 2017. 'Polycomb complexes PRC1 and their function in hematopoiesis', *Exp Hematol*, 48: 12-31.
Vinuesa, C. G., S. G. Tangye, B. Moser, and C. R. Mackay. 2005. 'Follicular B helper T cells in antibody responses and autoimmunity', *Nat Rev Immunol*, 5: 853-65.
Vora, K. A., E. Nichols, G. Porter, Y. Cui, C. A. Keohane, R. Hajdu, J. Hale, W. Neway, D. Zaller, and S. Mandala. 2005. 'Sphingosine 1-phosphate receptor agonist FTY720-phosphate causes marginal zone B cell displacement', *J Leukoc Biol*, 78: 471-80.
Wang, J. M., J. R. Chao, W. Chen, M. L. Kuo, J. J. Yen, and H. F. Yang-Yen. 1999. 'The antiapoptotic gene mcl-1 is up-regulated by the phosphatidylinositol 3-kinase/Akt signaling pathway through a transcription factor complex containing CREB', *Mol Cell Biol*, 19: 6195-206.
Wang, L., J. L. Brown, R. Cao, Y. Zhang, J. A. Kassis, and R. S. Jones. 2004. 'Hierarchical recruitment of polycomb group silencing complexes', *Mol Cell*, 14: 637-46.
Wang, Q., K. R. Kieffer-Kwon, T. Y. Oliveira, C. T. Mayer, K. Yao, J. Pai, Z. Cao, M. Dose, R. Casellas, M. Jankovic, M. C. Nussenzweig, and D. F. Robbiani. 2017. 'The cell cycle restricts activation-induced cytidine deaminase activity to early G1', *J Exp Med*, 214: 49-58.
Wang, T., V. Nandakumar, X. X. Jiang, L. Jones, A. G. Yang, X. F. Huang, and S. Y. Chen. 2013. 'The control of hematopoietic stem cell maintenance, self-renewal, and differentiation by Mysm1-mediated epigenetic regulation', *Blood*, 122: 2812-22.
Watterson, K. R., E. Johnston, C. Chalmers, A. Pronin, S. J. Cook, J. L. Benovic, and T. M. Palmer. 2002. 'Dual regulation of EDG1/S1P(1) receptor phosphorylation and internalization by protein kinase C and G-protein-coupled receptor kinase 2', *J Biol Chem*, 277: 5767-77.

Weih, D. S., Z. B. Yilmaz, and F. Weih. 2001. 'Essential role of RelB in germinal center and marginal zone formation and proper expression of homing chemokines', *J Immunol*, 167: 1909-19.
Wen, L., J. Brill-Dashoff, S. A. Shinton, M. Asano, R. R. Hardy, and K. Hayakawa. 2005. 'Evidence of marginal-zone B cell-positive selection in spleen', *Immunity*, 23: 297-308.
Wen, W., C. Peng, M. O. Kim, C. Ho Jeong, F. Zhu, K. Yao, T. Zykova, W. Ma, A. Carper, A. Langfald, A. M. Bode, and Z. Dong. 2014. 'Knockdown of RNF2 induces apoptosis by regulating MDM2 and p53 stability', *Oncogene*, 33: 421-8.
Whitcomb, S. J., A. Basu, C. D. Allis, and E. Bernstein. 2007. 'Polycomb Group proteins: an evolutionary perspective', *Trends Genet*, 23: 494-502.
Winkelmann, R., L. Sandrock, J. Kirberg, H. M. Jack, and W. Schuh. 2014. 'KLF2--a negative regulator of pre-B cell clonal expansion and B cell activation', *PLoS One*, 9: e97953.
Witt, C. M., W. J. Won, V. Hurez, and C. A. Klug. 2003. 'Notch2 haploinsufficiency results in diminished B1 B cells and a severe reduction in marginal zone B cells', *J Immunol*, 171: 2783-8.
Woo, C. J., P. V. Kharchenko, L. Daheron, P. J. Park, and R. E. Kingston. 2010. 'A region of the human HOXD cluster that confers polycomb-group responsiveness', *Cell*, 140: 99-110.
Woodland, R. T., C. J. Fox, M. R. Schmidt, P. S. Hammerman, J. T. Opferman, S. J. Korsmeyer, D. M. Hilbert, and C. B. Thompson. 2008. 'Multiple signaling pathways promote B lymphocyte stimulator dependent B-cell growth and survival', *Blood*, 111: 750-60.
Woodland, R. T., M. R. Schmidt, and C. B. Thompson. 2006. 'BLyS and B cell homeostasis', *Semin Immunol*, 18: 318-26.
Wu, H., V. Coskun, J. Tao, W. Xie, W. Ge, K. Yoshikawa, E. Li, Y. Zhang, and Y. E. Sun. 2010. 'Dnmt3a-dependent nonpromoter DNA methylation facilitates transcription of neurogenic genes', *Science*, 329: 444-8.
Wu, H., A. C. D'Alessio, S. Ito, K. Xia, Z. Wang, K. Cui, K. Zhao, Y. E. Sun, and Y. Zhang. 2011. 'Dual functions of Tet1 in transcriptional regulation in mouse embryonic stem cells', *Nature*, 473: 389-93.
Wu, X., J. V. Johansen, and K. Helin. 2013. 'Fbxl10/Kdm2b recruits polycomb repressive complex 1 to CpG islands and regulates H2A ubiquitylation', *Mol Cell*, 49: 1134-46.
Wu, Z., X. Jia, L. de la Cruz, X. C. Su, B. Marzolf, P. Troisch, D. Zak, A. Hamilton, B. Whittle, D. Yu, D. Sheahan, E. Bertram, A. Aderem, G. Otting, C. C. Goodnow, and G. F. Hoyne. 2008. 'Memory T cell RNA rearrangement programmed by heterogeneous nuclear ribonucleoprotein hnRNPLL', *Immunity*, 29: 863-75.
Wu, Z. L., S. S. Zheng, Z. M. Li, Y. Y. Qiao, M. Y. Aau, and Q. Yu. 2010. 'Polycomb protein EZH2 regulates E2F1-dependent apoptosis through epigenetically modulating Bim expression', *Cell Death Differ*, 17: 801-10.
Wu, Z., S. Zheng, and Q. Yu. 2009. 'The E2F family and the role of E2F1 in apoptosis', *Int J Biochem Cell Biol*, 41: 2389-97.
Xu, Z., and A. Weiss. 2002. 'Negative regulation of CD45 by differential homodimerization of the alternatively spliced isoforms', *Nat Immunol*, 3: 764-71.
Yabas, M., D. I. Godfrey, C. C. Goodnow, and G. F. Hoyne. 2011. 'Differential requirement for the CD45 splicing regulator hnRNPLL for accumulation of NKT and conventional T cells', *PLoS One*, 6: e26440.
Yamamoto, T., Y. Yamanashi, and K. Toyoshima. 1993. 'Association of Src-family kinase Lyn with B-cell antigen receptor', *Immunol Rev*, 132: 187-206.
Yamashita, M., M. Kuwahara, A. Suzuki, K. Hirahara, R. Shinnaksu, H. Hosokawa, A. Hasegawa, S. Motohashi, A. Iwama, and T. Nakayama. 2008. 'Bmi1 regulates memory CD4 T cell survival via repression of the Noxa gene', *J Exp Med*, 205: 1109-20.
Yang, X., R. K. Karuturi, F. Sun, M. Aau, K. Yu, R. Shao, L. D. Miller, P. B. Tan, and Q. Yu. 2009. 'CDKN1C (p57) is a direct target of EZH2 and suppressed by multiple epigenetic mechanisms in breast cancer cells', *PLoS One*, 4: e5011.

Yap, K. L., S. Li, A. M. Munoz-Cabello, S. Raguz, L. Zeng, S. Mujtaba, J. Gil, M. J. Walsh, and M. M. Zhou. 2010. 'Molecular interplay of the noncoding RNA ANRIL and methylated histone H3 lysine 27 by polycomb CBX7 in transcriptional silencing of INK4a', *Mol Cell*, 38: 662-74.

Ying, H., J. I. Healy, C. C. Goodnow, and J. R. Parnes. 1998. 'Regulation of mouse CD72 gene expression during B lymphocyte development', *J Immunol*, 161: 4760-7.

Yoon, S. O., X. Zhang, P. Berner, B. Blom, and Y. S. Choi. 2009. 'Notch ligands expressed by follicular dendritic cells protect germinal center B cells from apoptosis', *J Immunol*, 183: 352-8.

Yoshida, T., S. Y. Ng, J. C. Zuniga-Pflucker, and K. Georgopoulos. 2006. 'Early hematopoietic lineage restrictions directed by Ikaros', *Nat Immunol*, 7: 382-91.

Yu, J., C. Angelin-Duclos, J. Greenwood, J. Liao, and K. Calame. 2000. 'Transcriptional repression by blimp-1 (PRDI-BF1) involves recruitment of histone deacetylase', *Mol Cell Biol*, 20: 2592-603.

Yu, M., T. Mazor, H. Huang, H. T. Huang, K. L. Kathrein, A. J. Woo, C. R. Chouinard, A. Labadorf, T. E. Akie, T. B. Moran, H. Xie, S. Zacharek, I. Taniuchi, R. G. Roeder, C. F. Kim, L. I. Zon, E. Fraenkel, and A. B. Cantor. 2012. 'Direct recruitment of polycomb repressive complex 1 to chromatin by core binding transcription factors', *Mol Cell*, 45: 330-43.

Yusuf, I., X. Zhu, M. G. Kharas, J. Chen, and D. A. Fruman. 2004. 'Optimal B-cell proliferation requires phosphoinositide 3-kinase-dependent inactivation of FOXO transcription factors', *Blood*, 104: 784-7.

Zeidler, M., S. Varambally, Q. Cao, A. M. Chinnaiyan, D. O. Ferguson, S. D. Merajver, and C. G. Kleer. 2005. 'The Polycomb group protein EZH2 impairs DNA repair in breast epithelial cells', *Neoplasia*, 7: 1011-9.

Zhang, Q., S. K. Padi, D. J. Tindall, and B. Guo. 2014. 'Polycomb protein EZH2 suppresses apoptosis by silencing the proapoptotic miR-31', *Cell Death Dis*, 5: e1486.

Zhang, Y., T. Liu, C. A. Meyer, J. Eeckhoute, D. S. Johnson, B. E. Bernstein, C. Nusbaum, R. M. Myers, M. Brown, W. Li, and X. S. Liu. 2008. 'Model-based analysis of ChIP-Seq (MACS)', *Genome Biol*, 9: R137.

Zhang, Y., Y. Xiong, and W. G. Yarbrough. 1998. 'ARF promotes MDM2 degradation and stabilizes p53: ARF-INK4a locus deletion impairs both the Rb and p53 tumor suppression pathways', *Cell*, 92: 725-34.

Zhao, J., B. K. Sun, J. A. Erwin, J. J. Song, and J. T. Lee. 2008. 'Polycomb proteins targeted by a short repeat RNA to the mouse X chromosome', *Science*, 322: 750-6.

Zheng, X., A. S. Li, H. Zheng, D. Zhao, D. Guan, and H. Zou. 2015. 'Different associations of CD45 isoforms with STAT3, PKC and ERK regulate IL-6-induced proliferation in myeloma', *PLoS One*, 10: e0119780.

Zhou, W., P. Zhu, J. Wang, G. Pascual, K. A. Ohgi, J. Lozach, C. K. Glass, and M. G. Rosenfeld. 2008. 'Histone H2A monoubiquitination represses transcription by inhibiting RNA polymerase II transcriptional elongation', *Mol Cell*, 29: 69-80.

Zink, D., and R. Paro. 1995. 'Drosophila Polycomb-group regulated chromatin inhibits the accessibility of a trans-activator to its target DNA', *EMBO J*, 14: 5660-71.